Energy and Exergy Analysis in Spray Drying Systems

Perry Johnson

Under supervision by: Professor Timothy A.G. Langrish

A thesis submitted in fulfilment of the requirements of the degree of

Doctor of Philosophy

School of Chemical and Biomolecular Engineering

Faculty of Engineering and Information Technology

The University of Sydney

September 2019

Acknowledgements

The completion of this thesis would not have been possible without the assistance and support of many people. I would like to thank my supervisor, Professor Timothy Langrish. Your patience, understanding, guidance, constructive feedback, and support has been invaluable throughout this whole process – I cannot thank you enough. I would also like to thank the other academic staff at the school for various helpful tips, support, and experience.

Additionally, I would like to extend my thanks to my colleagues in the Department of Chemical and Biomolecular Engineering for making this experience enjoyable and rewarding. Particular thanks must be extended to the administration team for solving any and all administrative issues in a professional and friendly manner. I wish to thank Mr Ilya Popov for assisting me in cleaning up and editing my language use within this document to improve readability.

Finally, I wish to express my deepest thanks to my family and friends for their encouragement, support, and patience and understanding. One last special thank you to my various housemates over this period, for all of your support, encouragement, and motivation; this would have been much more challenging without you.

Mr Ilya Popov (Editor)

Mr Ilya Popov MPub (Sydney University) has worked as a sub-editor, editor, content manager, journalist, writer, and digital content coordinator in various industries including finance, law, gaming, travel, and assorted print and online media.

Ilya proofread and copy-edited Chapters 1-3 and 7-9 and provided recommendations regarding structure, ambiguity, repetition, and the use of clear language.

Statement of originality

This is to certify that to the best of my knowledge the content of this thesis is my own work. This thesis has not been submitted for any degree or other purposes.

I certify that the intellectual content of this thesis is the product of my own work and that all the assistance received in preparing this thesis and sources have been acknowledged.

Author Attribution Statement

Chapter 4

1) Johnson, P.W.;Langrish, T.A.G. Inversion temperature and pinch analysis, ways to thermally optimize drying processes. *Drying Technology, An International Journal*, 2011. 29(5): p. 488-507.

Chapter 4 of this thesis is published as the above [1], this chapter is the results and discussion section of that publication, with some material distributed through Chapters 1, 2, and 3.

Case studies were proposed, and data analysis and manuscript drafts were completed by me.

Chapter 5

2) Johnson, P.W.;Langrish, T.A.G. Exergy Analysis of a Spray Dryer: Methods and Interpretations. *Drying Technology, An International Journal*, 2018. 36(5): p. 578-596.

Chapter 5 of this thesis is published as the above [2], this chapter is the results and discussion section of that publication, with some material distributed through Chapters 1, 2, and 3.

Case studies were proposed, and data analysis and manuscript drafts were completed by me.

Chapter 6

3) Johnson, P.W.;Langrish, T.A.G. Interpreting exergy analysis as applied to spray drying systems. International Journal of Exergy (IJEX), 2020. 13(2): p. 120-149.

Chapter 6 of this thesis has been approved for publication as the chapter title [3] this chapter is the results and discussion section of that publication, with some material distributed through Chapters 1, 2, and 3.

Case studies were proposed, and data analysis and manuscript drafts were completed by me.

Abstract

Drying processes contribute a significant proportion of energy use within industry today, from food and pharmaceuticals to construction products. The need to find and improve methods to increase the energy effectiveness of drying processes without reducing product quality can have significant effects on both financial costs and the cost to the environment through direct or indirect greenhouse gas emissions. These methods, beyond what is already used in industry already (such as improved insulation), are required to be able to be used and understood to make a difference.

There are various tools and methodologies which can be used to analyse and estimate the effect of process changes on systems – from ideal rate comparison models (Inversion Temperature) to heat exchanger optimisation tools (Pinch Analysis), to a full energy utilisation integration (Exergy Analysis). It is important to understand when each method is suitable, and the benefits of each. For example, an Exergy Analysis will provide the same outcomes as a Pinch Analysis when dealing exclusively with heat recovery; but will be more challenging to apply.

The Inversion Temperature has been compared with a Pinch Analysis on a typical stand-alone dryer system. For the Inversion Temperature to be relevant, different evaporative gases needed to be compared. In this instance, superheated steam was compared with hot air. One of the results revealed that the steam dryer is likely to be smaller than that of the air system (given the same inlet temperature) based on the higher evaporation rate presented by the superheated steam system.

In order to compare the Inversion Temperature (rate-based estimation method) with Pinch Analysis (thermal flow model), a Pinch Analysis was applied to both systems, yielding reasonable results (over open systems in both cases) of 18% energy recovery for the air system and 8.4% (with 86.6% potential) energy recovery for the steam system.

The extra potential from the steam system is due to the outlet temperature being at a much higher temperature (100^{O}C vs 40^{O}C), meaning that, as part of an extended system, the steam dryer has the potential to also have lower energy costs. It is important to note that

the air dryer operates above its system's Pinch Temperature –meaning that any extra heat added to the system is lost, with extra cooling potentially needed.

By contrast, the steam dryer operates across its Pinch Temperature, meaning that the steam system is less sensitive to process changes than the air system in terms of the system's energy recovery potential. This is due to the steam system having a significant recycle component to it, as gas recirculation requires less energy than heating a colder feed stream (this is harder to do with air systems as the humidity increase per recirculation interferes with the driving force within the dryer, further reducing efficiency).

The use of exergy analysis over a single unit operation has been explored, showing that while a spray dryer is effective at rapidly drying particulate solids, the energy use is inherently inefficient. Defining the task as evaporation of water means that the task-based losses are in the order of 38% of energy being fed to the dryer, with energy efficiencies ranging from 30% on a transiting basis to 94% on a temperature and pressure (thermo-mechanical) basis.

Small optimisation opportunities exist, within the range of typical operating temperatures and flows, mainly confirming that existing optimisations on existing systems are suitable at this point. The shortcut technique using the Carnot efficiency and a first law (energy balance) is suitable on systems that rely on temperature effects (such as drying; pressure within the dryer is a secondary effect).

An exergy analysis has been extended to two different systems which support the dryer –an electrically supplied system (vapour recompression) and a typical natural gas-driven steam boiler system. The key results are that as the systems get larger and more complex, exergy losses tend to get higher, and the total exergy lost within both systems is significantly higher than just the dryer on its own.

Key metrics of energy flows, including evaporation potential, recovery potential, and some key factors, have been explored for each system. While these overall factors compare the systems, it is important to also analyse each unit's operation within each system to help focus on which part of each system has the most improvement opportunities. While the boiler-driven system is better based on several of the metrics, changing the valve in the

Vapour Recompression system to a work recovery turbine (to help drive the compressor) reduces the wasted work potential of that system significantly enough to make the system competitive (the valve accounts for more than 50% of that system's exergy loss).

A preliminary level of system costing has also been carried out, outlining the scale of the cost of each of the studied systems in this thesis. Carbon accounting has also been presented for the systems. Carbon accounting highlights how the electrically-driven system is likely to be less damaging to the environment as more renewable energy sources come online in Australia, and this is aligned with the operating cost differential. The Vapour Recompression system costs around 60% more to build and 20% more to operate under current energy costing scenarios. The capital cost is unlikely to converge over time. However, operating costs are likely to change significantly based on the cost of natural gas and electricity production costs changing over time.

INDEX

Table of Contents

Table of Figures

Table of Tables

List of Equations

Chapter 1 Introduction to the Study

1.1Project Introduction

Several authors have reviewed energy consumption in drying, including Baker [4], Al-Adwani [5] in fluidised bed drying, and McKenzie [6] in spray drying. Estimates for the percentage of industrial sector energy used by dryers are between 10%-25% [7-9]. In addition, a Warren Centre study at the University of Sydney on energy efficiency [10] found that the energy usage by the industry sector was 40% of the 3,000 PJ/annum of energy used in Australia between 1997-1999, at a cost of $16 billion/annum. This translates to a range of 120 - 300 PJ/annum used for drying in Australia during that time period on the basis of 10%-25% of the total energy use being used for drying; equivalent to $1.6 and $4 billion/annum associated with dryers alone during that period.

1.1.1The Scope of the Thesis

The main task of the thesis is to find a suitable method of saving energy and cost within drying systems, where a reduction of any margin could save industry millions of dollars per year, and finding further savings is considered challenging due to the low temperature of dryer outlets (typically below 100^{O}C) [11]. This assessment can be completed by using a variety of tools to determine if and how much energy can be saved in the drying processes. The scope includes the creation of a methodology which uses a combination of methods to assist in the optimisation of drying processes, including a kinetics comparison method, energy use and recovery, and exergy optimisation techniques.

As a part of this methodology, Inversion temperature (IT) was chosen as it presents a method of comparing the kinetics of two drying gases (in this study air and steam systems were compared). In this way, the IT method gives an indication of what drying gas is more likely to result in a smaller dryer at a given temperature, and potentially resulting in a more efficient process.

Another key tool which can be used is Pinch Analysis (PA), which aims to maximise heat (energy) recovery within a system, and this analysis was performed on the systems described in the comparison using IT in Chapter 4.

It is also important to discuss the potential to recover significant amounts of energy commonly discharged to the environment in the form of vapour from a spray-dryer exhaust. The recovery of this (environmentally discharged) excess energy is not a simple task, unless starting with a humid stream with a higher moisture content than the saturation conditions (cold temperature) that a coolant can provide, the vapour recovery will be low. This low recovery can be even more problematic for recirculation systems due to requiring more energy to reheat the dried vapour back to the dryer inlet temperature. If it was possible to extract a much larger proportion of the evaporation energy from the outlet gas stream, the energy recovery potential would become significantly more important. This issue is explained in more detail in Chapter 4. The utilisation of condensing humid air as an energy source and the potential energy quality that may be extracted from such a process.

PA is often confused with optimisation since it is used to optimise a significant part of the system. However, most systems do not rely solely on heat transfer or heat processes, generating pressure differentials and generating flow is generally done with non-heat sources such as electrically-driven pumps/compressors/blowers. PA does not easily integrate non-heat sources in a straightforward and easy-to-interpret manner, for that task it is better to integrate a more holistic method such as exergy analysis (ExA). ExA was used here to demonstrate the integration of non-heat energy within a system, including one of the key benefits of ExA over PA – in that ExA is based on the second law of thermodynamics.

Exergy (which ExA is based on) has also been referred to by several names historically, including Gibbs free energy, Availability, and Work Potential. While no single method exists to perform an ExA on systems, adding a procedure to assist with generating assumptions for a given system has been important. It is also important to determine the parts of a calculation which can be left out, in order to achieve this, understanding the system being studied is crucial. The second law of thermodynamics has been used to compare different energy sources for the same task within the system (such as electricity relative to direct fuel use).

A discussion of losses within a system and to the environment in terms of exergy is covered in Chapter 5; this is an important aspect of optimisation as it gives an indication that internal and external efficiency are not always linked. It is important to differentiate methods that

isolate the different losses, both to the environment and internally. The understanding of where the losses come from gives a better understanding of what a unit is doing and how efficient a unit operation is, in this case a dryer, in each context.

Chapter 6 discusses the potential to replace a boiler system with an electrically-driven vapour recompression system; this comparison is an illustrative example of where PA would be inappropriate. The discussion of losses within the system and to the environment is extended to include pressure-based losses. A cost comparison of potential changes within a system was also completed to demonstrate that cost is generally a good indicator for the likelihood of potential optimisations being adopted.

1.2Approach in the Thesis

The process of drying and the systems associated with drying are complex in nature, since simultaneous heat and mass transfers occur in most cases. In the case of spray drying, this occurs in a single vessel and is not straightforward in concept. To understand the nature of spray dryers, research into calculation models appropriate to approaching PA and ExA models of heat and mass transfer in the context of a spray dryer were researched, extending to integrating the heat and mass transfer device into larger systems. It was clear that taking the dryer and solids separator as a single unit reduced much of the complexity in modelling by allowing the gas side and liquids side of the dryer to be isolated, with the interaction being treated as occurring within both units in an ideal manner. This method is described in more detail in Chapter 3.

A mass and energy balance (MEB) was initially constructed for a spray dryer and was based on and inspired by the work of Langrish [12]. The following constraints and assumptions were used for the MEB:

- The dryer is a well-insulated adiabatic continuous co-current spray dryer.
- The dryer is well mixed and equilibrium limited [13, 14].
- The flow rate of warm gas entering the dryer is 21 $kg.s^{-1}$ and the liquid solution flow rate is 2.5 $kg.s^{-1}$ of 50 %wt milk solids.
- An outlet approach temperature of $20^{O}C$ was used for the PA and dryer outlet temperature. This assumption will be explained in the relevant sections.

- The dryer curve was not studied. Instead, the results of the mass and energy balance were utilised to represent the dryer.
- Utilities analysis was not undertaken in the calculation of IT or for the first stage of PA. The generation of the heat exchanger network diagram was not completed, since the system is too simple for this part of the pinch processes to be utilised effectively.
- The system boundaries are located where each inlet and outlet streams are found at ambient conditions.
    - This assumption regarding ambient conditions in and out of the system was made to ensure the maximum recovery potential could be determined. For example, if venting the dryer exhaust directly to the environment, no energy can be recovered. This also means that the maximum acceptable utility usage for the system can be calculated easily. Any increase in utilities from this point would be wasteful.
- The calculation of the solids feed side of the system may be estimated by replacing the mass and energy balance with that of an evaporation tower system, but is currently indicative of the energy usage scale between the two sides of the system. The higher resolution would not yield further system improvement potential unless integration of the internal heat profile of the dryer becomes an option.

The MEB model was created and developed using Microsoft Excel, which allows for process variations and plant-wide process changes to be calculated. The choice of using Excel over more complex, and expensive, mathematics programs such as Matlab was straightforward as the analysis was to be completed for a steady-state system. At one point, it was more beneficial to code the mathematics into Visual Basic to speed up the calculation process.

While researching and creating the MEB model, it was evident that it only applied to using air as a drying gas since the model was reliant on a humidity term. The MEB is the basis upon which the rest of the study was built and is referenced in Chapters 2 - 6. To include non-air-based drying, the model was also adapted to handle gases such as steam. This change allowed for a superheated steam (SHS) dryer to also be studied. During this phase it was thought that using SHS could improve energy recovery as the steam leaving the dryer

would be at a warmer temperature than the equivalent air temperature and would allow heat recovery by condensation.

Using the IT method was a reasonable approach for comparing these two dryer types. The information required for IT was relatively simple to gather, being the heat capacity and equilibrium data for the two systems (since this can be found from the results of the MEB). The results for IT were informative but incomplete, so the MEB was used as the starting point for a common thermal analysis such as PA; the combination of IT and PA is discussed in Chapter 4.

Both methods were missing key parts of a potentially more complete optimisation tool, with both methods studying different aspects — IT based on relative kinetics and PA based on heat recovery potential. Both methods ignored electrical and pressure-based energy. Though both electricity and pressure are important energy aspects in drying, where sub-ambient pressure improves drying rates, and compressing the outlet could pre-heat the exhaust gas, potentially recovering more energy, each is generally ignored during a conventional PA or is added at the end.

To reduce the need to integrate pressure and electricity into an optimisation methodology, there were a few options, from advanced PA, ExA, as well as a few other ideas (which are discussed in more detail in Chapter 2), it became evident that exergy was perhaps the most interesting due to its potential to be as inclusive as any other method while also being useful in describing parts of a process individually or collectively in a meaningful way. The visualisation of results from an ExA is important to improve the understanding of any system, and visualisations for an ExA were completed in several forms (since the visualisation methods in PA enhance the usability of the PA method). These visualisations are presented in Chapters 5 and 6.

The concepts that were developed included the following aspects:

- The concept of phase change incurring no change in exergy was an important concept. The effect of the evaporation exergy calculation is a significant part of the result.
- The analysis done has been on ideal systems, with the dryer being adiabatic and assumed to be equilibrium limited (or close to it).

Based on these assumptions and methods, several methods were discussed, and a brief introduction to these will follow:

1.3The Underlying Laws of Thermodynamics

There are four underlying laws of thermodynamics, which define the physical quantities such as temperature, energy, and entropy, and which characterise thermodynamic systems at thermal equilibrium. The laws describe how these quantities behave under various circumstances.

The four laws of thermodynamics are [15, 16]:

- Zeroth law of thermodynamics: If two systems are in thermal equilibrium with a third system, they are in thermal equilibrium with each other. This law helps to define the concept of temperature.
- First law of thermodynamics: When energy passes, as work, as heat, or with matter, into or out from a system, the system's internal energy changes in accord with the law of conservation of energy. Equivalently, perpetual motion machines of the first kind (machines that produce work with no energy input) are impossible.
- Second law of thermodynamics: In a natural thermodynamic process, the sum of the entropies of the interacting thermodynamic systems increases. Equivalently, perpetual motion machines of the second kind (machines that spontaneously convert thermal energy into mechanical work) are impossible.
- Third law of thermodynamics: The entropy of a system approaches a constant value as the temperature approaches absolute zero. With the exception of non-crystalline solids (glasses) the entropy of a system at absolute zero is typically close to zero and is equal to the natural logarithm of the product of the quantum ground states.

The third law has a negligible impact for systems above ambient temperature as it refers to the entropy of cryogenic systems, particularly those in near vacuum. The first and second laws will be referred to throughout this thesis.

1.4Pinch Analysis and Inversion Temperature Introduction

Many proposed solutions to energy use in drying tend to be based on a single method for studying energy quality and quantity measurements and methodologies. There are a few papers built around an optimisation algorithm that includes comparing set changes within

the system to an ideal case [17]. There is also some literature that compares or combines certain methodologies to create a more complete picture of other possible solutions. However, there is very little in the way of comparisons or integrations of methodologies to create a more complete picture of possible solutions in respect to drying, although some have an application - such as Zhelev's 'Cleaner flue gas and energy recovery through pinch analysis' [18, 19]. Of the many comparisons used in literature, simple efficiency calculations have primarily been used.

In some ways, pinch technology is an attempt to take the quality of the energy into account when analysing the energy systems, in a way that first law analysis (e.g. energy balances) does not. In first law analysis, 1 kW is just 1 kW, regardless of whether it is available at 50^{O}C or 250^{O}C. Pinch technology starts to introduce the idea that 1 kW at 250^{O}C is more useful (has higher quality) than 1 kW at 50^{O}C. Exergy takes the idea of energy quality a step further than pinch technology. This progression is explored in this thesis.

1.5Exergy Analysis for a Spray Dryer and Drying Systems

Optimising unit operations beyond the traditional methods of pinch, chemical reaction completion and energy requirements is necessary to further improve the efficiency of processes. One such method, exergy analysis, is proposed here as a way of optimising the overall energy requirements of drying processes. Exergy was first suggested in the 19^{th} century, starting with Gibbs, and then Carnot, but the development of the methodology halted until the mid-20^{th} century. The modern version of exergy had its primary development in engineering applications (called exergy analysis) between 1950 and 1990, with development continuing to this day [20, 21].

Due to its more complete and complex nature, exergy was thought cumbersome while giving relatively small gains relative to PA [20]. Today, however, PA is often undertaken as part of the design stage [22], before construction, and this leaves a place for further improvement or optimisation techniques to be used for retrofitting, or plant-wide changes.

There exist many challenges with introducing exergy as a concept to industry in general, as it does not follow the general rules associated with energy and is a comparison method with ideal-reversible systems, which are not realistic, and is more abstract in its interpretation than a standard heat analysis such as PA. One of the rules that exergy does not follow is

conservation — exergy is destroyed as it is used or converted. Exergy also does not have a negative value when a change is being determined; work can occur in both directions. For example, in cooling systems, the energy level may be negative (when compared with ambient conditions), but the exergy is positive as there is work potential [23].

Exergy is the study of available energy or the ability to do work. In the case of process integration and development, it represents the ability to utilise energy. Exergy analysis works to save as much available energy as possible by manipulating the whole processing system, just as PA saves thermal utility requirements. This exergy analysis may require more data than PA, including flow properties, pressure drops through unit operations and piping, chemical reaction energy changes, and momentum changes. As such, it is more difficult to collect data.

Some comparisons have been made between PA and exergy analysis, with a focus on the limitations of PA or problems associated with interpreting the results of exergy analysis. One example is the work of Wall and Gong [24], which illustrates how exergy analysis is useful at determining heat pump integration. This work may be compared with Krajnc and Glavic's work [25] on integrating heat pumps into a PA and its composite curves.

1.5.1The Application of Exergy Analysis

Exergy analysis has been used in industry to optimise energy loads on dryers and drying plants for many years with some success. The exergy of drying systems in the food industry has been explored broadly in the past [26-33], mainly focussing on tray drying with air as the drying gas. Topic [34] investigated drying systems in general, particularly the effects of a direct-fired burner, fuel consumption, mixing, and solids moisture content on the exergy usage of the studied drying system. The main result from that analysis was that the dryer was the dominant exergy inefficiency within the system. Other drying techniques have been explored, such as tray-type heat pump timber drying [35], solar-thermal [36], ground source heat-pump drying [37], and pharmaceutical products using a gas engine-driven heat pump dryer [38]. In general, the results of the exergy analysis suggest dryers have second law or exergy efficiencies in the order of 4%-25% [28, 34] compared with high-pressure gas boilers (60%-75%) [39, 40], and electrically-driven air compressors (70%-80%) [30]. Chapter 5 of this

thesis has reviewed the application of various exergy analysis and efficiency factors on a dryer in isolation.

1.5.2Exergy Analysis for Other Dryers

Tambunan *et al* [36] studied a solar kiln dryer and stated that the optimum result for a solar thermal storage charge-discharge (energy battery) system would require a maximum loss ratio (exergy loss to exergy input ratio) of 60% to be a reasonable practical replacement for direct solar drying, while the loss ratio of the studied system was as high as 86% — meaning that the current technology has made the solar thermal dryer inefficient for direct solar drying, even though the drying cycle can be extended by a few hours per day.

The work of Gungor *et al* [30, 38] states ranges of results for exergy analyses on gas-engine heat-pump dryer systems, with a focus on which parts of the system required further study. The Gungor study found that the exhaust air heat exchanger (3.08 MW/USD) and drying ducts (1.42 MW/USD) were the worst performers on an exergy loss per capital cost basis. This result allows studies of the energy saving to be focused on these two units. Gungor and Hepbasli have been studying ways to assist in targeting poor exergy performers in systems with respect to ground engine heat pumps used for drying [41-43]. Their method uses the complex and integrated method of exergo-economic analysis which integrates costing (both capital and operating) over the lifetime of the operation to determine long-term savings in cost and exergy. The method in this thesis is more basic in that it isolates the two aspects. This is discussed in more detail in Chapters 5-7.

Other additions to targeting methodologies have been focussing on loss types and cause-effect analyses [41, 43-47]. These metrics are useful for system-wide optimisations but are limited in their use for a single unit operation — such as the spray dryer studied in this work. However, the determination of inevitable losses (INE) is useful to determine an optimal or desired operating condition.

1.6Challenges with Exergy Optimisation

A challenge that exergy presents is in the interpretation of the results, which is complicated by the difference in exergy evaluation factors. Chapter 5 of this thesis compares the most common factors used within the exergy literature to explore why no consensus has been reached in this area. Aghbashlo and Erbay [48-53] have both studied spray-drying systems

using exergy analysis in an attempt to optimise the systems. Both concluded that spray drying is far from an ideal system (in terms of exergy), and work is required to find more efficient ways of drying wet particles.

The results of these studies found that the parametric analyses showed no peak values, having optima at the upper or lower limitations of the process variables. Erbay and Koca [49, 51] also studied the effect of atomisation pressure on white cheese spray-drying and suggested that the atomisation pressure was a significant area of exergy loss. This result occurs since pressure has a small effect on the system equilibrium, while having a large effect on exergy requirements (to pressurise the feed for the atomiser). The pressure is a requirement of the operating conditions, and to create flow (spray) within the dryer. Pressure optimisation on atomisers is a trade-off between particle size, orifice size and flowrate. As a result, pressure should be considered important, but secondary to temperature and flow, for energy optimisation in most cases.

Optimising the spray dryer for maximum exergy recovery while maintaining an acceptable product specification (based on these results) may be challenging. Aghbashlo [48] determined that upwards of 15% of exergy fed to the dryer is lost from the dryer, and over 30% is converted to entropy (unusable energy), with only 7% of the combined exergy feed being utilised for drying.

Another notable challenge that exergy presents is the interpretation of the results — an undertaking complicated by the difference in factors. Kuzgunkaya and Hepbasli [37] stated that “the results (of the exergy analysis) can focus an engineer’s attention on components where the greatest potential is destroyed and quantify the extent to which modification of one component affects, favourably or unfavourably, the performance of other components of the system”. This statement implies an ability to target and optimise systems without explicitly saying how, and this current work explores that area.

1.7Summary of Scope

This chapter introduced the various methods used within this thesis and the importance of comparing and combining various methodologies when applied to spray drying to develop an objective methodology to optimise the quality of the energy used, as well as the

quantity, while integrating different forms of energy into the analysis to allow for a simple comparison on the basis of cost and environmental impacts.

Throughout this thesis different directions are taking towards optimisation. This thesis tries to assess the use of different tools and measures that would help designers to answer the following spray drying design questions:

- Should air, steam or other gas be used as the drying gas?
- What are the optimal inlet conditions (temperature and flow)?
- What options for energy recovery are available?
- How can these be best employed and assessed?

With these questions in mind, it is possible to study the compatibility and suitability of a combined, or integrated, optimisation approach using IT, PA, and ExA for the purpose of optimising spray-drying systems.

Chapter 2 has continued the introduction to the tools within the thesis and is a study of relevant literature. The scope of the thesis beyond what is described in this Chapter is outlined.

Chapter 3 has introduced the underlying thermodynamic principles, including sample calculations, particularly for ExA. Chapter 3 also covers the many factors used within ExA and the basis for their calculations, the proper use for each of these factors is discussed in more detail in Chapters 5 and 6.

Chapter 4 has investigated the IT technique and PA to determine the suitability of both methods for early-stage design decisions and potential optimisation potential. Chapter 4 demonstrates that even a simple heat-recovery option can reduce utility usage by a significant amount. IT and PA share a consistent set of results which demonstrates the link between kinetic based models, and heat recovery, particularly in drying systems.

Chapter 5 has demonstrated the application of an ExA to a spray dryer as a single focused unit for optimisation potential. This chapter is important as it links with Chapter 6 in the way that the dryer is found to be one of the most restrictive units for optimisation in both

systems studied in Chapter 6. The investigation of the dryer in Chapter 5 also compares the use of several effectiveness factors using a dryer system case study. These factors are then discussed in terms of their usefulness as optimisation tools.

Chapter 6 has investigated the optimisation of a drying system, and shows that optimisation is not limited to just heat exchangers or kinetics as given by PA or IT. ExA is a powerful tool that needs help to be made accessible to engineers because it is not limited to just heat, as in PA, and has the potential to improve the understanding of the systems being analysed. While PA is limited to heat exchange networks, ExA may be completed on systems to find alternative non-temperature-based optimisation pathways — such as vapour recompression or the integration of heat pumps, for which PA is not equipped. Chapter 6 has also examined the benefits of ExA compared to PA for drying systems, as well as demonstrating that exergy is a straightforward analytical technique that allows integration beyond what is offered by PA. Several visualisation tools presented in the literature are compared to help define where the system can be improved the most.

Chapter 7 has compared exergy analysis with PA regarding the required information as well as on a 'time to do the analysis' basis – which is useful in understanding the close relationship between exergy analysis and the time and information required to do the analysis. This chapter provides a method of simplifying exergy analysis to make it more accessible to engineers as a tool for optimisation of both thermal and non-thermal systems. To help demonstrate the comparison between PA and exergy analysis, an initial cost analysis has been provided to illustrate both the potential improvements to the system as well as the implications of each analysis.

Chapter 8 completes a techno-economic analysis of each case studied within this thesis, the boiler driven air drying and superheated steam systems from Chapter 4 and the vapour recompression system in Chapter 6. A basic carbon accounting has also been done based on localised conditions (a high level of coal power generation in Australia's east coast). An attempt to link ExA and PA results to costing in a simple and meaningful manner was discussed in this chapter.

These energy analysis methods shown in this thesis are designed to be an addition to the optimisation process, assuming that all other avenues for traditional process energy loss minimisation (such as insulation and improved system seals) have been implemented.

This thesis focuses on energy quality in drying and drying systems, using the second and third laws of thermodynamics to add value to energy analysis above the value given by energy balances alone, which are essentially based on the first law of thermodynamics.

Chapter 2 A review of the Comparison Tools and Methods

2.1The Proposed Methods

The proposed solutions for optimising dryers and drying processes include various standardised methods, such as Pinch Analysis (PA), extended-PA, Gibbs-enthalpy plots, Exergy Analysis (ExA), extended-ExA, Emergy analysis, and the integration of other environmental tools such as life cycle assessments. Some comparisons that can be used as a guide are Wall and Gong [24] and Sorin [54] for Pinch vs. Exergy, Zhelev for Pinch with Emergy [18], Sciubba and Ulgiati for Extended Exergy vs. Emergy [55], Nilsson and Jørgensen [56, 57] for a combination of several methods.

The best way to learn the strengths and weaknesses of each of these methods, as applied to drying, is to test each on a simple system and compare the results in detail. One of the key areas of focus in this thesis is using multiple tools to find a more suitable optimisation than each can give on their own.

2.2Hot Air and Superheated Steam

Superheated steam drying was developed in the mid to late 19th century but received very little attention in industry until the energy crisis of the 1970's [58]. Steam drying has become increasingly popular for many applications in recent years as technology has improved. Steam drying has benefits over air drying in the following areas [8, 59, 60]:

- Since the dryer exhaust is steam, it is possible to recover the majority of the latent heat that is supplied to the dryer inlet stream. This energy can be used in another part of the plant or partially re-compressed for use elsewhere.
- There are no oxidative reactions with solid skim milk powder, meaning it is desirable for oxygen-sensitive products.
- Recovery and removal of toxic or organic liquids are easier.
- Sterilisation, deodorisation, and pasteurisation are side effects that can be beneficial.
- Better rehydration properties, porosity, and colour retention often result from this process.

However, there are some potential disadvantages of steam drying:

- There may be a larger energy requirements associated with steam recirculation [61].
- There is limited industrial experience of this process compared with air systems.
- The system may be more complex for pressure containment and minimisation of solids entrainment using separation equipment can be more complicated.
- Potentially a more corrosive environment for equipment.
- The solid temperature can be higher than in conventional hot air drying.
- A higher risk of condensation in solids recovery systems.

2.2.1Useful Comparisons

There are several useful comparisons of air and superheated steam drying for the food industry in Prachayawarakorn [62], which show that for some systems, steam is more suitable than air as a drying gas. Prachayawarakorn's research also covers the detrimental effects of the initial condensation period that comes with the use of superheated steam.

Wimmerstedt [58] also discussed the potential for process integration; his primary example was boiler fuel feed drying. This example has the potential to improve boiler energy efficiency, reduce the boiler size, and reduce the environmental impact of the plant. He also explains that, for a fully integrated plant, such as a town electricity and heating supply from a combined heat and power plant (CHP), there are significant exergy losses, meaning the overall amount of recoverable heat is lower from the CHP plant. However, the exergy losses do not outweigh the benefits in this particular application [58].

It is clear from the literature that steam drying has a superior ability to be integrated within larger systems (at least for heat recovery). Steam also has a higher potential to have other methodologies applied to the outlet gas for energy recovery, such as mechanical vapour recompression and heat pumps [58].

2.3Inversion Temperature

The inversion temperature is the temperature where one thermally-driven system dries material more quickly than another one. This applies to drying gases such as convective hot

air and superheated steam systems. This approach to separation systems has been known for well over a century and has become a ‘rule of thumb’ approach to the process design of dryers [58].

Costa and Neto De Silva [53] have made the following statements with regards to the application of IT to separation systems:

“The common perception of the drying process states that the air streams are more effective drying agents at low humidity and high temperature. However, this is true only below a given temperature.” [63]

Several works on this IT for air relative to steam systems have been produced over the years. One in particular [63] describes how several previous analyses of the inversion temperature provided varying results based on differing assumptions - such as keeping the outlet solids moisture content constant or keeping the input energy constant for the dryer. Quoted ranges for the inversion temperature are between $140^{O}C$ - $260^{O}C$ for previous works [63]. The primary basis for the inversion temperature analysis is that a wet surface releases unbound water into a stream of humid air or superheated steam [63].

The drying of unbound water is typically called the unhindered drying region, which may limit the range of the method if the material temperature being dried does not have a long unhindered drying period, particularly for large porous solids such as timber; the system being studied in this thesis is powdered skim milk with an initial moisture content of 50%. For the case of any hindered drying, the material temperature rises above the wet-bulb temperature (for hindered drying).

The drying rate through the both the hindered, and unhindered regions may be interlinked through the concept of a Characteristic Drying Curve or the Reaction Engineering Approach [64]. For the systems being studied in Chapter 4, the drying of milk is likely to be hindered. The small size of skim milk powder also means that the Characteristic Drying Curve is likely to be true [64]. This situation means that the IT will be higher than if they drying process was unhindered [60, 63, 65, 66].

2.3.1Inversion Temperature Methodologies

Costa and Neto da Silva developed a methodology to get a consistent result for the majority of conditions by studying the mass-transfer rates at the surface of the material [63], in this case moist skim milk powder. This method (Inversion Temperature) is useful in determining if it is best to make a major change in the system in terms of air vs steam, or consider the potential change as an option to save energy and costs without taking into consideration other factors like capital or maintenance costs.

Costa and Neto da Silva determined that a similar result to the localised and effective IT's may be achieved by assuming that the dryer approximates an adiabatic saturation chamber and that the heat and mass transfer occur under the conditions of the outlet for the dryer. This situation simplified the calculation of the IT by assuming that the dryer reaches equilibrium, which allows for a more flexible analysis, negating the effects of the localised mass transfer rates. The result of this simplifying assumption was similar to those of the more detailed drying rate analyses [63].

2.3.2Adiabatic Saturation Inversion Temperature

For the application of IT to this thesis, in particular Chapter 4, the assumption that the dryer acts as an adiabatic saturation chamber as described by Costa and Neto Da Silva [63] is used. This assumption allows a simple metric to be used at an early stage of the optimisation process.

The saturation conditions that relate to the inlet conditions of temperature and humidity are assumed to be the point at which all of the evaporation occurs. That assumption removes the need to determine specific, and local, evaporation fluxes, thus making this method independent of local kinetic variables, rather than based on equilibrium conditions [63]. Many IT methods work with localised conditions across a surface length through the dryer. Those methods are based on kinetic information, while ASIT is based on equilibrium information, which is easier to find. The ASIT is suitable for dryers of sufficient length that they achieve, or come close to, equilibrium.

In effect, this is a comparison of the ideal rate at which drying occurs, and the IT is where the steam drying rate becomes higher than the air drying rate [60, 63]. However, even if

these conditions are not met in real dryers, the analysis is sufficient to use as a starting point for later and more complete assessments, such as PA, process modelling, and dryer design.

ASIT can be defined as the ratio of heat flows for the system, this is shown in Equation 2-1

$$ASIT_W = T_{Sat_{\Delta V}} + \frac{\beta}{1-\beta}\left(T_{Sat_{\Delta V}} - T_{ST}\right) \quad 2\text{-}1$$

Where:

[63]

$$\beta = \frac{(m_{DA} + m_V)_{IN}}{m_{ST_{IN}}} \frac{Cp_{DA} + y_{IN} Cp_V}{1 + y_{IN}} \frac{1}{Cp_V} \frac{\Delta h_{\Delta V(T_{Sat\Delta V})}}{\Delta h_{\Delta V(T_{ST})}}$$

Where:

- $(m_{DA} + m_V)_{IN} = m_{Air}$=total wet air feed mass flowrate.
- $m_{ST_{IN}}$=total steam feed mass flowrate.
- Cp_i= specific mass heat capacity of each component.
- $\Delta h_{\Delta V(T_{Sat\Delta V})}$ and $\Delta h_{\Delta V(T_{ST})}$= latent heat of vaporisation at the saturation temperatures of the air and steam, respectively.
- $T_{Sat_{\Delta V}}$ and T_{ST} are the saturation temperatures of the air and steam, respectively.
- y_{IN} is the humidity of the feed air in $g_W.g_{DA}^{-1}$.

The pressure of the system is critical on the properties used within the calculation. It should also be noted that this calculation assumes that the solids temperature change is insignificant and that the evaporation occurs adiabatically (the two-step process is discussed later in this chapter).

2.4Pinch Analysis

There are several papers and books [23, 67-72] that address the PA of systems, but most are based on a rigid system structure, i.e., the major items are reactors, which cannot be manipulated or changed to make a more energy-efficient process. Most of the literature on PA has not focused on manipulating the system, but rather on heat exchange and the recovery network around the key systems. Many of these analyses do not include increased

capital and maintenance costs using a differential economic analysis of the plant, where the differences are created by the changes in the system structure.

In these papers and books, dryers are discussed in modest detail in terms of potential savings using a PA, due to the adiabatic nature of drying systems, blower requirements, and the low dew point temperatures of dryers exit stream(s). However, it is generally agreed that drying is a key area where energy savings need to be addressed.

There are several papers and books written by Kemp [61, 73, 74] that address the need to look at the actual processing arrangement and interactions for separation systems such as dryers, evaporators, and distillation columns. In these books [61, 73, 74], changes to the dryer were studied to fit the dryer around other sections of the plant, as opposed to studying the plant and manipulating it to fit around the dryer. Considering the significant energy usage of dryers, manipulating the system to fit around the dryer may result in reducing utility requirements more effectively.

Another factor that has not been included in any standardised PA reference is the electrical energy requirements. especially those involved in re-circulation or flow induction equipment, or electrical heating and cooling systems such as heating elements, refrigeration, and heat pump cycles. The interaction between electrical energy flows and pinch analysis has been studied [75], but the quality of any replacement energy source has not been considered, and an analytical approach to including energy quality in a pinch analysis needs to be developed to improve the understanding of such decisions. The proposed approach should encompass more energy solutions, such as open ended or closed circuit heat pumps [24, 25].

2.4.1Method for Pinch Analysis

Starting a Pinch Analysis

In order to begin a PA it is important to have a complete process ready to analyse. In that regard, at least the reactors and separators and recycle loops need to have been designed, during the early stage of process design, assuming the use of only utilities is acceptable (PA is a process that takes care of integrating the heat within the process). A mass and energy balance should be completed first.

Heat Profile Data Collection

Once the process has been designed to the point where a heat balance can be done, generating a table for heating and cooling requirements is the next step. The important information includes the heat gradient information (*m.Cp*) average data for each flow. The streams are required to be a new table row if the *m.Cp* value changes too dramatically. Once these values are generated, it is possible to split and combine energy within each temperature range. The data from **Error! Reference source not found.** are then used to c reate a pinch plot with combined hot and cold curves.

Composite Curves

Composite curves can be constructed to indicate the pinch temperature, and how to start generating the heat exchange network.

Integration Network Diagrams

Heat network diagrams are a way of pairing heat sources and heat sinks to minimise total utility requirements.

2.4.2Assumptions and Rules in Pinch Analysis

- Streams can be split, just like pipes
- Phase change should be separated to ease calculation, and better matching
- Heat must not be transferred across the pinch
- There must be no external cooling above the pinch
- There must be no external heating below the pinch
- Attempting to match heat profiles (*mCp*) as close as possible, for heat exchangers lead to better results.
- Do not ignore cost, there is a trade-off between capital and energy costs
- Keep refining the network, some better options may exist
- When designing the network, start at the pinch, and move towards the outer ends, this ensures that the utilities are used in more appropriate locations (in general).

A more detailed method and calculation is completed in Chapter 4.

2.5Combining Inversion Temperature and Pinch Analysis

Inversion temperature (IT) arises from a simplified kinetics model that can be used to compare the drying rates of different fluids into different gases within a dryer. In terms of drying, it refers to the temperature where two drying gases dry at the same rate [63]. This situation in effect means that using a different drying gas may become beneficial at different temperatures.

While the inversion temperature may not be explicitly stated in some other works, the same method has been used by several authors to compare superheated steam and hot air. Choicharoen *et al* [65] studied hot air against superheated steam in drying high-moisture content particulate materials.

The main benefits that were stated by Choicharoen of steam over air, on top of reduced energy consumption, was the higher temperature potential within the dryer, the improved recycle potential, and reduced re-heating energy requirement. Suvarnakuta *et al* [66] investigated low-pressure superheated steam with vacuum drying in molecular sieve beads. It was commented in the study by Suvarnakuta that while an inversion temperature existed for the constant rate period of drying, there existed no inversion temperature for the complete drying cycle, suggesting that superheated steam was not always superior.

It should be noted that the inversion temperatures were recorded near the high end of the tested temperature spectrum. The extrapolation from the modelling suggested no inversion point. The work of Suvarnakuta *et al* [66] would be significantly more useful with more studied operating points, three pressures and three temperatures make it difficult to draw a conclusion from when comparing the two systems. There are several different IT calculation methods outlined in the work of Costa and Neto De Silva [63].

The method applied in this work is the simplified Adiabatic Inversion Saturation Temperature (ASIT). The simplified form is more than adequate for this thesis because IT is used as a comparison and selection tool, and thus high levels of detail and modelling are not required.

In the case being studied, humid air and superheated steam are the two options chosen. These cases will be compared with the aid of PA, which studies heat exchange potential and heat recovery options of the process streams around the dryer.

The results from the inversion temperature have been used as the basis for the mass and energy balances. From these balances, the system limitations have been assessed, such as the minimum inlet gas temperature to dry the solids sufficiently. These results will be used to complete the PA by comparing the air and superheated steam systems on the basis of energy recovery and energy use per unit moisture evaporation. This situation is outlined in **Error! Reference source not found.**.

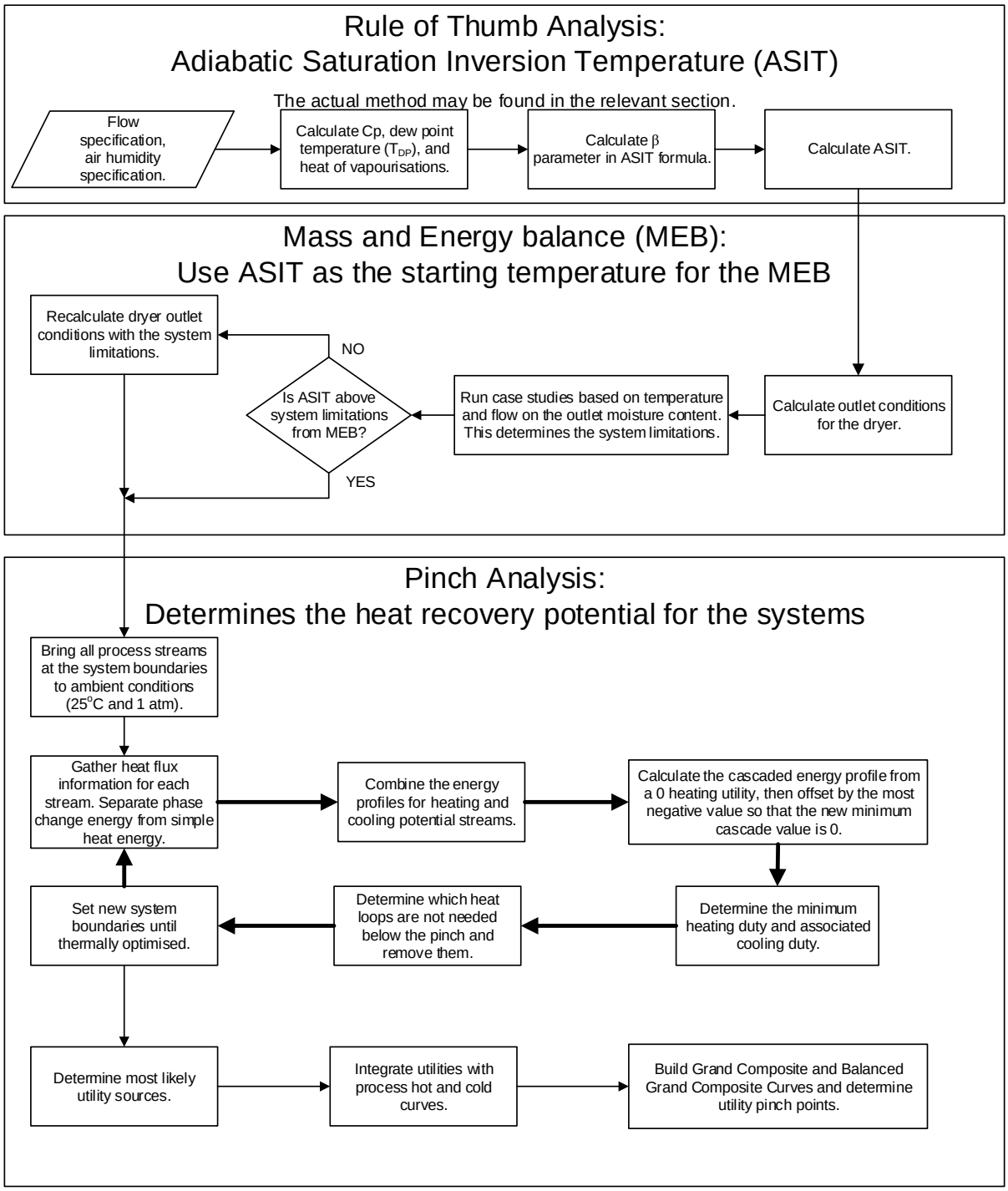

Figure 2-1: A diagram of the proposed optimisation process.

A comparison of the IT and PA methods is given in **Error! Reference source not found.**. This s ituation presents a basis for comparison for determining if the two methods give complementary results.

Table 2-1: A comparison of the IT and PA on some key properties.

Property	Inversion Temperature [63]	Pinch Analysis [61]
Basic Principle	Kinetic based comparison.	Thermodynamic optimisation.
Primary focus	Drying gas effectiveness within the dryer.	Heat recovery of external/ peripheral parts of the dryer.
Determines	Dryer inlet temperature, where during the constant rate period of drying, the drying rates of air and steam are the same.	Heat recovery potential based on an approach temperature.
Level of detail	There are various approaches for which different levels of detail are required.	High levels of analysis for heat exchanger networks can be done here.
Results accuracy	Approximate, can be used as a starting analysis or a rule of thumb for drying gas selection.	Dependent on approach temperature, which is related to heat exchanger sizing.
Scope	Can only be applied to a mass-transfer process, such as drying.	Can be used plant wide, used for heat exchanger network design.
Used here for	Estimating and comparing steam and convective air evaporation kinetics.	Determining the heat recovery potential.
Past usage	To select drying gases for drying based on the evaporation rates associated with each, after the effects of material sensitivity has been taken into consideration.	To optimise heat exchanger network design plant-wide. This has become a standardised optimisation tool within the design stages of a plant.

Error! Reference source not found. is the flowchart for the process used in Chapter 4. The r eason why the IT was used as a starting point for a MEB, and ultimately the PA, is so that a combination of a kinetics based and a thermodynamics-based models can be implemented into one analysis procedure. This combination has the potential to optimise the dryer systems without going into a high level of detail regarding the dryer design, and to help in the preliminary stages of the design process.

Combining kinetics and thermodynamics for optimisation is important in minimising equipment sizing (kinetics) and running costs due to energy (thermodynamics). The benefit of combining these two methods is that they complement each other by focussing on different aspects of the system. Both are simple and require readily available information to use.

PA is an example of a simple, robust methodology for thermal network and energy targeting. This method however, has a significant drawback in that it does not include energy types other than thermally-based enthalpy very well.

2.6Exergy Analysis

ExA requires more data than PA, including flow properties, pressure drops through operations and piping, chemical reaction energy changes, and momentum changes. As such, it is much harder to collect the data. This situation means that most exergy analyses are simplified versions of a total analysis. This simplification is generally done by removing some of the less significant parts of the analysis, such as the change of altitude, momentum, and dispersion work potential. The general equation for exergy is shown in Equation 2-2 [28, 35]. The analysis may be completed using known system equations, such as thermodynamic modelling or actual plant data [24].

Even though Wall and Gong [24] state there is limited potential to find appropriate heat pumping options with PA, there have been slight variations to include heat pumps and other mechanical equipment into a PA, as demonstrated by Krajnc and Glavic [25], Feng and Zhu [39], and Staine and Favrat [75]. Several other sources have stated that an exergy analysis is superior to PA [24, 34, 35, 70, 76, 77] due to it providing more options to improve the system and manipulate more forms of energy. Fushimi studied a self-heat recuperative air and steam dryer with the assistance of a VRC system for superheated steam [78], these results were compared on a pinch basis, and further verified with a preliminary exergy analysis.

There are several modified PA methodologies dealing with the integration of heat pumps into PA [23, 25]. The additions to the standard operating rules of pinch are that any heat pump must work across the pinch point in the reverse direction or the utilities will increase. Also, the higher the temperature change required, the lower the energy benefits become [23, 61, 74]. A heat pump example will be explored for this system to demonstrate the methods, and to compare them to an exergy analysis.

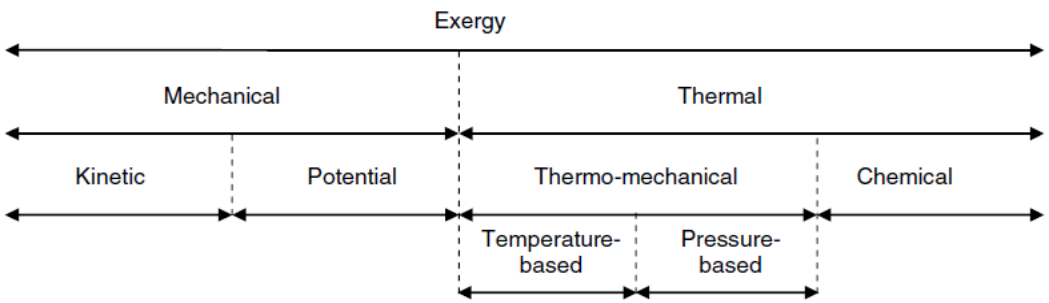

Figure 2-2: The breakdown of the most common exergy components [23].

$$ex = (u - u_0) + P_0(v - v_0) - T_0(s - s_0) + \sum_{i=0}^{\infty}(\mu_i - \mu_0)x_i$$

Internal Energy, Volume Work, Entropy, Chemical Potential

$$+g(z - z_0) + \frac{V^2}{2g} + E_i A_i F_i(3T^4 - T_0^4 - 4T_0 T^3)$$

Potential, Kinetic, and Radiation Energies

2-2 [35]

2.6.1Exergy and Efficiency Models

A review of several papers and their application of an exergy analysis to dryers has shown a variety of simplified models. To be more specific, Ozgener and Ozgener [33] present a model for a solar kiln dryer on a mass basis that takes many of the aspects of exergy into account presented here, including the effect of humidity, overall pressure changes, and dispersion to the environment. However, it is clear that the Ozgener study does not take evaporation or condensation into account when dealing with the exergy use.

Ozgener and Ozgener [33] also present some interesting results for the exergy efficiency of a dryer while key operational factors were changed over a range, such as residence time (0-18 hours), solar radiation levels (450-700 $W.m^{-2}$) and inlet gas temperature (40-50^{O}C). They also present several useful factors concerning exergy destruction, as well as a variety of other efficiency factors which are common in papers relating to exergy analysis. The Ozgener paper concludes that, since the study is based on solar energy within a greenhouse system, low solar energy input regions (non-tropical climates) will have low efficiencies, and low drying potentials.

Further research on exergy and dryers include a two-part paper by Cay [79, 80], which presents some practical ways of comparing different units within a system using exergy destruction per unit. The model used by Cay is the same as that of Ozgener and Ozgener [33]. The Cay papers are based on an air dryer in the textiles industry, which recirculates the outlet gas. Textiles are less likely to have solids entrainment issues, unlike the powder drying of milk solids studied in this current work. The air system studied here will initially be

treated as a once through system (no air recirculation). Different configurations can be modelled to determine the effect of changing the process variables, such as the recirculation rate or the outlet relative humidity.

A paper on exergy modelling by Aghbashlo, Kianmehr and Arabhosseini [26] uses only the temperature-based thermo-mechanical (TM) exergy component (shown in Equation 2-3), i.e. changes in system pressure are ignored, treating the system as an isobaric closed system.

$$ex_{TM}^{T} = \overline{Cp}\,(T - T_0) - T_0\overline{Cp}\ln\left(\frac{T}{T_0}\right) \qquad 2\text{-}3$$

The analysis in that paper is limited to the dryer and its thermal nature and does not consider the surrounding equipment. Aghbashlo *et al* [26] highlight a simple summarisation method for more complex systems. This method applies the idea of an exergy utilisation ratio (ExUR) (the used exergy per exergy input) to compare the effects of process changes. The ExUR is calculated in a similar fashion to the simple exergy efficiency.

$$ExUR = \frac{ex_{IN} - ex_{OUT}}{ex_{IN}} \qquad 2\text{-}4$$

Overall the work of Aghbashlo gives a brief starting point for thinking about applying a simple exergy model to a dryer to determine its thermal effectiveness [26]. This model has been simplified and tailored to the application and is likely to be misleading for other applications, such as those with significant pressure changes or vents to the environment.

A paper by Hepbasli [31] presents a method called exergoeconomic analysis. The focus of that paper is the cost of equipment and it treats exergy destruction per capital cost as the primary factor for optimisation, the equations are shown in Equation 2-5. This method may be considered when working with real systems, especially in the design and optimisation stages.

$$R = \frac{Loss\ rate}{Cost} \qquad 2\text{-}5$$

$$R_{Ex} = \frac{L_{Ex}}{K}$$

And

$$R_Q = \frac{L_Q}{K}$$

$$L = \text{consumption} + \text{loss rate}$$

$$L_{Ex} = \sum_{IN} Ex - \sum_{Products} Ex$$

$$L_Q = \sum_{IN} Q - \sum_{Products} Q$$

$$K = \text{Capital cost of equipment}$$

The main issue with this analysis method is that it depends highly on the timescale, since the capital cost is a once off, and the loss rate is ongoing.

Icier [32] compares the two most common exergy efficiency parameters and suggests the ratio of exergy outflow to exergy inflow rate (equation 2-9) is more meaningful in comparing different drying operations than the exergy used per specific exergy of evaporation (equation 2-8). The paper also introduces a factor called the improvement potential (IP), which is a method of calculating un-utilised lost exergy. The IP factor is a measure of how far apart of the plant is from ideal exergetic efficiency. Apart from being able to compare different parts of a plant, it can also be used to compare different designs for the same task, such as different dryers or drying gases. The equation for the improvement potential is shown below in Equation 2-6.

$$IP = (1 - \eta_{Ex})(E_{IN} - E_{OUT}) \quad \text{2-6}$$

$$\eta_{ex} = 1 - \frac{ex_{Loss}}{ex_{IN}} \quad \text{2-7}$$

$$\eta_{ex} = \frac{ex_{\Delta V}}{ex_{G_{IN}}} \quad \text{2-8}$$

$$\eta_{ex} = \frac{ex_{OUT}}{ex_{IN}} \quad \text{2-9}$$

$$\eta_{Task} = \frac{ex_{IN_{min}}}{ex_{IN}}$$

or 2-10

$$\eta_{Task} = \frac{ex_{IN_{ID}}}{ex_{IN}}$$

The difference between Equations 2-7 to 2-10 will be explained in Chapter 5 in more detail as the difference is significant for the results and application of its use. This IP factor was used to compare three different dryer types to determine which type was the most exergy efficient for each application. Icier's paper [32] was based on a laboratory-scale drying system. Since the dryers studied were run at atmospheric pressure, or close to it, the pressure-based exergy term was ignored in that study.

Dincer and Rosen [28] produced a book on the uses of exergy analysis in various forms including its usefulness in sustainable and environmental development, as well as industrial applications. While this book [28] is not comprehensive in its theoretical background on exergy, it does cover many practical applications in industrial and environmental approaches, including combining exergy with LCA and industrial ecology methods. This book [28] contains many practical applications of exergy analysis, but requires some understanding of exergy.

One of the most useful tables in the book is Table 1.1 on page 13 [28], which compares the properties of energy and exergy, reproduced here in Table 2-2.

Table 2-2: A comparison of energy and exergy (from [28]).

Property	Energy	Exergy
Dependency	Matter flow or energy flow.	Matter flow or energy flow and the local environment.
Conservation	ΔH=0	ΔEx=0 for reversible ideal systems. ΔEx≠0 for real systems.
Value	H>0, when in equilibrium with the environment.	Ex=0 when at the dead state. This means being in equilibrium with the local environment.
Consumption	Cannot be created or destroyed.	Destroyed (consumed) in real (irreversible) processes, but not destroyed in reversible processes.
Forms	Many forms, measured individually.	Many forms, measured on the ability to produce work.
Usefulness	Measure of quantity.	Measure of quantity and quality.

Chapter 2 of Dincer and Rosen [28] goes into significant detail regarding different reference-state models, and different efficiency calculations that have been presented, including a short discussion on each of their merits. The chosen method for the reference environment is the “natural environment sub-system” [28] as described in the discussion on the reference state.

Chapter 6 of Dincer and Rosen [28] examines in more detail the methodology for dealing with a psychrometric process, and Chapter 8 of Dincer and Rosen [28] builds on this by analysing a variety of air dryers using exergy analysis.

This review is not however, a comparison of work on exergy analysis alone. Rather it is a comparison and discussion of the usefulness of the various factors used within the literature to compare systems. A brief of some of the key results are described in the introduction to give context for the discussion.

2.6.2Efficiency factor use

The INE calculation is one of many metrics that may be used to interpret the data given by exergy analysis, along with many efficiency factors in use, some of which are presented here. The review of exergetic indicators by Zisopoulos *et al* [81] indicates the complexity in understanding exergy analysis. This variety of preliminary interpretations is one of the main challenges with exergy analysis, and a standard has yet to be accepted. A conceptual breakdown analysis of the factor types is presented in Chapter 5, which indicates the desired, and effective, usefulness of each factor type regarding process efficiency calculations.

For example, many factors only work across mass-transfer devices, such as the evaporation efficiency $\eta_{\Delta V.Ex_{IN}}$ while others only work on a phase-to-phase basis, such as the solids exergy efficiency K_{Ex} or the gas exergy efficiency η_{Ex_G}. While these factors are useful, their use is limited in explaining a system, while more overarching factors can be misleading and harder to interpret in terms of what each unit is trying to achieve. For example, the simple efficiency η_{Ex} shows the overall exergy efficiency of the system, but does not explain whether the exergy is being utilised or is part of system inefficiencies or emissions. Using an item-by-item task efficiency requires a more detailed analysis.

There has also been work done with artificial neural network (ANN) methods on exergy analysis of drying systems, but this method is more complicated than the exergy calculation method which it is intended to emulate [82-84]. ANN's should only be a tool for exergy analysis and should not be an alternative to exergy calculations, not a potential model-fitting and extrapolation tool.

As part of this work, a variety of factor types have been applied and discussed, to help guide engineers about the appropriate use of effectiveness factors in optimisation methods.

2.6.3Reference Conditions and the Dead State

The reference state refers to the reference temperature, pressure and environmental chemical state used for the calculations. In this work, 25^{O}C (298.15 K) and 101.325 kPa (1 atm) have been used for the reference temperature and pressure. For the dead state, the composition of the two phases has been used. In the case of the gas phase, the composition shown in Table 2-3 has been used, so as to be consistent with standard atmospheric conditions [85].

Table 2-3: Assumed dead-state and composition used for the gas phase. (These can be assumed to also be the air feed properties)

Air Component	Dead state partial pressure (bar)	Feed partial pressure (bar)	Feed mass fractions
O_2	0.2039	0.2099	0.2335
N_2	0.7578	0.7802	0.7599
CO_2	0.000355	0.0004	0.0006
H_2O	0.022	0.0096	0.0060
Inert (mainly Ar)	0.015945	-	-
Other useful properties			Units
Humidity (Y)	14	6	$g_W.kg_{DA}^{-1}$ *
T	25	25	^{O}C
P	1	1	atm

***NOTE 2-1: Dry air constitutes the dead state O_2, N_2, and CO_2 compositions only.**

Since a condensed phase (both solids and liquids) is present, it is necessary to consider any components that exist within that phase, which are not in equilibrium with the vapour phase. This dead-state parameter changes significantly depending on the composition of the materials being studied.

There are several ways of representing the condensed phase in the literature [21, 85-89]. The general pathway for calculating chemical potential energy is to assess the energy change for diffusing the chemical with consideration to the natural concentrations found in the environment. For this step, this chemical must be reduced or oxidised to these natural components, mainly CO_2, O_2, N_2, SO_2, and H_2O. The most common pathway for this process is generally assumed to be combustion in the environment. The overall composition change of oxygen in the environment is assumed to be negligible for the process. For most cases, the chemical potential is equivalent to the higher heating value (HHV).

For this work, the condensed phase has been assumed to be an ideal mixture of solids and pure water in equilibrium with the partial pressure of water in the gas phase. Therefore, the condensed phase has been assumed to be independent of the gas phase, but in equilibrium with the gas/vapour. There is a small fraction of sulphur in SMP (~9.04×10^{-3} mol of S per mol of H_2O produced from SMP). The effect of sulphur is smaller than the accuracy of the data used to calculate the value of the calculation of chemical exergy, and is not considered in this work. This assumption means that the condensed phase may be assumed to be pure water (after the reaction).

2.6.4Transiting Exergy

Transiting exergy refers to a component that has an insignificant contribution to, or interaction with, the unit operation [90, 91]. For example, if no chemical reaction or phase change takes place across a unit or system, the exergy associated with this movement across the unit or system is not taken into account for the change calculation within that unit or system. This assumption mainly affects the chemical potential energy of the SMP (which is likely to be unchanged) with the evaporation of water from the solids being the only change to that phase. SMP may also be assumed to be relatively inert in the environment due to its long shelf life, even in high humidity environments [92].

2.6.5Mole and mass calculation bases

It is common in the literature for exergy calculations to be calculated on a mass basis – particularly those used for space heating and air conditioning texts [93-97].

Exergy is generally expressed on a mass basis, resulting in cumbersome formulae, so this section will use a molar basis to show that an exergy analysis is quite straightforward on a

molar basis. While the mass basis makes more sense in real processing plants, introducing concepts in a complex manner is not amenable to readers wanting to use it. A simple presentation is fine to start with, then afterwards, you can give the reader the more practical form of the equations.

The formulae for Thermomechanical (TM) exergy remain the same with a domain change. However, the chemical and diffusion exergy changes significantly. This change can be seen by comparing Equations 2-46 and 2-11. As Equation 2-11 is presented on a molar basis, the calculation for the component-specific R value is not needed, and the mole fractions are relatively simple to calculate. The definition of chemical potential is given on a molar basis, which means that the mass basis (which only works in this form for a binary system) is needlessly complex due to the basis conversions required throughout the equation.

$$ex = \left(\frac{Cp_{DA} + yCp_V}{1+y}\right)T_0\left(\frac{T}{T_0} - 1 - \ln\left(\frac{T}{T_0}\right)\right) + \left(\frac{R_{DA} + yR_V}{1+y}\right)T_0 \ln\left(\frac{P}{P_0}\right) + T_0\left(R_{DA}\left(\frac{1}{1+y}\right)\ln\left(\frac{1+y_0}{1+y}\right) + R_V\left(\frac{y}{1+y}\right)\ln\left(\frac{y}{y_0}\frac{1+y}{1+y_o}\right)\right) \quad 2\text{-}11$$

$where$:

$$y = \frac{m_V}{m_{DA}}, y_0 = \frac{m_{V_0}}{m_{DA_0}}$$

$$R_{DA} = \frac{\bar{R}}{mm_{DA}}, R_V = \frac{\bar{R}}{mm_V}$$

$$ex = (x_{DA}Cp_{DA} + x_VCp_V)T_0\left(\frac{T}{T_0} - 1 - \ln\left(\frac{T}{T_0}\right)\right) + \bar{R}T_0 \ln\left(\frac{P}{P_0}\right) + \bar{R}T_0\left(x_{DA}\ln\left(\frac{x_{DA}}{x_{DA_0}}\right) + x_V \ln\left(\frac{x_V}{x_{V_0}}\right)\right) \quad 2\text{-}12$$

where:

$$x_{DA} = \frac{n_{DA}}{n_{DA} + n_V}, x_V = \frac{n_V}{n_{DA} + n_V}$$

$$n_{DA} = \frac{m_{DA}}{mm_{DA}}, n_V = \frac{m_V}{mm_V}$$

Alternatively, mole fractions from humidity and molar mass:

$$x_{DA} = \frac{1}{1 + y\frac{mm_{DA}}{mm_V}}, x_V = \frac{y\frac{mm_{DA}}{mm_V}}{1 + y\frac{mm_{DA}}{mm_V}}$$

In addition, the calculation of exergy for a liquid differs slightly, in that the pressure-based exergy is not defined solely on the phase being calculated. The liquid phase exergy is pressure-based and, as a result, has a significant dependence on the gas phase. This form does not differ between a molar and a mass basis. The liquid phase specific exergy may be calculated using Equation 2-13.

$$ex_L = Cp_L T_0 \left(\frac{T}{T_0} - 1 - \ln\left(\frac{T}{T_0}\right)\right) + \left(P - P_{T^{Sat}}\right) v_{Sat.L(T)} - \bar{R} T_0 \ln\left(\frac{P_V}{P_{T^{Sat}}}\right) \quad 2\text{-}13$$

Calculating exergy on a molar basis leaves the equations in a simpler and straightforward form (compared with the mass equivalent). The mass basis is useful for thermo-physical calculations, but becomes very complex for chemical potential calculations. This situation means that the basis for the calculation becomes important, particularly when it comes to more complex systems.

2.6.6Efficiency Factors

There are several efficiency factors used to determine the system, or unit efficiency with respect to exergy. In this work, the following definitions have been used:

$$IP = (1 - \eta_{ex})(ex_{IN} - ex_{OUT}) \quad 2\text{-}6$$

Where:

η= Exergy efficiency can be defined by one of Equations 2-7 to 2-10.

$$\eta_{ex} = 1 - \frac{ex_{Loss}}{ex_{IN}} \quad 2\text{-}7$$

$$\eta_{ex} = \frac{ex_{\Delta V}}{ex_{G_{IN}}} \quad 2\text{-}8$$

$$\eta_{ex} = \frac{ex_{OUT}}{ex_{IN}} \quad 2\text{-}9$$

$$\eta_{Task} = \frac{ex_{IN_{min}}}{ex_{IN}}$$

or 2-10

$$\eta_{Task} = \frac{ex_{IN_{ID}}}{ex_{IN}}$$

The above efficiency factors (Equation 2-6) take the entire exergy calculation into account for each unit. Equation 2-7 represents the basic (or standard) exergy efficiency, while Equation 2-8 represents the evaporation efficiency common to much of the literature when referring to dryers, and Equation 2-9 represents the simple exergy efficiency, which is the easiest to calculate. The main difference between Equations 2-7 and 2-9 is that, for real systems, losses occur between the unit and the environment (typically through heat loss via equipment walls).

For this work, these two are identical since loss represents change over the unit (i.e. loss=out-in). However, these factors may not be useful in determining the true effect of system factors on a unit. To determine a more appropriate efficiency for these cases, a transiting exergy factor may be used. The simple transiting calculation is shown in Equation 2-14:

$$ex_{Trans} = ex - ex_{inert} \quad 2\text{-}14$$

$$\eta_{Trans} = \frac{ex_{OUT} - ex_{Trans}}{ex_{IN} - ex_{Trans}} \quad 2\text{-}15$$

In practice, this is not a simple calculation when dealing with large systems, but a simplified method of determining transiting exergy may be used, and this calculation is discussed in Chapter 5. In order to determine many of these factors, intermediate calculations are required. For example, the evaporation rate and gas phase evaporation potential are required for the evaporation efficiency calculation (Equation 2-8). Some key items of information used to calculate the efficiency factors are $Q_{\Delta T.G}$ and $Ex_{\Delta T.G}$ These are the energy and exergy changes associated with the gas side of the dryer on a temperature basis only, while assuming that no mass transfer has taken place (chemical exergy is ignored). These factors are defined by Equations 2-15 and 2-16, respectively.

$$Q_{\Delta T.G} = \dot{n_{G_{IN}}}\overline{Cp_G}\left(T_{G_{IN}} - T_{G_{OUT}}\right) \quad 2\text{-}16$$

$$Ex_{\Delta T.G} = \dot{n_{G_{IN}}}\overline{Cp_G}\left(T_{G_{IN}} - T_{G_{OUT}} - T_0 \ln\left(\frac{T_{G_{IN}}}{T_{G_{OUT}}}\right)\right) \quad 2\text{-}17$$

Some other parameters may be used to describe the system, which are the ideal evaporation potentials: $\dot{m_{\Delta V_{ID.Q}}}$ and $\dot{m_{\Delta V_{ID.Ex}}}$. On an energy and exergy basis they are determined by Equations 2-8 and 2-9, respectively.

$$\dot{m_{\Delta V_{ID.Q}}} = \frac{Q_{\Delta T.G}}{\Delta Q_{\Delta V}} \quad 2\text{-}18$$

$$\dot{m_{\Delta V_{ID.Ex}}} = \frac{Ex_{\Delta T.G}}{\Delta Ex_{\Delta V}} \quad 2\text{-}19$$

The effect of evaporation is not just a thermal effect, but also contains a change of exergy associated with the diffusion change or inter-phase mass transfer (chemical potential change). This situation is important to note for systems that are open to the environment.

The evaporation efficiency may be defined on a mass flow basis ($\eta_{\Delta V_{ID.Q}}$), where the actual evaporation is divided by the evaporation potential on a first law basis.

$$\eta_{\Delta V_{ID.Q}} = \frac{\dot{m_{\Delta V}}}{\dot{m_{\Delta V_{ID.Q}}}} \quad 2\text{-}20$$

The evaporation efficiency may be defined on the basis of the gas feed energy or exergy ($\eta_{\Delta V.Q_{IN}}$ Equation 2-21 and $\eta_{\Delta V.Ex_{IN}}$ Equation 2-22, respectively).

$$\eta_{\Delta V.Q_{IN}} = \frac{\dot{m_{\Delta V}}\dot{\Delta h_{\Delta V}}}{\dot{m_{G_{IN}}}Cp_G\left(T_{G_{IN}} - T_0\right)} \quad 2\text{-}21$$

$$\eta_{\Delta V.Ex_{IN}} = \frac{\dot{m_{\Delta V}}\dot{\Delta ex_{\Delta V}}}{\dot{m_{G_{IN}}}Cp_G\left(T_{G_{IN}} - T_0\left(1 - \ln\left(\frac{T_{G_{IN}}}{T_0}\right)\right)\right)} \quad 2\text{-}22$$

Other methods exist for discussing the exergy efficiency system. For example, Feng and Zhu [39, 98] proposed using the omega factor (Ω) to simplify the use of exergy analysis to provide a simple graphical method similar to the grand composite curves used commonly in PA. The method can be applied to unit operations, streams or systems in the same manner.

However, there are some rules that must be followed for the method to be useful. The general form of Ω is shown in Equation 2-22.

$$\Omega = \frac{Exergy\ (Ex)}{Energy\ (Q)} \qquad 2\text{-}23$$

Where Ω can be simplified for several conditions:

For Work: $$\Omega = 1 \qquad 2\text{-}24$$

For Heat: $$\Omega = \eta_{Carnot} = 1 - \frac{T}{T_0} \qquad 2\text{-}25$$

And for steady-state flow:

$$\Omega = \frac{\Delta Ex}{\Delta H} \qquad 2\text{-}26$$

Due to the definition of Ω, the value is greater than unity for expansion processes, and less than unity for compression processes. In the case of expansion processes, the exergy loss can be defined as the area between the Ω=1 line and the system curve, i.e. regardless of the value of Ω, the exergy loss can still be defined as the area between two lines. In the case of work (in or out), the second line corresponds to Ω=1 [39, 98].

One of the concerns with ExA is that the basis for which the comparison is made is often unrealistic. As a result of this criticism, research has been done to characterise the difference between inevitable (*INE*) and avoidable (*AVO*) exergy losses within systems [98]. The important aspect of inevitable loss is its relationship with the minimum loss associated with the task, or the unit operation performing the task. In this case, it represents the loss associated with evaporating the liquid from the solid. Typical unit operations may be determined based on the relationship with the Carnot efficiency, or the minimum entropy generation for non-thermal systems.

Assuming that the dryer acts to evaporate water and assuming that the exergy loss associated with evaporation is small, Equation 3 from [98] may be used to calculate the inevitable exergy loss associated with the evaporation of water using hot gas. This calculation is presented here as Equation 2-27.

$$INE = Q_{Transfer.G} T_0 \left(\frac{1}{T_{\Delta V.max}} - \frac{1}{T_{G_{IN}.max}} \right) \quad \text{2-27}$$

Assumptions used for Equation 2-27 include:

- $T_{\Delta V.max} = \left(T_{DP_{OUT}}, T_{S_{OUT}}\right) + \Delta T_{min}$corresponding to the offset temperature assumption used in the model.
- $T_{G_{IN}.max}$ the feed gas inlet temperature.
- $Q_{Transfer.G}$ is the overall change in energy on the gas side of the dryer.
- $Q_{Transfer} = Q_{\Delta T_{G_{IN}}} = Q_{\Delta V_G}$(based on Equation 2-21).

Other unit operations have used a similar calculation based on the Carnot efficiency for each task or unit operation [98].

The basis for the calculation of the exergy loss for an ideal dryer is that the exergy associated with the internal mass transfer is negligible (isothermal). The inevitable exergy loss will be due to the difference between the feed gas temperature and the evaporation temperature within the dryer. Another way to determine the exergy loss is to calculate the entropy generated by the ideal drying process. It should be noted that, for simple unit operations, this may be done using the first law analysis as the basis. This method assumes that the change of exergy is only thermally based (Carnot efficiency). A discussion of the INE calculation methodology is provided in Chapter 5.

Another use for the inevitable loss is to determine the unit efficiency relative to its potential efficiency. This can be seen in Equation 2-29, which represents a more detailed version of Equation 2-7 in that it takes the minimum potential loss and compares it with the actual loss, which provides a useful factor for describing how close to ideal the task operates.

$$1 - \frac{INE}{Ex_{IN}} = \frac{Ex_{IN} - INE}{Ex_{IN}} = \frac{AVO}{Ex_{IN}} \quad \text{2-28}$$

This factor can also be used to describe energy effectiveness on a first law basis when replacing exergy with energy (as shown in Equation 2-28).

$$1 - \frac{INE}{H_{IN}} = \frac{H_{IN} - INE}{H_{IN}} = \frac{AVO_H}{H_{IN}} \quad \text{2-29}$$

2.6.7Summary of Exergy Formulae

The general forms of enthalpy, entropy and chemical-potential exergy used within this study are shown in Equations 2-10 to 2-45.

General Form

$$ex = (h - h_0) - T_0(s - s_0) + \sum_{i=0}^{inf}(\mu_i - \mu_0)x_i \quad \text{2-30}$$

***NOTE 2-2: This is the shortened version of the exergy definition; the full version includes all forms of work, including potential energy, kinetic energy, radiation, etc, as shown in Equation 2-2.**

Enthalpy Terms

$$h_i^T = Cp_i(T - T_0) \quad \text{2-31}$$

and

$$h_{\Delta V}^T = \left[\overline{Cp_V}(T - T_0) + \overline{\Delta h_{\Delta V.0}}\right] \quad \text{2-32}$$

$$h^{CH} = \sum_i x_i h_i^{CH} \quad \text{2-33}$$

where:

$$h_i^{CH} = HHV_i = 341C + 1{,}323H + 68S + 15.3A - 120\,(0 + N) \quad \text{2-34}$$

in $\%wt$ using the general reaction form [99]

$$X_i + v_1O_2 \leftrightarrow V_2CO_2 + v_3H_2O + v_4N_2 + v_5S_{Solid} + v_6Ash \quad \text{2-35}$$

where: v_j *"is the set or molar reaction coefficient(s)"*

Entropy Terms

$$T_0 s_i^T = T_0 Cp_i \ln\left(\frac{T}{T_0}\right) \quad \text{2-36}$$

and

$$T_0 s_{\Delta V}^T = T_0\left[\overline{Cp_V}\ln\left(\frac{T}{T_0}\right) + \overline{\Delta s_{\Delta V.0}}\right] \quad \text{2-37}$$

Exergy Terms

Thermo-mechanical Exergy Terms

$$ex^{TM} = h^{TM} - T_0 s^{TM} \quad \text{2-38}$$

$$ex_T^{TM} = \sum_i x_i(h_i^T - T_0 s_i^T) \quad \text{2-39}$$

$$ex_{P_G}^{TM} = \bar{R}T_0 \ln\left(\frac{P}{P_0}\right) \quad \text{2-40}$$

$$ex_{P_{S\&L}}^{TM} = T_0\overline{v_{Ave}}(P - P_0) \quad \text{2-41}$$

Chemical Potential and Diffusion Exergy Terms

$$ex_G^{diff} = \bar{R}T_0 \sum_i x_{i0} \ln\left(\frac{p_{i0}}{p_{i00}}\right) \quad \text{2-42}$$

$$ex_{S\&L}^{diff} = T_0 \sum_i x_{i0}\overline{v_{i0}} \ln\left(\frac{x_{i0}}{x_{i00}}\right) \quad \text{2-43}$$

$$ex_{S\&L.G}^{diff} = \bar{R}T_0 \sum_i x_{i0}\overline{v_{i0}} \ln\left(\frac{p_{i0}}{p_{i00.Sat}}\right) \quad \text{2-44}$$

$$ex^{CH} = \sum_i x_i ex_i^{CH} \quad \text{2-45}$$

where:

$$ex_i^{CH} = \beta_i \times LHV_i \quad \text{2-46}$$

$$\beta_i = 1.047 + 0.0154\frac{H}{C} + 0.0562\frac{O}{C} + 0.5904\frac{N}{C}\left(1 - 0.175\frac{H}{C}\right) \quad \text{[99]}$$

in $\%wt$

2.6.8Assumptions

- Air has been assumed to be an ideal gas for all calculations.
- Water properties have been taken from steam tables at the calculated partial pressures, assuming ideal interactions with dry air.
- Heat loss within the system has been ignored for all calculations, but has been discussed conceptually.
- The modelled system is a short-form spray dryer with a solution flow of 2.5 $kg.s^{-1}$ (50% solids content), with a feed of 21 $kg.s^{-1}$ moist air flow at 190^{O}C.
- Feed gas temperatures and flows were changed to test optimisation potentials.
- The SMP (Skim Milk Powder) Water mixture has been assumed to be an ideal mixture while being limited by the moisture isotherm typical of SMP at lower moisture contents [1, 12].
- The dryer outlet has been assumed to have a temperature difference between the gas and solid phases of 20^{O}C to allow for equilibrium not being reached in the dryer [1, 13].
- The air feed to the dryer has been assumed to be at standard conditions, which are shown in Table 2-3.
- For chemical calculation purposes, SMP has been assumed to have an average molecular weight of 342.3 $kg.mol^{-1}$ and a chemical formula of ($C_{12.66}H_{23.66}O_{8.82}N_{1.69}S_{0.05}$). This value was calculated based on a proximate analysis of 8.5% whey, 41.5% casein, and 50% lactose (dry ash free weight basis) [100-104].

While the assumptions for the isotherm being the limiting point for solid moisture and the temperature offset at the outlet may seem contradictory, the two have interactions through most of the drying curve. The isotherm is based on the solids temperature, while the gas temperature is based purely on the mass and energy balance. For the initial part of the dryer, the drying is purely related to surface moisture evaporation, which is unhindered by the solid.

However, once the surface moisture is removed, the isotherm interacts with the system as a measure of “resistance” to evaporation and is linked heavily with gas-side partial pressure and the solids moisture content. Employing a temperature offset to the gas side and bringing the system to thermal equilibrium (with the offset in place) is a reasonable way of estimating system inefficiency. Since the isotherm is the limiting moisture content (minimum for a given temperature) of the solids, the mass balance can be based off that, and as long as there is enough energy in the gas side of the dryer to evaporate that amount of water, the temperature can be estimated.

The Mass and Energy balance is iterative with the gas and solids temperature converging (with the offset) to a single point of convergence. The only time when the isotherm is not limiting in the method, when the gas inlet temperature is too low to complete the required evaporation to reach the isotherm for the given outlet conditions. This approach is covered in more detail later in this chapter in the discussion of the two-step calculation method.

2.6.9Overview of Exergy

Exergy is the sum of the physical and chemical exergy, and generally the chemical exergy is orders of magnitude larger than the physical exergy, particularly for low temperature processes with organic materials or fuel, as they are equivalent to the HHV [99, 105, 106]. For this reason, segregating the two components of the exergy calculation may allow more meaningful analysis to be carried out.

In terms of chemical exergy, cases exist where components exist in multiple phases, for example both the gas and the condensed, or S&L (Solids and Liquids) phase. The calculation for that component is slightly different, in that it accounts for the interaction with the gas phase (typically replacing x_0/x_{00} with $p_0/p_{SAT.0}$) while referring to the condensed component fraction as shown in Equations 2-41 and 2-42. The most common example of this situation is water, as it is part of the environment in both gaseous and liquid states. This situation means that humidity is taken into account when dealing with the condensed phase, so when evaporation takes place within the dryer, the diffusion potential changes significantly for both phases, not just the gas phase. This calculation is completed by using Equation 2-43.

The diffusion potential is typically ignored in exergy calculations due to the magnitude being much smaller than the reaction potential. In the case of transiting exergy, this part of the calculation becomes more important.

Equations 2-30 and 2-35 are typical of the literature, i.e. they represent calculations for constant heat capacity values. Since a system with phase changes is being studied in this thesis, a more appropriate calculation method has been given in Equations 2-31 and 2-36. A combination of the two methods has been used, since many components do not have a significant change in heat capacity over the calculation range. Air and the SMP have been assumed to have a constant heat capacity, while the heat capacity of water has been sourced from steam tables.

The generic equation for exergy, which is valid for all conditions, has been shown in Equation 2-10. This definition has been applied to all conditions, and as the components of exergy (enthalpy, entropy and chemical potential) are state variables, exergy is inherently a state variable. This situation means the path for the calculation does not matter.

2.7Exergy Analysis and Other Assessment Tools

There have been several proposed options to combine both work and thermal energy into one method, most of which are based on exergy or the Gibbs free energy methods. There are also several approaches and attempts to combine the PA and ExA, with varying degrees of success [23, 39, 54, 107].

Exergy analysis and variations thereof are beneficial to systems where pressure drops and other work-related information are known. However, this does not take into account the differences between the quality of different energy sources, and ignores the environmental impacts of the process, which is where extended exergy analysis and emergy analysis are appropriate [55, 56, 108].

Extended exergy and emergy are biosphere energy assessment tools that need a substantial amount of data, and use many assumptions, to determine the overall environmental ‘energy loading’. The difference between extended exergy analysis and ordinary exergy analysis is the scope of the process. Standard exergy analysis studies the immediate process, including the on-site utilities production, and extended exergy analysis examines the exergy

cost associated with how the offsite utilities and services are created. Emergy analysis uses tabulated data for base energy sources, such as coal, natural gas and even wind and rain energy. With a common set of units, in this case solar equivalent Joules (se-J), from these base energy sources, each conversion process can be given a conversion factor and all energy sources can be compared on a common basis. This approach in effect gives an overall system energy usage [55].

Other methods like Life Cycle Assessments (LCA) have a basis in different environmental impact loads. With each of these methodologies - from IT, to PA, ExA, Emergy, LCA etc., more information is required to complete each analysis. This trend is a good indication that each of these methods should be applied at different stages of the process, making modifications to the overall design at each stage [56]. Optimising at each of the stages should reduce the effects of the change at each later stage.

For example, IT requires kinetic information for unit operations, PA requires heat exchange thermal requirements, ExA requires the addition of pressure, chemical composition, and electrical requirements for a basic analysis. Emergy requires solar profiles, environmental variables, physical profiles and building material assessments, while LCA requires specific details regarding potential pollutants, not just CO_2. Any of these methods can be used at the start, but typically LCA, IT and PA are suitable for preliminary stages with ExA and Emergy more suited for mid to post design stages, respectively.

It must also be noted that, since some of these later steps can only occur when the process is finalised, they become more of an auditing tool, rather than design tools, like PA and ExA.

2.8Emergy, Extended-ExA and LCA

These methods are focused on auditing and have not been used so much in optimisation, so they have not been used so much in this chapter.

The difference in auditing and design in this context means that IT, PA and ExA can influence the design and construction of a project, making it potentially optimised from the start. Auditing tools, such as Emergy, LCA and Extended-ExA lead to retro-fitting options, or benchmarking, and as such any recommendation given by those tools tend not to be implemented due to a higher cost, both in downtime and capital. In the manner of

optimisation, it is important to make gains as early as feasibly possible in a design process. While optimisation is key in the design phase, retrofitting can lead to significant improvements, particularly in lean times of profit and increased energy costs.

2.9Two-step calculation for drying

Before any short-cut mass and energy balances can be made, it is worth looking at the long form of the mass and energy balances (sample calculations for the dryer outlet may be seen in Chapter 3).

2.9.1Mass Balance

A mass balance in theory is quite simple, material in equals material out, this is shown in 2-47. But this is not enough, because rarely is a system containing a single material, so to complement this a component balance, or an atom balance (Equation 2-48) may be paired with 2-47 to give more detail.

$$\sum m_{IN} = \sum m_{OUT} \tag{2-47}$$

$$\sum_i n_{i.IN} = \sum n_{i.OUT} \tag{2-48}$$

Where:

i refers to individual components or atoms (in the case of reactions)

2.9.2Energy Balance

Along the same lines as the mass balance, the energy balance refers to the first law of thermodynamics in that “Energy cannot be created or destroyed”. As part of that it can be equated in the same manner as the mass balance as shown in equation 2-49. It is important to note that in most cases both Q_{IN} and Q_{OUT} can be measured, Q_{Loss} is generally only estimated or derived as it is harder to measure directly.

$$\sum Q_{IN} = \sum Q_{OUT} + \sum Q_{Loss} \tag{2-49}$$

Where:

Q is the energy, which may come in many forms

Q_{Loss} is the loss to the environment

While in many cases this is over simplified, on a simple energy basis the energy is linked to the mass balance in that mass is a component of energy, for parts of the system which contain no reactions, energy is simplified to that shown in equation 2-50

$$\Delta Q = mCp\Delta T$$

Where:

ΔQ is the change in energy

m is mass

Cp is the heat capacity at constant pressure

ΔT is the change in temperature

2-50

Phase change energy is defined per material and is independent of the other materials, only relying on pressure and temperature, the basic change equation is shown in 2-51.

$$\Delta Q = m_{\Delta V}\lambda$$

Where:

ΔQ is the energy change

$m_{\Delta V}$ is mass of phase change

λ is the heat of change per mass

2-51

Given these equations, all non-reactive systems may be solved to balance both mass and energy.

2.9.3Dryer Simplification

If it is assumed that the solids side of the dryer has a small change in energy and exergy compared with the gas side of the dryer, the analysis or mass and energy balance may be simplified significantly as shown in Equation 2-52.

$$\dot{m_G} Cp_G \left(T_{G_{IN}} - T_{G_{OUT}}\right) = \dot{m_{\Delta V}} \lambda_{G_{OUT}} \quad \text{2-52}$$

Where Equation 2-52 applies, the energy associated with reducing the feed gas to the temperature of the outlet is used for evaporating the moisture of the solids at the outlet gas temperature. This method is useful for determining evaporation efficiency.

Another key result of splitting the calculation into two parts and isolating the solids and gas phases for the calculation is that the change in energy and exergy on the solids side of the dryer is insignificant compared with the change associated with the gas side using a two-step method (heat and mass transfer separated).

The assumption can be illustrated in Figure 2-3. The bulk of the exergy change is due to the large temperature change, which means the simplified dryer assumptions are reasonable on the gas side.

On the solids side (light grey lines in Figure 2-3), enthalpy and exergy are very similar and small, and the sensible heat effect is small and insignificant in comparison. These calculations demonstrate that the assumption of treating the dryer as a water evaporator is a good estimate in exergy terms, since the deviation from the overall exergy profile is small. Mass transfer and evaporation affect the enthalpy significantly, but has little effect on the exergy change.

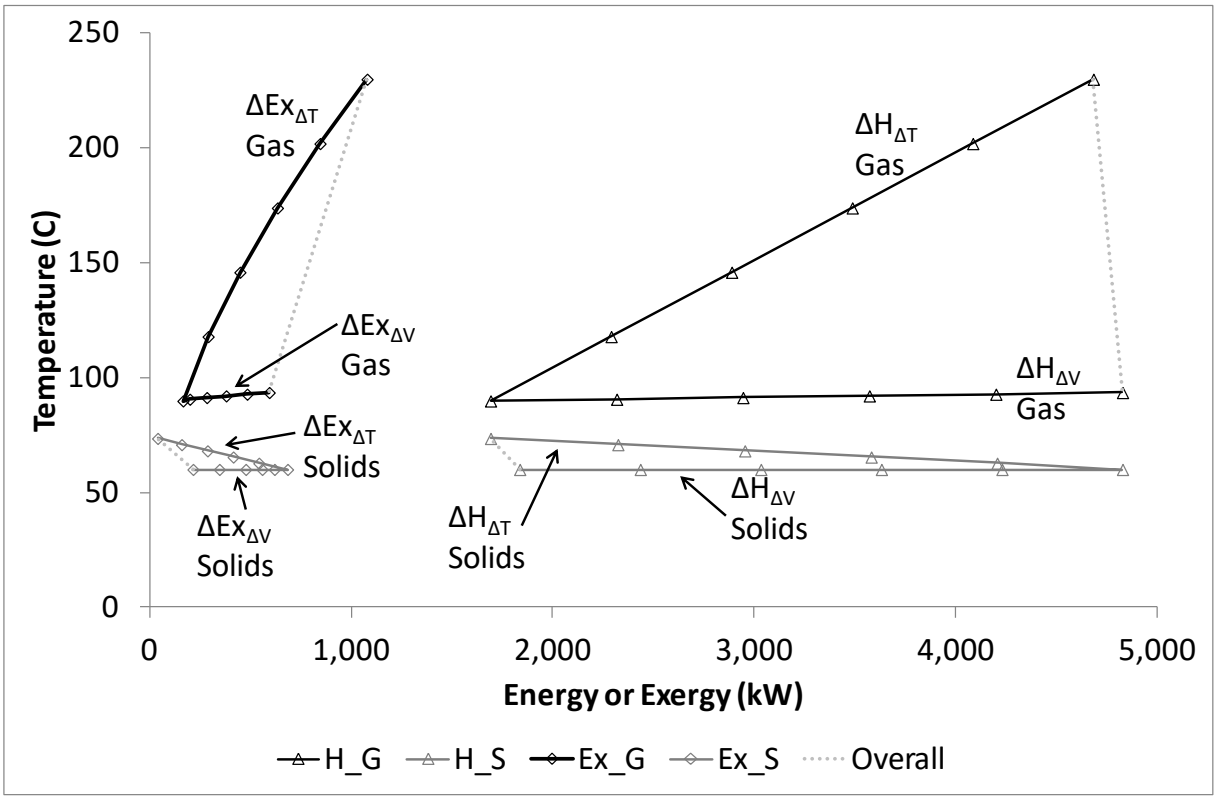

Figure 2-3: The effect of feed temperature on maximum efficiency (note that the H_S line is shifted to the right by 1,200 kW for ease of reading).

Figure 2-3 is an example of the enthalpy and exergy plots (in-out analysis) for the system, with an inlet temperature of 230^{O}C. The change in energy and exergy on the solids side is insignificant compared with the change associated with that of gas using a two-step method (heat and mass transfer separated).

The overall energy change may be the same, but the change of exergy associated with evaporation is small (nearly zero) and the effect of temperature on energy and exergy values is more important in this instance. The assumption that the exergy change is associated with the gas phase is valid for this system as the temperatures are quite low. However, at much higher temperatures this might not be true. Dryers typically operate below 300^{O}C, and for that range the change in exergy associated with the solids phase is insignificant (provided the outlet solids temperature remains below the boiling point of water).

Chapter 3 An Introduction to the Calculation of Energy and Exergy Efficiency

This chapter aims to introduce the calculations, methodologies and assumptions which will be used for the rest of the thesis, along with this will be a derivation of exergy from first principles and several sample calculations.

3.1Nomenclature

Within this work, there are several methods being studied. The following nomenclature has been adapted from several sources to be consistent in this work.

Table 3-1: The main nomenclature and symbols used within this work.

Symbol	Description	Symbol	Description
m	mass (kg) (or $\dot{m}$ flowrate (kg.s^{-1}))	T	Temperature (K)
n	moles (kmol) (or $\dot{n}$ flowrate (kmol.s^{-1}))	V	Velocity (m.s^{-1})
h	Specific enthalpy (kJ.mol^{-1})	H	Enthalpy (kJ)
e	Specific exergy (kJ.mol^{-1})	Ex	Exergy (kJ)
u	Specific internal energy (kJ.mol^{-1})	E_i, A_i, F_i	Radiation energy co-efficients
s	Specific entropy (kJ.mol^{-1}.K^{-1})	S	Entropy (kJ)
v	Specific volume (m^3.kg^{-1}, or m^3.kmol^{-1})	Q	Energy (kJ)
x	Component fraction	F	Flow
g	Gravity constant (9.81 N.kg^{-1} on earth)	LHV	Lower Heating Value (kW.kg^{-1})
z	Height (m)	HHV	Higher heating value (kW.kg^{-1})
y	**Humidity (g_W.kg_{DA}^{-1}) unless stated otherwise**	$ASIT$	Adiabatic Saturation Inversion Temperature
mm	Molecular mass (kg.kmol^{-1})	$SMER$	Specific Moisture Extraction Ratio
p	Partial Pressure (Pa, kg.m^{-1}.s^{-2})	P	Pressure (Pa, kg.m^{-1}.s^{-2})
Cp	Heat Capacity at constant pressure (kJ.kg^{-1}.K^{-1})	$\overline{Cp}$	Average Heat Capacity at constant pressure (kJ.kg^{-1}.K^{-1})
R	Specific gas constant (when paired with subscript)	$\bar{R}$	Ideal Gas Constant (J.K^{-1}.mol^{-1})
	Loss rate per cost ratio (in Eq. 2-5)		
EUR	Energy Utilisation Ratio	$ExUR$	Exergy Utilisation Ratio
L	Loss	K	Cost of equipment
IP	Improvement Potential	PI	Process Irreversibility
MC	Moisture Content (a combination of Y and X)	PFD	Process Flow Diagram
X	Solids moisture ratio (g_W.kg_S^{-1})	INE	Inevitable loss (minimum for task)
S_W	Specific exergy saving	AVO	Avoidable loss (the remaining loss)
Δ	Change	$\|\#\|$	Absolute value
β	A ratio of evaporation energy used in the ASIT calculation	Ω	A Quality factor based on the ratio of exergy and energy
	A estimated conversion factor for LHV to chemical exergy		
γ	mole fraction	θ	Gas to solids flow ratio
μ	Chemical potential energy (kJ.kmol^{-1})	S_W	Specific exergy saving
η	Efficiency	Ψ	Superheat number
λ	is the heat of change per mass (also $\Delta h_{\Delta V}$)		

Table 3-2: The subscripts, sub-subscripts and superscripts used within this work.*

Symbol	Description	Symbol	Description
Sat	Saturation (generally part of Temperature	DA	Dry Air part
IN	Into the unit/or system	V	Vapour Water part
OUT	Out of the unit/or system	L	Liquid water part
DP	Dew Point (Temperature)	W	Water
WB	Wet Bulb (Temperature)	S	Dry Solids part
1	State 1 (T,P)	ST	Steam
2	State 2 (T_0,P)	ΔV	Change in vapour (evaporation)
0	Reference state (T_0,P_0)	i	Each individual component raw state
00	Dead state (T_0,P_0,μ_0)	j	Each individual component product
T	Thermal (ΔT) basis	Q	Energy basis
P	Mechanical (ΔP) basis	Ex	Exergy basis
TM	Thermo-mechanical (ΔT, ΔP) basis	K	Cost
CH	Chemical Potential Basis	min	Minimum
G	Gas Basis	max	Maximum
$S\&L$	Solid and Liquid or condensed phase	ID	Ideal
$Loss$	Loss portion (has several definitions)	$inert$	The part that does not change
$Task$	Based on the task of the unit/system	$Carnot$	Carnot Factor
$Trans$	Transiting factor	$Transfer$	Part that is transferred
INE	Inevitable loss (minimum for task)	SP	Sticky Point
AVO	Avoidable loss (the remaining loss)	Hot	Hot side
Gen	Generated	$Cold$	Cold side
$Prod$	Product Basis	Cap	Capital cost basis
ave	Average	Rec	Recovery Potential
Mix	Mixing	$simple$	Simple (not complicated)
rxn	Reaction	$fuel$	Fuel

***NOTE 3-1: Each subscript may be used as a sub-subscript.**

3.2Grouping of Factors

There are many different efficiency factors that may be used to describe a system. Each has advantages and disadvantages when applied to either a drying unit or a larger system. To clarify, a larger system will typically include heating and cooling in order to support the dryer unit or may refer to a much larger scope when dealing with a dryer unit integrated into a larger processing plant. This section discusses the merits of each factor.

Firstly, it is useful to divide the factors into groups. There are two ways of doing this. One is to assess the information level (or complexity) of each factor, as shown in Table 3-3.

Table 3-3: The information levels for different exergy factors.

Level	Brief of level	Examples	Eq. Refs
0	Does not use thermodynamics (parametric level)	$\frac{m_{\Delta V}}{m_{G_{IN}}}$	Eq. 2-19
1	Does not use exergy (first law/mass-energy balance)	$\eta_{\Delta V.Q_{IN}}$ $\dot{m_{\Delta V}}_{ID.Q}$ $1-\frac{INE}{H_{IN}}$	Eq. 2-20 Eq. 2-17 Eq. 2-28
2	Simplistic factors based on raw results, some are case specific, described in Table 3-4.	$\eta_{ex}=1-\frac{ex_{Loss}}{ex_{IN}}$	Eqs. 2-39 to 2-41, 2-27, 2-25

		$\eta_{ex} = \frac{ex_{\Delta V}}{ex_{G_{IN}}}$ $\eta_{ex} = \frac{ex_{OUT}}{ex_{IN}}$ $\eta_{max} = 1 - \frac{INE}{Ex_{IN}}$	
3	Factors which assess the specific task (more detailed). These are typically based on factors shown in level 1 and 2 (above).	η_{ex}^{Trans} η_{Task}	Eq. 2-14 Eq. 2-9
4	Factors which are not efficiency but are used to interpret results based on levels 2 and 3 (above).	IP	Eq. 2-4

The second way is to group the factors on a calculation basis. For example, some of the factors focus on entire systems, or a set task, or neglect a part of the system, whether it be gas flow, solids flow, or evaporated moisture. For the system being studied, the key factor is the energy used to achieve the task of evaporation. A summary of several factor types is presented in Table 3-4.

Table 3-4: A summary of the features of different efficiency factors found in the exergy literature.

Factors		Use/Features
Overall (O)	[23, 31, 33, 35, 85, 94, 96, 109, 110]	Good to determine exergy use items. Not good for finding ineffective units.
Gas Side (G)	[27, 35]	Good when most of the systems energy is found on the gas side of the system. Not appropriate where condensed phase chemical exergy is significant.
Evaporation (V)	[26, 28, 33-35, 76, 94, 96, 111]	Exergy per evaporated moisture, good for dryer/evaporator. Poor for utilities and system wide analysis.
Solid Side (S)	[70]	Suitable for dryers and evaporators, essentially a solids throughput comparison. Only suitable for systems with multi-phase systems.
Other Factors (F)	[79, 89, 112, 113]	These are generic, and have either no basis for comparison, can be used on streams, or change specifically with each unit type.
-Process Irreversibility (PI)	[91]	This is the entropy generated in each unit. Limited in an optimisation approach.
-Quality Factor (Ω)	[114]	Quality of the system, exergy/energy. Can be used on streams (abs), or units (change). May give negative or inflated qualities for systems with high chemical exergies.
-Task Efficiency (IP)	[30-32]	Based on the ideal exergy use for a task. Defining the task exergy may not be straightforward in some cases.
-Exergy Cost Factor (K)	[29]	This is a late stage factor that includes a cost analysis and is used as a comparison between systems on a cost and exergy basis.

An important aspect when discussing the efficiency is the purpose of the dryer. The exergy cost and associated factors consider the best exergy efficiency possible for a particular item

(more specifically, the dryer). The exergy cost factor (K) [29] has the potential to give a good basis for optimising such an exergetic perspective.

The factors that are used in this work are shown in Equations 2-6 to 2-10. Equations 2-6 to 2-10, and 2-14 to 2-15 show factors that are used extensively in the literature. The key is to understand which factors are suitable for use in each application. For example, Equation 2-7 is only suitable in applications where evaporation occurs, such as dryers and evaporators. The improvement potential (IP; shown in Equation 2-4) is a factor derived from the unit efficiency and is an indication of how much exergy is being wasted compared with an ideal but not necessarily realistic set of unit operations.

This method allows for different types of unit operations to be grouped into one factor while maintaining a useful metric for the entire system. For example, the dryer uses a different efficiency factor to a heat exchanger. The dryer (D-1) may use Equation 2-7 while a heat exchanger uses Equations 2-8 or 2-14 to describe the efficiencies. Equation 2-8 is the simple efficiency commonly used, while Equation 2-14 is the transiting exergy. Overall efficiencies or an overall factor–such as the IP–are useful in monitoring changes in the optimisation of specific units by accounting for the effects on other units. Equation 2-6 provides an indication of how a real unit operation has an inherent efficiency.

Exergy loss may be defined in several ways. The most common method is in the second bracket of Equation 2-6 (ex_{IN}-ex_{OUT}). Others, such as the task efficiency (Equation 2-9) take into account how much of the loss is associated with the process and how much is lost to the environment (typically through heat loss).

The Ω factor represents the quality (or quality change) and is useful as a metric to simplify systems. This factor works as a targeting metric – similar to the ones used in PA. The main issue occurs when units such as expanders are used to convert work potential to work. This situation typically gives a value that is greater than unity for Ω. The value of Ω then requires manipulation to fit within the range of (0-1) required for a graphical representation using Ω vs H. Since Ω is a quality factor that can be used to describe unit operations and streams, it has the potential to simplify the interpretation of exergy analysis optimisation algorithms [114].

3.3Efficiency Factors

3.3.1Overall Energy Efficiencies

Simple Energy Efficiency

The simple energy efficiency calculation is determined by the energy transferred and the energy lost to the surroundings, as shown in Equation 3-1.

$$\eta_{Q1} = \frac{h_{IN} - Q_{Loss}}{h_{IN}} = \frac{h_{OUT}}{h_{IN}} \quad 3\text{-}1$$

This equation represents the energy loss as a fraction of what is fed into the process and can be applied to a unit or process equally effectively. Applying this method using plant data is equivalent to taking the heat losses to the surroundings into account.

If working with real plants, it is important to approach each item from its ideal perspective and to then determine the deviation from this — represented by Q_{Loss}. This procedure will help in understanding what part of the process requires process changes or insulation.

Energy Utilisation Ratio

The energy utilisation ratio (EUR) represents the energy used compared against the total energy entering the process. The relationship with Equation 3-1 is shown in Equation 3-2.

$$EUR = \frac{h_{IN} - h_{OUT}}{h_{IN}} \quad 3\text{-}2$$

3.3.2Gas Side Energy Efficiency

This parameter was created for this work as a comparative measure related to the unit exergy efficiency, as presented by Ceylan [35].

Unit Energy Efficiency

The unit energy efficiency is shown in Equation 3-3.

$$\eta_{Q_G} = \frac{h_{G_{OUT}}}{h_{G_{IN}}} \quad 3\text{-}3$$

3.3.3Evaporation Energy Efficiencies

These efficiencies are commonly used to compare the energy use of dryers, evaporators, and other mass transfer units, based on the energy entering the process. Unlike the other energy efficiencies, these factors are application specific.

Evaporation Energy Ratio

$$\eta_{Q_{\Delta V}} = \frac{h_{G_{IN}} - h_{G_{OUT}}}{\dot{m_{\Delta V}}} \quad 3\text{-}4$$

This factor, Equation 3-4, is simple because it represents the change in specific enthalpy of the gas stream compared with the amount of water evaporated, which means that it is independent of gas flow rate, but strongly dependent on the evaporation rate.

Specific Moisture Extraction Rate (SMER)

SMER represents the amount of moisture removed per energy input, shown in Equation 3-5.

$$SMER = \frac{\dot{m_{\Delta V}}}{\sum Q_{IN}} \quad 3\text{-}5$$

This factor has been used to compare the energy use of different dryers per unit of evaporated water [115].

3.3.4Solid Side Energy Efficiency

This factor was created for this work as a comparison measure with the exergy cost factor, as presented by Sieniutycz [70]. The unit of comparison for exergy is the dry solids flow.

Solids Energy Efficiency

The solids energy efficiency is shown in Equation 3-6.

$$\eta_{Q_S} = \frac{h_{G_{IN}} - h_{G_{OUT}}}{\dot{m_{S_{IN}}}} \quad 3\text{-}6$$

This factor can be useful in comparing the energy associated with producing a unit of solids. This means that despite it not being popular, it does incorporate a useful unit (energy per flow of solids) to compare different operating conditions. This factor is capable of comparing dryers of different capacities in a useful way.

3.3.5Overall Exergy Efficiencies

These efficiencies are able to be used as simple exergy efficiency measures. Unlike the overall energy efficiency calculations presented above, exergy is consumed in a process, and as such, ideal systems do not have the same exergy input as that at the outlet. These factors may be applied to individual systems and overall systems alike.

Simple Exergy Efficiency

$$\eta_{Ex1} = \frac{ex_{OUT}}{ex_{IN}} \quad 3\text{-}7$$

Equation 3-7 is very simple and determines how much exergy has been used in each unit operation or for an entire process. Equation 3-1 is the energy equivalent.

Exergy Utilisation Ratio

The energy utilisation ratio is the change of exergy to the exergy input. This is called a utilisation ratio because it represents the exergy use within the system. This ratio has the same treatment as the energy utilisation ratio (Equation 3-2), as shown in Equation 3-8.

$$ExUR = \frac{ex_{IN} - ex_{OUT}}{ex_{IN}} = 1 - \eta_{Ex1} \quad 3\text{-}8$$

3.3.6Gas Side Exergy Efficiency

If it is determined or assumed that the non-gaseous phases of a system have a negligible effect on the overall exergy calculation [35], then it is appropriate to apply exergy efficiency calculations to the gas-phase parts of the system alone.

Unit Exergy Efficiency

This factor, Equation 3-9, suggests that the liquids and solids phases in drying processes do not undergo significant exergy change, so it is suitable to determine the gas phase exergy-use ratio [35]. In order to compare this ratio with the equivalent energy efficiency, the ratio uses the gas side energy as the basis for comparison (Equation 3-3).

$$\eta_{Ex_G} = \frac{ex_{G_{OUT}}}{ex_{G_{IN}}} \quad 3\text{-}9$$

3.3.7Evaporation Exergy Efficiencies

These efficiencies are commonly used to compare the exergy use of dryers, evaporators, and other mass transfer units, based on the exergy input to the system. Unlike the other exergy efficiencies, these factors are specific to the task of evaporation.

Evaporation Exergy Ratio

$$\eta_{Ex_{\Delta V}} = \frac{ex_{IN} - ex_{OUT}}{\dot{m_{\Delta V}}} \quad 3\text{-}10$$

This factor (Equation 3-10) is equivalent to Equation 3-4; it provides a factor that can be used to compare process changes with the evaporation exergy use. Ultimately, this factor is limited in its usefulness in process optimisation since it is limited to the dryer.

Exergetic Moisture Extraction Rate (EMER)

EMER represents the amount of moisture removed per unit exergy input, as shown in Equation 3-11.

$$EMER = \frac{\dot{m_{\Delta V}}}{\sum E_{IN}} \quad 3\text{-}11$$

This factor has been used to compare the exergy use of different dryers per unit of evaporation [115], and can be compared with Equation 3-5.

Drying Exergetic Efficiency

This efficiency ratio, Equation 3-12, compares the amount of exergy used in the evaporation within a dryer with the exergy provided by the drying gas at the inlet [76].

$$\eta_{Ex_{Drying}} = \frac{\Delta E_{\Delta V}}{E_{G_{IN}}} = \frac{\dot{m_{\Delta V}}\left(e_{L_{OUT}} - e_{L_{IN}}\right)}{\dot{m_{G_{IN}}} e_{G_{IN}}} \quad 3\text{-}12$$

This factor is specific to drying and evaporation systems and can be used as a comparison ratio of different dryer types because it uses a common factor to compare dryer types, called a functional unit. This factor is different to the form of Equations 3-4 and 3-5 and should not be used in conjunction with it.

3.3.8Solid Side Exergy Efficiency

In drying processes, it is important to note that the dry solid is the product of the process, and there is a need to associate the exergy cost with creating that product. There are two

ways of doing this: by comparing dryers based on their solids capacity or on their evaporation capacity. The evaporation efficiencies are more popular because the focus is related to the evaporation, which is the main purpose of the dryer. However, the solids factor was proposed by Sieniutycz [70] and will be discussed here.

Exergy Cost and Associated Factors

This method of comparison assesses how much exergy is used in producing the solid product [70]. Equation 3-13 shows what the factor represents.

$$K_{Ex} = \frac{\Delta ex}{\dot{m_{S_{IN}}}} = \frac{ex_{IN} - ex_{OUT}}{\dot{m_{S_{IN}}}} \quad 3\text{-}13$$

There are several equations that need to be coupled with this, as shown by Equations 3-14, 3-15, and 3-16:

$$\theta = \frac{\dot{m_{DA_{IN}}}}{\dot{m_{S_{IN}}}} \quad 3\text{-}14$$

$$ex_{IN} = \theta ex_{Gas_{IN}} + ex_{S_{IN}} \quad 3\text{-}15$$

$$ex_{OUT} = \theta ex_{Gas_{OUT}} + ex_{S_{OUT}} \quad 3\text{-}16$$

These equations can be combined in different ways to give different factors:

K (Equation 3-17), η_K (Equation 3-18), and S_W (Equation 3-19) as shown here:

$$K = K_{Ex} + K_{Cap} = \frac{ex_{IN} - ex_{OUT}}{\dot{m_{S_{IN}}}} + \theta\lambda \quad 3\text{-}17$$

λ represents the ratio of change of capital cost for a change in the gas-to-solids flow ratio (θ). This factor is useful when comparing the effect of changing a piece of equipment to handle improved exergy efficiency and could be used as a justification to either change or not change a process.

The solids exergy efficiency (η_K) can now be defined as:

$$\eta_K = 1 - \frac{ex_{IN} - ex_{OUT}}{ex_{IN}} \quad 3\text{-}18$$

The next factor that can be found is the specific exergy saving (or cost).

$$S_W = \frac{\Delta[ex_{IN}(1-\eta_K)]}{X_{IN} - X_{OUT}} \quad \text{3-19}$$

Where the delta refers to a deviation from the optimum, or current point if used as a starting point, and iteration occurs until the optimum solution is found.

Also, X_{IN} and X_{OUT} refer to the solids moisture ratio at the feed and outlet of the dryer, respectively.

3.3.9Process Irreversibility

This factor (Equation 3-20) studies how much entropy is generated in a system. It presents a way of finding changes within the system to reduce the amount of entropy generation, or to reduce the irreversibility of a system [91].

$$PI = \sum_{IN} Ex_i - \sum_{OUT} Ex_i = T_0\left(\sum_{OUT} S_i - \sum_{IN} S_i\right) = T_0 \Delta S_{Gen} \quad \text{3-20}$$

This calculation, however, is not particularly helpful; this is because it can only indicate improvement, but not how improved the system is. It does not indicate whether the entropy is generated as a requirement of the process. As a result, optimisation using the process irreversibility method is not realistic due to the trial and error approach that occurs with it. The next two methods that use some of the above factors are useful in describing the limitations of exergy efficiency and the deviation of the current process from that upper limit.

3.3.10Energy Level or Quality Factor

This comparison method assesses the ratio of exergy to enthalpy for a single point or item in a larger system to determine its quality [39, 114]. This quality factor (Equation 3-21) may be used to replace the temperature axis on pinch plots to allow exergy quality to be plotted against the cumulative energy flows of a system [39, 114].

$$\Omega = \frac{Ex}{H} \; OR \; \frac{\Delta Ex}{\Delta H} \quad \text{3-21}$$

Equation 2-42 can be combined with the idea of Inevitable (*INE*) and Avoidable (*AVO*) exergy losses to produce an effective way of identifying process exergy inefficiencies [39, 98]. The *INE* and *AVO* exergy losses can be described by Equations 3-22 and 3-23 [39, 98].

$$Ex_{Loss} = Ex_{AVO} + Ex_{INE} \quad 3\text{-}22$$

$$Ex_{AVO} = Ex_{Prod} \frac{ExUR_{max}}{(1 - ExUR_{max})} \quad 3\text{-}23$$

These additional equations are applied as though there is a minimum driving force applied to each process to achieve the same goal. Equation 3-23 determines the inevitable exergy losses, and the remaining portion is the avoidable part of the exergy loss. These losses can include heat losses from equipment walls, process limitations that require flow or energy compensations to overcome, process technological limitations, and utility mismatching. The minimum driving force calculation can also assist in determining a more effective pinch offset temperature [98]. In this instance, the 20˚C ΔT_{min} assumption is used to be consistent with the assumptions used for the PA shown in Chapter 4.

3.3.11Task Efficiency

The task efficiency (Equation 3-24) is defined more generally than the exergy cost, and is commonly used in the literature [28, 31, 56] to describe how different something is from the exergetic optimum.

$$\eta_{Task} = \frac{Ex_{IN_{min}}}{Ex_{IN}} \quad 3\text{-}24$$

Equation 3-24 represents a deviation from an optimum, which has the same purpose as Equations 3-22 and 3-23, but in a more generic form.

This efficiency (Equation 3-24) is found in case studies, which find a best-case scenario, and as a result, the efficiency is less useful during the design stage, but is shown to be more useful for process modelling and the optimisation of existing processes.

3.4Summary of Formulae

The temperature-based thermo-mechanical exergy (of components, which have a constant Cp), is shown in Equation 3-25.

$$ex_T^{TM} = \sum_i \left[\overline{Cp_i}(T - T_0) - T_0 \overline{Cp_i} \ln\left(\frac{T}{T_0}\right) \right] \quad 3\text{-}25$$

The temperature-based thermo-mechanical exergy of that part of the system that undergoes phase change is shown as Equation 3-26.

$$ex_T^{TM} = \Delta V \left(\overline{Cp_V} \left[T - T_{DP} - T_0 \ln\left(\frac{T}{T_{DP}}\right) \right] + \overline{Cp_L} \left[T_{DP} - T_0 - T_0 \ln\left(\frac{T_{DP}}{T_0}\right) \right] + \Delta h_{\Delta V} - T_0 \Delta s_{\Delta V} \right) \quad 3\text{-}26$$

The pressure-based thermo-mechanical exergy for gas components is shown in Equation 3-27.

$$ex_{P_G}^{TM} = \bar{R} T_0 \ln\left(\frac{P}{P_0}\right) \quad 3\text{-}27$$

The pressure-based thermo-mechanical exergy for solid and liquid components is shown in Equation 3-28.

$$ex_{P_{S\&L}}^{TM} = \overline{v_{ave}}(P - P_0) \quad 3\text{-}28$$

The chemical-based exergy for mixing of gaseous components from one concentration to another, reversibly, is shown in Equation 3-29.

$$ex_{i_G}^{CH} = T_0 \bar{R} x_{i_{oo}} \ln\left(\frac{\gamma_{i_0}}{\gamma_{i_{oo}}}\right) \quad 3\text{-}29$$

The chemical-based exergy for mixing for solid and liquid components from one concentration to another, reversibly, is shown in Equation 3-30.

$$ex_{i_{S\&L}}^{CH} = T_0 \bar{R} x_{i_{oo}} \ln\left(\frac{P_{i_0}}{P_{i_{oo}}}\right) \quad 3\text{-}30$$

A summation of the different temperature-based thermo-mechanical component enthalpies gives:

$$h_{TM}^T = h_{DA_1} + h_{S_1} + h_{L_1} + h_{V_2} + h_{\Delta V}^T \quad 3\text{-}31$$

The summation of the different temperature-based thermo-mechanical component entropies gives:

$$T_0 s_{TM}^T = T_0 s_{DA_1} + T_0 s_{S_1} + T_0 s_{L_1} + T_0 s_{V_2} + T_0 s_{\Delta V}^T \quad 3\text{-}32$$

The relationship between Equations 3-31 and 3-32 in terms of exergy is shown in Equation 3-33:

$$ex_{TM}^T = h_{TM}^T - T_0 s_{TM}^T \quad 3\text{-}33$$

The summation of the different pressure-based thermo-mechanical component enthalpies gives:

$$h_{TM}^P = h_{DA_2} + h_{S_2} + h_{L_0} + h_{V_2} + h_{\Delta V}^P \quad 3\text{-}34$$

The summation of the different pressure-based thermo-mechanical component entropies gives:

$$T_0 s_{TM}^P = T_0 s_{DA_2} + T_0 s_{S_2} + T_0 s_{L_0} + T_0 s_{V_2} + T_0 s_{\Delta V}^P \quad 3\text{-}35$$

The relationship between Equations 3-34 and 3-35 in terms of exergy is shown in Equation 3-36:

$$ex_{TM}^P = h_{TM}^P - T_0 s_{TM}^P \quad 3\text{-}36$$

Given the enthalpy and entropy, the pressure-based exergy of the phase change component is given in Equation 3-37:

$$ex_{\Delta V}^P = h_{\Delta V}^P - T_0 s_{\Delta V}^P \quad 3\text{-}37$$

Summation of the different components exergies is given in Equation 3-38:

$$ex^{CH} = ex_{DA}^{CH} + ex_V^{CH} + ex_L^{CH} + ex_S^{CH} + ex_{\Delta V}^{CH} \quad 3\text{-}38$$

Given the enthalpy and entropy, the chemical-based exergy of the phase change component is shown in Equation 3-39:

$$ex_{\Delta V}^{CH} = h_{\Delta V}^{CH} - T_0 s_{\Delta V}^{CH} \quad 3\text{-}39$$

The overall summation of the different components of the enthalpy system is:

$$h = h_{TM}^T + h_{TM}^P + h_{\Delta V}^{CH} \quad 3\text{-}40$$

The overall summation of the different components of the exergy system is:

$$ex = ex_{TM}^{T} + ex_{TM}^{P} + ex_{\Delta V}^{CH} + ex^{CH} \quad 3\text{-}41$$

The quality factor equation is:

$$\Omega = \frac{ex}{h} \quad 3\text{-}42$$

The quality factor equation is a representation of the work potential of a system as a function of the enthalpy within that system [24, 40, 114, 116]. The part of the enthalpy that can be used to do work and the part of the enthalpy that has no work potential can be determined simply by using Equations 3-40 and 3-41. This determination is a useful way of describing the potential work in a system as a function of enthalpy, which is commonly used as the basis of most energy calculations for thermal systems.

Many exergy efficiency factors apply to operations and units, while this factor can be used at any point in a process independently and represents a combination of both pressure and temperature. This factor has been used for the exergy analysis visualisations to compare the results with those of pinch analysis.

3.5Derivation of exergy terms from first principles

When doing thermodynamic calculations, like an exergy analysis, it is the standard convention to work on a molar basis. There are no molar component changes within this system, so working on the mass basis is possible, but this is not always the case, and as such, the molar basis will be used.

The single-phase component terms should be multiplied by their molar fraction in order to get their partial effect on the system. The simple equality shown in Equation 3-43 indicates that the mole fractions of all components in the total system must add to unity.

$$1 = \sum_{i} x_i \quad 3\text{-}43$$

Since there is a phase change within the system, the constant Cp assumption will not work for that component, so each component should be considered separately. Taking the part of the phase change component that changes phase separately and combining the other components is a good idea, but for this example, the components will have their subscripts written as follows.

- The dry air (DA)
- The solids (S)
- The liquid (L), that stays liquid in both states
- The water vapour (V), that stays in the vapour phase in both states
- The phase change (ΔV), this is just the part of that component that changes phase within the calculation domain.

Recall the general exergy formula, Equation 3-44.

$$ex = (u - u_0) + P_0(v - v_0) - T_0(s - s_0) + \sum_{i=0}^{\infty}(\mu_i - \mu_0)x_i + g(z - z_0) + \frac{V^2}{2g} + E_i A_i F_i (3T^4 - T_0^4 - 4T_0 T^3) + \text{any other exergy terms} \quad 3\text{-}44$$

This equation can be simplified for this system by making the following assumptions [35]:

- The potential and kinetic energy terms are considered insignificant for this system
- The system contains no radiation exergy (it does not emit any significant energy through radiation, it is not hot enough or radioactive in any way)
- There are no other forms of work potential in or on the system not already accounted for in Equation 3-44
- Enthalpy contains internal energy and pressure volume work (Equation 3-45)

$$h = u + Pv \quad 3\text{-}45$$

Substituting Equation 3-45 and the other statements into Equation 3-44, this equation simplifies to the one under study, Equation 3-46.

$$ex = (h - h_0) - T_0(s - s_0) + \sum_{i=0}^{\infty}(\mu_{i_0} - \mu_{i_{00}})x_i \quad 3\text{-}46$$

Using (T, P) as the initial conditions, and (T_0, P_0) as the reference conditions, Equation 3-46 changes its notation to become Equation 3-47.

$$ex = [h(T,P) - h(T_0,P_0)] - T_0[s(T,P) - s(T_0,P_0)] + \sum_{i=0}^{\infty} \left(\mu_{i_0} - \mu_{i_{00}}\right)_{T_0,P_0} x_{i_0} \quad \text{3-47}$$

Since the different components of exergy are separated, they can be addressed one step at a time, to make it easier to follow.

Since exergy is a measure of the potential ideal work of a system, it is more convenient to change the temperature under constant pressure first, and then change the pressure isothermally at the reference temperature. This procedure makes sense since, in order to run isothermally, energy must be transferred between the process and the environment to keep the temperature constant. This situation means that the best path to take to determine the exergy is to determine the temperature-based exergy component, at constant pressure and composition, then the pressure-based exergy component at constant temperature and composition.

3.5.1Temperature based exergy

Therefore, initially the isobaric exergy change should be investigated, which is the exergy change associated with the temperature change ($T_0 \rightarrow T$) only. This exergy change is called the temperature-based thermo-mechanical component of exergy (e_{TM}^{T}), as categorised in Figure 2-2. This component is represented by Equation 3-48.

$$ex_{TM}^{T} = h(T,P) - h(T_0,P) - T_0[s(T,P) - s(T_0,P)] \quad \text{3-48}$$

So, consider the general definitions of both enthalpy, Equation 3-49, and entropy, Equation 3-50.

$$dH = mCpdT + \left[V - T\left(\frac{\partial V}{\partial T}\right)_P\right] dP \quad \text{3-49 [117] p183}$$

$$dS = \frac{mCpdT}{T} - \left(\frac{\partial V}{\partial T}\right)_P dP \quad \text{3-50 [117]}$$

It is reasonable that these parts can be separated into both temperature and pressure-based terms to solve this problem, since the temperature-based exergy is determined first, the term $dP = 0$. Equation 3-49 then simplifies to Equation 3-52, assuming a constant Cp value (phase change should be dealt with separately to constant Cp changes).

$$dH = mCpdT + \cancelto{0}{\left[V - T\left(\frac{\partial V}{\partial T}\right)_P\right] dP} \quad 3\text{-}51$$

$$H^T = m\int_{T_0}^{T} Cp\, dT = n\int_{T_0}^{T} \overline{Cp}\, dT$$

$$h^T = Cp(T - T_0) \quad 3\text{-}52$$

$Units\ of\ h$: $\frac{Q}{M.T}T = \frac{Q}{M}$

$Where$:

$Q\ = energy\ (Joules)$

$M = unit\ of\ comparison\ (mol, g, m^3, etc.)$

$T\ = temperature\ (K, ℃, R, °F)$

$Cp = specific\ heat\ capacity, dependent\ on\ the\ desired\ units$

Now it is necessary to solve the entropy component of Equation 3-48 to find the overall temperature based thermo-mechanical component of the exergy for the stream.

Now manipulate Equation 3-50, in the same way as Equation 3-49, i.e. the term that relates to the $dP = 0$. Equation 3-50 simplifies to be Equation 3-55, assuming a constant Cp value; again: the phase change component will be discussed separately.

$$dS = \frac{mCpdT}{T} - \cancelto{0}{\left(\frac{\partial V}{\partial T}\right)_P dP} \quad 3\text{-}53$$

$$S^T = \int_{T_0}^{T} \frac{mCpdT}{T} = \int_{T_0}^{T} \frac{n\overline{Cp}dT}{T} \quad 3\text{-}54$$

$$T_0 s^T = T_0 Cp \ln\left(\frac{T}{T_0}\right) \quad 3\text{-}55$$

$$Units\ of\ T_0 s: T\frac{Q}{M.T} = \frac{Q}{M}$$

These units are consistent with the units for specific enthalpy as above.

Therefore, by substituting Equations 3-52 and 3-55 into Equation 3-48, Equation 3-56 is obtained for systems with constant Cp, and the molar basis is to be used, so the Cp is in its molar form.

$$ex_{TM}^{T} = \overline{Cp}\,(T - T_0) - T_0\overline{Cp}\ln\left(\frac{T}{T_0}\right) \qquad 3\text{-}56$$

For systems that invoke a phase change (ΔV, this can be found via a simple mass balance), such as the system being studied, it is important to treat the system with special care. The saturation properties at the phase change interval are required, and the enthalpy and entropy should be calculated in three distinct stages.

First it is necessary to determine the properties of the vapour at the conditions for both temperatures, T and T_0. The required properties are listed in Table 3-5.

Table 3-5: The required information, to be calculated for the phase change component of the system.

Required Information	
γ_{V_1}	Mole fraction of vapour in the gas phase at point 1[NOTE 3-2]
γ_{V_2}	Mole fraction of vapour in the gas phase point 2[NOTE 3-2]
P_{V_1}	Partial Pressure of vapour at point 1
$P_{V_2}^{Sat}$	Saturation pressure of vapour at point 2
T_{DP}	Dew point temperature for partial pressure at point 1

NOTE 3-2: It is important to note here that γ_V is Gas phase specific and γ_L is S&L phase specific

The first part of the analysis is to determine the static properties, in other words, the properties that will not change with the composition of Point 2 (treating Point 1 as static) and are dependant only on temperature and pressure. These properties are calculated in Equations 3-59, 3-60 and 3-61. Equation 3-61 is also used as the initial guess for the sorption isotherm method.

Without the isotherm, the calculation method is:

1. γ_{V_1} using (eq. 3-57)
2. P_{V_1} using (eq. 3-58)

3. T_{DP} using (eq. 3-59)
4. $P_{V_2}^{Sat}$ using (eq. 3-60)
5. γ_{V_2} using (eq. 3-61)
6. Convert back to total moles of each component (eq. 3-62)

$$\gamma_V = \frac{n_V}{(n_V + n_{DA})} = \frac{x_V}{(x_V + x_{DA})} \quad 3\text{-}57$$

$$P_i = \gamma_i P \quad 3\text{-}58$$

$$T_{DP} = \frac{3816.44}{18.3036 - \ln\left(\frac{P_V}{133.3}\right)} + 44.12 \quad 3\text{-}59$$

$$P_{V_0}^{Sat} = 133.3 \times \exp\left(18.3036 - \frac{3816.44}{T_0 - 44.12}\right) \quad 3\text{-}60$$

$$\gamma_V^{Sat} = \frac{P_V^{Sat}}{P} \quad 3\text{-}61$$

$$n_V = \frac{\gamma_V n_{DA}}{(1 - \gamma_V)} \quad 3\text{-}62$$

The following equality represents a limit for T_{DP}. If it is too high, then Y is too high (the humidity is too high), and there is too little mass-transfer driving force for drying. The other limiting condition (lower limit) is in place for calculation modelling consistency. With iterative calculations, overshoots occur, and this statement is intended to limit an overshoot.

$$\begin{aligned} &\boldsymbol{IF}\ T_{DP} \geq\ T, T_{DP} = T \\ &\boldsymbol{IF}\ T_{DP} \leq\ T_0, T_{DP} = T_0 \end{aligned} \quad 3\text{-}63$$

For this example, T_0 is the dead state temperature, in this case 25^{O}C (298.15 K), T is the gas temperature at the outlet of the dryer and T_{DP} is within the temperature range as outlined by Equation 3-63, and condensation will occur as the stream cools from $T \rightarrow T_0$.

This method using steps 1 to 6 above represents a simplification, that is, the liquid water and the vapour in the air are in equilibrium, meaning that it is assumed that the solid is assumed to be non-hygroscopic, and as such does not interact with the system. This

situation is not the case with skim milk powder [92]. As a result, the sorption isotherm should be included.

During the sample calculation, both methods have been compared to determine if making the simplification is appropriate for an exergy analysis. The sorption isotherm has been used in the mass and energy balance calculation over the dryer. This isotherm was used to determine the outlet equilibrium solids moisture content.

The sorption isotherm used here applies to skim milk powder and is shown in Equation 3-64 [12, 14]. This equilibrium moisture content is expressed on a mass per mass basis, so it is necessary to convert it back to a molar basis for this analysis, shown as Equation 3-65.

$$\frac{\gamma_L}{\gamma_S} = 0.1499 \times \exp\left[-2.306 \times 10^{-3} \times T_0 \times \ln\left(\frac{P_V^{Sat}}{P_V}\right)\right] \frac{kg_L}{kg_S} \times \frac{342.29}{18.015} \frac{\frac{kg_S}{kmol_S}}{\frac{kg_L}{kmol_L}} \quad 3\text{-}64$$

$$\frac{\gamma_L}{\gamma_S} = 2.8481 \times \exp\left[-2.306 \times 10^{-3} \times T_0 \times \ln\left(\frac{P_V^{Sat}}{P_V}\right)\right] \frac{kmol_L}{kmol_S} \quad 3\text{-}65$$

To continue, the phase compositions must be studied. Equation 3-57 has the required form. The solids and liquids combined ($S\&L$) phase, needs to be accounted for, and this phase is represented by Equation 3-66.

$$\gamma_L = \frac{n_L}{(n_L + n_S)} = \frac{x_L}{(x_L + x_S)} \quad 3\text{-}66$$

Combining Equations 3-65 and 3-66, and solving for n_{L_2} gives Equation 3-67, which is what will be used to balance the component between the two phases, Gas and S&L.

$$n_L = \frac{\gamma_L}{\gamma_S} \times n_S \quad 3\text{-}67$$

The water component balance formula is shown in Equation 3-68.

$$n_{V_2} = n_{V_1} + n_{L_1} - n_{L_2} \quad 3\text{-}68$$

Using algebra to solve for the mole fractions of each component, Equation 3-69 is used.

$$x_i = \frac{n_i}{n} \tag{3-69}$$

The solution procedure is not straightforward. There is now an iterative calculation that needs to take place, and the method is listed here:

1. γ_{V_1} and γ_{DA_1} using (eq. 3-57)
2. P_{V_1} using (eq. 3-58)
3. T_{DP} using (eq. 3-59)
4. $P_{V_2}^{Sat}$ using (eq. 3-60)
5. γ_{V_2} initial guess using (eq. 3-61)

Then iteration needs to be done on steps 6 to 10.

6. P_{V_2} using (eq. 3-58)
7. γ_{L_2} using (eq. 3-65)
8. n_{L_2} using (eq. 3-67)
9. n_{V_2} using (eq. 3-68)
10. γ_{V_2} new using (eq. 3-57)

When a stable solution has been reached, it is necessary to determine if the system is within the limitations of both phases. For this, these limitations need to be known. Equation 3-70 states that the vapour must not be supersaturated, in which case the system is gas-side limited, and the isotherm calculation becomes redundant at this point.

$$n_V(Actual) = \min(n_V(Isotherm), n_V^{Sat}) \tag{3-70}$$

Once this number of moles has been determined, the final mole fractions can be calculated using Equations 3-68 and 3-69.

Now that the compositions of points 1 (T, P) and 2 (T_0, P) have been determined, the enthalpy and exergy changes associated with the difference can be derived.

It is necessary to calculate $\Delta h_{\Delta V}$ to find the enthalpy change due to condensation and evaporation. For this calculation, data from the steam tables should be used. The $\Delta h_{\Delta V}$ can be found directly, or by using Equation 3-71.

$$\Delta h_{\Delta V} = h_{Sat.V}(T_{DP}) - h_{Sat.L}(T_{DP}) \quad 3\text{-}71$$

The calculation of $\Delta s_{\Delta V}$ is required to find the entropy change due to condensation and evaporation: the steam tables are used to determine $\Delta s_{\Delta V}$. This step can be done directly, or by using Equation 3-72.

$$\Delta s_{\Delta V} = s_{Sat.V}(T_{DP}) - s_{Sat.L}(T_{DP}) \quad 3\text{-}72$$

Now the sum of the parts of the phase change components is calculated. The various parts of the enthalpy calculation are:

1. The enthalpy of the liquid up to the dew point temperature ($T_{DP} - T_0$)
2. The enthalpy of the phase change ($\Delta h_{\Delta V}$)
3. The enthalpy of the gas phase up to the working temperature ($T - T_{DP}$)

This summation is shown as Equation 3-73.

$$h_{\Delta V} = x_{\Delta V}\left[\overline{Cp_V}(T - T_{DP}) + \overline{\Delta h_{\Delta V}} + \overline{Cp_L}(T_{DP} - T_0)\right] \quad 3\text{-}73$$

Now the sum of the parts of the phase change components is calculated, only for the entropy terms. This calculation is shown in Equation 3-74. After collecting like terms, this equation simplifies to give Equation 3-75.

$$T_0 s_{\Delta V} = T_0 x_{\Delta V}\left[\overline{Cp_V}\ln\left(\frac{T}{T_0}\right) + \overline{\Delta s_{\Delta V}} + \overline{Cp_L}\ln\left(\frac{T_{DP}}{T_0}\right) - \overline{Cp_V}\ln\left(\frac{T_{DP}}{T_0}\right)\right] \quad 3\text{-}74$$

$$T_0 s_{\Delta V} = T_0 x_{\Delta V}\left[\overline{Cp_V}\ln\left(\frac{T}{T_{DP}}\right) + \overline{\Delta s_{\Delta V}} + \overline{Cp_L}\ln\left(\frac{T_{DP}}{T_0}\right)\right] \quad 3\text{-}75$$

As a result, the exergy of the part of the system that undergoes phase change is shown in Equation 3-76.

$$\begin{aligned} ex_{TM}^{T} = x_{\Delta V}\Bigg[&\overline{Cp_V}\left[T - T_{DP} - T_0\ln\left(\frac{T}{T_{DP}}\right)\right] \\ &+ \overline{Cp_L}\left[T_{DP} - T_0 - T_0\ln\left(\frac{T_{DP}}{T_0}\right)\right] + \Delta h_{\Delta V} - T_0\Delta s_{\Delta V}\Bigg] \end{aligned} \quad 3\text{-}76$$

3.5.2Pressure based exergy

This model is however far from complete, and there are other factors (pressure) involved in an exergy analysis beyond this point, if Equation 3-47 is recalled.

$$ex = [h(T,P) - h(T_0,P_0)] - T_0[s(T,P) - s(T_0,P_0)] + \sum_{i=0}^{\infty} \left(\mu_{i_0} - \mu_{i_{00}}\right)_{T_0,P_0} x_{i_0} \quad 3\text{-}47$$

To determine what is left in terms of the thermo-mechanical exergy, it is necessary to subtract what has been determined, or Equation 3-48, and the chemical exergy, from Equation 3-47. Therefore, the remaining parts of the exergy analysis are equal to the difference, as shown in Equation 3-77.

$$ex_{TM} - ex_{TM}^{T} = [h(T,P) - h(T_0,P_0)] - T_0[s(T,P) - s(T_0,P_0)] - \left[h(T,P) - h(T_0,P) - T_0\left(s(T,P) - s(T_0,P)\right)\right]$$

$$ex_{TM} - ex_{TM}^{T} = h(T,P) - h(T_0,P_0) - h(T,P) + h(T_0,P) - T_0[s(T,P) - s(T_0,P_0) - s(T,P) + s(T_0,P)]$$

$$ex_{TM} - ex_{TM}^{T} = -h(T_0,P_0) + h(T_0,P) - T_0[-s(T_0,P_0) + s(T_0,P)] \quad 3\text{-}77$$

From this equation, it is clear that some thermo-mechanical exergy remains in terms of a change in pressure, at constant temperature, so that Equation 3-78 is then obtained.

$$ex_{TM}^{P} = ex_{TM} - ex_{TM}^{T} = h(T_0,P) - h(T_0,P_0) - T_0[s(T_0,P) - s(T_0,P_0)] \quad 3\text{-}78$$

Again, each enthalpy and entropy term are to be calculated, as done above for the temperature-based exergy. The important difference here is that, since this component of exergy is isothermal, another way needs to be found of describing enthalpy and exergy without using temperature as the change (driving force which has the potential to create work). The general definitions of enthalpy and entropy need to be revisited to assess what effect changing the pressure has on the system.

Recall Equations 3-49 and 3-50.

$$dH = mCpdT + \left[V - T\left(\frac{\partial V}{\partial T}\right)_P\right] dP \quad 3\text{-}49$$

$$dS = \frac{mCpdT}{T} - \left(\frac{\partial V}{\partial T}\right)_P dP \quad 3\text{-}50$$

It is clear that a way of describing $\left(\frac{\partial V}{\partial T}\right)_P$ for each phase needs to be found. The ideal gas law has been assumed for the gas phase; therefore, the change in volume with the change in temperature at constant pressure is equal to $\left(\frac{n\bar{R}}{P}\right)_P$ (Using $PV = n\bar{R}T$).

For the pressure-based exergy, the temperature is constant (Isothermal process). Since there is no temperature change, $dT = 0$ and $T = T_0$. With this information, Equation 3-49 solves to give Equation 3-79 for gas systems and Equation 3-80 for solid and liquid systems.

$$dH_G^P = \cancel{Cp\,dT}^{\,0} + \left[V - T\left(\frac{n\bar{R}}{P}\right)_P\right] dP \qquad 3\text{-}79$$

$$dH_{S\&L}^P = \cancel{Cp\,dT}^{\,0} + \left[V - T\left(\frac{\partial V}{\partial T}\right)_P\right] dP \qquad 3\text{-}80$$

For this part, T is constant, so $dT = 0$ and $T = T_0$, so Equation 3-79 can be solved.

$$dH_G^P = \left[V - T_0\left(\frac{n\bar{R}}{P}\right)_P\right] dP$$

$$H_G^P = \int_{P_0}^{P} \left[\frac{n\bar{R}T_0}{P} - T_0\left(\frac{n\bar{R}}{P}\right)_P\right] dP \qquad 3\text{-}81$$

$$H_G^P = n\bar{R}T_0 \int_{P_0}^{P} \left[\frac{1}{P} - \left(\frac{1}{P}\right)_P\right] dP$$

$$H_G^P = n\bar{R}T_0 \left[\ln\left(\frac{P}{P_0}\right) - \ln\left(\frac{P}{P_0}\right)\right]$$

$$H_G^P = 0 \qquad 3\text{-}82$$

Now that the enthalpy is known for the gas system, a way of describing $\left(\frac{\partial V}{\partial T}\right)_P$ for the solids and liquid phase must be found. This partial derivative represents the thermal expansion of the material at a constant pressure. From the literature, this term may be represented as Equation 3-83. For most solids and liquids, this term is negligible under most circumstances, and is ignored. However, it can become significant (high pressure systems), so it will be investigated further.

$$\left(\frac{\partial V}{\partial T}\right)_P = \beta V \qquad 3\text{-}83$$

[16] p246

By substituting Equation 3-83 into Equation 3-84, there is:

$$dH_{S\&L}^P = \left[V - T_0\left(\frac{\partial V}{\partial T}\right)_P\right] dP \qquad 3\text{-}84$$

$$H_{S\&L}^P = \int_{P_0}^{P} (V - T_0 \beta V) dP \qquad 3\text{-}85$$

By assuming that β is constant within the working range.

$$H_{S\&L}^P = (1 - T_0\beta) \int_{P_0}^{P} V dP \qquad 3\text{-}86$$

$$H_{S\&L}^P = V(1 - T_0\beta)(P - P_0) \qquad 3\text{-}87$$

Using the same method and assumptions that were applied to the enthalpy terms in Equation 3-50, now consider what the pressure-based entropy becomes. For the gas system, this becomes Equation 3-89, and for the solids and liquids, this becomes Equation 3-91.

$$dS_G^P = \frac{\cancel{CpdT}}{T}_{0} - \left(\frac{n\bar{R}}{P}\right)_P dP$$

$$dS_G^P = \int_{P_0}^{P} -\left(\frac{n\bar{R}}{P}\right)_P dP \qquad 3\text{-}88$$

$$dS_G^P = -n\bar{R} \int_{P_0}^{P} \left(\frac{1}{P}\right)_P dP$$

$$S_G^P = -n\bar{R} \ln\left(\frac{P}{P_0}\right) \qquad 3\text{-}89$$

Now that the gas phase has been solved, the solids and liquids phase can be obtained from Equation 3-54.

$$dS_G^P = \frac{\cancel{CpdT}}{T}_{0} \beta V dP \qquad 3\text{-}90$$

$$dS_{S\&L}^{P} = -\int \beta V dP$$

$$S_{S\&L}^{P} = -\beta V(P - P_0) \quad \text{3-91}$$

Recall Equation 3-77, where the pressure-based thermo-mechanical exergy was defined as.

$$ex_{TM} - ex_{TM}^{T} = -h(T_0, P_0) + h(T_0, P) - T_0[-s(T_0, P_0) + s(T_0, P)] \quad \text{3-77}$$

Some of the common terms cancel each other out when combined, as shown by Equations 3-92 and 3-93.

$$H_G^P - T_0 S_G^P = n\bar{R}T_0[0] — T_0\left(-n\bar{R}\ln\left(\frac{P}{P_0}\right)\right)$$

$$H_{Ga}^P - T_0 S_G^P = n\bar{R}T_0 \ln\left(\frac{P}{P_0}\right) \quad \text{3-92}$$

To then turn this equation into the form that is required, specific exergy for the gas phase components, divide by n to get Equation 3-93.

$$ex_{TM_G}^P = \bar{R}T_0 \ln\left(\frac{P}{P_0}\right) \quad \text{3-93}$$

Similar manipulation for the solids and liquids gives Equation 3-95.

$$H_{S\&L} - T_0 S_{S\&L} = V(1 - T_0\beta)(P - P_0) — T_0(-\beta V[P - P_0])$$
$$H_{S\&L} - T_0 S_{S\&L} = V(P - P_0)[1 - T_0\beta + T_0\beta] \quad \text{3-94}$$

$$H_{S\&L} - T_0 S_{S\&L} = V(P - P_0) \quad \text{3-95}$$

Dividing by n gives the specific exergy for the solids and liquids phase components, shown in Equation 3-96.

$$ex_{TM_{S\&L}}^P = \overline{v_{ave}}(P - P_0) \quad \text{3-96}$$

This manipulation simplifies the calculation in terms of exergy change. The thermal expansion coefficients are not required for the exergy calculations but may be required for enthalpy calculations.

It is necessary to find $\overline{v_{Ave}}$ to solve this in one step. This can be done using Equation 3-97.

$$\overline{v_{ave}} = \sum_i \gamma_{i_{S\&L}} \overline{v_i} \qquad 3\text{-}97$$

Because the pressure-based exergy occurs in a closed system, it is important to find the phase change component, as was done with the temperature based thermo-mechanical exergy. The main point of difference is that the pressure system will be at a constant temperature, so the saturation pressure will not change. Following the same method as listed above will result in new compositions for point 0, or the reference state (T_0, P_0). Equation 3-70 must be observed in this situation also, as the pressure change thermo-mechanical exergy is calculated as if in a closed system.

It is clear then that this new phase change component must be treated separately, as was done with the temperature-based change.

Since the partial pressure changes, but the temperature does not, the dew-point temperature is not suitable to find the enthalpy and entropy of evaporation. In this case, the partial pressure of water vapour (P_{V_2}) should be used, as in Equations 3-98 and 3-99.

$$\Delta h_{\Delta V} = h_{Sat.V}(P_V) - h_{Sat.L}(P_V) \qquad 3\text{-}98$$

$$\Delta s_{\Delta V} = s_{Sat.V}(P_V) - s_{Sat.L}(P_V) \qquad 3\text{-}99$$

Since there is no change of temperature and replacing the temperature basis with the pressure basis above, Equation 3-73 becomes Equation 3-100.

$$h_{\Delta V}^P = x_{\Delta V}\left[\overline{\Delta h_{\Delta V}} + \overline{v_L}(1 - T_0\beta_L)(P - P_0)\right] \qquad 3\text{-}100$$

Similarly, for Equation 3-74, becomes Equation 3-101.

$$T_0 s_{\Delta V} = T_0 x_{\Delta V}\left[-\bar{R}\ln\left(\frac{P}{P_0}\right) + \overline{\Delta s_{\Delta V}} - \overline{v_L}\beta_L(P - P_0)\right] \qquad 3\text{-}101$$

Combining Equations 3-99 and 3-100 to get the result for exergy, gives Equation 3-102.

$$ex_{TM}^P = x_{\Delta V}\left[T_0\bar{R}\ln\left(\frac{P}{P_0}\right) + \overline{\Delta h_{\Delta V}} - \overline{\Delta s_{\Delta V}} + \overline{v_L}(P - P_0)\right] \qquad 3\text{-}102$$

3.5.3Chemical exergy

There is one more component to the exergy analysis, as suggested by Equation 3-47.

$$ex = [h(T,P) - h(T_0,P_0)] - T_0[s(T,P) - s(T_0,P_0)] + \sum_{i=0}^{\infty}\left(\mu_{i_0} - \mu_{i_{00}}\right)_{T_0,P_0} x_{i_0} \quad \text{3-47}$$

Where: 3-103

$$\mu_i = \Delta G_i = \Delta h_i(\gamma_i) - T_0 \Delta s_i(\gamma_i) \quad \text{[16] p 323}$$

As a result, the chemical exergy component is simplified to Equation 3-104 once any phase changes have been taken into account, such as by using the sorption isotherm.

$$ex^{CH} = \sum_{i=0}^{\infty}\left(\mu_{i_0} - \mu_{i_{00}}\right)_{T_0,P_0} x_{i_{00}} \quad \text{3-104}$$

Since there is no change in temperature or system pressure, the enthalpy term is equal to zero, by definition, so Equation 3-103 becomes Equation 3-105. This part of the analysis represents what happens in an open system with no composition change, but where there is a change in concentration.

To elaborate, this determines the work potential that is lost in the form of the chemical composition of a system output changing to be in equilibrium with the environment. An example is the diffusion of water vapour from a liquid surface at its saturation pressure to the pressure of the water vapour in the environment.

This calculation is simplified compared with reality by taking the temperature and pressure considerations separately. For most parts of a chemical plant, this calculation can be largely ignored but should be taken into consideration when calculating the feeds, products and waste products of the process.

$$\mu_i = -T_0 \Delta S_i(\gamma_i) \quad \text{3-105}$$

[16] p 318

Since there is no chemical reaction in this system, only with the entropy associated with mixing with the environment remains to be determined.

For gas systems, the entropy of mixing is defined as the ratio of the pressure from the pure component to the partial pressure of the component; this entropy term is shown in Equation 3-106.

$$\Delta S_{i_{Mix}} = \bar{R} \ln\left(\frac{P}{P_i}\right) \quad 3\text{-}106$$

Equation 3-106 then represents the pressure-based entropy of relating the pure component to its partial pressure, which is represented by Equation 3-58.

$$P_i = \gamma_i P \quad 3\text{-}58$$

Substituting Equation 3-58 into Equation 3-106 may be simplified further to give Equation 3-107, which is the equation for the entropy of mixing, as shown by Sussman [16].

$$\Delta S_{i_{Mix}} = -\bar{R} \ln(\gamma_i) \quad 3\text{-}107$$

[16]
p 321

Since there is a difference in composition compared with the environment, there is a difference in the free energy of mixing in the gas phase. This change represents the reversible work potential of taking the compositions to that of the dead state. There is then the potential to extract work from the system. Even if this work is not technologically feasible to extract, it must be taken into account for an exergy analysis of an open system and becomes what is known as lost work in a later part of an exergy analysis.

Substituting Equation 3-107 into Equation 3-105 gives the chemical potentials of the system at the reference and dead states, Equations 3-108 and 3-109, respectively.

$$\mu_{i_0} = \Delta G_{i_0} = T_0 \bar{R} \ln\left(\gamma_{i_0}\right) \quad 3\text{-}108$$

$$\mu_{i_{00}} = \Delta G_{i_{00}} = T_0 \bar{R} \ln\left(\gamma_{i_{00}}\right) \quad 3\text{-}109$$

From here, these terms can be directly substituted into Equation 3-104, and simplifying gives Equation 3-110.

$$ex^{CH} = \sum_{i=0}^{\infty} \left[T_0 \bar{R} \ln\left(\gamma_{i_0}\right) - T_0 \bar{R} \ln\left(\gamma_{i_{00}}\right)\right]_{T_0, P_0} x_{i_0} \quad 3\text{-}110$$

$$ex^{CH} = T_0 \bar{R} \sum_{i=0}^{\infty} x_{i_{00}} \left[\ln \left(\frac{\gamma_{i_0}}{\gamma_{i_{00}}} \right) \right]_{T_0, P_0}$$

It is important to consider each phase independently here, because each phase acts differently when mixed.

The gas phase chemical exergies can be calculated using Equation 3-29.

$$ex_{i_G}^{CH} = T_0 \bar{R} x_{i_{00}} \ln \left(\frac{\gamma_{i_0}}{\gamma_{i_{00}}} \right) \quad \text{3-29}$$

Now the phase specific molar fractions need to be found, using Equation 3-57.

$$\gamma_{i_G} = \frac{x_i}{x_G} \quad \text{3-57}$$

The above formulation works well for ideal gas systems. However, for ideal liquid and ideal solids, this does not hold true.

"*The free energy of mixing of liquid or solid solutions is equal to the free energy of mixing of the vapour mixtures that are in equilibrium with these solutions. The reason for this is that there is no change in free energy when one moves matter from one equilibrium phase to another.*" - [16] p319.

This statement means that the exergy for mixing of ideal liquid and solid-phase components is equal to the change in the free energy of the component vapour. The mixing of this phase is then calculated by the change from each component's saturation pressure, to the actual vapour pressure of the mixture. This result is then the pressure-based exergy calculated for $P_{i_0}^{Sat}$ to $P_{i_{00}}$ for each component in the solid and liquid phases.

Since this is an open system, and the solids and liquid phases are in equilibrium with the gas phase, via the sorption isotherm, $P_{L_{00}} = P_{V_{00}}$ and since the solid has no significant vapour pressure, it is assumed that it is already in equilibrium, and the vapour pressure remains constant (P_0), or at the dead state condition for this part of the analysis.

A sorption isotherm is used to determine the equilibrium state with the environment. This equilibrium state is then used as the composition of the dead state. The sorption isotherm used for skim milk powder is shown in Equation 3-65.

The solution procedure is the same as with the temperature-based exergy term. There is now an iterative calculation that needs to take place, and the method is listed again here:

1. γ_{V_0} using (eq. 3-57)
2. P_{V_0} using (eq. 3-58)
3. T_{DP} using (eq. 3-59)
4. $P_{V_{00}}^{Sat}$ using (eq. 3-60)
5. $\gamma_{V_{00}}$ initial guess using (eq. 3-61)

Then iteration needs to be done on steps 6 to 11.

6. $P_{V_{00}}$ from (eq. 3-58)
7. n_{L_0}, n_{V_0} using (eq. 3-62)
8. $\gamma_{L_{00}}$ using (eq. 3-65)
9. $n_{L_{00}}$ using (eq. 3-67)
10. $n_{V_{00}}$ using (eq. 3-68)
11. $\gamma_{V_{00}}$ new using (eq. 3-57)

Equation 3-70 should not be applied here, since the chemical exergy accounts for the transfer between closed and open systems. Assuming a rapid transfer of vapour away from the liquid surface, the vapour pressure will be taken as that of the dead state. From here, the solid and liquid phase mixing exergies can be found. Recall Equation 3-107, which is the general definition of mixing entropy.

Now that the component fraction that changes phase has been obtained, it is necessary to take that into account. As with the pressure-based exergy, the enthalpy and entropy of evaporation should be determined at the vapour pressure of the solution, as shown in Equations 3-111 and 3-112.

$$\Delta h_{\Delta V} = h_{Sat.V}(P_V) - h_{Sat.L}(P_V) \qquad 3\text{-}111$$

$$\Delta s_{\Delta V} = s_{Sat.V}(P_V) - s_{Sat.L}(P_V) \qquad 3\text{-}112$$

All of the resulting vapour is to be used in the gas phase equation (Equation 3-29), while the remaining liquid needs to be calculated using the solids and liquids phase exergy calculation, Equation 3-30.

$$\Delta S_{i_{Mix}} = \bar{R} \ln\left(\frac{P}{P_i}\right) \quad 3\text{-}107$$

Since the pressure of the ideal solution is the vapour pressure of the solution at the reference state, the pure component saturation pressure is the starting pressure i.e. $P = P_{i_0}^{Sat}$. As a result, Equation 3-107 becomes Equation 3-113 for point 0, and Equation 3-114 for point 00.

$$ex_{i_0}^{CH} = T_0 \bar{R} x_{i_{00}} \ln\left(\frac{P_{i_0}^{Sat}}{P_{i_0}}\right) \quad 3\text{-}113$$

$$ex_{i_{00}}^{CH} = T_0 \bar{R} x_{i_{00}} \ln\left(\frac{P_{i_{00}}^{Sat}}{P_{i_{00}}}\right) \quad 3\text{-}114$$

The change in chemical exergy is then the difference between 3-113 and 3-114, or Equation 3-115.

$$ex_{i_0}^{CH} - ex_{i_{00}}^{CH} = T_0 \bar{R} x_{i_{00}} \ln\left(\frac{P_{i_0}^{Sat}}{P_{i_0}}\right) - T_0 \bar{R} x_{i_{00}} \ln\left(\frac{P_{i_{00}}^{Sat}}{P_{i_{00}}}\right) \quad 3\text{-}115$$

Since $T_0 = T_{00}$ and $P_0 = P_{00}$, $P_{i_0}^{Sat} = P_{i_{00}}^{Sat}$. Equation 3-115 then solves to give Equation 3-116.

$$ex_i^{CH} = T_0 \bar{R} x_{i_{00}} \ln\left(\frac{P_{i_{00}}}{P_{i_0}}\right) \quad 3\text{-}116$$

NOTE 3-3: In this case, the terms P_{i0} and P_{i00} represent the vapour pressures of component *i* at the reference and dead state conditions, respectively.

Equation 3-117 represents the summation of the chemical exergy components.

$$ex^{CH} = ex_{DA}^{CH} + ex_V^{CH} + ex_L^{CH} + ex_S^{CH} + ex_{\Delta V}^{CH} \quad 3\text{-}117$$

Chapter 4 Inversion Temperature and Pinch Analysis

This chapter has been published in the journal "Drying Technology" [1] and shows the ability of pinch analysis and the inversion temperature to assist in process selection and optimisation techniques for drying systems.

This analysis is suitable for all dryer applications, as long as the inlet conditions to the dryer are sufficient to dry the product sufficiently. The effects of humidity and flowrate on the inversion temperature have also been studied in this work.

This inversion temperature is an example of a simple rule of thumb for drying agent selection and should only be used as a starting point in initial design considerations. More rigorous macro-scale energy analyses should then be used to confirm the results. This more rigorous analysis should include both thermal and mechanical work as sources of energy, as well as the cost potential of these energy sources.

4.1Constraints/Assumptions

- The dryer is a well-insulated adiabatic continuous co-current short-form spray dryer.
- The dryer is well mixed and equilibrium limited [13, 14].
- The flow rate of gas entering the dryer is 21 $kg.s^{-1}$, and the liquid solution flow rate is 2.5 $kg.s^{-1}$ of 50 wt% milk solids.
    - This assumption was used to be representative of what is found industrially after milk has been evaporated in a pre-process and is still sufficiently free flowing to pass through the nozzle in the spray dryer [14, 118, 119].
- An approach temperature of $20^{O}C$ will be used for the pinch analysis and dryer outlet temperature [13].
    - This is a well known to industrial operators in the Australian and New Zealand dairy industry.
    - Another reason for this offset was to use a simplistic method to estimate internal losses, as the dryer would not come to equilibrium. It does not come exactly to equilibrium – see my main point above.

    - A short form dryer may not have enough contact time to get a closer exit temperature (this could essentially estimate a dryer that is too small for the flow).

- The drying rate will not be studied, instead the results of the mass and energy balance will be utilised to represent the dryer.

- Utilities analysis will not be undertaken here, and neither will the heat exchanger network diagrams, as the system is too simple for these pinch processes to be utilised effectively.

- The system boundaries are where each inlet and outlet stream are found to be at ambient conditions.

4.2Inversion Temperature

The inversion temperature for the system, which will be studied throughout this chapter, can be found using the methodology as set out by Costa and Neto da Silva [63]. This comparison between air and steam systems applies for very specific conditions, namely the unhindered drying period. This procedure then determines at what temperature the drying rate is the same for both the convective air and superheated steam dryers, meaning that the size of the dryer is then the same.

Since an adiabatic dryer is mainly being discussed, it is worth noting that a simplified Adiabatic Saturation Inversion Temperature (ASIT) was used to determine the result. Because of the nature of the information required for the inversion temperature calculation, there is no need for an initial mass and energy balance (MEB) over the system. This situation means that, from this inversion temperature analysis, it is possible to find a suitable starting temperature to use for the MEB in the next stage.

The dryer will be assumed to approach equilibrium between the gas and solids at the outlet. A justification for this assumption is the works of Ozmen and Langrish [14], and Bahu [13] , who found that this assumption was a reasonable first estimate for the conditions of the gas and the solids at the end of many co-current spray dryers. For the analysis, the dryer will be coupled with the separation device into one unit, for the purposes of simplifying the analysis. This procedure gives two streams in and two streams out.

4.2.1Required Data

- Inlet Flows
- Condition of inlet flows (humidity, temperature, flow rate)
- Latent heat of vaporisation of the evaporating fluid (water):
    - At $100^{O}C$, and
    - At the inlet dew point temperature
- Dew point temperature at the inlet; and
- Specific heat capacities of the system (Cp's).

4.2.2Discussion

The resulting inversion temperature is $182^{O}C$ for a humidity of 6 $g_W.kg_{DA}^{-1}$. This temperature is within the specified range for inversion temperatures as shown in Figure 5 from Costa and Neto da Silva [63]. It must also be noted that this result is independent of the dryer system. The mass and energy balance requirements for the dryer are not taken into consideration as the ASIT is a kinetic-based parameter.

The sensitivity of this analysis is important in that the inlet humidity of the air changes constantly, along with the flowrates of both the solids mixture and the drying gas. This change will inevitably alter the results based on the factors shown within the β parameter in Equation 2-1. The effect of humidity on the ASIT is shown in Figure 4-1.

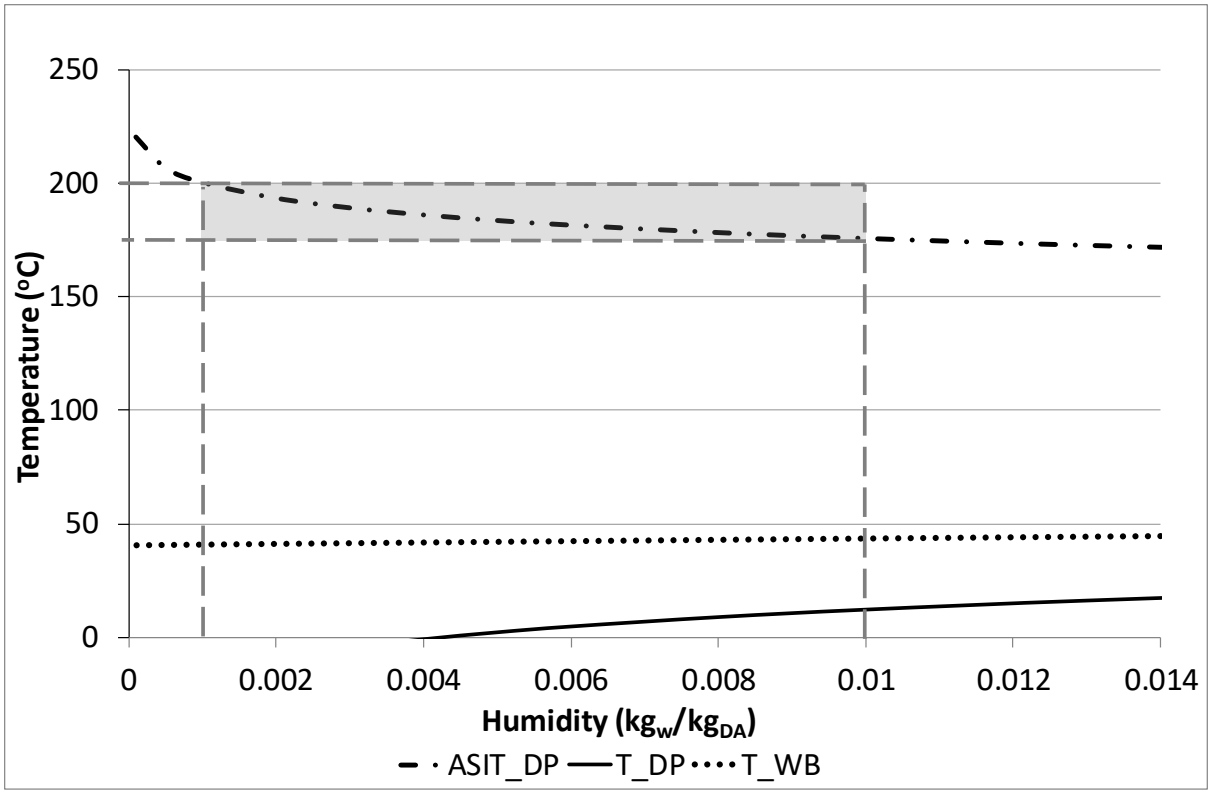

Figure 4-1: The effect of inlet air humidity on the ASIT. The steam to air flowrate ratio is constant (1 on a mass basis).

Figure 4-1 shows that the inlet humidity does not have a large effect on the inversion temperature until the inlet humidity becomes very small (below 2 $g_W.kg_{DA}^{-1}$). The inversion temperatures range between 170-200^{O}C for the studied conditions.

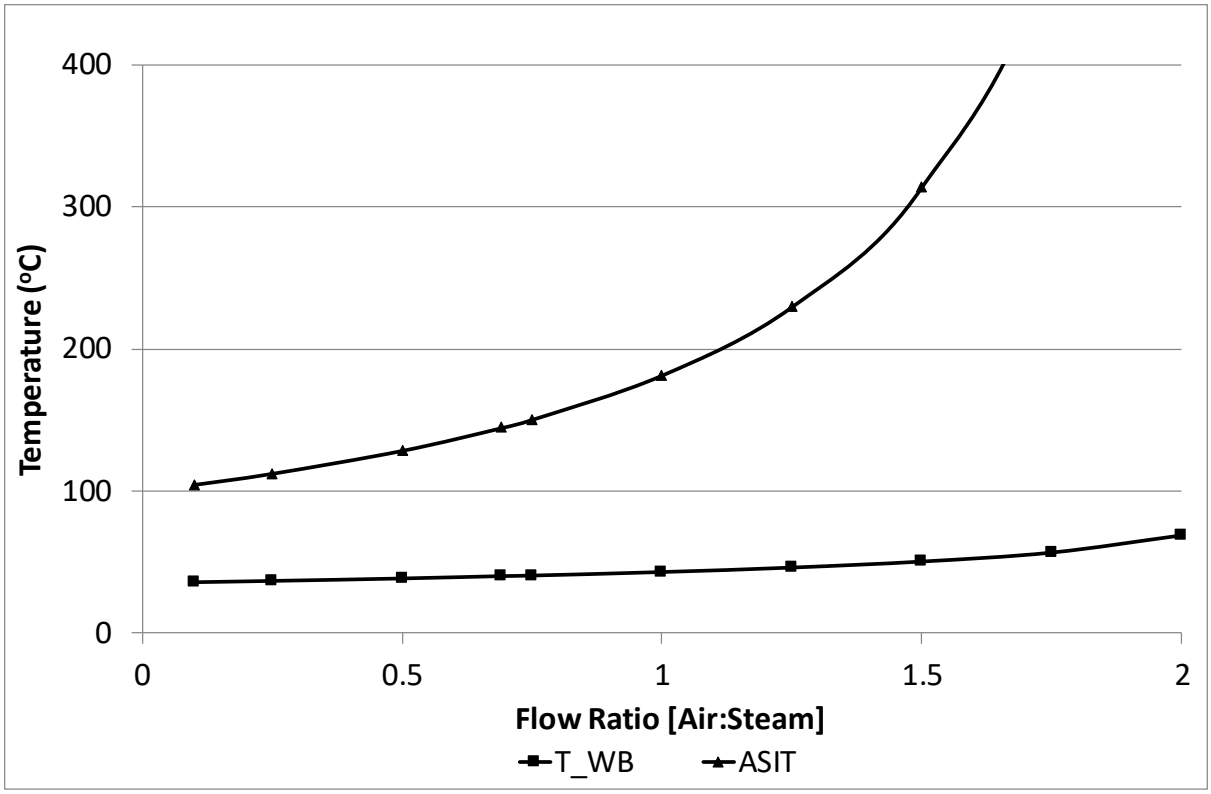

Figure 4-2: Effect of flow ratio on the ASIT, humidity fixed at 6 $g_W.kg_{DA}^{-1}$.

Figure 4-2 shows the effect of using a different mass flow rate of air and steam on the inversion temperature. This effect does have a limit, due to the term β/(1-β) in Equation 2-1, where β is a function of the mass flow ratio of humid air and steam being used, which means β must be less than unity. The relationship between the flow ratio and ASIT is clear from Figure 4-2. If it is assumed that the flow variations are similar in both the air and steam systems, then there is no need to go into further detail regarding the effect of this parameter.

4.3Mass and Energy Balances for the Dryers

For any detailed thermodynamic analysis of processes, the MEB's need to be completed first. A brief explanation of the assumptions and methods will be discussed before comparing the results of using the ASIT with a PA.

A case study of the temperature effects on the dryness of the solids at the outlet was completed to ensure that the dryer had sufficient energy to dry the solids. The results are

shown in Figure 4-3. The shaded region shows a region where there is insufficient energy to dry the solids. This occurs at an inlet gas temperature below 184^{O}C.

It is clear that the inversion temperature of 182^{O}C is below the lower limit of an effective dryer, i.e. 184^{O}C, for the steam dryer. The air dryer has a much lower outlet temperature limitation, and as a result it can operate at much lower inlet temperatures. The required energy for the steam system is considerably lower for all temperatures above this restriction. As seen in Figure 4-3, the steam system achieves lower solids moisture contents than the air system above an inlet gas temperature of 184^{O}C.

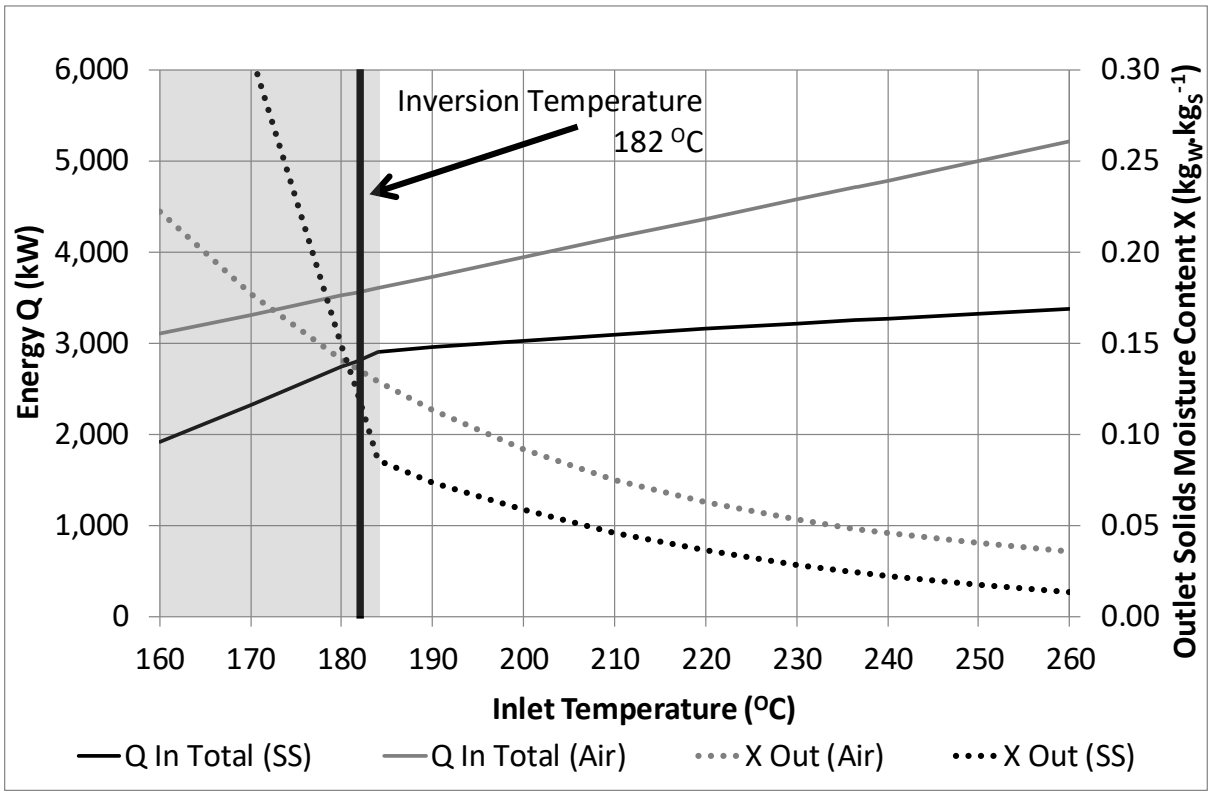

Figure 4-3: The effect of temperature on effectiveness of the dryer. Flowrates constant at 21 kg.s^{-1}.

4.3.1Convective Air Dryer

A simple system will be studied in this chapter, consisting of an air pre-heater, solution pre-heater, spray dryer, solids separator, and some coolers, as shown in Figure 4-4. The mass and energy balance over the studied dryer system is based on the work of Reay [120]. The following assumptions have been used to assess the mass balance and to ensure that the inversion temperature can be compared fairly with the PA.

The solids temperature was not allowed to drop below the dew-point temperature of the outlet conditions, and the gas outlet temperature from the dryer system is offset by 20^{O}C, i.e. the outlet stream of gas is 20^{O}C hotter than the solids outlet. This offset has been assumed primarily to represent some driving force remaining at the outlet of the dryer, and to represent the pseudo temperatures to be applied to the dryer streams for the PA. This offset is reasonable according to the literature [61].

The process given in Figure 4-4 shows humid air (S-01 to S-03) entering the pre-heating sequence of exchangers (E-1 and E-2) before entering the dryer (D-1) at 190^{O}C. The wet solids stream (S-08 to S-09) is pre-heated (E-4) to 60^{O}C before entering the dryer. S-04 is an intermediate stream between the dryer and solids-separation device (C-1). This is a mixed phase stream of very humid gas and dried solids. The solid phase (S-10) and gas phase (S-05) are separated here and both are cooled back to ambient conditions, the gas via a 2-stage process including the pre-heater (E-1) and E-3, while the solids are cooled using E-5.

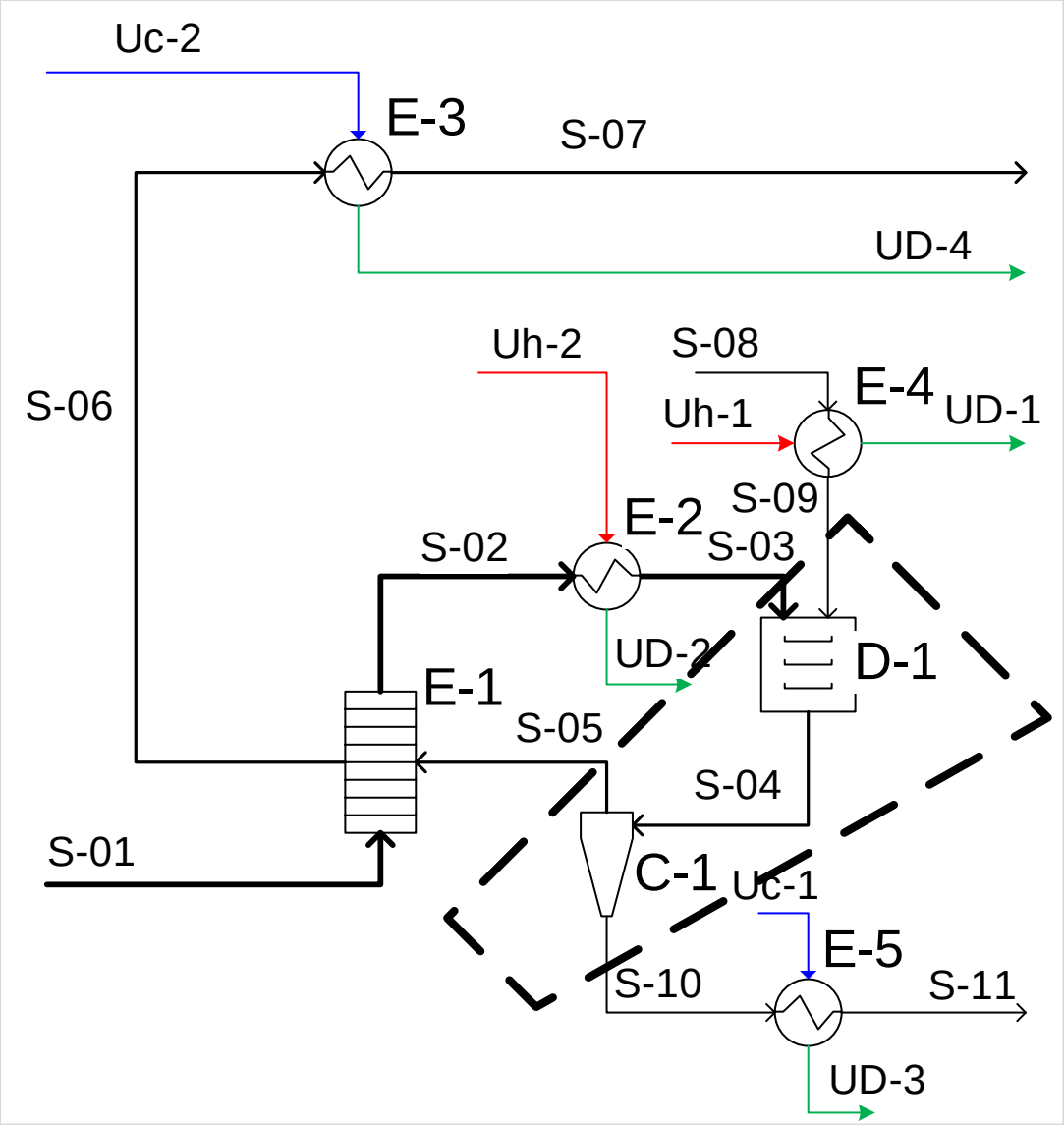

Figure 4-4: A PFD of the tested system with a convective air dryer. The region in the dashed box refers to Figure 4-8 and Figure 4-9. Refer to Table 4-1 for stream descriptions and mass and energy balance.

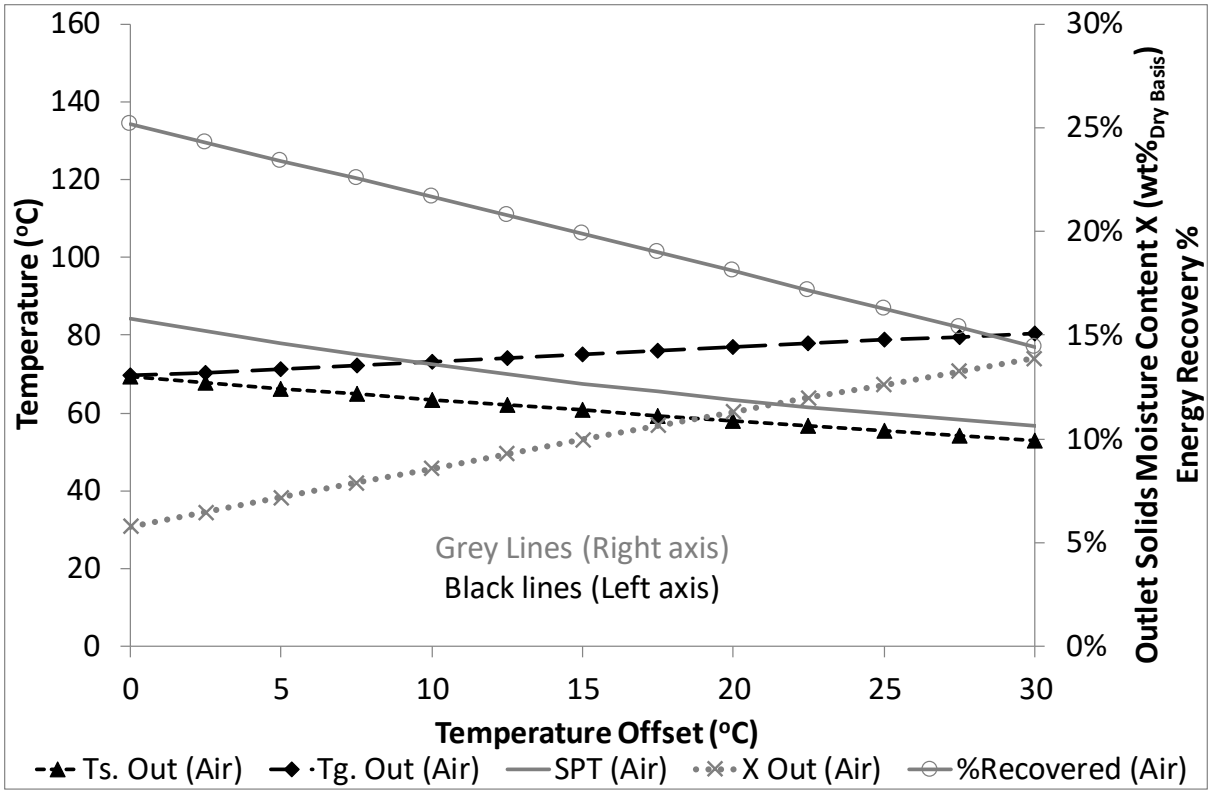

Figure 4-5: The effect of dryer outlet ΔT on energy recovery and outlet solids moisture content (Air).

Figure 4-5 shows the effect of changing the temperature offset for the dryer outlet on the air dryer. As the temperature offset increases, the recovered energy (from the PA) decreases, while the outlet solids moisture content increases. The Sticky Point Temperature (T_{SP}) has been plotted here to show that its calculated value is equally affected by the offset since it is closely linked to the solids moisture content at the outlet of the dryer. While the outlet temperature cannot be controlled in any sensible manner, this shows how important the design of the dryer is, the closer to equilibrium (left side) of the plot you can achieve, the more efficient the system becomes.

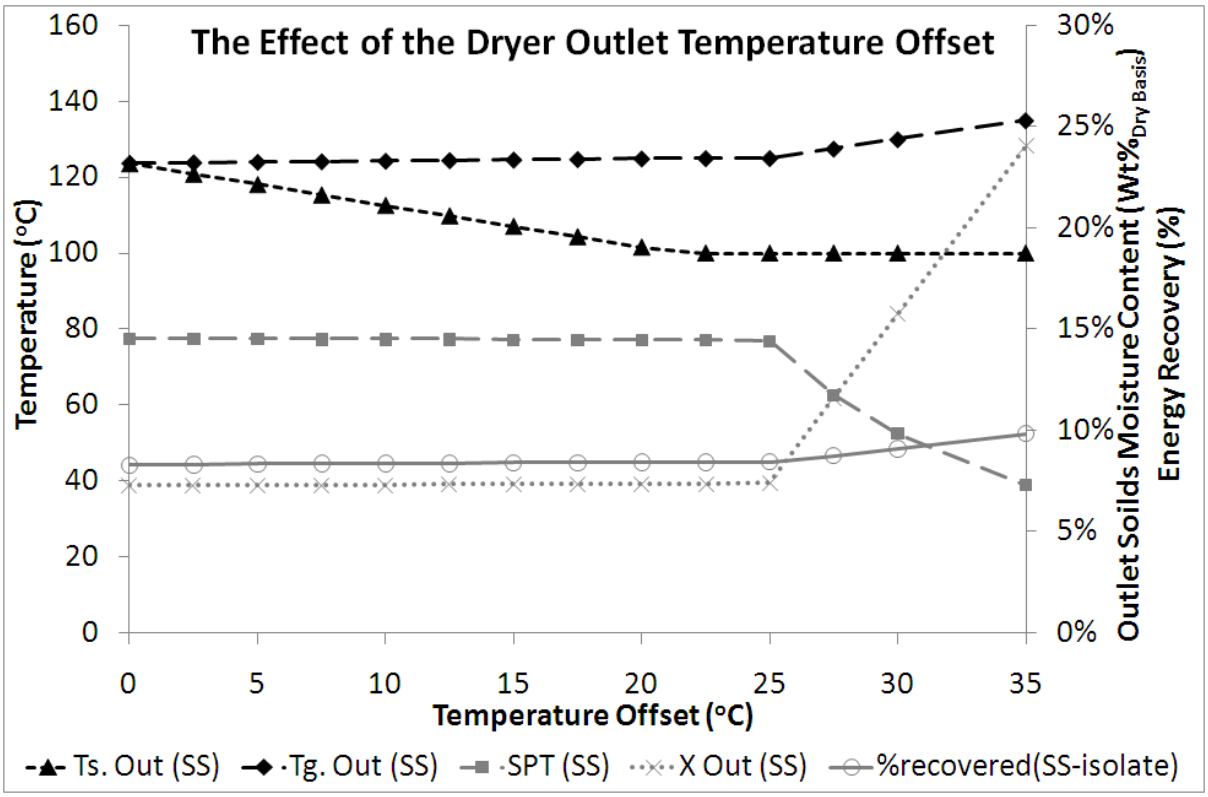

Figure 4-6: The effect of dryer outlet ΔT on energy recovery and outlet solids moisture content (SS).

Figure 4-6 shows the effect of changing the temperature offset for the dryer outlet, with the superheated steam dryer. As the temperature offset increases, the solids temperature is affected more, until the solids temperature reaches 100^{O}C. The solids moisture content is not affected by this temperature offset below an offset of 25^{O}C. Due to the conservative approach taken in the PA, an offset of 20^{O}C was chosen to allow a simple integration of the dryer with the analysis.

In order to prepare for the PA, it is essential to specify the system inlet and outlet conditions at ambient conditions (25^{O}C, 1 atm), or the lowest temperature present in the system. This assumption gives the maximum energy recoverable from these streams while also maximising the cooling utility requirements for this minimum heating. If cooling these streams is found to be wasteful, or not required, then these coolers may be simply removed to create a more realistic energy solution.

If it is found that the given conditions are not sufficient to achieve good overall drying, the dryer inlet temperature should be manipulated to the point where it is sufficient. In this

instance 190^{O}C is used as it is above the minimum inlet temperature of 184^{O}C. The results of the MEB for the system are shown in Table 4-1.

Table 4-1: The mass and energy balance (MEB) results for the air system in Figure 4-4.

Stream Properties						
Stream	**Description**	**Temp.**	**Cp**	**Enthalpy**	**Flowrate**	**Humidity**
Name		**^{O}C**	**kJ.kg^{-1}.K^{-1}**	**kW**	**kg.s^{-1}**	**g_W.kg_{DA}^{-1}**
S-01	Fresh air inlet	25	1.01	811	21	6.0
S-02	Pre-heated air	58	1.01	1,508	21	6.0
S-03	Air feed to dryer	190	1.01	4,296	21	6.0
S-04	Dryer outlet	77	1.10	4,722	23.5	59.1
S-05	Humid air out	78	1.05	4,604	22.11	59.1
S-06	Exchanged gas out	48	1.05	3,905	22.11	59.1
S-07	Ambient flue gas	25	1.13	1,686	22.11	22.5
S-08	Ambient solution feed	25	2.84	178	2.5	
S-09	Solution feed	60	2.84	426	2.5	
S-10	Solids removal	59	1.77	146	1.39	
S-11	Ambient solids	25	1.77	62	1.39	

The evaporation of liquid into gas occurs gradually through the dryer and not stepwise, meaning there is no particular point or preferred region in the dryer where the evaporation change occurs. This energy system cannot be easily represented as a function of temperature, as pinch plots. In order to do a MEB over the dryer, a linear approximation, or in-to-out calculation, of the profile of energy as a function of temperature in the dryer has been used. This procedure is a suitable estimate, particularly for this early stage of the analysis, as it may be used to find better operating conditions in terms of overall energy solutions. Taking all of these considerations and limitations into account, Table 4-2 was constructed. The results for S-04 (Outlet 4g and Outlet 4s in Table 4-2), when combined, represent the section between the dryer and the separator. The results of these intermediate streams were found by treating the dryer as two systems, one as a heat exchanger and one other as a mass transfer unit. These 'internal' results have been used for the Conservative Region Estimate (CRE) used in the PA.

Table 4-2: Results of the MEB for the convective air dryer.

Convective Air Dryer Mass Balance							
Stream	**Flow**	**Temp**	**Humidity**	**$Water_{Liq}$**	**Solids**	**Wet Gas**	**Ave C_p**
Symbol	**Q**	**T**	**Y**	**L_w**	**S**	**G_w**	**C_p**
Units	**$kg.s^{-1}$**	**^OC**	**$g_w.kg_{DA}^{-1}$**	**$kg.s^{-1}$**	**$kg.s^{-1}$**	**$kg.s^{-1}$**	**$kJ.kg^{-1}K^{-1}$**
Gas In (3)	21	190	0.006	-	-	21	1.01
Sol^n In (9)	2.5	60	-	1.25	1.25	-	2.84
Outlet (4g)	21	75.69	0.006	-	-	21	1.01
Outlet (4s)	2.5	55.69	-	0.1	1.25	1.15	1.83
Outlet (5)	22.15	73.57	0.061	-	-	22.15	1.06
Outlet (10)	1.35	57.59	-	0.1	1.25	-	1.71

However, an overall MEB approach, by definition, cannot find internal operational savings. Determining the inlet and outlet conditions is critical for managing the energy potential of the system and is a simple starting point before the design of the actual drying unit is needed or the dryer is modelled.

4.3.2Superheated Steam

Using similar conditions to the example for hot air, it is possible to compare superheated steam as a water-stripping agent in a spray-drying system. The first point that should be considered in this new system is to keep the steam as close to atmospheric pressure as possible throughout the process to reduce the amount of electrical energy to be used for fans, blowers or compressors, and to minimise the operating costs associated with pressure vessels.

Because steam is being used in this process, it has the potential to reduce the energy requirements of the pre-heaters, since the steam may be recirculated readily. For superheated steam to be effective, the outlet temperature for the dryer must be above the dew-point, or condensation temperature (100^OC at 1 atm). The condensation temperature is traditionally manipulated using pressure changes in the system, e.g. a low condensation temperature may be achieved in a partial vacuum. The system that is to be represented here is shown in Figure 4-7.

For this system to be compared with the previously studied air system, the basis for comparison that was chosen was the inlet conditions for the dryer, or the 190^OC gas inlet temperature. This basis then allowed for a comparison of the overall mass and energy transfer and the evaporation efficiencies for both systems.

The model that was used is a slight variation on the MEB described for the air system, based on the works of Reay and Langrish [12]. The biggest difference is that the humidity (Y) in the air system was replaced by the superheat number (Ψ) for the steam system. The definition of this parameter is shown in Equation 4-1. This number is the ratio of the actual steam vapour pressure to the steam saturation pressure.

$$\Psi = \frac{p_V}{p_{V_{Sat.T}}} \qquad 4\text{-}1$$

A mass and energy balance over the dryer was completed and the results are shown in Tables 4-3 and 4-4. The process depicted in Figure 4-7 shows the steam system being studied. The process starts with the wet solids stream (S-08 to S-09) being heated to 60^{O}C before entering the dryer (D-1). The steam returning side of the loop (S-01) this stream is re-heated to the gas inlet temperature via a heat exchanger (E-2) before being entering the dryer. The dryer outlet (S-04) represents the mixed phase exiting the dryer and entering the solids recovery stage where the solids are removed (S-10) from the steam recycle system (S-05) and cooled (E-5). From this point, the evaporated moisture (S-05) is purged (S-06) through a control valve or automatic relief system and then condensed and cooled (E-3).

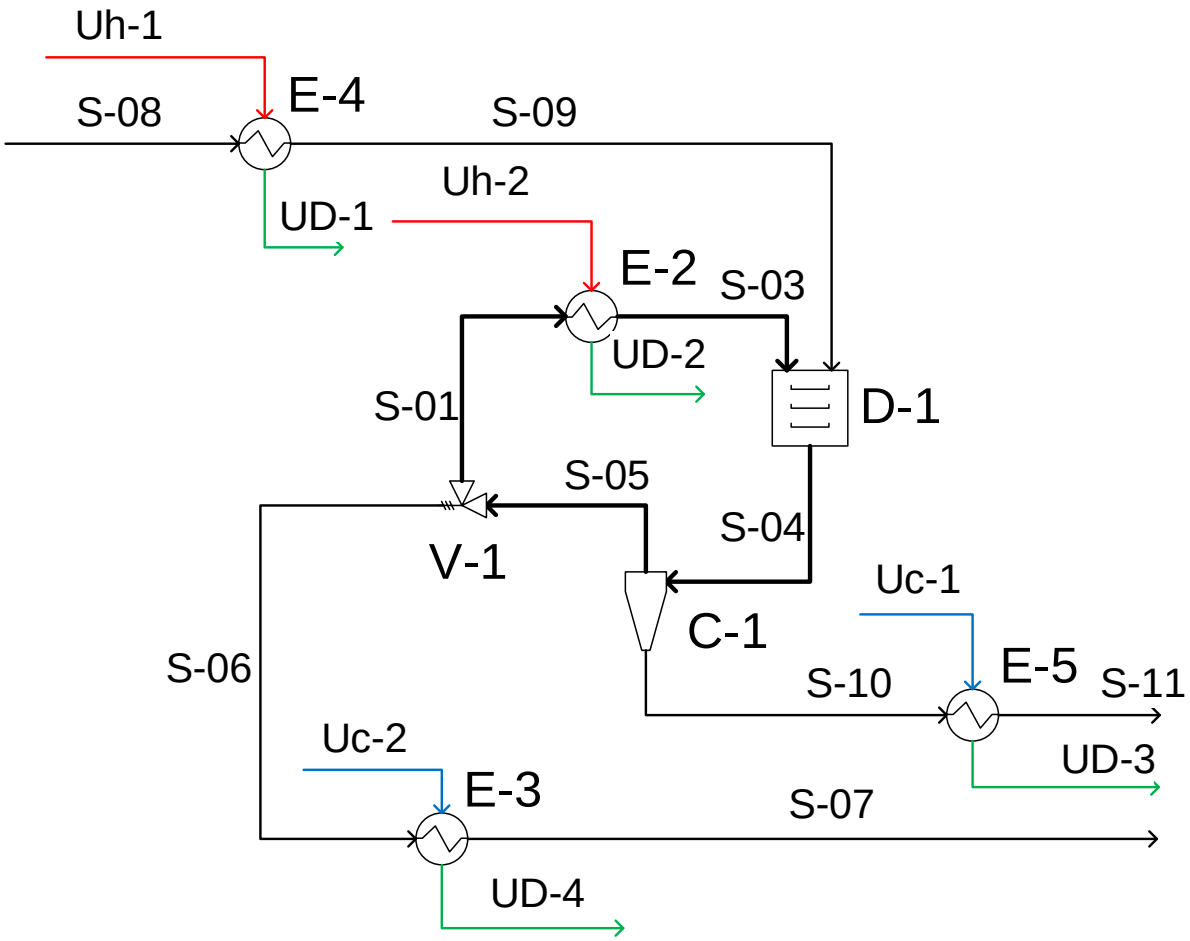

Figure 4-7: A PFD of the superheated steam system. Refer to Table 4-3 for stream descriptions and mass and energy balance.

Table 4-3: The MEB results for the steam system shown in Figure 4-7.

Stream Properties						
Steam	**Description**	**Temp.**	**Cp**	**Enthalpy**	**Flowrate**	**Superheat**
Name		**^{o}C**	**kJ.kg^{-1}.K^{-1}**	**kW**	**kg.s^{-1}**	**Number**
S-01	High quality steam recycle	124.9	2.0	52,568	21.0	0.438
S-03	Steam feed to dryer	190.0	2.0	55,270	21.0	0.081
S-04	Dryer outlet	123.7	2.0	55,696	23.5	0.454
S-05	Steam out	124.9	2.0	55,467	22.2	0.438
S-06	Steam purge	124.9	2.0	2,899	1.2	0.438
S-07	Purge to ambient	25.0	4.2	121	1.2	
S-08	Ambient solution feed	25.0	2.8	178	2.5	
S-09	Solution feed to spray dryer	60.0	2.8	426	2.5	
S-10	Solids removal	101.6	1.7	229	1.3	
S-11	Solids to ambient	25.0	1.7	56	1.3	

Table 4-4: Results of the MEB for the superheated steam dryer.

Superheated Steam Dryer Mass Balance							
Stream	**Flow**	**Temp**	**Superheat Number**	**$Water_{Liq}$**	**Solids**	**Steam**	**Ave Cp**
Symbol	**Q**	**T**	**Ψ**	**L_w**	**S**	**G_w**	**C_p**
Units	**$kg.s^{-1}$**	**^oC**	**$atm.atm^{-1}$**	**$kg.s^{-1}$**	**$kg.s^{-1}$**	**$kg.s^{-1}$**	**$kJ.kg^{-1}.K^{-1}$**
Gas In (3)	21	190	0.081	-	-	21	1.98
Sol^n In (9)	2.5	60	-	1.25	1.25	-	2.84
Outlet (4g)	21	125.7	0.427	-	-	21	1.98
Outlet (4s)	2.5	105.7	0.818	0.09	1.25	1.16	1.82
Outlet (5)	22.16	124.9	0.438	-	-	22.16	1.98
Outlet (10)	1.34	101.6	-	0.50	1.25	-	2.27

4.4Pinch Analysis

In order to apply PA to drying, it is important to determine a method of addressing composition changes over units, such as the evaporation of water and direct contact heat and mass transfer within the dryer. This consideration will help with the visualisation aspects of PA, especially when considering options to integrate the dryer into larger systems.

For a general starting method, based on the works of Kemp [61, 74], it is recommended to ignore any internal processes, such as the inner workings of the dryer and focus on the energy flows on either side of the drying system.

Once the MEB's have been completed on the peripheral systems (Tables 4-1 and 4-3), it is possible to combine each of the potential heating (hot side) and cooling (cold side) streams for the system to give a simple view of the energy flows over each temperature range. Some pinch texts [23-25, 61, 69] recommend using a pseudo-temperature for each of the streams i.e. a temperature offset between interacting streams.

This approach is required to get a reasonable offset. For this work 20^OC was assumed, and this was based on the typical starting assumptions presented by Kemp [61]. The purpose of this energy offset is to ensure that the representation of the system is feasible and does not violate any kinetic or thermodynamic laws e.g. Heat is not transferred against a temperature gradient.

The large temperature offset is also used for the dryer (even though it is specific to heat exchange systems) for a few reasons. The first being for consistency within the PA, in order to allow for the visual representation of the dryer to be consistent with the system, having a

different pseudo temperature difference may offset the dryer's position on the plot, even to the point of causing an edge case inconsistency in the PA where the dryer incorrectly resides entirely above the pinch point. The second is to allow for a simple estimate for thermal efficiency losses of drying (a deviation from an outlet equilibrium), which may be a result of the drying resonance time being shorter than required.

4.4.1Adding the Dryer to Pinch

In this work, the addition of the energy changes within the dryer to the PA was used to demonstrate how the energy within the dryer may be used or augmented to save the external energy inputs.

In order to show a representation of what may be happening within the dryer, a linear approach at two extremes was used, these two extremes can be defined as the sensible heat load, and the evaporative heat loads in isolation as shown in the two-step method outlined in Chapter 2, the resulting triangle being the possible area of the dryer curve. This approach then provides generalised regions for where the dryer system curves would most likely to be located, which will be further referred to as a Conservative Region Estimate (CRE). Similar approaches have been used to estimate energy profiles in other mass and energy transfer systems with some success [19].

The three lines of the CRE boundary are:

- The thermal only energy change, i.e. if each side of the dryer remains a separated stream throughout the dryer, as shown in Figure 4-8, at the same overall composition throughout the dryer, reaching an equilibrium temperature. The overall outlet solids moisture content is unchanged, i.e. if the dryer is a heat exchanger only.

- The in-out line, representing the results from the MEB. This line is the overall result of the other two lines, the thermal change, and the non-thermal change.

- The remaining difference that is required from the thermal line and the MEB line represents the non-temperature related energy changes within the dryer and separator. This line is close to horizontal on the plot.

It is important to note that the exit stream of a co-current dryer is typically well mixed and not two separated streams. For the overall system of drying to be considered, the system shown in Figure 4-9 is combined and used as the dryer component of the analysis.

These three lines give the two regions as shown in Figure 4-10, which are to be accompanied by the hot and cold composite curves for the pre- and post-treatment flows before and after the dryer. This approach is based purely on a MEB, not a dryer kinetics model, and because of this point, it should only be used as a guide.

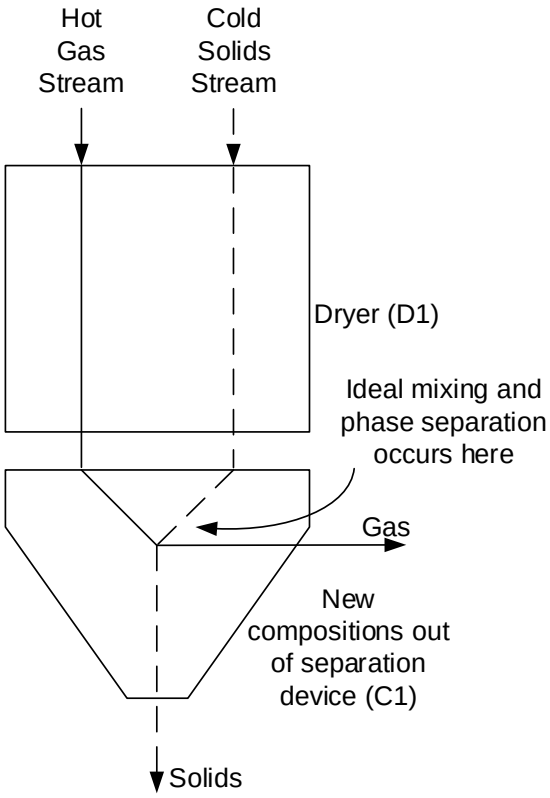

Figure 4-8: The representation of the MEB simplification for the dryer and solids removal system.

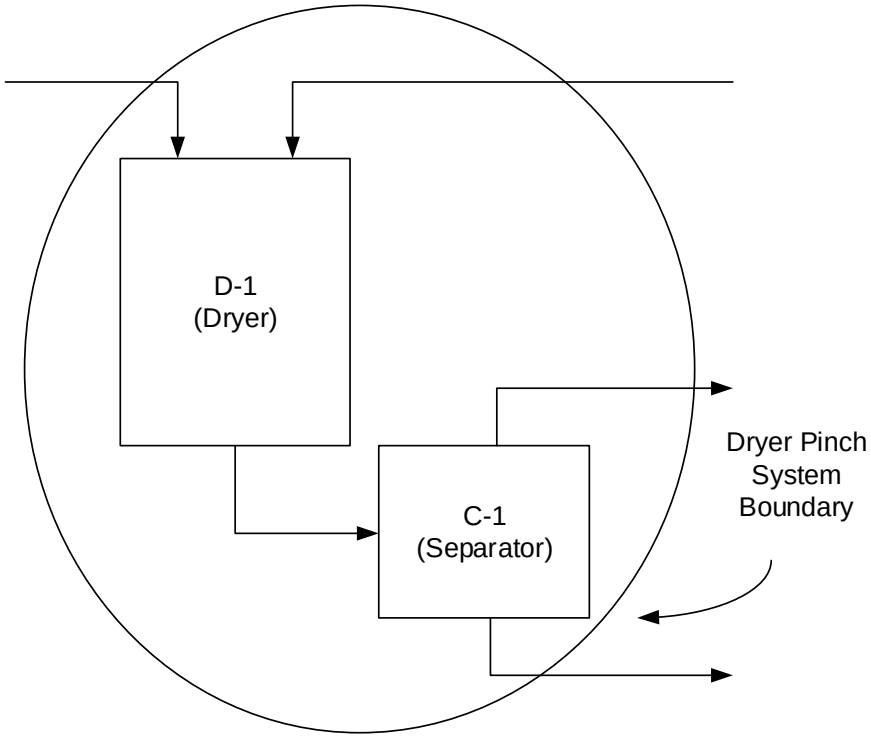

Figure 4-9: The system boundaries for the dryer system curves used in PA.

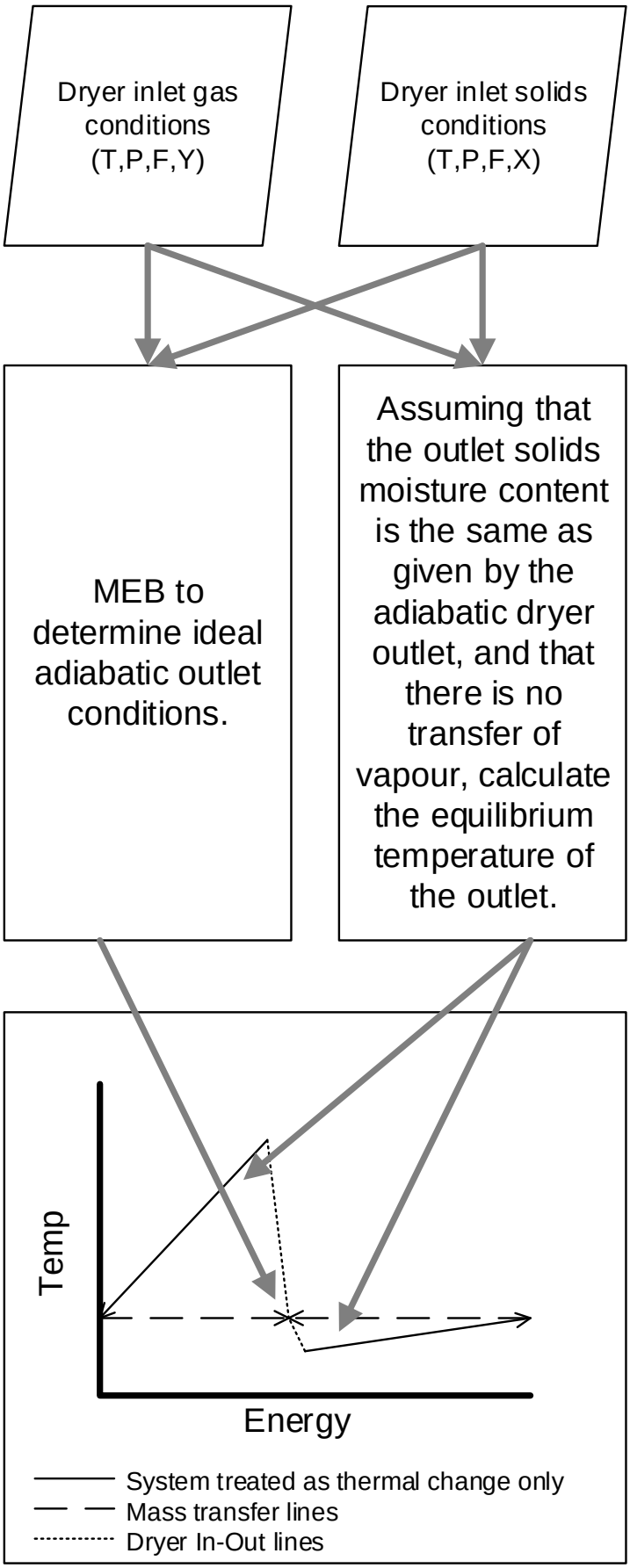

Figure 4-10: The flowchart for calculating the estimates for the different regions.

Required Data

This method requires:

- Temperature changes in all streams
- Flow rates
- Heats of reaction (if any)
- Heat capacities of each stream
- Phase change information

Methodology

Firstly, the temperature-energy profiles for all of the streams need to be recorded in a table as it is necessary to determine if the streams need cooling (hot side) or heating (cold side).

A temperature offset is applied to each side: (+) for cold and (-) for hot side. These offsets are needed to create more realistic temperature profiles and to allow for the stream temperatures to never meet exactly (a finite temperature approach) at the ends of the heat exchangers. In this example $20^{O}C$ was used ($+10^{O}C$ to the cold side, $-10^{O}C$ to the hot side). This offset was selected based on the texts of Kemp [61], where $20^{O}C$ was used as a reasonable starting point. This offset can be changed at a later stage of the design process to optimise each heat unit further.

The streams are named as follows:

- H1: the solids cooling to ambient conditions
- H2: the flue cooling to saturation
- H3: the flue to ambient cooling (mixed simple and phase change)
- C1: the solids feed pre-heater
- C2: the air feed pre-heater (heat exchanger)
- C3: the air feed heater

The intermediate steps for the phase change have been omitted here since there is no clear temperature or curve for the air/water system within the dryer, so a linear end point analysis was chosen. This estimation method results in a more detailed energy profile needing to be analysed when designing the heat exchanger, or a conservative view on the sizing will need to be utilised in any design stage of the analysis.

Temperature ranges need to be determined based on the streams. Each starting and ending point for a stream should have a temperature associated with it. For example, stream H2 goes from 63.6^{O}C down to 23.7^{O}C, while H1 goes from 47.6^{O}C down to 15^{O}C (from the MEB in Table 4-1). In this case, it would represent three temperature regions: one where only H1 needs cooling, one where both H1 and H2 need cooling, and one where only H2 needs cooling. This analysis is repeated until all stream temperature ranges are met, as shown in Table 4-5.

Table 4-5: The stream profile table used for pinch analysis (Air).

Temp. (^{O}C)	**<-- 15**	**<-- 23.7**	**<-- 35**	**<-- 47.6**	**<-- 63.6**	**<-- 67.6**	**<-- 70**	**<-- 180**	**<-- 200**	**Total (kW)**	**m.Cp (kW.K^{-1})**
H1 (10-11)	20.1	26.2	29.1	-	-	-	-	-		75.3	2.3
H2 (5-6)	-	264.7	294.3	373.7	-	-	-	-		932.8	23.4
H3 (6-7)	1,966.5	-	-	-	-	-	-	-		1,966.5	226.6
C1 (8-9)	-	-	89.4	113.5	28.6	17.1	-	-		248.6	7.1
C2 (1-3)	-	-	265.8	337.6	84.9	51.0	2,323.4	422.4		3,485.2	21.1
Dh (3-5)	-	-	-	-	10.1	6.1	277.0	-		293.2	2.5
Dc (9-10)	-	-	-	-	-	293.2	-	-		293.2	121.5

Further clarification on Table 4-5 is that the each cell within the table is the energy load for that stream between the temperature in the column, and the temperature in the column to the right – for example the cell (row H2, column <--35) refers to the energy required in that interval, as shown here.

$$\Delta H = mCp\Delta T$$
$$= 23.4 \times (47.6 - 35)$$
$$= 294.3\ kW$$

Where:

$$mCp = 23.4\ kW.K^{-1}$$
$$\Delta T = (47.6 - 35)\ K$$

This table (Table 4-5) is a useful intermediate step for pinch analysis as it then allows for the addition of energy loads within each temperature interval, so batch processing can be achieved in a straightforward manner. From here, the summation of the total heating and cooling requirements within each temperature region are accumulated and tabulated in the first three columns of Table 4-6.

The temperature change in the region (column 4) and average heat flux is found (column 5) in Table 4-6, and then the total required energy per region is calculated (column 6). Alternatively, the energy per region may be found directly from columns 2 and 3 using Equation 4-2. These interval energy requirements are then summed cumulatively, or cascade from hot to cold representing a system where the excess heat from one interval is fed into the next.

$$interval\ energy = \sum (|Q_{Hot}| - |Q_{Cold}|) \quad \text{4-2}$$

-[61]

In order to find the required utilities, the cascaded energy profile should be used. The minimum heat required for the system is the most negative number, highlighted for ease of viewing in Table 4-6. This minimum heat is then used to start the new summation from hot to cold, giving the minimum heating utility requirement and the required cooling utility.

Table 4-6: The overall profile and cascade pinch profiles (Air).

	Hot (kW)	Cold (kW)	ΔT (K)	Cp_H-Cp_C ($kW.K^{-1}$)	Interval (kW)	Cascade (kW)	New (kW)
Heat Utility						**0.0**	**3,036.6**
200-180	0.0	422.4	20.0	-21.1	-422.4	-422.4	2,614.2
180-70	0.0	2,323.4	110.0	-21.1	-2,323.4	-2,745.9	290.7
70-67.59	0.0	68.1	2.4	-28.2	-68.1	-2,814.0	222.6

67.59-65.69	0.0	53.5	1.9	-28.2	-53.5	-2,867.5	169.1
65.69-63.57	0.0	59.9	2.1	-28.2	-59.9	-2,927.5	109.2
63.57-47.59	373.7	451.1	16.0	-4.8	-77.3	-3,004.8	31.8
47.59-35	323.4	355.3	12.6	-2.5	-31.8	**-3,036.6**	0.0
35-23.68	290.9	0.0	11.3	25.7	290.9	-2,745.7	290.9
23.68-15	1,986.5	0.0	8.7	228.9	1986.5	-759.2	2,277.4
Cold Utility							**2,277.4**

From Tables 4-5 and 4-6, it is clear that the pinch temperature is 35^{O}C where the cascaded energy flow is at its minimum.

The composite curve(s) can be constructed from the last column of Table 4-6. Taking the hottest temperature as the utility point, i.e. for the hot curve, the lowest point is at 15^{O}C, while the lowest temperature for the cold curve is 35^{O}C. The overall or Grand Composite Curve (GCC) is the plot of the right-most column as a function of temperature; the GCC is the cascade energy plot and is very useful for system integrations.

4.4.2Pinch Analysis: Convective Air Dryer

The hot and cold side composite curves for this system are shown in Figure 4-11. Using the cooling utility calculated in Table 4-6 as the offset for the hot process curve prevents any negative net energy flows, and ensure that no part of the cold side curve is above the hot side curve. The additions of the dryer curves to these plots, Figures 4-11, 4-13, and 4-14 (which were calculated based on the procedure described in the section 4.4.1), can be important in energy utilisation and auditing, so several different ways of doing this step have been investigated.

Figure 4-11 shows the potential regions where the dryer is most likely to operate. This is an important visualisation as it shows both the thermal changes and the overall dryer curves, with the resulting line representing the mass transfer component of the drying system as described in section 4.4.1.

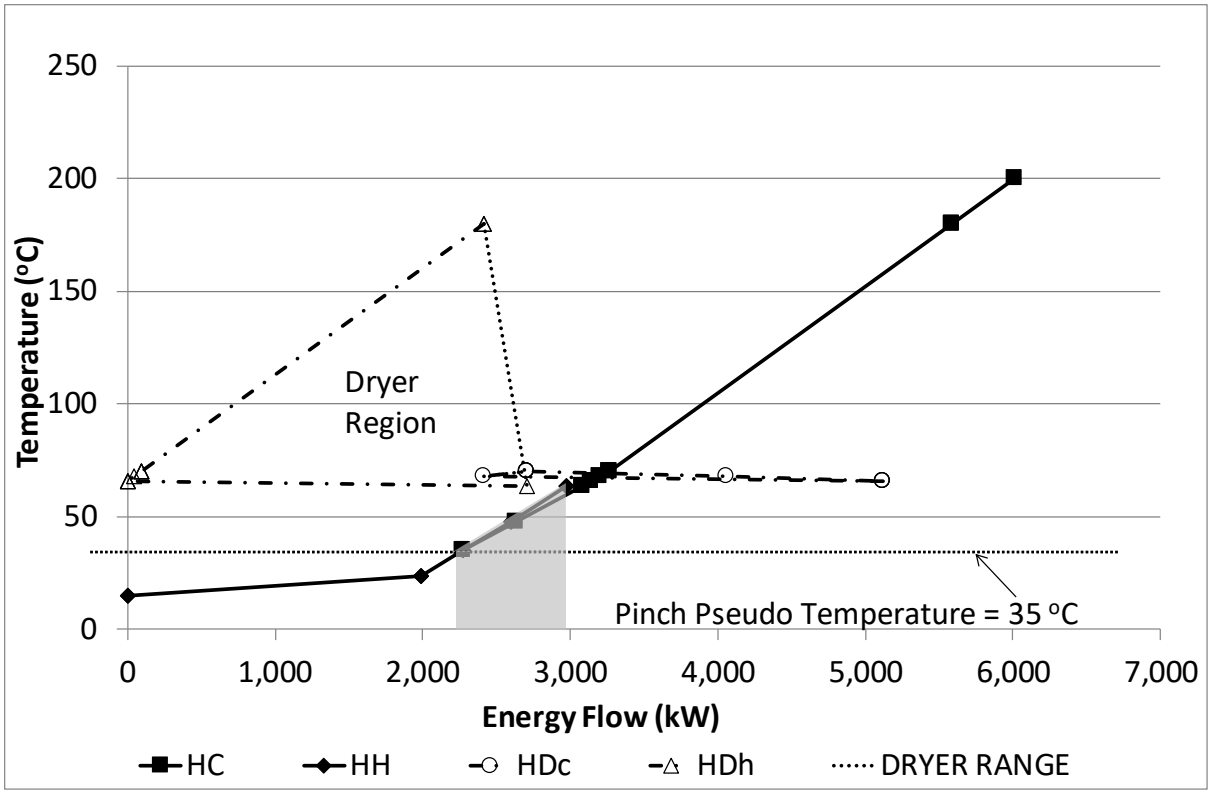

Figure 4-11: Pinch plot for the convective air dryer system with the dryer triangles (Figure 4-10) as described on page 113 (Conservative Regions Estimate).
NOTE 4-1: HC refers to enthalpy of cold, HH refers to enthalpy of hot, HD refers to enthalpy of each dryer section.

The above representation of a pinch plot involving a dryer (Figure 4-11) is simple in nature and has the core components of the external systems. It is clear that the system pinch temperature is different to the outlet temperature of the dryer, which is the internal pinch for the dryer. Given this and observing that there is very little energy recovered from condensation in the flue gas, it appears that the system is not operating at its full potential. This situation can also be seen in Figure 4-11.

The effectiveness of heat recovery using PA may be increased by reheating the flue gas and recirculating the humid air to another drying stage. This process would then increase the moisture content of the flue gas to the point where condensation can occur at a high enough temperature to recover even more energy. This hypothesis will not be tested here as only a single-stage dryer has been studied for this chapter.

Removing the extra cooling equipment (solids cooler and secondary flue cooler) provides a very similar result, since the flue-feed exchanger is represented by the grey region on Figure

4-11, of which the lower end is the pinch temperature. This heat exchanger is useful in reducing the total energy requirements of the plant by as much as 25-30% at higher inlet temperatures (220^{O}C or more). A saving of 18% occurs from pre-heating the feed gas and solids feed with the outlet gas, compared with a non-recovery system for an inlet gas temperature of 190^{O}C.

This exchanger becomes more important as the inlet gas temperature rises. This result occurs because both the outlet temperature and the outlet humidity (not to be mistaken with relative humidity) also rise, allowing more condensation to occur in the heat exchanger. As the feed temperature increases, the total energy requirement also needs to increase, giving an increased effectiveness, allowing the energy recovery percentage to increase only slightly, meaning the total energy wasted increases significantly. The total energy saving found within the air system at 190^{O}C is estimated to be 670 kW, with a further 3.0 MW required for the system, giving an outlet moisture content of 113 $g_W.kg_S^{-1}$. Increasing the inlet temperature to 220^{O}C yields figures of 24% recovery with 1.08 MW saved and 3.1 MW still required for an outlet solids moisture content of 62 $g_W.kg_S^{-1}$. The results of this sensitivity analysis can be seen in Figure 4-12.

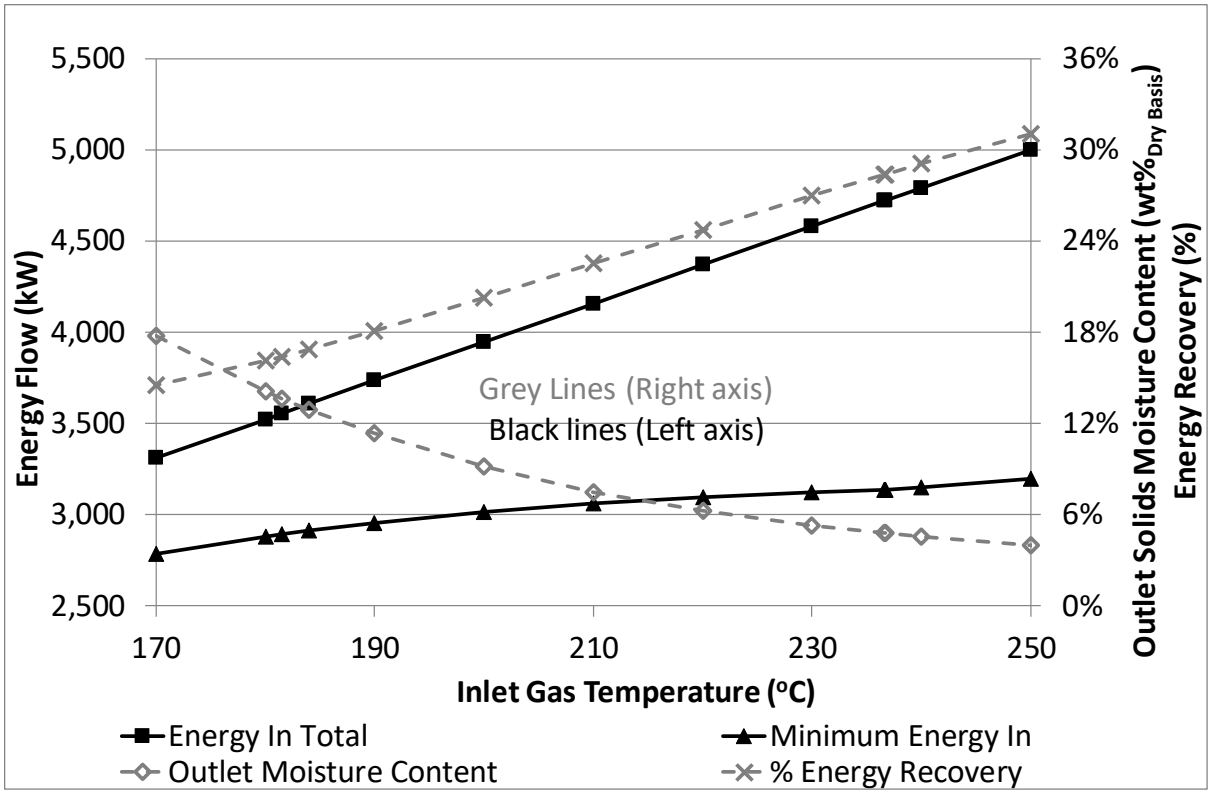

Figure 4-12: The effect of inlet air temperature on the PA of the convective air system.

Figure 4-13 shows only the in-out curves for the dryer. Figure 4-13 is a simplified version of Figure 4-11 and is an overall representation of the final dryer system. Note also that these curves have not been added to the pinch plot, as no integration is available at this stage. If there was a heat source that needed to be cooled before being discharged, it could be used as a temperature booster within the dryer, or be integrated into the pre-heating system.

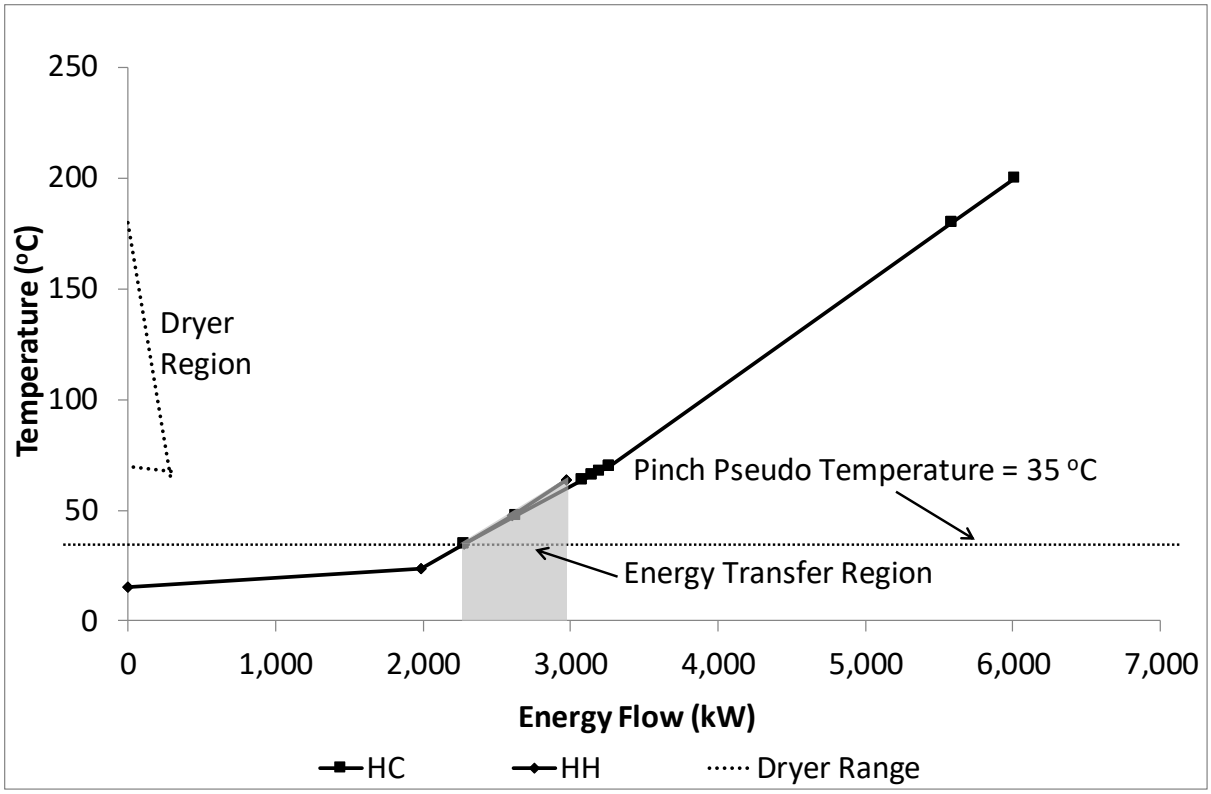

Figure 4-13: The in-out pinch analysis of the convective air dryer (using end points only).
NOTE 4-2: The Dryer Region shown in this image differs from that in Figure 4-11 due to only showing the endpoint (overall) lines, this was used to highlight the difference between internal and external effects more clearly.

These curves show that there is no unique way to represent the system for all conditions and dryer arrangements, or for an overall analysis of the system, to identify energy saving areas. Ideally if the actual dryer profiles are determined, they should be put in place of the dryer region or in-out representations shown here.

Figure 4-14 shows the Grand Composite Curve (GCC), discussed after Table 4-6, for the air dryer system and is very useful for utility analysis and process options. The GCC is constructed by calculating the net surplus energy per interval available in the system and is a useful way to see the pinch point(s). The GCC is the representation of the final column of Table 4-6 and is the easiest graphical approach to determine the optimum utility qualities and quantities required. For this work and this simple two-stream system, this analysis is adequate. For more complex systems, a full PA is required to make an informed choice regarding the heat exchanger network required.

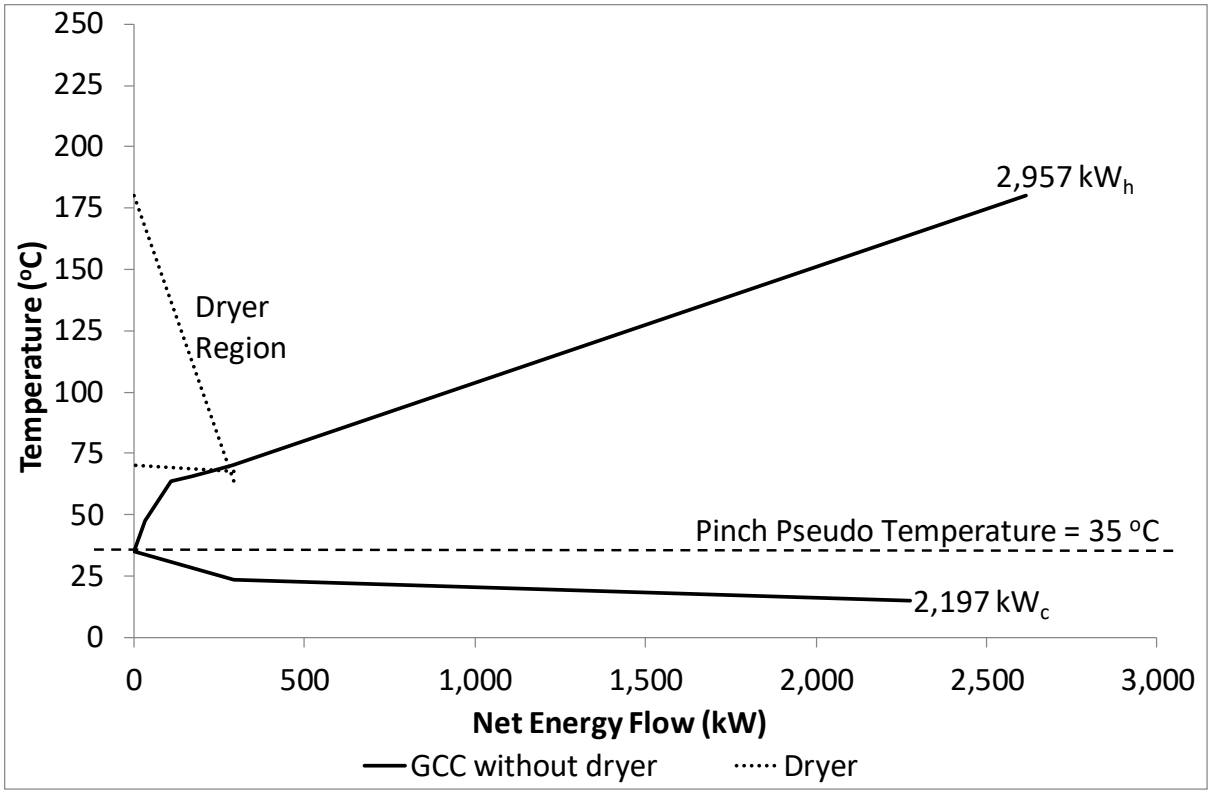

Figure 4-14: The GCC for the air system, which is the graphical representation of the last column in Table 4-6.

Now that the analysis for the air system has been completed, the superheated steam examples will be analysed and the results of these two PA will be compared with the results of the inversion temperature to demonstrate the suitability of both methods for rapid analysis as a starting point for an energy evaluation of drying systems.

In order to compare these convective air results with those of the steam example, the procedure will be repeated for the superheated steam example. Pinch Analysis: Superheated Steam Dryer

The streams are named as follows:

- H1 : the solids cooling to ambient
- H2a : the flue cooling system (steam to dew point)
- H2b : the flue cooling system (steam to condensate)
- H2c : the flue cooling system (condensate to ambient)

- C1 : the solids pre-heater
- C2 : the steam re-heater

The hot and cold curves for the purge valve example are shown in Figures 4-15, and 4-16. Tables 4-7 and 4-8 are the pinch tables for the steam system utilising a partial condenser as the steam purge device.

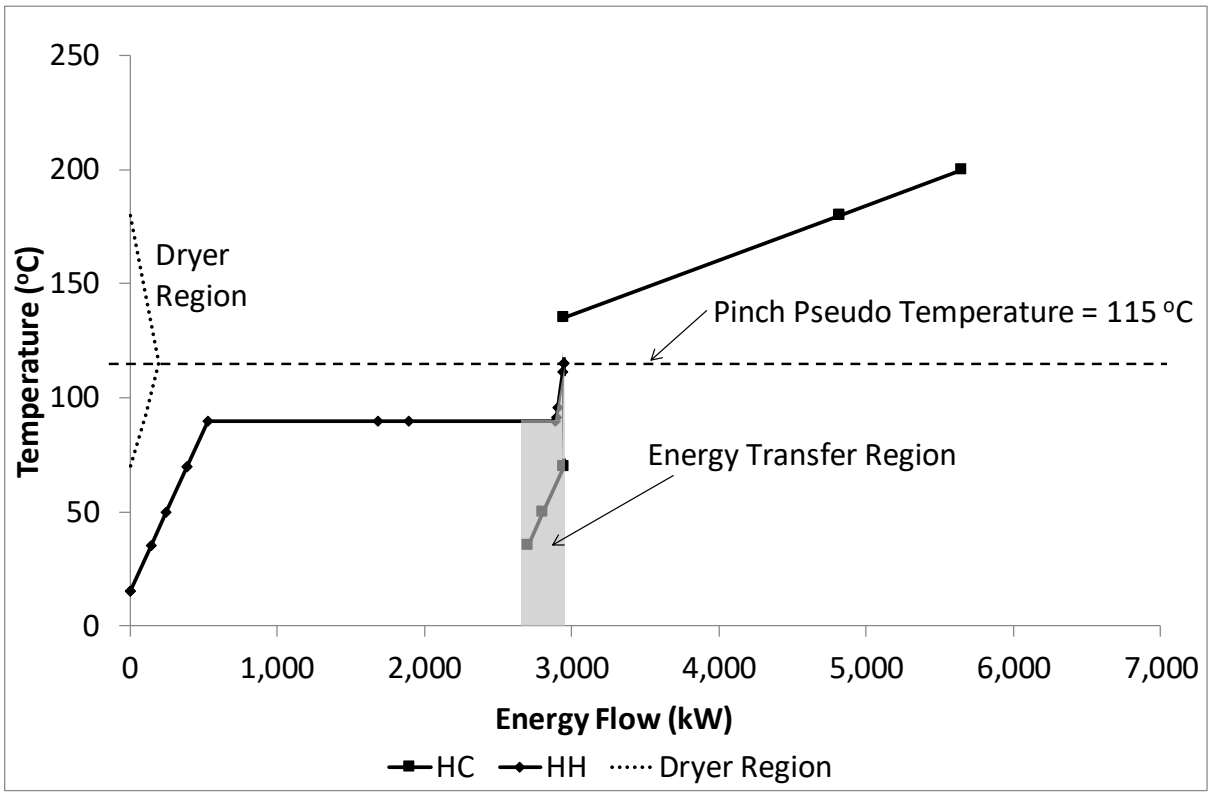

Figure 4-15: The hot and cold curves for the superheated steam dryer.

Table 4-7: The stream profile table used for PA (SS).

Temp. (^{O}C)	<-- 15	<-- 35	<-- 70	<-- 90	<-- 91.6	<-- 95.7	<-- 111.6	<-- 114.9	<-- 115.7	<-- 134.9	<-- 180	<-- 200	Total (kW)	Cp ($kW.K^{-1}$)
H1 (10-11)	45.2	79.1	45.2	3.6	-	-	-	-	-	-	-		**173.0**	**2.3**
H2a ($6\text{-}7_{DP}$)	-	-	-	3.6	9.5	36.3	7.6	-	-	-	-		**56.9**	**2.3**
H2b (6-7c)	-	-	-	2,358	-	-	-	-	-	-	-		**2,357.9**	**--**
H2c (6-7a)	96.9	169.6	96.8	-	-	-	-	-	-	-	-		**363.2**	**4.8**
C1 (2-3)	-	-	-	-	-	-	-	-	-	1,873	829.8		**2,702.4**	**41.5**
C2 (8-9)	-	248.6	-	-	-	-	-	-	-	-	-		**248.6**	**7.1**
Dh (3-5)	-	-	-	-	-	-	-	2.5	57.9	136.4	-		**196.8**	**3.0**
Dc (9-10)	-	-	4.6	7.5	19.6	75.1	-	-	-	-	-		**196.8**	**4.7**

Table 4-8: The overall profile and cascade pinch profiles (SS).

RANGE	Hot (kW)	Cold (kW)	ΔT (K)	Cp_H-Cp_C ($kW.K^{-1}$)	Interval (kW)	Cascade (kW)	NEW (kW)
Heat Utility						**0.0**	**2,702.4**
200-180	-	829.8	20.0	-41.5	-829.8	-829.8	1,872.6
180-134.9	-	1,872.6	45.1	-41.5	-1,872.6	**-2,702.4**	-
134.9-114.9	-	-	20.0	-	-	**-2,702.4**	-
114.9-111.56	7.6	-	3.3	2.3	7.6	-2,694.8	7.6
111.6-95.7	36.3	-	15.9	2.3	36.3	-2,658.5	43.9
95.7-91.6	9.5	-	4.1	2.3	9.5	-2,649.0	53.3
91.6-90	2,365.1	-	1.6	1,478.2	2,365.12	-283.9	2,418.4
90-70	142.0	-	20.0	7.1	142.0	-142.1	2,560.3
70-35	248.6	248.6	35.0	-	-	-142.1	2,560.3
35-15	142.1	-	20.0	7.1	142.1	-	2,702.4
Cold Utility							**2,702.4**

Comparing this example with that of the air system above, the energy savings are 250 kW of the 2,950 kW total heating requirement. This amount is a saving of 8.4%, but this is not where the greatest saving can come from the steam system. Taking into account the lower region of condensation below the system pinch, and the dryer outlet temperature, there is still another 2,450 kW of energy available in the form of condensing steam, producing a total energy recovery potential of 91%.

This amount is sizable and can be integrated readily with other systems. Hence, for this example, the air system has a better internal energy saving potential of 18% compared with

the 8.4% for the steam system, while the steam system has far better overall energy saving potential when integrated with other unit operations. This result occurs because the steam system has the ability to recover all of the latent heat of evaporation from the steam by condensing the outlet vent stream.

The result of changing the inlet temperature on the energy saving potential of the steam system is shown in Figure 4-16. It is clear that, when compared with Figure 4-12, the steam system is far less sensitive to changes in the inlet temperature than the air system. The GCC for the steam system is shown in Figure 4-17.

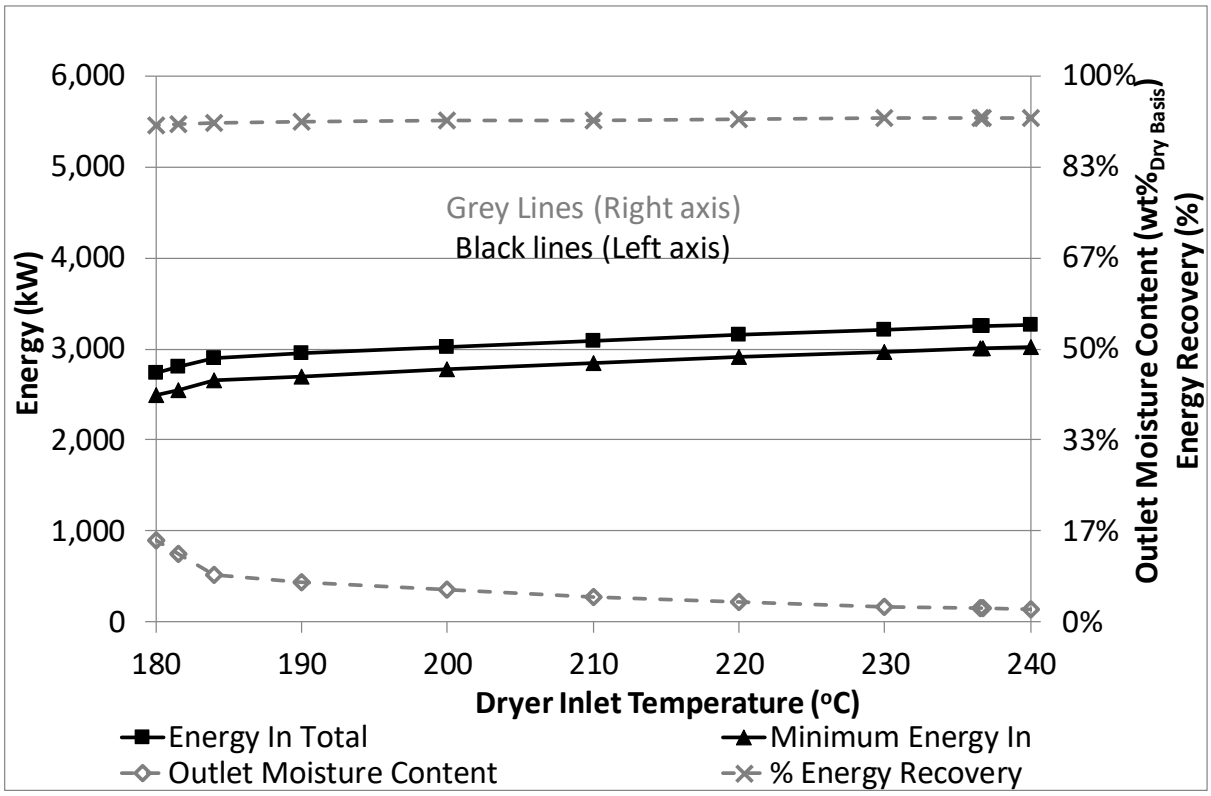

Figure 4-16: The effect of temperature on the steam system (sensitivity).

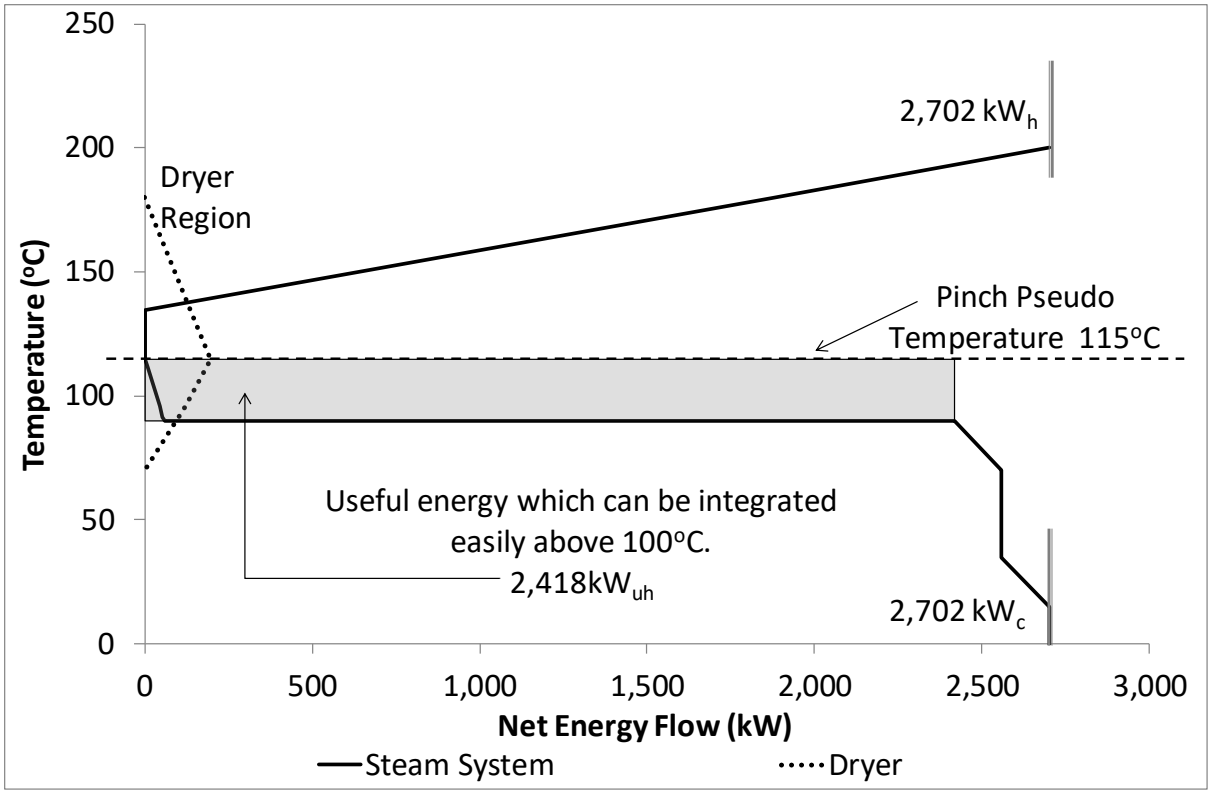

Figure 4-17: The GCC for the superheated steam system, which is the graphical representation of the last column in Table 4-8.

4.4.3Pinch Discussion

Within the steam system, the pinch temperature is the same temperature as the outlet to the dryer. This result is a good indication that the dryer is the pinch limiting unit for the system, and the pinch analysis will be highly reliant on the conditions leaving the dryer. As a result of this, the most important changes to the system are to the dryer, and not to the peripheral system. This situation is not the same for the air system, with a pinch temperature that is close to ambient conditions. This result indicates that the energy recovery system is the most important component of that thermal system.

From the GCC's for the air and superheated steam systems (shown in Figure 4-18), it is clear that the energy profiles within the dryers are not too dissimilar (based on the input-output analysis). The hot side (top part of the curve) is almost identical between the air and steam systems, until the steam system hits the pinch. The gas temperature for the air system keeps dropping at the same energy rate until it reaches its equilibrium point, which is much cooler.

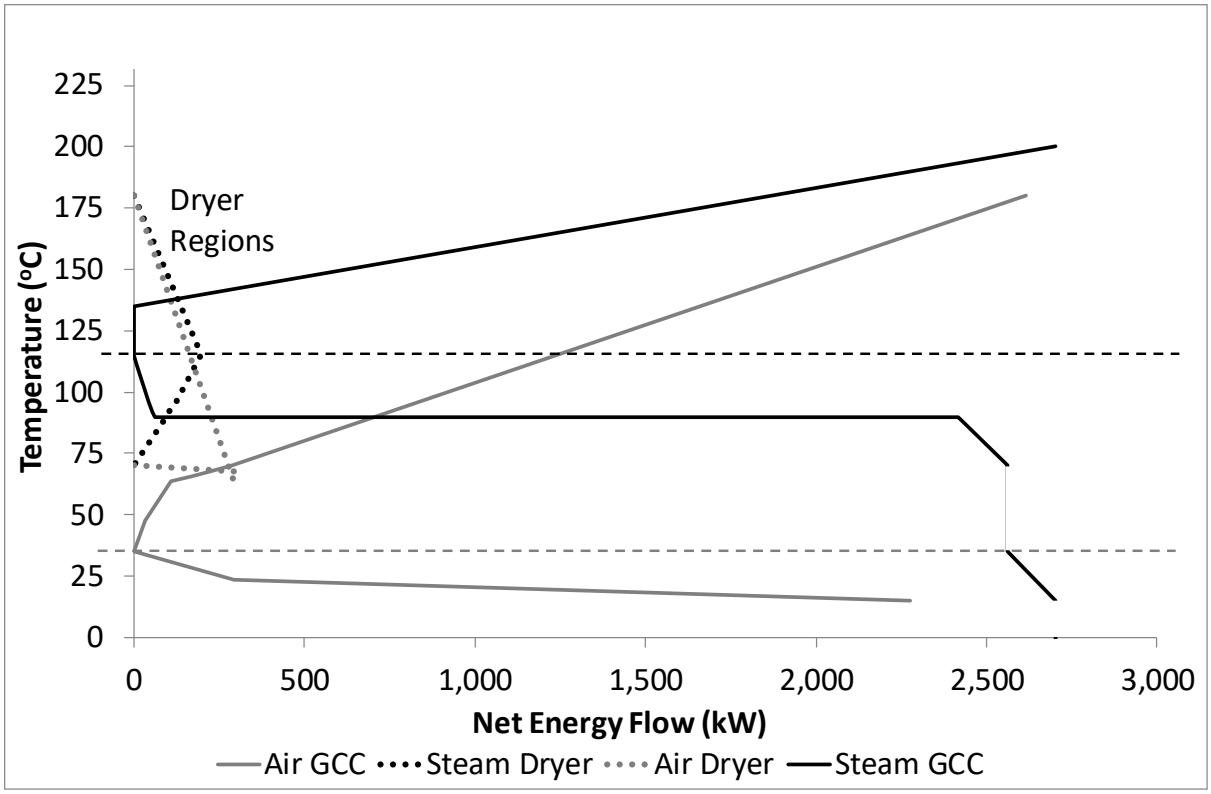

Figure 4-18: A direct comparison between the air and superheated steam dryer GCC curves.

The energy for the external systems are significantly different, especially below the pinch temperatures, which means that there is more need for cooling fluid overall in a superheated steam system than for an air system and with a larger range of temperatures. This situation may become more significant when the system boundaries are changed, i.e. removal of the extraneous cooling heat exchangers such as the solids cooler (E-5) and the condensate cooler (E-3) (from Figure 4-4). Also note the sharp profile at the pinch for both systems, which may allow the use of a heat pump or a similar change based on an exergy analysis.

4.5Discussion

There are physical limitations to both dryers that have been taken into consideration, such as the dew point temperatures for the outlet (saturation conditions). Adding these limitations to the dryer model and adding an offset between the solids and gas outlet temperature of 20^{O}C, as described in the mass balance section (Sections 2.9.1 and 3.5), it becomes clear that the system limitations occur above the 182^{O}C ASIT. This result means

that there is not enough energy to dry the solids sufficiently below the calculated limit of 184^{O}C.

In this section, only a MEB over the dryer has been utilised, and as such a drying-rate model has not been used to confirm the findings of the inversion temperature. Instead a PA has been used to confirm if the dryer system is related to the energy utilisation within the dryer itself. The results of the PA confirm that the steam system is indeed less energy intensive, which results in a better energy recycle potential, as shown in Figure 4-18. This has implications for the difference in total energy savings and for energy utilisation. Energy savings will ultimately occur on the heat recovery and recycle sides of this analysis, while the rate at which the dryer operates is more linked to the size and effectiveness of the dryer (which are not studied in detail here).

A sensitivity analysis was carried out for the MEB model and PA results, and Figures 4-19, 4-20 and 4-21 show the results of this analysis.

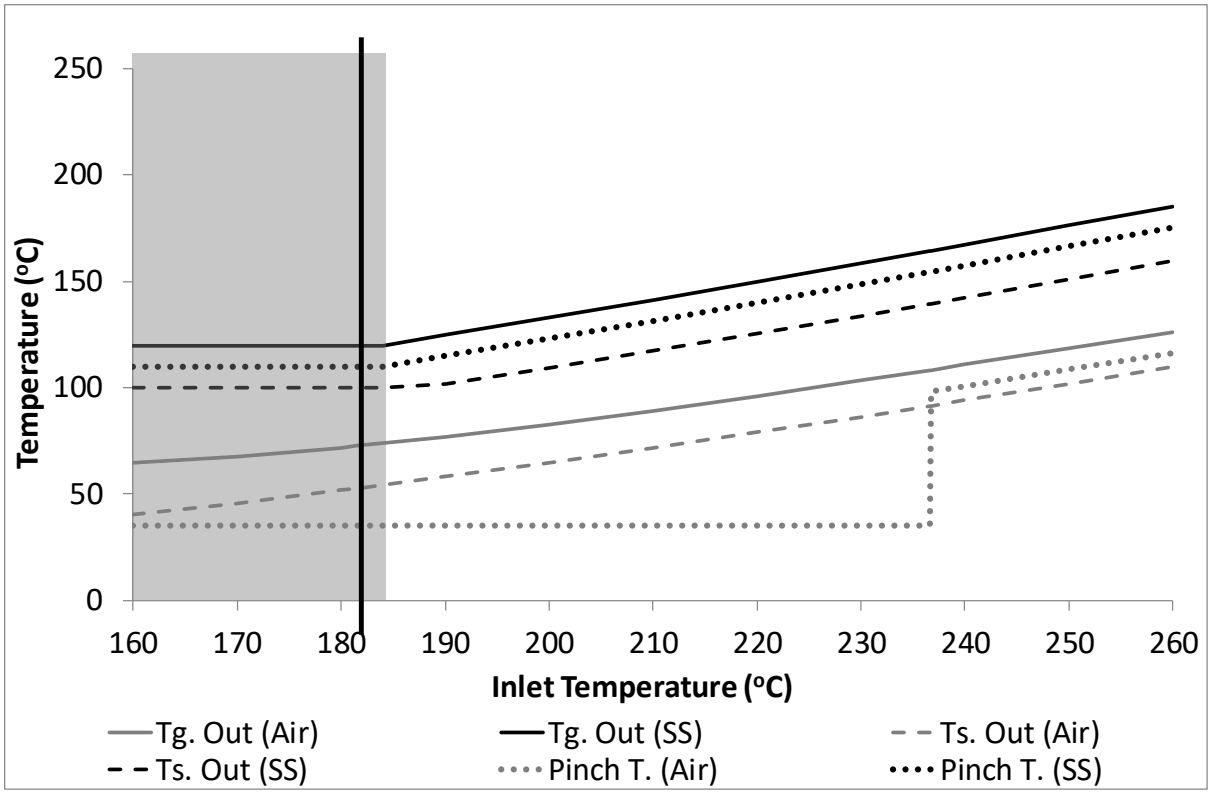

Figure 4-19: The temperature profiles of the dryers as a function of inlet gas temperature (21 kg.s^{-1} air flow rate).

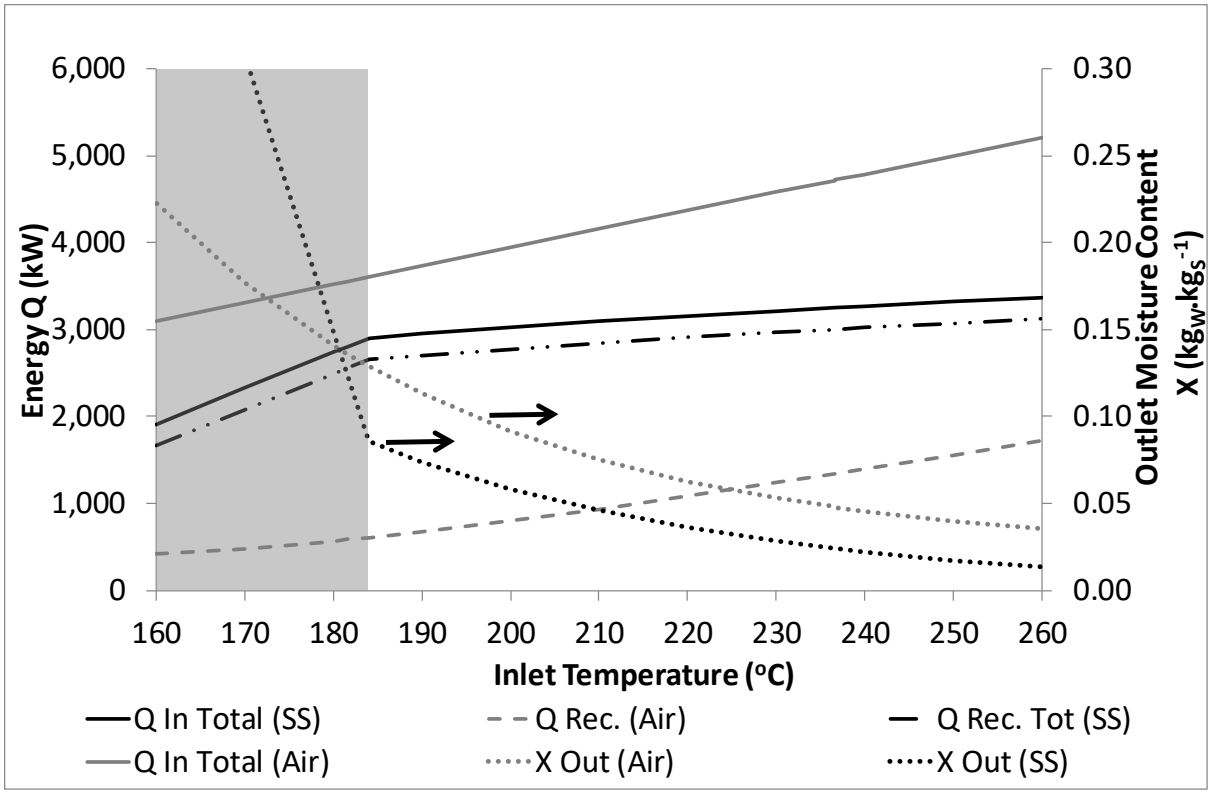

Figure 4-20: The energy profiles of the dryers as a function of the inlet gas temperature (21 kg.s^{-1} air flow rate). Lines are on the left axis unless marked.

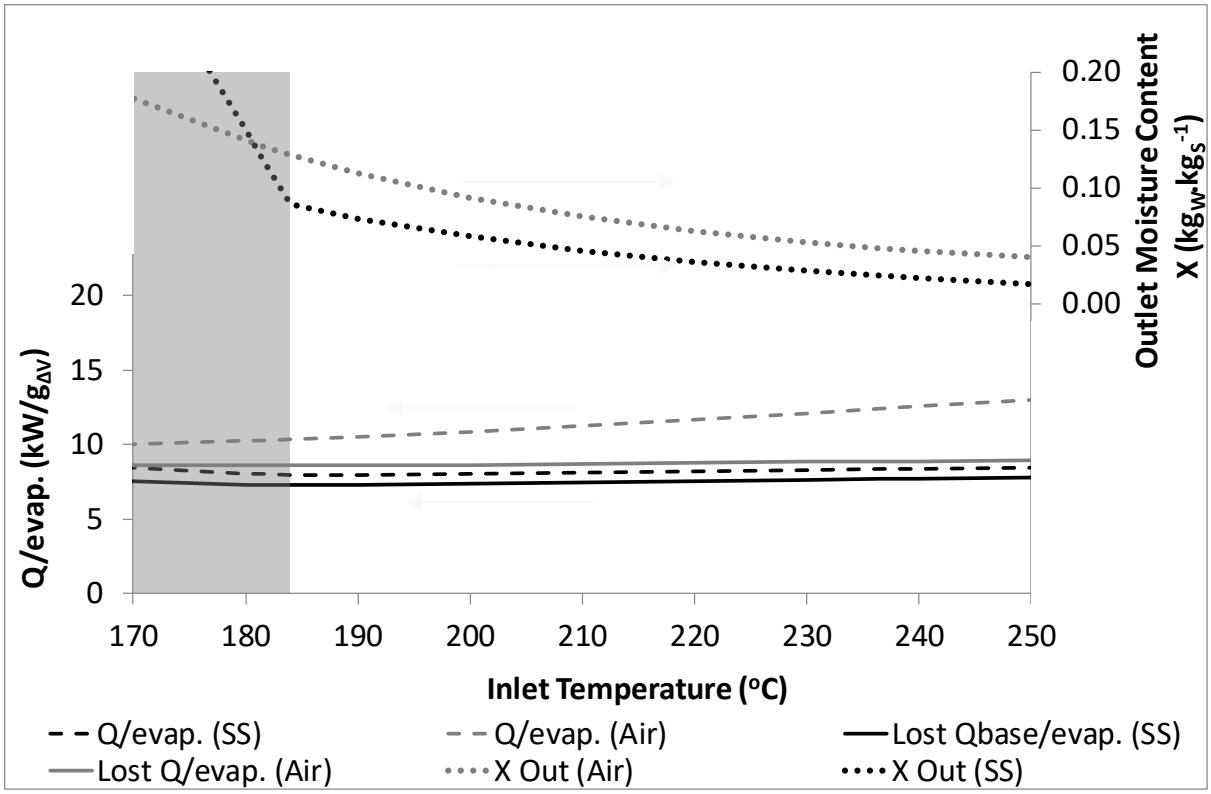

Figure 4-21: The energy use and loss per moisture evaporation profiles for the dryer, as a function of the inlet gas temperature (21 kg.s^{-1} air flow rate).

The pinch temperatures for each system are also plotted in Figure 4-19, and from this figure it becomes clear that the dryer is the limiting unit of the PA for the steam system. The pinch temperature is approximately equal to the dryer outlet temperatures, indicating that the dryer outlet is the pinch point. However, it is not the pinch point for the air system since 35^{O}C is the pinch temperature for inlet gas temperatures up to 238^{O}C. Above 238^{O}C the outlet temperature becomes the same as that of the steam system.

Noticeable results from Figure 4-20 are that the direct recoverable energies from both the air and steam systems are small in comparison with the required energies. The gradient of the recovered energy for the air dryer is still not as steep as the inlet energy gradient, which means that more energy is being wasted. On the other hand, looking at the overall energy recovery profile for the steam system *Q. Rec. Tot (steam)*, this curve closely follows the inlet energy requirements, meaning that the total recoverable energy for the steam system is quite high.

It must also be noted that, since the steam system is primarily a recycle system, the start-up energy requirements have not been considered, and would become less significant the longer the system is in continuous operation. Figure 4-20 also has the plot of the moisture content of the solids at the outlet, which shows a diminishing effect of temperature on the evaporation of moisture above 184^{O}C. This effect relates to outlet solids moisture specifications. For example, for a moisture content of 0.05 kg of water per kg of solids, the steam inlet temperature required is 205^{O}C, while the air system requires 232^{O}C.

Figure 4-21 shows the energy required per unit of evaporated water. It is clear that air requires more energy in relation to steam as the specified moisture content decreases and the inlet gas temperature increases. From these plots it appears that the steam system is less reliant on the inlet temperature being above 184^{O}C than the air system; the air system wastes more energy for every kg of evaporated water above this temperature. The steam system also has the same trend, but it is far less severe.

Figure 4-21 also shows that the energy lost for the steam system stays low at higher temperatures, while the air system loses more energy as the temperature increases. This effect is also seen in Figures 4-12 and 4-16. Since the steam system includes a recycle where the excess steam is purged continuously, the pinch energy profile is almost identical to the heating requirement for the system. Another side effect is that, since all of the feed is purged at ambient conditions and fed at ambient conditions (in this analysis), all the evaporated liquid is condensed, and thus the cooling requirements will match the heating requirements for the superheated-steam system.

This result suggests the inversion temperature is useful for dryer sizing because it is a kinetics-based estimate of drying. This feature is not sufficient to understand the energy utilisation within or around the dryers, so it is important that the inversion temperature is integrated with a MEB to determine any system limitations, which the IT does not take into consideration. From there a simple PA can be used to further optimise the system in terms of heat recovery, or the thermodynamic performance of the system. In effect, the combined approach of the drying kinetic parametric analysis and a system-wide thermodynamic analysis can give a more balanced assessment of the system than either on its own. The inversion temperature gives an indication of dryer size by using a kinetics-based evaluation,

similar to a capital cost (CAPEX) comparison, while the pinch temperature, which determines recoverable energy by using a thermodynamic method, produces an operational cost comparison (OPEX), even if other factors are not taken into account, such as capital costs for other equipment, labour costs, maintenance, and other running costs.

It must also be noted that the air system is more sensitive to inlet gas temperature changes than the steam system, as shown in Figure 4-20, where the required energy input for the air system *Q in Total (Air)* increases significantly with temperature, while the steam system does not. This result means the steam system is less sensitive to temperature changes for energy utilisation within the dryer than the air system, yet both are equally sensitive in terms of the outlet solids moisture content as a function of inlet gas temperature fluctuations.

Also, for the calculated IT, the flow rates of the humid air and superheated steam systems were the same. This situation means the comparison would not be complete without comparing the effect of gas flow on the system. This comparison has been done for the same values as for the temperature profiles (Figure 4-22, 4-23, and 4-24). The mass flow rate of air is assumed to be equal to the mass flow rate of steam.

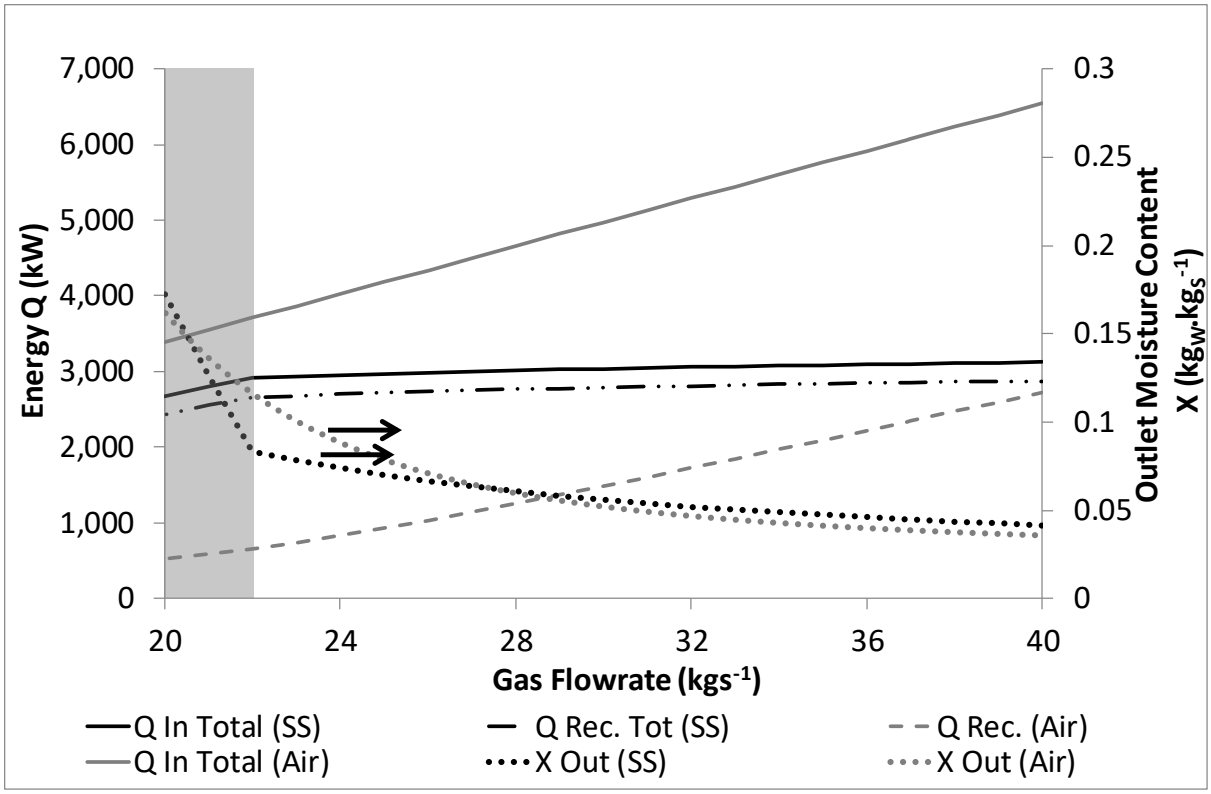

Figure 4-22: The energy profiles of the dryers as a function of inlet gas flowrate, at an inlet gas temperature of 182^{O}C. Lines are on the left axis unless marked.

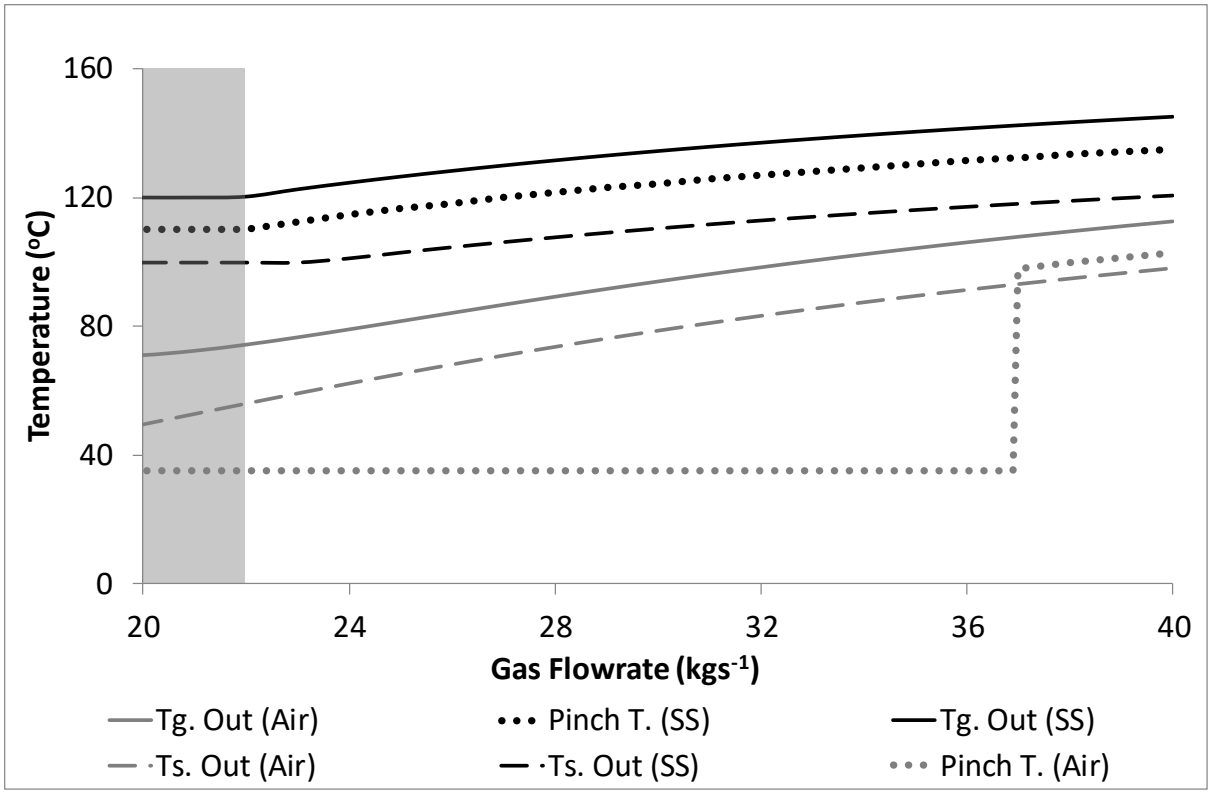

Figure 4-23: The temperature profiles of the dryers as a function of inlet gas flowrate, at an inlet gas temperature of 182^{O}C.

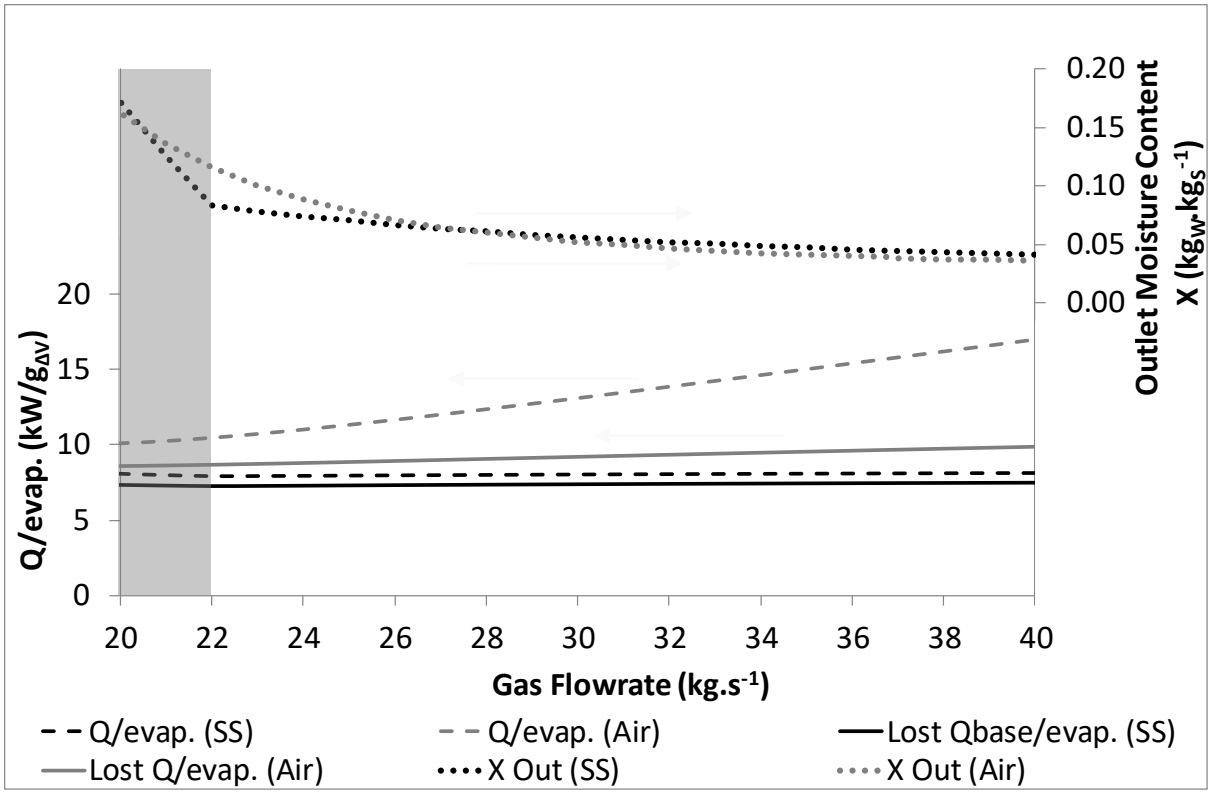

Figure 4-24: The energy use and loss per moisture evaporation profiles for the dryer, as a function of the inlet gas flowrate, at an inlet gas temperature of 182^{O}C.

From Figure 4-22, it is evident that the steam system begins to work effectively at a flow rate above 22 kg.s^{-1} for the calculated inversion temperature of 182^{O}C. Another noticeable result from Figure 4-22 is where the solids moisture content is plotted as a function of the energy profiles for the systems. It appears that the steam system and the air system have similar changes based on the change of flow, with the air system getting marginally better (lower outlet moisture content) than the steam system as the gas flowrate increases. When this is compared with the effects of temperature, it is apparent that the gas flow has as much influence on the two systems as the temperature does, with the flow having a greater effect than the temperature.

Figure 4-23 shows the effect on the various temperatures for the drying systems. From this result, it appears that changing the flowrate has a similar effect to increasing the inlet temperature. The main result that can be seen in this figure is that the pinch temperature for the air system changes from 35^{O}C to the solids outlet temperature above 37 kg.s^{-1} for the studied system. This is an important result because the energy that is wasted in the air

system increases above this flow rate and the energy recovery per unit of moisture evaporated increases.

Figure 4-24 shows that the flow rates of the two systems have very little impact on their energy recovery profiles. The gradient of all the curves (e.g. energy used per unit of water evaporated) is steeper for the effect of the inlet air temperature than for the effect of the gas flow rate. This result means that changing the flow rate of gas (within the plant limits) may be a better option for saving energy while ensuring that the material is adequately dried than to consider changing the system temperature. The disadvantage of this, however, is that for a higher gas flow rate, a larger blower or fan is required, taking more non-thermal energy to circulate the drying gas within the drying system.

Since the analysis has not studied the rate at which the drying occurs, only the mass and energy balance around the dryer, no conclusions can be reached from this analysis about the dryer size, or capital cost, except the indication from the ASIT that the drying rate is faster for superheated steam than air above 182^{O}C. It must be noted that the ASIT is based on the drying kinetics within the unhindered period of drying and is not a complete drying kinetics model, and this point should be considered when using it as a basis for comparing air and steam drying without other justifications. As with the temperature-based comparison of steam and air energy usage, it is clear that the air system is more energy sensitive to changes in inlet gas flowrate than the steam system, as shown by the slopes of the total energy requirement lines in Figure 4-24.

From the above analysis, steam drying outperforms air drying in many aspects, yet it is still not widely used in industrial drying processes. This outcome may be due to other factors involved in the differences between the systems, such as the larger compressor or blower used for steam recirculation than for the air system, and the potential for solids to be entrained into the recycle stream, which can damage such devices (blowers, compressors, injectors, etc.) and higher fouling rates on both the heat-transfer surfaces and within the dryer for steam drying [59].

4.6Conclusions

The inversion temperature for this system was estimated at 182^{O}C. Since this temperature is just below the temperature (184^{O}C) where the steam dryer reaches a feasible outlet

condition (outlet solids temperature above the dew point), superheated steam dryers are likely to be smaller than air dryers for all feasible drying conditions, while the air system allows for lower inlet temperatures to be used.

The recoverable (saved) energy from both the air and steam systems is high using PA at the studied conditions. Pre-heating the feed gas and solids with the dryer outlet gases yields energy savings of 18% for the air system and 8.4% for the steam systems. The steam system has an extra 86.6% of recoverable energy from the condensing of excess steam (a total of 91%), which can be integrated throughout the plant. This result shows that this rapid analysis can identify a sizable energy saving using the two techniques, IT and PA.

Other key results from this analysis are that the steam dryer sets the pinch temperature, while the air dryer does not set the pinch temperature, but rather the fresh inlet gas temperature does. This result means that steam drying, when run at 1 atm, works across the pinch, while the air dryer works above the pinch on its own i.e. the steam dryer is easier to integrate into other systems. The steam system also has less sensitivity to temperature and flow changes in terms of energy requirements than the air system. This outcome is due to the steam circuit being a recycle stream rather than a once-through system which is commonly used for air drying.

From the above discussions it appears that, as a rapid analysis, IT and PA are complementary. They provide an engineer with quick assessment tools that compares the potential fixed and variable costs associated with different drying gases. This method indicates that the superheated steam dryer has both a faster drying rate (in the unhindered drying period) and a higher energy recovery potential than the air system.

Chapter 5 Exergy Analysis of the Dryer

The following chapter is work on the exergy analysis of a dryer with a focus on the factors with potential use for the specific unit operation, using the same case as Chapter 4, and the same input and outlet conditions.

5.1Results and Discussion

5.1.1Basic Results from the Dryer

Table 5-1: The raw exergy and enthalpy results, from the two-step calculation assumption.

	T(^{O}C)	MC (g.g^{-1})	Ex_{TM}	Ex_{CH}	Ex_{diff}	Ex	H_{TM}	H
Dryer G_{IN},T_{IN}	190	Y=0.006	720	-	31.6	751	3,830	3,830
***Dryer G_{IN},T_{OUT}**	68.8	Y=0.006	62.6	-	31.6	94.2	1,200	1,200
Dryer G_{OUT},T_{OUT}	68.8	Y=0.059	69.0	-	390	459	4,020	4,020
Dryer S_{IN},T_{IN}	60	X=1	13.6	25,200	594	25,800	249	23,500
***Dryer S_{IN},T_{OUT}**	48.8	X=0.121	6.39	25,200	594	25,800	169	23,500
Dryer S_{OUT},T_{OUT}	48.8	X=0.121	2.26	25,200	71.8	25,200	59.6	23,400

***NOTE 1: An intermediate step for both phases within the dryer has been used to determine the difference between the evaporation/mass transfer and temperature effects within the dryer.**

Table 5-3 shows that the magnitude of the chemical exergy associated with the solids is higher than the other exergies. The change of diffusion exergy associated with the condensed phases is significant and should not be ignored in this case, as it contributes to the losses of exergy (in the material flows) to the environment from the process. The separation of mass transfer and heat transfer has been demonstrated previously in Chapter 3 and further discussion about this situation is given later. Now the factors that give further insights into the system are presented.

5.1.2Factors

It is important to start with the assumptions (Table 5-2) and the base factors for the following calculations. For example, Table 5-3 shows the basic factors that may be extracted from a simple analysis of energy and exergy.

Table 5-2: Assumptions and simple factors used for the ideal dryer calculation.

Assumption/Factor	Value	Unit
$T_{S_{IN}}$	60 (333.15)	C (K)
$T_{G_{IN}.max} = T_{G_{IN}}$	190 (463.15)	C (K)
Dryer evaporation $(\dot{m_{\Delta V}})$	1.099	$kg_W.s^{-1}$
$T_{\Delta V.ID}$	68.8 (342)	C (K)
$m_{\Delta V_{ID}.Q}$	1.15	$kg_{\Delta V}.s^{-1}$
$\Delta Q^{TM}_{\Delta V@T_S}$	2,385	$kJ.kg_{\Delta V}^{-1}@T_S$
$\Delta Ex^{TM}_{\Delta V@T_S}$	176	$kJ.kg^{-1}@T_S$

$$\begin{aligned} \dot{m_{\Delta V}} &= \dot{m}^{OUT}_{V.ID} - \dot{m}^{IN}_{\Delta V} \\ &= 1.28 - 0.13 \\ &= 1.15\ kg.s^{-1} \end{aligned}$$

Where: ideal conditions refer to the dryer reaching equilibrium at the outlet, this gives a suitable maximum evaporation rate for the dryer inlet conditions.

The remaining properties in Table 5-2 are from the mass and energy balance for an ideal system, with $\Delta Q^{TM}_{\Delta V@T_S}$ and $\Delta Ex^{TM}_{\Delta V@T_S}$ representing the latent heat and exergy of vaporisation of water at the outlet temperature, the exergy of evaporation is calculated by subtracting Equation 3-72 from 3-71 to give Equation 5-1.

$$\begin{aligned} \Delta Ex^{TM}_{\Delta V@T_S} &= \Delta h_{\Delta V} - T_0 \Delta s_{\Delta V} = \Delta Q^{TM}_{\Delta V@T_S} - \mathrm{T}_0 \Delta S^{TM}_{\Delta V@T_S} \\ &= h_{Sat.V}(T_S) - h_{Sat.L}(T_S) - T_0(s_{Sat.V}(T_S) - s_{Sat.L}(T_S)) \end{aligned} \quad 5\text{-}1$$

5.1.3Factor Types

There are several layers of factors that need to be considered, especially since some factors follow from other ones. An example of this development is the improvement potential (IP), which uses a previous efficiency factor to determine the ideality of a system. The usefulness of a factor is related to the level of information used for the calculation of the factor.

The simplest factors are based on ideal systems, mass-transfer estimates or mass and energy balances (Levels 0 and 1). The next level (Level 2) includes the second law efficiencies, such as the exergy efficiency factors discussed in the above section (Section

5.1.2). These factors on their own can be misleading and hard to interpret, especially for larger and more complex systems. The distinction between the levels can be seen in Table 5-3. This point will now be discussed in more detail.

Table 5-3: Resulting factors for the dryer-solids separator system using the levels described in Table 3-3.

Factor #		Parametric	Q Based	Ex based	Compound Exergy	Scale (IP)
		Level 0	Level 1	Level 2	Level 3	Level 4
1	$\frac{\dot{m}_{\Delta V}}{\dot{m}_{G_{IN}}}$	0.05				
2		$\eta_{\Delta V_{ID.Q}}$	93%			
3		$1-\frac{INE_G}{Q_{G_{IN}}^{TM}}$	75.4%			
4		$1-\frac{INE^{TM}}{Q_{IN^{TM}}}$	84%			
5		$\frac{\Delta Q_{\Delta V}}{Q_{G_{IN}}}$	68%			
6			$\frac{\Delta Ex_{\Delta V}}{Ex_{G_{IN}}}$	38%		
7			$\frac{Ex_{OUT}}{Ex_{IN}}$	97%		
8			$1-\frac{INE^{TM}}{Ex_{IN}^{TM}}$	10%		
9			$1-\frac{INE}{Ex_{IN}^{-CH}}$	31%		
10			$1-\frac{INE_G}{Ex_{G_{IN}}}$	-26%		
11			$1-\frac{INE}{Ex_{IN}^{Trans}}$	34%		
12			$\Omega^{TM}=\frac{\Delta Ex^{TM}}{Q_{IN}^{TM}}$	20%		
13			$\frac{Ex_{OUT}^{TM}}{Ex_{IN}^{TM}}$	9.7%		
14			$1-\frac{Ex_{Loss}}{Ex_{IN}^{-CH}}$	39%		
15			$1-\frac{INE_{\Delta V.G}^{\Delta T}}{Ex_{G.IN}}$	15%		
16				η_{Trans}	70%	
17				η_{Task} *	38%	
18					IP_{Trans}	250
19					IP_{Task}	722
20					$IP_{\frac{OUT}{IN}}$	26

***NOTE 2: Can be selected from other factors, in this case, Factor 6 is appropriate due to evaporation being the task.**

The more complex that an efficiency factor is, the greater is the importance of defining the basis. The task efficiency (Level 3) is a way of basing the factor on what is important. An

example of a suitable task efficiency for the dryer is the evaporation of water, and this basis has been used as the basis for the task efficiency of the dryer. This factor should be modified on a thermal basis (per J) rather than a mass-transfer basis (per kg) (for simplicity). This procedure creates a more compatible and meaningful set of factors, rather than the basic set of factors, which are the input and output calculations.

The results for the ranges of factors are shown here in Table 5-3. It appears that the parametric factor (Level 0) is useful only to size the flow system. The energy-based factors (Level 1) can be more meaningful, mainly in terms of assessing where the energy is being transferred inside the system.

For example, Factor 5 ($\Delta Q_{\Delta V}/Q_{G.IN}$) describes how much of the input energy from the gas stream is utilised through evaporation within the system, which partly explains the potential technological or task energy efficiency. Another aspect is the effect of the gas-side only calculations, or ignoring the condensed phase (shown by the difference between Factors 3 and 4). This difference is expanded further when the chemical potential energy is included on the solids-side (the factor becomes very close to unity).

Simple Factors

Simple factors include all of the Levels 0, 1 and some of the Level 2 factors. Simple factors that are used to describe a unit operation or system are shown in Table 5-3. Flow ratios (Level 0) can be useful for design metrics, while energy use ratios and first law energy efficiency methods (Level 1) are useful to determine energy losses to the environment and process energy inefficiencies. In order to determine the exergy efficiency, which is a measure of process irreversibility, the process objective and ideal process become more important.

The most commonly used exergy efficiency factor is Factor 7, which is known as the basic or simple exergy efficiency. Factor 7 is the general efficiency factor used to explain losses at a fundamental level. Ideally, this parameter should be split into factors to explain the loss to the environment and for internal use, as part of a systems approach. This point has partly been addressed in the work of Gungor [41] regarding endogenous / exogenous exergy losses. The advanced method is more about unit operation interactions than a simplified used/vented approach.

Due to the over-arching nature of this factor (Factor 7), the chemical potential term tends to dominate the exergy analysis in systems where the chemical potential term is applicable. For this unit operation (drying), it is important to note that this factor is close to unity. This situation means that the majority of exergy fed to the dryer goes to the environment. Since this factor only assesses the inputs and outputs of the unit operations in the system, it gives very little information about the system itself. The effects of assuming that this part of the chemical exergy is insignificant in the process are discussed below.

Factor 13 assesses only the thermo-mechanical (ΔT, ΔP) exergy use, which ignores the chemical potential and environmental chemical equilibrium (diffusion) components of the exergy calculation. These thermo-mechanical (only) factors can be useful for units that only undergo temperature and pressure changes (that do not cause phase change or chemical change), such as heat exchangers without phase change. However, for a dryer, these are inappropriate due to the way in which the dryer behaves (mass transfer creates a change of diffusion potential, through phase change).

Another consideration is the importance of carefully selecting a factor set that describes the system in a descriptive manner. For this consideration, factors that are more complex can be used to help with the interpretation of the results. The task and transiting efficiencies have been used here, and these efficiencies are discussed next.

Task and Transiting Efficiencies

Defining the objective, or task, for a unit operation in a system can help to simplify the interpretation of the results from an exergy analysis. In this case, the task for the dryer is to evaporate water from the solids, so for the dryer the task efficiency is defined by Factor 6. The evaporation efficiency of the dryer (Factor 17) is 38%, which is low compared with the overall efficiency (93%). This case is an example of how some of the simpler factors can be misleading if used without prior understanding of the task. Factor 6 can be used to improve the efficiency of the dryer in doing its task, but not necessarily the overall exergy use. Improving the exergy use for evaporation may make the dryer less efficient overall, or reduce the effectiveness of the system surrounding the dryer. The task efficiency does not take these factors into account. This situation means that, in order to improve the dryer,

improving the task efficiency should not be done on its own, but by determining its effect on the other units (including utility usage).

The large change in efficiency by just removing the chemical energy of the SMP from the equation is significant (97% Factor 7 vs. 70% Factor 17). This large change is due to the scale of the chemical exergy, and that it is entering and leaving the system unchanged. This situation means that keeping this component of exergy actively in the calculations can be misleading.

Considering the transiting exergy is more complex than assuming that the chemical exergy is insignificant, which has been done for the majority of factors. For example, for the solids feed stream (S-9), the total exergy is 25,800 kW, with 25,200 kW of that being chemical exergy, leaving 607 kW of non-chemical exergy in the thermo-mechanical exergy and the diffusion potential. Using the transiting method described above, the exergy value for this stream becomes 533 kW, because part of the thermal exergy, and part of the diffusion exergy, is removed from the calculation as well.

The total feed exergy to the dryer changes from 26,500 kW to 1,360 kW by removing the chemical exergy, then to 1,180 kW of affected exergy (exergy which takes part in the process, using the true definition of transiting exergy), while the outlet exergy from the dryer changes from 25,700 kW to 533 kW to 250 kW across the three methods.

What becomes important is that the change does not vary between the three methods (825 kW for all three methods). Any factor that includes the gas feed exergy, feed exergy or outlet exergy varies significantly with the different methods. One important result is that it is possible to establish the exergy losses due to the dryer, and the losses due to the product and by-products leaving the dryer.

Effect of the Evaporator Assumption

The value of INE_G (Factor 3) uses the assumption that the dryer can be split into two unit operations, one being a purely heat-transfer device, and the other being a pure mass-transfer device, taking only the heat-transfer part (ΔT) into the calculation. This difference in the definition leads to a much larger transfer of energy for the gas value (2,600 kW vs. 190 kW). By the definition given for INE in the literature (for an evaporator), it is important

to use the gas transfer value, not the overall transfer value [98]. The definition is based on the Carnot efficiency, which takes into account the temperature-based energy-transfer potential only. For non-thermal-based systems, the definition reverts to its simpler form, in that the INE value is the entropy generated in the ideal system (based on the desired task). For evaporation as an example, this INE value becomes $T_0\Delta S_{gen.ID}$, which may also be calculated by ΔH_{ID}-ΔEx_{ID} [98].

Assuming that the dryer acts as an evaporator alone ignores the exergy changes associated with the mixing and separation of the streams (mass transfer), leading to only part of the process being analysed. The assumption implies that the water vapour is generated by indirect heating, while spray dryers often use direct heating. This assumption is not suitable for spray dryers in exergy terms, as it assumes that a part of the process includes isothermal mixing.

Instead of simplifying the dryer, it is important to determine a suitable INE formula for what the task involves. The definition of the task efficiency is important here. For example, since the task of the dryer is to evaporate water (the evaporator assumption), it is also changing the humidity and the solids moisture content. The effect of changing the diffusion potential in the condensed phase is significant. Given this information, it is possible to define more than one INE calculation to describe the system [42].

This concept has also been discussed for drying units (Equations 21 and 22 of Liu *et al* [121]) with the focus on the approach temperature of the unit operation being the main inevitable loss of exergy (in this case $20^{O}C$ is used). The main issue with the simplification given by Liu *et al* [121] is that the paper assessed a scenario whereby it is possible to pair similar heat profiles, meaning it creates evaporation by using condensation with an indirect heat exchanger internal to a fluidised bed dryer. The form of drying used by Liu *et al* is not suitable to be used for the application of spray drying as the potential to pair these two process streams internal to a dryer is less likely in practice. The comparison of the method including the method used by Liu *et al* is shown below.

$$INE_{\Delta V.G}^{\Delta T} = \left(H_{G.OUT}^{Y_{IN}} - H_{G.IN}^{Y_{IN}}\right)T_{00}\left(\frac{1}{T_{OUT.ID}} - \frac{1}{T_{G.IN}}\right) \qquad 2\text{-}27$$
$$= 592\ kW$$

$$INE_{MIX.G}^{\Delta V} = \left(H_{G.OUT}^{Y_{IN}} - H_{G.OUT}^{Y_{OUT}}\right)T_{00}\left(\frac{1}{T_{P_{sat.OUT}}} - \frac{1}{T_{OUT.ID}}\right) \quad 5\text{-}2$$
$$= 197\ kW$$

$$INE_{\Delta V}^{\Delta T} = \left(H_{OUT}^{Y_{IN}} - H_{IN}^{Y_{IN}}\right)T_{00}\left(\frac{1}{T_{OUT.ID}} - \frac{1}{T_{G.IN}}\right) \quad 5\text{-}3$$
$$= 594\ kW$$

$$INE_{MIX}^{\Delta V} = \left(H_{OUT}^{Y_{IN}.X_{IN}} - H_{OUT}^{Y_{OUT}X_{OUT}}\right)T_{00}\left(\frac{1}{T_{P_{sat}}} - \frac{1}{T_{OUT.ID}}\right) \quad 5\text{-}4$$
$$= 195\ kW$$

$$INE_{Dryer} = INE_{\Delta V}^{\Delta T} + INE_{MIX}^{\Delta V} \quad 5\text{-}5$$
$$= 788\ kW_G : 789\ kW_{overall} : 818\ kW_{ID.overall}$$

$$INE_{Dryer.ID} = -T_0\Delta S_{Dryer.ID} \quad 5\text{-}6$$
$$= \Delta Ex_{G.ID} - \Delta H_{G.ID} + \Delta Ex_{S\&L.ID} - \Delta H_{S\&L.ID}$$
$$= 845\ kW = Ex_{Loss.ID} \quad **$$
$$= 825\ kW\ (actual)$$

Liu: $$INE_{\Delta T.ID} = (m_S\Delta S_S + m_{LW}\Delta S_{LW})\Delta T_{min} \quad 5\text{-}7$$
$$= -235\ kW \quad *$$ [121]

Liu: $$INE_{\Delta V.ID} = m_{LW}\frac{\Delta H_{\Delta V}}{T_{\Delta V}}\Delta T_{min} \quad 5\text{-}8$$ [121]
$$= 178\ kW$$

Liu: $$INE_{\Delta T.min} = INE_{\Delta T.ID} + INE_{\Delta V.ID} \quad 5\text{-}9$$
$$= 56\ kW$$

NOTE 3: This negative value is due to the overall outlet temperature being below the solids feed temperature.
***NOTE 4: Exergy loss and INE are always positive (negative exergy loss is not possible for real systems).**

It is important at this point to discuss the various equations presented above. Equation 2-27 represents the gas phase thermal loss due to non-mixing evaporation (or indirect evaporation). Equation 5-2 is the paired term for Equation 2-27 in that it is the gas phase exergy loss associated with the mixing and change of gas humidity in the process.

Equations 5-3 and 5-4 are the same as Equations 2-27 and 5-2, except they take into account the overall system, not just the gas phase. An important point here is that the change associated with each aspect of the system (-2,600 kW for evaporation and 2,600 kW for temperature change) is non-zero, while the overall change will be. Equation 5-6 shows the calculation of INE using the base definition for the ideal case (while showing the result of the studied system).

Equation 5-5 is the summation and comparison of the two pathways, including the case where the dryer reaches equilibrium at the outlet (considered to be the ideal system). Equations 5-7, 5-8 and the result 5-9, represent the method shown in Liu *et al* , and these results are different due to the assumptions regarding only the use of indirect heating (ideal case), which is not always used for a spray dryer (direct heating).

The assumption that the dryer acts in a similar way to an evaporator (Equation 2-27) only accounts for part of the inevitable loss, or part of the task. What this situation implies is that, based on evaporation alone, a dryer is an efficient method of only doing evaporation. Considering the mass-transfer component changes this situation significantly (15% Factor 15 to 39% Factor 14 inevitable loss), which means that the dryer is more efficient for one part of the task it is undertaking (solids drying), but less efficient for evaporating water. These two tasks may seem similar, and for many indirect dryer operations, they would be the same. Due to the nature of spray drying, however, the loss associated with mixing the evaporated moisture and the hot gas generates significant losses; these mixing-based losses demonstrate the importance of efficiency factor selection. The evaporation potential decreases significantly along the length of the dryer as the moisture content in the solids increases and the humidity increases, which also reduces the evaporation driving force within the system. The longer the dryer the lower the evaporation efficiency becomes, even while the evaporation total increases, this is what is the main implication of saying the dryer is good at drying the solids (total evaporation), and not as efficient at evaporating water (evaporation energy).

The difference between the results of the gas side assumption (equilibrium between final solids and the outlet gas), and the overall calculations (Equations 2-27 and 5-2 vs. Equations 5-3 and 5-4), is less than 5%. This small difference shows that the gas-side assumption is a

reasonable method to simplify the calculations in this case. This situation may not be the case for other [non-drying] systems, particularly those that have high chemical exergy that is used within the system.

The hybrid methods that use the INE factor in an efficiency calculation (Factors 9 to 11) can lead to some informative results since the INE factor describes the minimum or ideal loss for a unit operation. This situation allows a maximum efficiency factor (based on the current conditions) to be determined, and to use this factor to explore optimisation pathways for this unit operation. For example, the optimal point may change due to the way that INE is calculated (gas in and out condition assumptions) for the dryer.

Another point to note is the check calculation of INE (Equation 5-6) that resulted in a similar number to the $Ex_{Loss.ID}$. This similarity is an important confirmation of the INE calculation, where the actual loss of exergy is lower (the ideal dryer assumption is that it reaches equilibrium). In this case the dryer that reaches equilibrium is less energy efficient than the tested dryer (ΔT_{OUT}=20^{O}C) (20 kW INE_{Loss} better off). This situation arises because for the ideal system more energy is used to evaporate more of the water at a lower efficiency. This situation also increases the amount of water vapour being discharged thus increasing the outlet diffusion potential exergy. This result may lead to considering multi-stage drying options where practical.

Detailed Factor Methods

Since it is possible to determine the inevitable exergy loss (INE), it is also possible to estimate the maximum possible efficiency. In this case 1-INE_{Loss}/Ex_{IN} is used (Factor 14), providing a value of 39%. Comparing this value with the task efficiency (Factor 17: 38%) leads to a similar result.

Improvement potential is another useful method, because the improvement potential gives a scale for the inefficiency, not just the percentage value. The IP value uses the task efficiency to back-calculate the lost exergy due to the inefficiency (Equation 2-6). Having a scale is important when targeting where the largest losses are, or where the easiest changes can be made. For this comparison the task efficiency, or the INE efficiency, is useful to target the largest exergy inefficiencies.

Sample Calculations for Table 5-3

These factors, and data used to calculate them is shown below in Appendix B.

Factor 1

Evaporation per gas feed flow

$$\frac{\dot{m_{\Delta V}}}{\dot{m_{G_{IN}}}} = \frac{m_{V_{OUT}} - m_{V_{IN}}}{m_{G_{IN}}} = \frac{1.224 - 0.125}{21} = \frac{1.099}{21} = 0.053$$

Factor 2

Ideal evaporation rate

$$\eta_{\Delta V_{ID.Q}} = \frac{\dot{m_{\Delta V}}}{\dot{m_{\Delta V_{ID.Q}}}} = \frac{\dot{m_{\Delta V}}}{\frac{Q_{\Delta T.G}}{\Delta Q_{\Delta V}}} = \frac{\dot{m_{\Delta V}}}{\frac{Q_{G_{IN}} - Q_{G_{@T_{S_{IN}}}}}{\Delta H_{\Delta V_{@T_{S_{IN}}}}}}$$

$$= \frac{1.099}{\frac{(3831.0 - 1053.4)}{2357.7}} = \frac{1.099}{\frac{2777.4}{2357.7}} = \frac{1.099}{1.178} = 93\%$$

Factor 3

Avoidable Exergy Loss Quotient using a modified Carnot equation for the gas side only

$$1 - \frac{INE_G}{Q_{G_{IN}}^{TM}} = 1 - \frac{Q_{G_{IN}}^{TM} \times T_{00} \times \left(\frac{1}{T_{OUT_{ID}}} - \frac{1}{T_{G_{IN}}}\right)}{Q_{G_{IN}}^{TM}}$$

$$= 1 - 298.15 \times \left(\frac{1}{341.26} - \frac{1}{488.15}\right)$$

$$= 1 - 0.246 = 75.4\%$$

Factor 4

Avoidable exergy Loss Quotient on a Thermal basis only

$$1 - \frac{INE^{TM}}{Q_{IN^{TM}}} = 1 - \frac{2669.9 \times 0.246}{4079.5} = 1 - \frac{658}{4079.5}$$

$$= 1 - 0.161 = 83.9\%$$

Factor 5

Evaporation to gas energy in ratio (Evaporation Energy Efficiency)

$$\frac{\Delta Q_{\Delta V}}{Q_{G_{IN}}} = \frac{m_{\Delta V} \times \Delta h_{\Delta V@T_{OUT}}}{Q_{G_{IN}}} = \frac{1.099 \times 2353.2}{3831}$$

$$= \frac{2585.7}{3831} = 67.5\%$$

Evaporation to gas energy in ratio (Evaporation Exergy Efficiency)

Factor 6

$$\frac{\Delta Ex_{\Delta V}}{Ex_{G_{IN}}} = \frac{m_{\Delta V} \times \left(\Delta h_{\Delta V@T_{OUT}} - T\Delta s_{\Delta V@T_{OUT}}\right)}{Ex_{G_{IN}}}$$

$$= \frac{1.099 \times (2353.2 - 2094.41)}{751}$$

$$= \frac{284.4}{751} = 37.9\%$$

Simple Exergy Efficiency

Factor 7

$$\frac{Ex_{OUT}}{Ex_{IN}} = \frac{25{,}691}{26{,}516} = 97\%$$

Thermal based avoidable loss ratio

Factor 8

$$1 - \frac{INE^{TM}}{Ex_{IN}^{TM}} = 1 - \frac{658}{733.1} = 10.3\%$$

Avoidable loss ratio excluding chemical based exergy

Factor 9

$$1 - \frac{INE}{Ex_{IN}^{-CH}} = 1 - \frac{INE_{\Delta V}^{\Delta T} + INE_{MIX}^{\Delta V}}{Ex_{IN}^{-CH}}$$

$$= 1 - \frac{774 + 147}{1358.3} = 1 - \frac{921}{1358.3} = 32.2\%$$

Gas side based avoidable loss ratio

Factor 10

$$1 - \frac{INE_G}{Ex_{G_{IN}}}$$

$$= 1 - \frac{Q_{G_{IN}}^{TM} \times T_{00} \times \left(\frac{1}{T_{OUT_{ID}}} - \frac{1}{T_{G_{IN}}}\right)}{Ex_{G_{IN}}}$$

$$= 1 - \frac{Q_{G_{IN}}^{TM} \times 298.15 \times \left(\frac{1}{341.26} - \frac{1}{488.15}\right)}{Ex_{G_{IN}}}$$

$$= 1 - \frac{3{,}831 \times 0.246}{751}$$

$$= 1 - \frac{943}{751} = -26\%$$

NOTE 5-1: The value is negative since the INE term is based purely on temperature change, and this does not take the evaporation into account correctly. As a result, the INE value is larger than the exergy input value. This value was taken as positive in the table.

Transiting based inevitable loss ratio

Factor 11

$$1 - \frac{INE}{Ex_{IN}^{Trans}}$$

$$= 1 - \frac{784}{650.5 + 533.1} = 1 - \frac{784}{1{,}183.7}$$

$$= 1 - 0.662 = 33.7\%$$

Omega Value based on the exergy change of the gas side relative to energy feed

Factor 12

$$\Omega^{TM} = \frac{\Delta Ex^{TM}}{Q_{IN}^{TM}}$$

$$= \frac{825}{4{,}080} = 20\%$$

Simple exergy ratio

Factor 13

$$\frac{Ex_{OUT}^{TM}}{Ex_{IN}^{TM}}$$

$$= \frac{71.3}{733.1} = 9.7\%$$

Non-chemical potential loss factor

Factor 14

$$1 - \frac{Ex_{Loss}}{Ex_{IN}^{-\mathrm{CH}}}$$

$$= 1 - \frac{\Delta Ex_G + \Delta Ex_{S\&L}}{Ex_{IN}^{-CH}}$$

$$= 1 - \frac{291.8 + 533.1}{1{,}358}$$

$$= 1 - \frac{825}{1{,}358} = 39\%$$

The two-step assumption efficiency ratio

Factor 15

$$1 - \frac{INE_{\Delta V.G}^{\Delta T}}{Ex_{G_{IN}}}$$

$$= 1 - \frac{638}{751} = 15\%$$

The transiting exergy efficiency

Factor 16

$$\frac{Ex_{IN}^{Trans} - Ex_{OUT}^{Trans}}{Ex_{IN}^{Trans}}$$

$$= 1 - \frac{Ex_{OUT}^{Trans}}{Ex_{IN}^{Trans}}$$

$$= 1 - \frac{358.8}{1{,}184} = 70\%$$

The task-based exergy efficiency
The task is determined by the unit operation, in this case evaporation

Factor 17

$$\boldsymbol{\eta_{Task}} = \textbf{Factor 6} = \frac{\Delta Ex_{\Delta V}}{Ex_{G_{IN}}}$$

$$= \mathbf{38}\%$$

Improvement Potential on a Transiting basis

Factor 18

$$(1 - \eta_{ex}^{Trans})(Ex_{IN}^{Trans} - Ex_{OUT}^{Trans})$$

$$= (1 - 70\%)(1{,}184 - 359) = 250\ kW$$

Improvement Potential on a Transiting basis

Factor 19

$$(1 - \eta_{ex}^{Task})(Ex_{IN} - Ex_{OUT})$$

$$= (1 - 38\%)(26{,}516 - 25{,}691) = 722\ kW$$

Improvement Potential (simple)

Factor 20

$$(1 - \eta_{ex})(Ex_{IN} - Ex_{OUT})$$

$$= \left(1 - \frac{Ex_{OUT}}{Ex_{IN}}\right)(Ex_{IN} - Ex_{OUT})$$

$$= \left(1 - \frac{25{,}691}{26{,}516}\right)(26{,}516 - 25{,}691) = 26\ kW$$

Improvement Potential (TM)

Factor 20a

$$(1 - \eta_{ex}^{TM})(Ex_{IN}^{TM} - Ex_{OUT}^{TM})$$

$$= \left(\frac{Ex_{OUT}^{TM}}{Ex_{IN}^{TM}}\right)(Ex_{IN}^{TM} - Ex_{OUT}^{TM})$$

$$= \left(\frac{71.3}{733.1}\right)(733.1 - 71.3) = 64\ kW$$

5.1.4The Effect of Inlet Gas Temperature on Efficiency

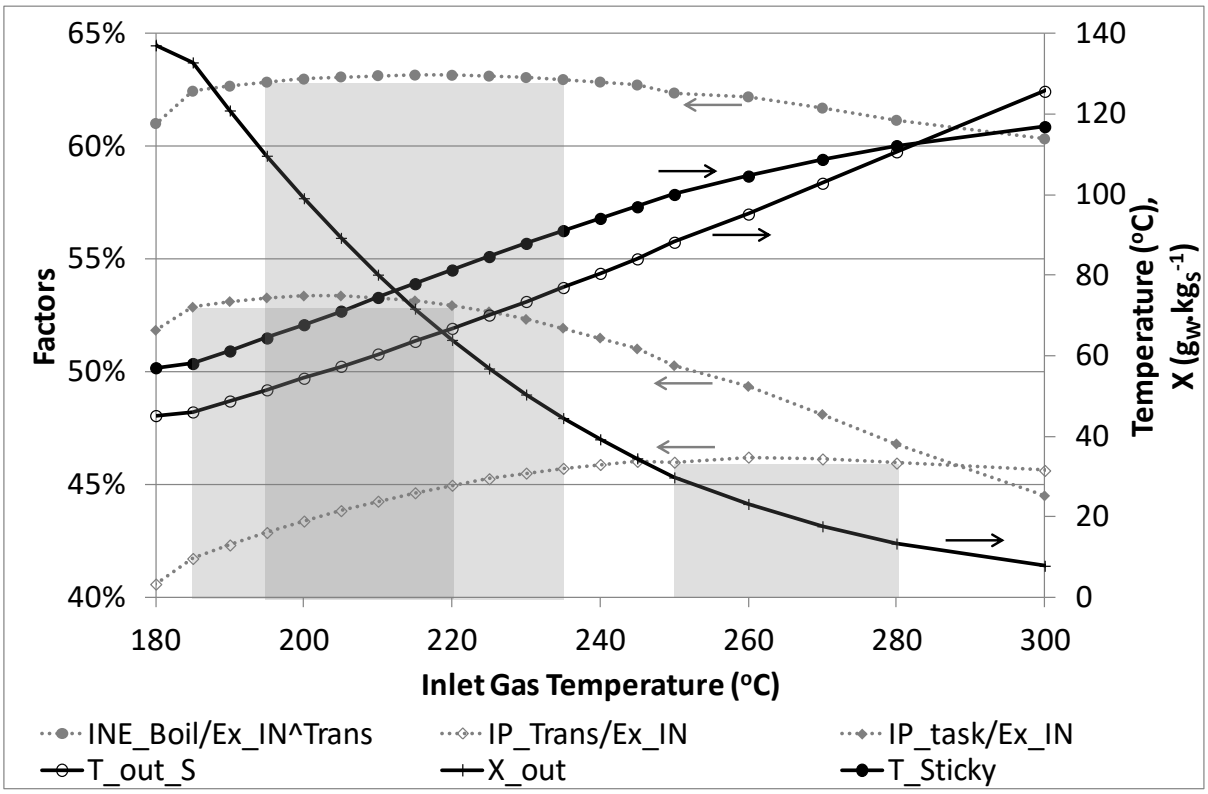

Figure 5-1: The effect of the inlet gas temperature ($T_{G.IN}$) on selected efficiency factors and outlet parameters.

Figure 5-1 shows the effect of the inlet gas temperature on several efficiency factors and outlet parameters. The first one to note is the outlet moisture content, which decreases with increasing temperature. The two temperatures shown are the outlet solids temperature (20^{O}C less than the outlet gas temperature) and the sticky-point temperature (a physical property). The result shows that, at higher temperatures, any benefit to energy would be negated by the solids fouling the walls of the dryer and downstream equipment including the separator (this occurs at a gas feed temperature of around 280^{O}C).

A point of interest is just after 185^{O}C, when the solids outlet temperature is 60^{O}C. This point is important because the dryer acts isothermally (on an external view, not internally), as the solids appears to not change temperature within the dryer, and this point is the basis of the two-step calculation method discussed earlier.

The three other factors shown here are important since they have maxima (while all the other studied factors have a monotonic relationship with the inlet temperature). These

three are the ratio or inevitable energy loss (INE) to exergy feed (INE/Ex_{IN}), the ratio of transiting improvement potential to exergy feed (IP_{Trans}/Ex_{IN}) and the task improvement potential to exergy feed ratio (IP_{Task}/Ex_{IN}).

The INE/Ex_{IN} factor shows that a gas feed temperature between 220^{O}C - 250^{O}C leads to the highest proportion of inevitable loss to the feed exergy input (there are two losses here: one to the environment and the other associated with the process). The effect of temperature changes the INE/Ex_{IN} factor within a range of 60% - 63% over the range of temperatures considered here, with the maximum ratio occurring on the high end of typical operational conditions for this type of dryer (190-230^{O}C inlet gas temperature).

The maximum is preferred in this case as it is suggesting that the loss is significantly related to the task of the dryer, and this occurs around 220^{O}C. The reason for this is likely connected with the solids moisture content and outlet solids temperature trade-off. As the outlet solids temperature increases, energy is wasted heating it, while evaporation decreases as the inlet temperature increases.

Another factor shown is the ratio of *IP* (on a transiting basis) to the exergy feed. This factor indicates that the process has the highest improvement potential at a higher temperature range (250^{O}C - 280^{O}C) than the *INE* ratio. The range of the IP_{Trans}/Ex_{IN} ratio within the potential operating range is from 41% to 46%, which is quite a small range, indicating that drying in general is inefficient in terms of exergy. While the ratio of *INE* to exergy feed ratio gives an indication of how much exergy from the feed is being wasted, the *IP* to exergy feed ratio gives an indication of how optimised the process is. The higher the *IP*, the further from ideal is the system.

There is a slight difference between the transiting *IP* and the task *IP* ratio, with the $Task_{IP}$ ratio showing a similar shape to the INE/Ex_{IN} curve. This ($Task_{IP}$) factor shows a maximum point even earlier than the other discussed factors. The worst performing temperature range based on evaporation, which is the task of the dryer, is close to the practical low limit of operations (185^{O}C - 215^{O}C) with a steady improvement as the outlet moisture ratio decreases. This maximum is due to the factor being based on the evaporation potential. At low temperatures, more of the energy will be used in heating the droplets to the evaporation equilibrium point rather than evaporating the water, meaning the energy is not

being used for the task. At higher feed temperatures, this becomes a smaller loss proportionately; the evidence was presented in Chapter 2.

A trade-off on energy/evaporation and energy lost in the solids is evident in these three factors being discussed. In this case, the aim is for a maximum *INE* to Ex_{IN} ratio, and a minimum *IP* to Ex_{IN} ratio. This situation leads to a trade-off between the evaporation task and the other two factors, leading to an optimal operating point somewhere between 200^{O}C and 220^{O}C (which is typical in industry).

5.1.5Factors Overall Discussion

The exergy-based factors (Level 2) are more numerous than those used for exergy (Level 1). This situation arises because of the potential to explain more deeply what the exergy is doing, not just where it is going. Factor 6 is related to Factor 5, comparing the evaporation with the energy supplied in the gas phase. Factor 6 is used for the task efficiency here because it explains the system (not just the dryer) in a meaningful manner.

Using a variety of factors to describe a system is important, since there is not really a 'one-size-fits-all' factor that is simple to use. Following the task efficiency path requires critical thought about what each unit (or the system as a whole) is trying to accomplish, while other factors determine the closeness to an ideal system. The large range of factor types means that breaking the factors into these 'complexity levels' helps to assess what each factor aims to achieve and why some factors should be used relative to others.

In summary, the basic procedure to use these factors in a meaningful manner is as follows:

- Consider what each operation is trying to achieve.
- Determine what task is being performed.
- Simplify the exergy calculation to compare with the task only, ignoring what is inert in the system.
- Determine the meaningful efficiency (task, transiting, TM, evaporation) for each unit operation (or system/sub-system).
- Target the lowest efficiency areas and determine the scale of the IP.

- Study ways of improving the targeted area (change of temperature, pressure, utilities).

This process is a simple heuristic approach to using exergy factors to target process improvements. Other methods (such as graphical ones) exist, such as the Ω-H plot [114], which may make complex process optimisation easier. However, this procedure requires breaking each type of unit into groups; expanders, for example, require a factor manipulation to bring the omega value inside the 0-1 range. Another visualisation method (Grassman diagrams) has been explored in this chapter.

5.2Visualisation Methods

There are several methods to visualise the results of an exergy analysis, the most common of which is a Grassman diagram. For this unit operation pairing, the diagram is shown in Figure 5-2. This diagram represents the exergy flows into and out of the dryer (D-1) and separator (C-1).

From this diagram, the main exergy destruction pathways may be determined for the dryer.

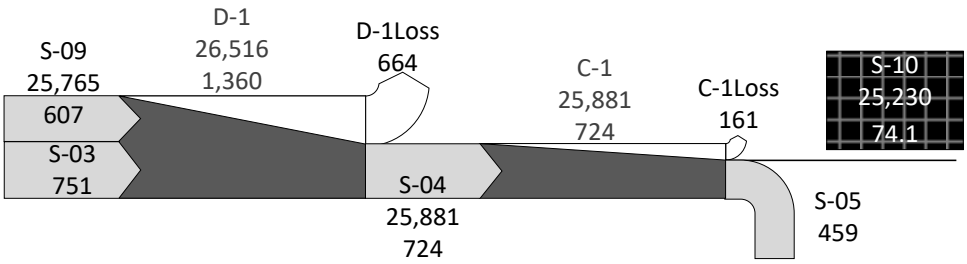

Figure 5-2: Grassman Diagram for Dryer (D-1) and Separator (C-1).
NOTE 5-2: For the solids side (S-09, S-04, S-10) there are two number layers: the top one is the total exergy, inclusive of the chemical exergy, and the smaller number (bottom) indicating only the thermo-mechanical exergy. This shows the importance of using a transiting exergy approach.

For more complex systems, the Grassman diagram becomes more useful in helping to interpret the exergy analysis [37]. In Figure 5-2, there are two numbers associated with each of the streams that highlight the difference between thermo-mechanical and total exergy. The significance of the chemical exergy can be seen in the condensed phase streams, containing the solids. The diagram is drawn with the thermo-mechanical exergy values due to the scale (when showing 25,900 vs 751, the diagram is meaningless).

The Grassman diagram shows the potential to separate the efficiency factor clearly, with the 'waste' flows showing exergy use and loss for each unit, while the flows into and out of the system show cost and environmental losses. There is the potential to segregate the efficiencies in this manner. For example, the waste values are 825 kW, while the loss to the environment is associated with the gas flue stream (459 kW). This situation means there are two sources of exergy losses from the system, but the losses from the units (internal) can be split further into the inevitable loss (INE) and the avoidable loss (AVO), which is a way of describing ideal process losses. The ideal system loss (ideal or INE) within the dryer chamber is 662 kW (based on an evaporator assumption presented in Chapter 2 (Two-step calculation for drying)), which means the avoidable loss is actually only 591 kW (based on evaporation alone).

Another method of visualising a system in exergy terms is to utilise the omega factor (mentioned earlier) as a function of enthalpy [39, 98]. Combining this with INE can be beneficial to illustrate the practical exergy and energy efficiencies. For a single unit operation, this method is less suitable, but is shown as an illustrative example (Figure 5-3).

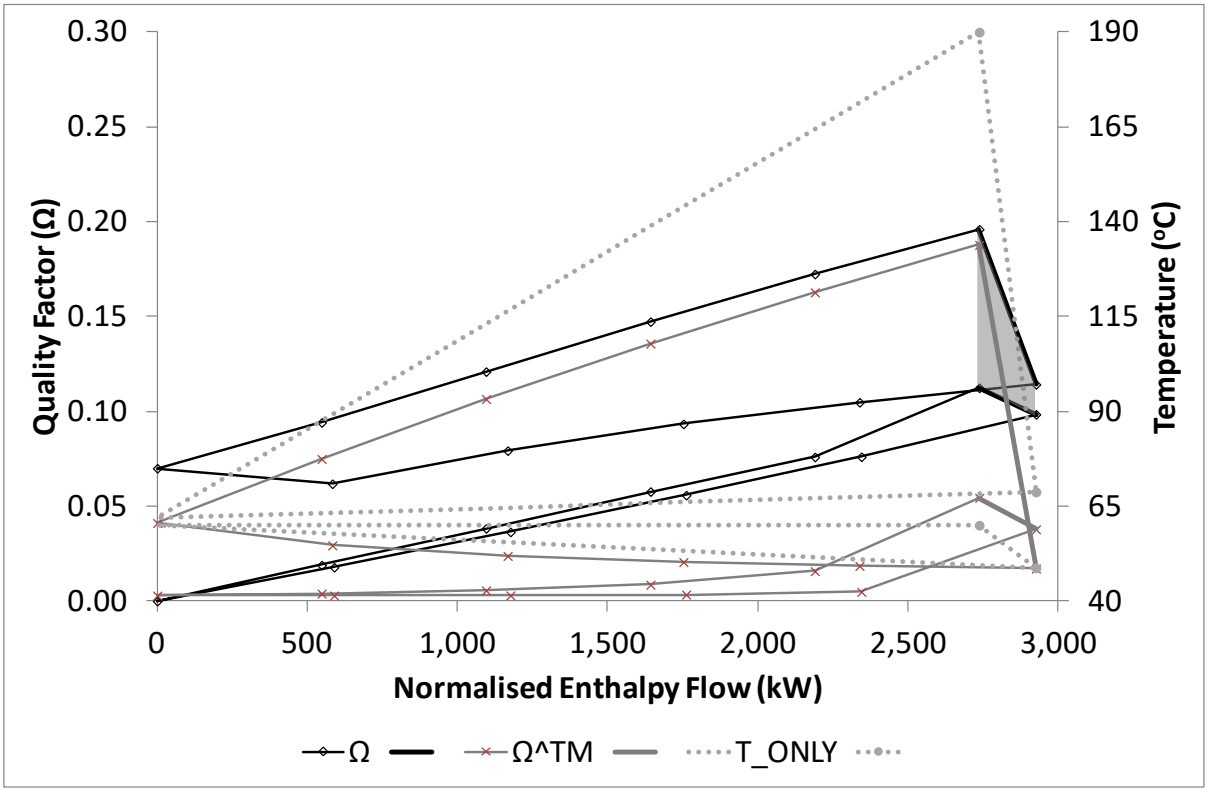

Figure 5-3: The Omega-Enthalpy diagram of the dryer (as a two-step heater, and a mass transfer system).

For Figure 5-3, the area between the curves represents the loss associated with the driving force of the system , but does not constitute all of the inevitable losses. The area below each curve represents the change in exergy. The total change within the system is 825 kW_{ex}, while the shaded area in Figure 5-3 represents 112 kW. This shaded area in Figure 5-3 is an approximate measure of loss associated with the driving force of the system [39, 98]. The dark grey curve (offset to the black one) shows only the thermo-mechanical effects for the system, which shows that the diffusion potential changes are significant for the gas side of the system, and almost exclusively represent the total exergy changes associated with the condensed phase. It is possible to split the exergy use value into the avoidable and inevitable losses to further find an optimum, but that method works better for process optimisation [39, 98].

5.3Implications and Conclusions

The dryer is inherently inefficient in exergy terms at evaporating the water from the solids. The losses associated with the task are 38%, while the losses associated with the mass transfer and heat transfer are 94% (thermo-mechanical IN/OUT) and 30% (transiting) respectively. This exergy efficiency range is significant considering the overall exergy efficiency is nearly 100% over the entire exergy spectrum. The IP of 575 kW for the feed of 722 kW shows that the dryer does not appear to be an exergy efficient way of performing this task, but does not offer an alternative method. The effect of feed temperature for several key variables shows that, depending on the basis of efficiency, various factors give significantly different optimal operating points. For this system, the optimum operating range in terms of the inevitable exergy loss method is between 215^{O}C and 250^{O}C, which is typical of the conditions currently used in industry [122]. There appears to be no suitable ‘one-size-fits-all’ efficiency factor for an exergy analysis. A variety of factors, which may be defined as a group, can be used such as the task efficiency (on the task for the unit operation) and the practical efficiency (based on the task). The INE method is a potential shortcut technique based on the Carnot efficiency and a first law analysis, but there are some limitations for processes that are not exclusively thermal, where an entropy balance is more correct. The INE method still shows potential as a starting basis of comparison because it shows the scale and the efficiency together, which are both important for targeting areas of the process to improve, without doing a full exergy analysis.

Chapter 6 Exergy Analysis of Spray Dryer Systems

This Chapter follows a similar treatment as that presented in the previous chapter, but applies to larger systems associated with the dryer. This chapter tests a traditional boiler based system against a Vapour Recompression (VRC) system. This demonstrates the flexibility of exergy analysis for dealing with non-thermal (VRC) systems.

This is followed by a methods comparison, where a boiler-driven system (Case 1) is compared with an electrically-driven vapour recompression (VRC) case (Case 2) over a variety of common factors.

6.1Assumptions

The assumptions for this work are the same as in Section 4.1 and Chapter 5, with the following additional assumptions covering the other parts of the systems. The minimum temperature approach for heat exchange has been taken as 20^{O}C for this system, since most heat is exchanged between two gases. This assumption is reasonable, according to the literature [61, 69].

- The compressor used in the Case 2 has been assumed to have an adiabatic efficiency of 75%, which is within the typical range for rotary type compressors [123].
- Natural gas fuel has been assumed to be pure methane (CH_4) for calculation purposes.
- The fuel-to-air ratio used in the boiler system has been assumed to be 1:18 on a mass basis. This ratio was calculated on the basis of a 7.5% (by mass) excess air requirement – typical of natural gas systems [124].
- The burner used in the boiler system is assumed to have a combustion-to-energy conversion efficiency of 80% (meaning an extra 20% in fuel requirements has been calculated for the feed) [124, 125].
- The combined dryer and gas solids separator have been assumed to be the base unit around which the optimisation occurs. These units have been assumed to be fixed and they have been kept the same between the different case studies.

- The pressure of the outlet of the compressor was determined based on the temperature requirements of the gas pre-heater.

6.2Determining a suitable calculation basis

The main factors used to describe the system may be defined on two bases, a total in basis, or gas side in basis. The difference in the basis may seem significant, but it has been demonstrated to be insignificant for most calculations [16]. For a full list of methods, refer to Chapters 3 and 5. There are several efficiency factors used to determine the system (or unit) efficiency with respect to exergy.

Simple efficiency is defined as the ratio of the outlet exergy to that at the inlet, as shown in Equation 6-1. This factor may be contrasted with the dryer's (and thus the system's) task efficiency factor given in Equation 6-2.

$$\eta_Q = \frac{H_{OUT}}{H_{IN}} \text{ and } \eta_{ex} = \frac{Ex_{OUT}}{Ex_{IN}} \quad 6\text{-}1$$

$$\eta_Q = \frac{H_{\Delta V}}{H_{G_{IN}}} \text{ and } \eta_{ex} = \frac{Ex_{\Delta V}}{Ex_{G_{IN}}} \quad 6\text{-}2$$

The evaporation values refer to the energy and exergy used (under ideal conditions) to evaporate the water used within the system (as opposed to the potential to evaporate).

The values associated with the inlet ($H_{G_{IN}}$and $Ex_{G_{IN}}$) refer to the potential energy and exergy in the gas entering the dryer. These values may be replaced with fuel use when referring to the system calculations, where fuel refers to the energy added to the system from external sources (i.e. electricity or the chemical energy from natural gas).

In contrast, the parameters used for Equation 6-1 are associated with the feeds (IN) and products (OUT) of the system in simple terms. Each of these factors can be further manipulated to refer to just the thermo-mechanical (TM) flows, transiting factors, or other factors. These factors were discussed in the previous Chapter (Chapter 5).

The key compound factors refer to the Improvement Potential (IP), the Inevitable loss (INE), and task efficiency and recoverable energy/exergy factors. The list of useful factors in exergy

analysis is significant and can be confusing. The previous chapter discussed several of these factors in relation to the dryer unit operation. The IP can be defined by Equation 2-6.

$$IP = (1 - \eta_{ex})(Ex_{IN} - Ex_{OUT}) \quad 2\text{-}6$$

Where:

η_{ex} = Exergy efficiency, defined by one of Equations 2-7 to 2-10.

The above efficiency factor takes the entire exergy calculation into account for each unit. However, this factor may not be useful in determining the true effect of system factors on a unit. To determine a more appropriate efficiency for these cases, a transiting exergy factor may be used. The simple transiting calculation is shown in Equations 6-3 and 6-4.

$$Ex_{Trans} = Ex - Ex_{inert} \quad 6\text{-}3$$

$$\eta_{Ex}^{Trans} = \frac{Ex_{Trans.OUT}}{Ex_{Trans.IN}} \quad 6\text{-}4$$

It is important to recognise that part of this calculation is defined by the definition of exergy (the dead state). If the dead state is not the same as the standard state (typically used in thermodynamics), the change associated with this unobtainable state is therefore already removed. Transiting exergy refers to a component that has an insignificant contribution to, or interaction with the unit operation.

In this work, the INE method is mentioned as a comparison with other factors. This method has been explored in the previous chapter and is not explored here due to its limited potential in a system. The INE method uses the Carnot efficiency method to short cut an exergy analysis for a single unit operation (or system in a limited manner), and gives a potential exergy loss target. The calculation of an inevitable loss is based on the unit task and varies with different units. For example, calculating the INE for a compressor is significantly different to a dryer, and a heat exchanger is different again. Another issue with the INE method is that it generally excludes non-temperature-based energies using the basic methodology, and becomes difficult to interpret for more complex systems where a full exergy analysis is preferred.

In terms of the INE, the overarching definition is the minimum entropy generation required to perform the task.

$$INE = -T_0 \Delta S_{ID.min} \quad 6\text{-}5$$

6.3Case Studies

6.3.1Case 0: No heat recovery option

The base case (Case 0) scenario is identical to Case 1, with the difference being the omission of the economiser (E-1) and boiler system (R-B1, E-B1, E-B2) attached to the dryer system. This dryer system is used as a common part of the two cases, and allows the definition of a target. This situation means that this case is an open-cycle system. Since no heat recovery system is installed in Case 0 it can be used as a basis upon which to justify improvements (in industry, the current system is typically used).

6.3.2Case 1: Boiler Case

The process shown in Figure 6-1 features humid air (S-01 to S-03) passing through a pre-heating sequence of exchangers (E-1 and E-2) before entering the dryer (D-1) at 190^{O}C. The wet solids stream (S-08 to S-09) is pre-heated (E-3) to 60^{O}C before entering the dryer. S-04 is an intermediate stream between the dryer and solids separation device (C-1), which is a mixed phase stream of very humid gas and dried solids. In C-1 the solids phase (S-10) and gas phase (S-05) are separated and the gas is used to partially preheat the feed gas (E-1).

The boiler plant must run at temperatures over 210^{O}C to preheat the feed gas; this process requires pressures in excess of 16 Bar. In terms of the utilities streams shown in Figure 6-1 (also shown below), the steam system is linked, in that Uh-3 is the combined flow of Uh-1 and Uh-2, and similarly UD-3 is the combined flow of UD-1 and UD-2.

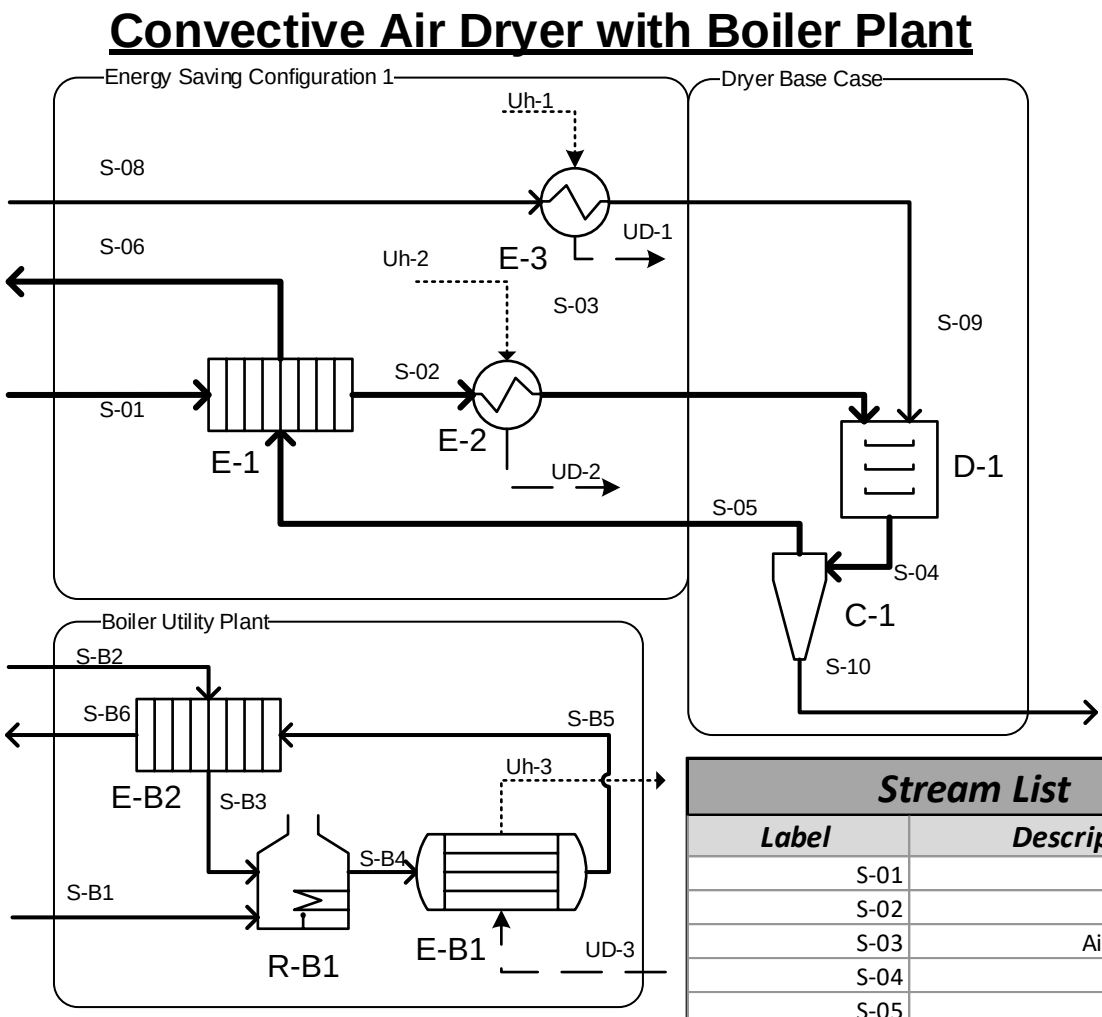

Stream List	
Label	**Description**
S-01	Fresh Air Inlet
S-02	Preheated Air
S-03	Air Feed to Dryer
S-04	Dryer outlet
S-05	Humid Air out
S-06	Exchanged Gas out
S-08	Ambient Solution Feed
S-09	Solution Feed to Spray Dryer
S-10	Dry Solids Out
S-B1	Fuel Feed
S-B2	Fresh Air to Burner
S-B3	Preheated Air to Burner
S-B4	Burner Outgas
S-B5	Spent Burner Exhaust
S-B6	Boiler Exhaust
UD-1	Solution Preheater Condensate
UD-2	Dry Air Preheater Condensate
UD-3	Boiler Condensate feed
Uh-1	Solution Preheater Steam
Uh-2	Dry Air Preheater Steam
Uh-3	Boiler Steam

Equipment List	
Label	**Description**
C-1	Gas Solids Separation Device
D-1	Convective Spray Dryer
E-1	Dryer Economiser
E-2	Steam-Air Preheater
E-3	Steam-Solution Preheater
E-B1	Boiler Tubes
E-B2	Boiler Economiser
R-B1	Methane Burner

Figure 6-1: The steam heated convective air dryer developed in the Pinch Analysis (Case 1).

6.3.3Case 2: Vapour Recompression Case

The process shown in Figure 6-2 features humid air (S-01 and S-03) entering the pre-heating heat exchanger (E-1) before entering the dryer (D-1) at 190^{O}C. The wet solids stream (S-08 to S-09) is pre-heated (E-3) to 60^{O}C before entering the dryer. S-04 is an intermediate stream between the dryer and the solids separation device (C-1), which is a mixed phase stream of very humid air and dried solids. In C-1, the solid phase (S-10) and gas phase (S-05) are separated. The gas is fed into a compressor (C-2) to heat the gas to 210^{O}C (S-06) to fully preheat the feed gas (E-1) and then has its pressure reduced using a valve (C-1) before being discharged (S-12).

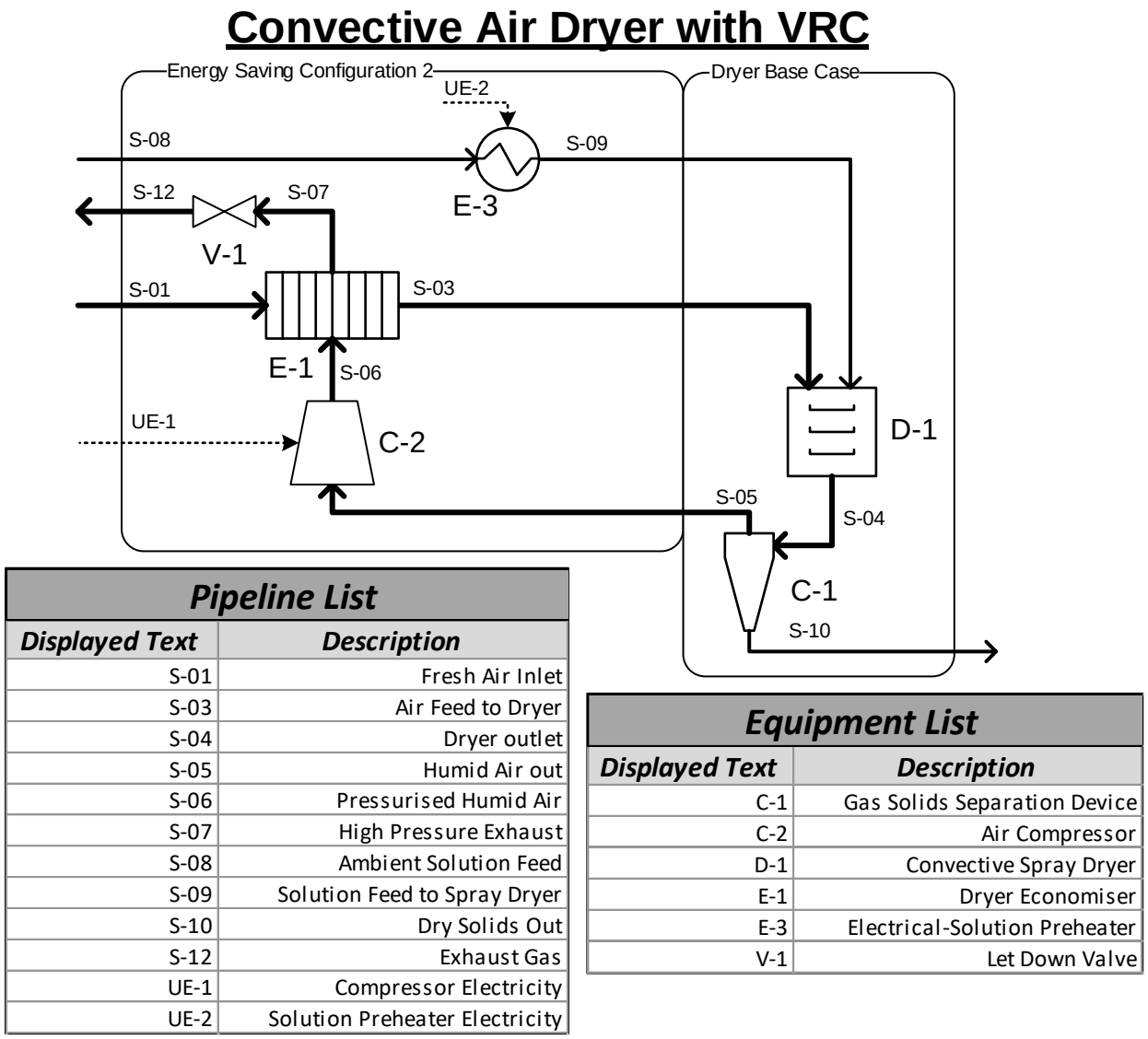

Pipeline List	
Displayed Text	**Description**
S-01	Fresh Air Inlet
S-03	Air Feed to Dryer
S-04	Dryer outlet
S-05	Humid Air out
S-06	Pressurised Humid Air
S-07	High Pressure Exhaust
S-08	Ambient Solution Feed
S-09	Solution Feed to Spray Dryer
S-10	Dry Solids Out
S-12	Exhaust Gas
UE-1	Compressor Electricity
UE-2	Solution Preheater Electricity

Equipment List	
Displayed Text	**Description**
C-1	Gas Solids Separation Device
C-2	Air Compressor
D-1	Convective Spray Dryer
E-1	Dryer Economiser
E-3	Electrical-Solution Preheater
V-1	Let Down Valve

Figure 6-2: The system in Figure 6-1 with a VRC system installed to replace the boiler system (Case 2).

6.4Results and Discussion

6.4.1Energy flows

Case 0

$$H_{G_{IN}} = 3{,}525\ kW \qquad Ex_{G_{IN}} = 720\ kW$$

$H, Ex_{G_{IN}}$ = energy or exergy given to the gas side of the system in total = S-01to S-03

Note: in the case of the TM basis, this is identical given the feed is at 25℃

These Case 0 values provide a basis for comparison with Cases 1 and 2.

Case 1

$$H_{IN}^{TM} = 362\ kW \qquad Ex_{IN}^{TM} = 0\ kW$$
$$H_{IN_{Tot}} = 27{,}547\ kW \qquad Ex_{IN_{Tot}} = 29{,}745\ kW$$
$$H_{IN}^{Trans} = 3{,}941\ kW \qquad Ex_{IN}^{Trans} = 4{,}484\ kW$$

Note that these numbers do not balance the energy from the feed. The following outlet energy numbers refer to losses to the environment in the products and flue streams. The main difference in the TM result is due to the conversion of fuel (chemical energy) to thermal energy within the system.

$$H_{OUT}^{TM} = 4{,}070\ kW \qquad Ex_{OUT}^{TM} = 26\ kW$$
$$H_{OUT.Tot} = 27{,}370\ kW \qquad Ex_{OUT.Tot} = 25{,}763\ kW$$
$$H_{OUT}^{Trans} = 3{,}774\ kW \qquad Ex_{OUT}^{Trans} = 503\ kW$$

These results may be compared with the inlet values to illustrate the change within the system:

$$\Delta H^{TM} = -3{,}709\ kW \qquad \Delta Ex^{TM} = -26\ kW$$
$$\Delta H = \Delta H^{Trans} = 177\ kW \qquad \Delta Ex = \Delta Ex^{Trans} = 3{,}982\ kW$$

While the raw numbers (IN and OUT) for transiting values are significantly different to the total, and the TM values, the overall change within the system is the same as the overall change. This allows for a better picture of what the system is doing. The change is generally

used in many efficiency factors, and the context given with the transiting values are important to analyse improvement opportunities.

If the calculation were repeated only on the gas side of the system, it would be possible to determine which phase is the most limiting in the system, and which part of the system requires a greater focus.

$$\Delta H_G^{TM} = -3{,}649\ kW \qquad \Delta Ex_G^{TM} = -23.7\ kW$$
$$\Delta H_{G.Tot} = \Delta H_G^{Trans} = 236\ kW \qquad \Delta Ex_{Tot} = \Delta Ex_G^{Trans} = 3{,}462\ kW$$

The reason for checking whether the gas side calculation is close to the actual change (an important step towards simplification) is that it can lead to less complex calculations and still provide meaningful results in terms of the optimisation potential for the dryer. In this instance, the gas side accounts for 98% of the change on an energy basis and 90% on an exergy basis.

Case 2

$$H_{IN}^{TM} = 4{,}714\ kW \qquad Ex_{IN}^{TM} = 4{,}455\ kW$$
$$H_{IN.Tot} = 28{,}014\ kW \qquad Ex_{IN.Tot} = 30{,}238\ kW$$
$$H_{IN}^{Trans} = 4{,}408\ kW \qquad Ex_{IN}^{Trans} = 4{,}977\ kW$$

Note: These numbers do not 'balance', and the following outlets refer to losses in the products and other outlets (i.e. the outlet is not at the same temperature and pressure as the inlet due to unit inefficiencies on energy losses).

$$H_{OUT}^{TM} = 1{,}873kW \qquad Ex_{OUT}^{TM} = 12.3\ kW$$
$$H_{OUT.Tot} = 25{,}173\ kW \qquad Ex_{OUT.Tot} = 25{,}474\ kW$$
$$H_{OUT}^{Trans} = 1{,}567\ kW \qquad Ex_{OUT}^{Trans} = 213\ kW$$

These results may be compared to give the change within the system:

$$\Delta H^{TM} = 2{,}842\ kW \qquad \Delta Ex^{TM} = 4{,}443\ kW\ ^*$$
$$\Delta H = \Delta H^{Trans} = 2{,}842\ kW \qquad \Delta Ex = \Delta Ex^{Trans} = 4{,}763\ kW$$

NOTE 6-1:* The exergy is high since the electrical energy was added to the TM calculation for simplicity.

If the calculation were repeated on just the gas side of the system, it would be possible to determine which phase is the limiting one in the system:

$$\Delta H_G^{TM} = \Delta H_{G.Tot} = \Delta H_G^{Trans} = 2{,}653\ kW \qquad \Delta Ex_G^{TM} = 4{,}196 kW$$

$$\Delta Ex_{G.Tot} = \Delta Ex_G^{Trans} = 3{,}995\ kW$$

Summary

It is important to note that Case 2 has a higher energy (4,408 kW versus 3,941 kW) and exergy feed (4,977 kW versus 4,484 kW) load than Case 1, meaning that for the same task, Case 1 has a lower energy and exergy cost. Another important aspect of these results is that the outlet thermal energy being sent to the environment is significant in both systems and is higher in Case 1 than Case 2 (3,774 kW versus 1,873 kW energy) and (26 kW versus 12.3 kW exergy). The overall loss is higher due to the change in composition from the feed (environmental) air. The difference in the thermal and total loss to the environment is important and leads to the recovery potential metric discussed below.

6.4.2Evaporation Potential

A metric that can be used to define efficiency is the task efficiency. To determine this metric, the evaporation potential must be established first. This assessment can be done by assuming that all the energy spent within a process is used to evaporate water under ideal conditions.

Comparing the evaporation potential with the actual evaporation from Case 0 can lead to some meaningful results.

Case 0

Actual (calculated) evaporation values:

$$\dot{m} = 1.18\ kg.s^{-1} \qquad \dot{n} = 0.065\ kmol.s^{-1}$$

$$H_{\Delta V} = 2{,}591\ kW \qquad Ex_{\Delta V} = 272\ kW$$

The evaporation potential is a useful calculation for a dryer (and can be translated to the system), as it relates to the task of the dryer and the linked systems. Using the values for the evaporation energy and the exergy of water at the constant temperature of the preheated wet solids stream (S-09) (60^{O}C), it is possible to determine the evaporation potential of water using the two-step method outlined in the two-step calculation. The values of $\Delta H_{\Delta v}$ and $\Delta Ex_{\Delta v}$ at 60^{O}C (2,360 kJ/kg and 144 kJ/kg, respectively) can be used to determine the potential to generate evaporate water using the two-step calculation of the dryer outlined

in [2]. The evaporation potential can then be compared with the actual evaporation produced by the dryer to obtain the evaporation efficiency.

$$\eta_{\Delta V.H_{G.IN}} = \frac{\dot{n_{\Delta V.act}}}{\dot{n_{\Delta V.pot_Q}}} = \mathbf{79\%} \quad 6\text{-}6$$

$$\eta_{\Delta V.Ex^{TM}_{G.IN}} = \frac{\dot{n_{\Delta V.act}}}{\dot{n_{\Delta V.pot_{Ex}}}} = \mathbf{41\%} \quad 6\text{-}7$$

Where

$$\dot{n_{\Delta V.pot_Q}} = \frac{\dot{n_{G_{IN}}}\overline{Cp_G}(T_G^{IN} - T_S^{IN})}{\Delta H_{\Delta V@T_S^{IN}}} \quad 6\text{-}8$$

And

$$\dot{m_{\Delta V.pot_{Ex}}} = \frac{\dot{m_{G_{IN}}}\overline{Cp_G}\left(T_G^{IN} - T_S^{IN} - T_0 \ln\left(\frac{T_G^{IN}}{T_S^{IN}}\right)\right)}{\Delta H_{\Delta V@T_S^{IN}} - T_0 \Delta S_{\Delta V@T_S^{IN}}} \quad 6\text{-}9$$

The evaporation potential efficiency determines the task efficiency of the dryer on both an energy and exergy basis; these efficiency factors determine one of the optimisation targets for the system.

Case 1

It is also important to consider the fuel energy (energy added to the system that is not part of the processing streams, e.g. natural gas and electricity) fed into a system. This is the energy value of the natural gas or electricity added to run a system, which is generally higher than what is used to preheat air for a dryer. The results of lost efficiencies within a system, be it fuel burning or shaft losses, means the total energy and exergy required to drive a system will naturally be higher than the ideal requirement for just a dryer.

The main losses associated with losses from the fuel to the product are conversion losses. These losses are associated with an 80% burning loss along with heat transfer effectiveness, heat loss to the environment and performing other tasks. Heat recovery and pressure-work recovery are ways of minimising these losses, but can only partially minimise the increase in fuel use. These increased numbers for Case 1 are:

$$H_{fuel} = 3{,}885\ kW \qquad Ex_{fuel} = 3{,}959\ kW$$

The evaporation potential associated with these fuel values, given the same conditions for the dryer stated above, provide the following values:

$$n_{\Delta V.\dot{f}uel.Q} = 0.0928\ kmol.s^{-1} \qquad n_{\Delta V.\dot{f}uel.Ex} = 0.8882\ kmol.s^{-1}$$

It should be noted that the calculated values above, of evaporation potentials, are determined by the energy available within the fuel-source dedicated to the task of evaporating water at the solids inlet temperature. These values lead to system-wide evaporation efficiencies of:

$$\eta_{\Delta V.H_{fuel}} = 71\% \qquad \eta_{\Delta V.Ex_{fuel}^{Trans}} = 7.4\%$$

Both efficiencies drop significantly when compared with Case 0 (79% to 71% and 41% to 5%). This result is expected since more energy is needed (in the form of fuel) than the recovery using the economiser.

The maximum heat recovery potential is around 84% of what is needed to pre-heat the feed (at the current conditions), considering that the burner in the boiler system is assumed to be 80% efficient, and that the heat recovery in the system is quite low (20% of maximum potential), the extra heat losses associated with the system are significant.

Another reason why the fuel-based factors are lower is that the boiler section of the case is not 100% efficient. Given this information, the resulting amount of fuel energy is higher than ideally required.

Case 2

It is also important to consider the 'fuel' energy fed into the system. This is the energy value of the natural gas or electricity added to run the system, and is generally higher than what is used to preheat the drying gas for the dryer. The result of lost efficiencies within a system means that the total energy and exergy required to drive the system will naturally be higher than the ideal requirement for just the dryer. These increased numbers for Case 2 are:

$$H_{fuel} = 4{,}408\ kW \qquad Ex_{fuel} = 4{,}455\ kW$$

The evaporation potential associated with these fuel values, given the same conditions for the dryer stated above, gives the following figures.

$$n_{\Delta V.\dot{f}uel.Q} = 0.104\ kmol.s^{-1} \qquad n_{\Delta V.\dot{f}uel.Ex} = 0.999\ kmol.s^{-1}$$

It should be noted here that the above calculated values of evaporation potentials apply if all the energy available within the fuel source were dedicated to the task of evaporating water at the solids inlet temperature. These evaporation potentials lead to system-wide evaporation efficiencies of:

$$\eta_{\Delta V.H_{fuel}} = 63\% \qquad \eta_{\Delta V.Ex_{fuel}^{Trans}} = 6.5\%$$

Summary

As the required heating in Case 0 is added using utilities (i.e. with no attempt to use heat recovery), the energy and exergy costs are quite high, and the exergy lost to the environment is high (due to the extra fuel required for the utilities and warm dryer flue gas). This situation is useful as a base case for comparison with proposed improvements.

Based on the overall factors, the energy utilisation may be defined as the ratio of the energy input to the energy added to perform the task. On an item-by-item basis, this definition is refined to be closer to the task efficiency. On an energy basis, it is appropriate to define this value as the energy added to the system per kilogram of evaporated water.

Table 6-1: Summary of Energy flows for the base comparison.

Case 0	Case 1	Case 2
$H_{IN}^{TM} = 3{,}773\ kW$ $H_{IN} = 27{,}379\ kW$ $H_{IN}^{Trans} = 3{,}774\ kW$ $H_{G.IN} = 3{,}525\ kW$	$H_{IN}^{TM} = 362\ kW$ $H_{IN} = 27{,}547\ kW$ $H_{fuel} = 3{,}885\ kW$	$H_{IN}^{TM} = 4{,}714\ kW$ $H_{IN} = 28{,}014\ kW$ $H_{fuel} = 4{,}408\ kW$

NOTE 6-2: The $H_{G.IN}$ term is a close representation of the H_{IN}^{TM} term. The 248 kW difference is associated with the solid stream (S-09) being above ambient temperature (60^{O}C).

Each of the three cases perform the same amount of evaporation. The H_{IN}^{TM} term used for the three cases is difficult to use due to the difference in the nature of the energy sources. In Case 1, the fuel used in the boiler is counted in the fuel and the total value, but is chemical in nature and is not counted in the TM energy. In Case 2, electricity is the fuel and is included in the TM energy. Given this difference, it is important to use a comparable information set. The H_{fuel} values for Cases 1 and 2 are equivalent, and this parameter shows a much higher energy requirement for Case 2 than for Case 1 (13%).

Comparing these values with the energy required for the dryer, there is an energy requirement improvement in Case 2. The higher fuel energy requirement for Case 1 also indicates a higher rate of energy loss per task.

6.4.3Flue Gas Recovery Potential

The flue gas recovery potential is calculated by:

$$\Delta H_{Rec} = H_{G.OUT} - H_{G.OUT@T_0} \quad \text{6-10}$$

$$\Delta Ex_{Rec} = Ex_{G.OUT} - Ex_{G.OUT@T_0} \quad \text{6-11}$$

Case 0

The energy (and exergy) recovery potential is important in defining the system. Based on the gas side of the dryer, the excess energy is associated with the heat in the increased temperature of the outlet (compared with the raw air feed temperature of 25^{O}C). In the case of the dryer:

$$\Delta H_{Rec} = 2{,}992\ kW \qquad \Delta Ex_{Rec} = 274\ kW$$

$$\Delta Ex_{Rec}^{TM} = 69\ kW$$

It is important to note that the exergy-based recovery potentials are different. This difference is due to the composition change. A significant amount of exergy is lost to the environment in the form of diffusion losses. What is more important is that a large amount of the energy potential is associated with the condensation of the water at the reference temperature (25^{O}C). Since the gas outlet has a dew point of 43.1^{O}C, potential condensation energy (to a dew point of 25^{O}C) is included.

While the exergy factor considers the composition (and the TM value does not), a driving force exists with the environment in terms of the water content being close to (or at) saturation conditions, rather than at dead state conditions. This driving force is considered to be an unrecoverable loss.

From this potentially recoverable exergy, only 25% (69 kW of 274 kW) is recoverable as heat. While using this energy is not practical (reusing heat close to the dead state temperature is difficult), it provides a target to aim for when applying the same method to the systems in the other two cases.

Case 1

Other areas of interest are environmental and system losses. For Case 1, the lost energy to the environment is in the form of flue gas from both the dryer air and boiler system flue gas. These losses are significant, with the heat loss from the cooled air being used to preheat the feed gas.

$$\Delta H_{Rec} = 2{,}485\ kW \qquad \Delta Ex_{Rec} = 223\ kW$$

$$\Delta Ex_{Rec}^{TM} = 18.6\ kW$$

A significant proportion of the lost energy is not associated with thermally-based energies (only 18.6 kW of the 223 kW). This result means that the majority of the lost energy is unrecoverable (92%) using simple heat exchange, and is due to the change in the air composition within the system. Also, if we compare this 18.6 kW to the potential 69 kW from just the dryer, 27% of the potential energy is not recovered. This result is due to the limitations given by the approach temperature ($\Delta T=20^{O}C$) and its effect on heat exchangers within the system.

Case 2

Other areas of interest are the environmental and system losses. For Case 2, the lost energy to the environment is in the form of flue gas from dryer air. This loss is significant and more complex than that of Case 1 due to the use of the valve V-1. Prior to V-1, the gas temperature is $62^{O}C$ and contains significant amounts of water vapour, and the pressure is also significant being at 3.56 Bar. After V-1 the conditions change to ambient pressure and $22.5^{O}C$, which is significant in that the outlet temperature is below ambient ($25^{O}C$).

$$\Delta H_{Rec} = 2{,}883\ kW \qquad \Delta Ex_{Rec} = 56.9\ kW; 2{,}721\ kW(pre\ valve)$$

$$\Delta Ex_{Rec}^{TM} = 10\ kW; 2{,}516 kW(pre\ valve)$$

A significant proportion of the lost energy is not associated with thermally-based energies (only 10 kW of the 56.9 kW). This result means that the majority of the remaining energy is unrecoverable (82%) using simple heat exchange. Also, comparing the 10 kW to the potential 69 kW from Case 0, 85% of the potential energy is not recovered. The main loss for this system is associated with pressure since an adiabatic valve has been assumed at the outlet of the system. A pressure recovery expander (turbine) may be installed in a real system to minimise this loss further at an increased cost. The loss associated with this valve on exergy terms is 2,664 kW. This valve also has the potential to condense the excess water vapour, leading to this large energy loss.

6.4.4Solids Heat Recovery Potential

It is important to discuss the loss of energy associated with the product stream (dried solids) as it is difficult to recover the heat from this part of the system. The solids stream leaves Case 0 (and subsequently Cases 1 and 2) at 48.8^{O}C which is significantly higher than the ambient temperature (25^{O}C). This leads to an extra 88 kW of enthalpy which is wasted from the feed heaters, equating to 7 kW of TM exergy being wasted. The solids may still attempt to absorb moisture from the environment unless further cooling takes place, and this has the potential to waste up to 72 kW of diffusion energy (if the solids behave in a thermodynamically ideal manner). This result is not significant when compared with the recovery potential of the gas and will not be considered further.

6.4.5Improvement Potential

Case 0

The factors discussed above are simple in interpretation and calculations, with many of them not requiring exergy to be calculated at all. However, many factors based on exergy in literature are not as straightforward to interpret. One such method, *IP*, is another way of interpreting losses within a system. IP does not provide a target, but it does have the potential to be used for optimisation through case studies.

$$IP^{Task} = 490\ kW \qquad IP^{Trans} = 542\ kW$$

$$IP = 598\ kW$$

The IP shifts the efficiency factor back into the scalar domain by utilising the lost exergy (or entropy generation) value. This approach is similar to the INE method. However, since this is determined in the exergy domain, it has the potential to be more informative (since INE is more of a 'short-cut' method). The other benefit of IP over the INE method for systems is that the definition is applicable on the simple efficiency basis, or task, depending on the level of information required. The INE factor is only suitable for use on an item-by-item basis, because the calculation of the inevitable loss is based on the unit task and varies with different unit operations. For example, calculating the INE for a compressor is significantly different to the dryer, and a heat exchanger is different again. These differences mean it is actually more meaningful to assess the system as a whole. INEs for individual unit operations will be discussed later.

It is important to note that the INE value for the dryer is 669 kW [2], which is the theoretical minimum exergy loss associated with the ideal process of drying.

Case 1

The evaporation and recovery potentials are useful in explaining how the expanded system reduces the overall efficiency of the dryer when changing the basis from the dryer-based factors to fuel-based factors. The effects of including the system (as opposed to on an item by item basis) on the other factors such as the IP, INE, and other efficiency factors are significant. These are explored here.

The INE of the system is challenging to define. For example, it may be defined relative to the sole task of drying (in which case it is the same as that of Case 0), or it may be defined per plant zone (the boxed areas of the plant diagrams), or defined as a combination of individual unit operations. The INE method is best defined as the third option (each unit separately defined) and this is explored in the work of Feng [39, 98].The IP is a useful factor for a system.

$$IP^{Task} = 3{,}668\ kW \qquad IP^{Trans} = 3{,}708\ kW$$

$$IP = 3{,}711\ kW$$

These results are significantly larger value than that of Case 0, which is due to the increased complexity of the system, with extra losses associated with the conversion of fuel in the process (similar to the change in evaporation potential).

Case 2

For consistency between the cases, the evaporation and recovery potentials that are useful in explaining how the expanded system reduces the overall efficiency of the dryer are explored here. The following results for IP were obtained.

$$IP^{Task} = 4{,}146\ kW \qquad IP^{Trans} = 4{,}559\ kW$$

$$IP = 4{,}457\ kW$$

Each of the IP values are significantly larger than that of Case 0, and this is due to the increased complexity of the system, with extra losses associated with the conversion of fuel in the process (similar to the change in evaporation potential).

The improvement potential is 20% higher than Case 1 (3,711 kW vs 4,457 kW). This result means that Case 2 is less effective at the task overall, but at this level it is hard to pinpoint why (although the valve is the major concern), or what part of Case 1 is the main contributor. An item-by-item analysis is required for a better understanding, and this is explored later.

6.4.6Efficiency Factors

Base factors

Many efficiency factors that can be used to describe a system are simple, while others require interpretation, each giving insight to the process; the simple efficiency factor (for example) provides an indication of exergy use within a system compared with what is entering a system. The following factors (with differing calculation bases) are calculated using Equation 12.

$$\eta_{Ex.simple} = \frac{Ex_{IN} - Ex_{OUT}}{Ex_{IN}} \qquad 12$$

Table 6-2: Summary of simple efficiency factors.

Case 0	Case 1	Case 2
$\eta_{Ex.simple}^{TM} = 90.3\%$	$\eta_{Ex.simple}^{TM} = 99.5\%$	$\eta_{Ex.simple}^{TM} = 99.9\%$
$\eta_{Ex.simple}^{Trans} = 65.7\%$	$\eta_{Ex.simple}^{Trans} = 88.8\%$	$\eta_{Ex.simple}^{Trans} = 95.7\%$
$\eta_{Ex.simple} = 3.1\%$	$\eta_{Ex.simple} = 23.5\%$	$\eta_{Ex.simple} = 15.8\%$

The energy recovery within each system results in an improvement in efficiency. While the efficiency values are lower overall for Case 2 than for Case 1, the remaining losses occur to the environment. These results provide a starting point for sensitivity analyses. Case 1 has a higher overall simple efficiency – implying that it involves a higher exergy use within the system (i.e. less wasted exergy), but a lower transiting efficiency (i.e. it has a greater loss to the environment than Case 2).

Task Factors

The previous factors assessed the overall energy and exergy loss within and around a system. However, systems are designed to perform a task — in this instance, evaporating water to dry a solid sufficiently. For the task of evaporation, the dryer performs quite poorly on an exergy basis (and as a result, typically occurs in a relatively compact unit).

Table 6-3: Summary of task factors.

Case 0	Case 1	Case 2
$\eta_{\Delta V.H_{G.IN}} = 79\%$	$\eta_{\Delta V.H_{fuel}} = 71\%$	$\eta_{\Delta V.H_{fuel}} = 63\%$
$\eta_{\Delta V.Ex_{G.IN}^{TM}} = 40.5\%$	$\eta_{\Delta V.Ex_{fuel}^{Trans}} = 7.4\%$	$\eta_{\Delta V.Ex_{fuel}^{Trans}} = 6.5\%$

Both systems have reduced task efficiencies, particularly on an exergy basis. The lost effectiveness is lower in Case 2 — i.e. less exergy loss is associated with the task, so more of the loss is associated with the rest of the system. However, the target is to meet (or exceed) the results of Case 0. As such, Case 2 is a better option due to its higher task efficiency.

6.5Item-by-Item results

6.5.1Case 1

Table 6-4: An item-by-item analysis of Case 1.

	H_{IN}	Task	H_{Task}	Task (%)	IP	AVO/IN (%)	Ex_{IN}	Ex_{OUT}	Task	Task (%)	IP	IP/IN (%)
E-1	3,714	Heat	507.7	13.7	3,206	0.00	428	397	19.2	4.5	408.5	95.5
E-2	4,580	Heat	3,018	65.9	1,563	41	1,439	1,599	700.3	48.7	738.6	51.3
D-1+C-1	3,774	Evap	2,777	73.6	996	6.6	1,255	430	783.6	62.4	471.4	37.6
E-3	249	Heat	248.5	99.9	0.3	8.9	566	535	13.5	2.4	552.8	97.6
E-B2	866	Heat	315	36.4	551	0.4	215	196	69.9	32.6	144.6	67.4
R-B1	4,256	Rxn	3,547	83.3	709	34.3	4,032	2,648	3,360	83.3	672.1	16.7
E-B1	5,239	Heat	3,270	62.4	1,970	15.3	3,606	1,754	585	16.4	3,022	83.8

The key results from Table 6-4 indicate that the dryer economiser (E-1), the dryer (D-1+C-1) and the boiler heat recovery exchanger (E-B2) have the lowest task efficiencies on an energy basis. The solids preheater (E-3), the economiser (E-1), and the boiler steam heater (E-B1) are the worst task performers on an exergy basis. However, looking at the IP for these units, the large-scale losses are associated with the steam exchanger (E-B1), the dryer gas preheater (E-2), and the boiler reactor (R-B1). From these results, the focus on improving the system lies in the boiler package part of the system.

AVO/IN has been calculated based on the energy transfer per unit as defined in the work of Feng [39, 98] for the AVO (1-INE) value and the value of the transiting exergy feed per unit. The higher this number, the worse the performance – which means similar results to that of the IP. The INE/AVO method may present a reasonable short-cut estimate on a unit-by-unit analysis, but is challenging to define for entire systems.

6.5.2Case 2

Table 6-5: An item-by-item analysis of Case 2.

	H_{IN}	Task	H_{Task}	Task (%)	IP	AVO/IN (%)	Ex_{IN}	Ex_{OUT}	Task	Task (%)	IP	IP/IN (%)
E-1	7,042	Heat	3,525	50.1	3,517	0.2	3,793	3,595	719.5	19.0	3,073	81.0
C-2	7,042	Comp	3,328	80.0	1,575	24.6	4,634	3,793	3,365	80.0	927	20.0
D-1+C-1	3,774	Evap	2,777	73.6	996.3	6.6	1,255	430	783.6	62.4	471	37.6
E-3	249	Heat	248.5	100.0	0.0	9.6	770	535	13.5	1.8	757	98.2
V-1	3,551	Expand	2,048	57.6	1,507	71.2	2,875	211	2,664	92.7	211	7.3

The key results from Table 6-5 indicate that the valve (V-1), the economiser (E-1), and the dryer (D-1+C-1) are the worst performers on an energy task basis. The solids pre-heater (E-3), the economiser (E-1), and the dryer (D-1+C-1) are the worst performers on an exergy task basis. However, looking at the IP for these units, the large-scale losses are associated with the economiser (E-1), the dryer (D-1+C-1), and the valve (V-1). From this, the focus on improving the system lies in improving these three units.

Comparing these results with those of Case 1 indicates a significant improvement on an item-by-item basis, while the IP for the economiser is significantly higher (3,073 kW) than the pre-heating train in Case 1 (409 kW). This result has occurred since the outlet of the economiser on the discharge side has a significantly higher amount of energy that is not recovered.

The importance of the results associated with the valve (V-1) in Case 2 shows the importance of pressure based energy recovery, the exergy being lost to the environment within this unit (or if it is not even installed) is significant, even if the pressure is not as high as that of the boiler in Case 1.

6.6Overall Discussion

It is important to compare these results to provide a context for potential system improvements that an exergy analysis may yield for a system that includes a dryer.

It is important to note that while the discussion below is focussed on the inlet gas temperature, the results are very similar with respect to changing the gas flow rate. Adding the case study for those does not differ substantially from that of Chapter 4. In saying that, since the variables being studied are energy-based variables, temperature and flow are heavily involved in that base definition, which does suggest that changing temperature and flow in an inverse manner (to keep feed energy constant) will yield similar results.

6.6.1Comparison of case studies

The base case outlines the potential recoverable energy for the system to benchmark the two cases; its task is focused on evaporating water. When assessing the system as a whole, this (water evaporation) becomes the task for the entire system, thereby allowing different cases to be analysed and compared.

An exergy analysis of the system focuses on other factors outside the heat flow and an energy balance. For example, on an energy basis, a dryer is a reasonable unit of operation for the task of evaporating water. However, the amount of lost exergy indicates that the unit uses significant amounts of high quality energy to perform the task.

- On the energy per evaporation basis, Case 1 is superior. While more of the fed energy in Case 2 is converted directly into the potential to evaporate water in the dryer (on a fuel basis), much of it is wasted directly to the environment. In comparison, Case 1 has fuel losses associated with the conversion of fuel to heat.

- On the energy recovery basis, Case 1 is preferred. While the recoverable energy is higher in Case 2, sizeable amounts of this energy are due to pressure. Both systems have low outlet temperatures and identical recovery losses associated with the product being warm.

- If only base factors are considered, then Case 1 is superior due to its total exergy use and loss to environment being lower than Case 2. If the pressure-based exergy is recovered in Case 2, this result is reversed.

- For task factors, Case 1 is preferred, as the task is based on evaporation.

6.7Implications for the system

Two key variables that may potentially be manipulated are the dryer gas inlet temperature and the dryer gas feed flowrate. The effects of these changes on several efficiency factors and quality metrics are shown and discussed here.

To have a basis of comparison with the dryer only, the dryer factors are shown in Figure 6-3. It must be noted that a dryer gas inlet temperature below $170^{O}C$ results in the dryer not reaching the isotherm at equilibrium, and the outlet equilibrium temperature is below the outlet dew point temperature. This result means that there is not enough energy in the feed gas to fully dry the solids.

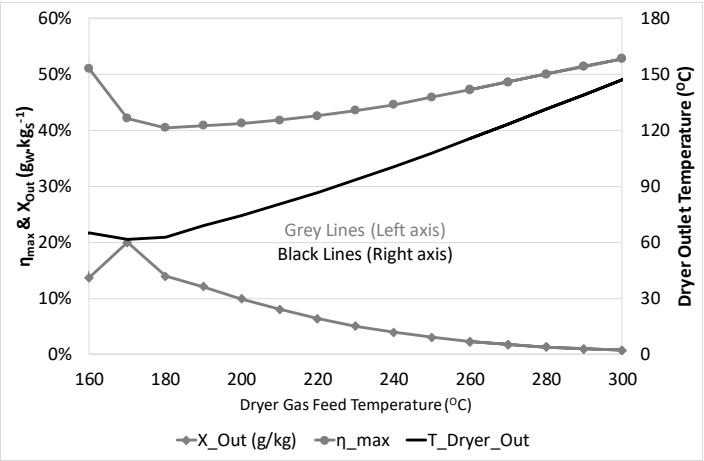

Figure 6-3: Dryer maximum efficiency, outlet moisture content for the dryer against gas feed temperature.

Figure 6-3 shows the relationship between the effect of changing the inlet gas temperature on the maximum efficiency of the dryer, the outlet dryer temperature, and the outlet moisture content. This relationship is important because it gives two system limitations and a target for efficiency when dealing with the system.

The maximum efficiency is determined by the boiler assumption used for the calculation of the INE factor, and this calculation may be found in Chapter 4.The outlet gas temperature is the outlet gas temperature given the offset of 20^{O}C of the outlet gas temperature above the outlet solids temperature.

The limits given in Figure 6-3 are inlet gas temperatures of 180^{O}C and 250^{O}C. Below 180^{O}C there is not enough energy in the gas to effectively dry the solids. The upper limit given (250^{O}C) arises because, at this temperature the outlet gas temperature reaches 100^{O}C which increases the risk of over drying or oxidation of the powder. A more reasonable limit would be when the solids reaches 100^{O}C (so given the offset, 265^{O}C is used as the inlet temperature). Due to these limits, any optima outside of the range (180^{O}C -265^{O}C) should be considered impractical.

Based on this information, the maximum efficiency (Figure 6-3) is at its lowest at the lowest point in the range, and steadily increases to the upper limit of the range.

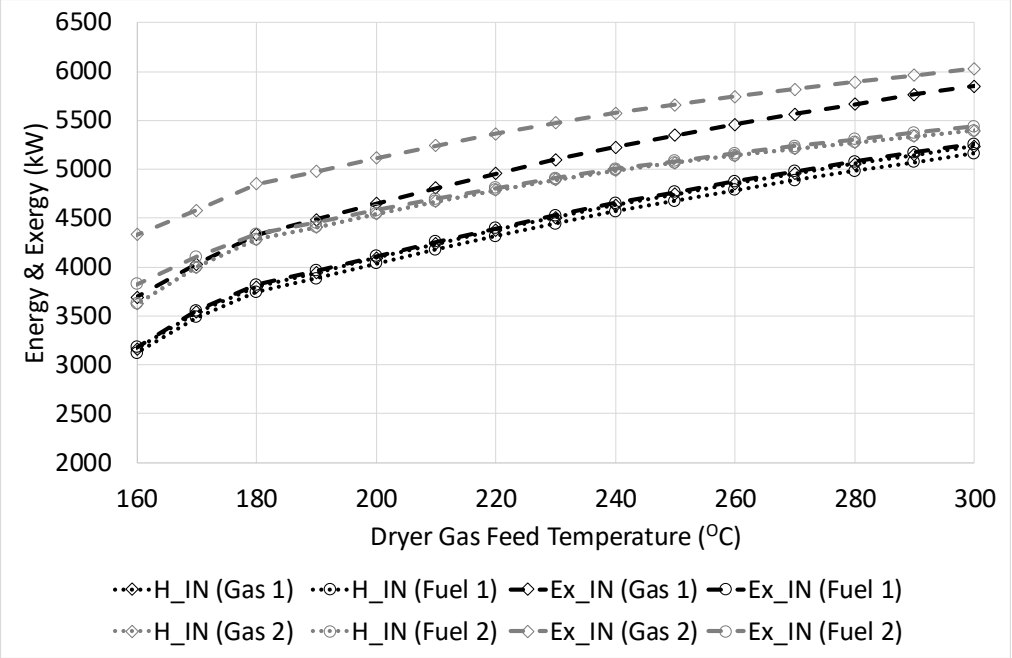

Figure 6-4: Inlet and Outlet Energy and Exergy flows for Case 1 (Black) and Case 2 (Grey) against feed gas temperature.

Figure 6-4 shows the energy and exergy profiles of both cases over a range of inlet gas temperatures. These are generally following the same shape (Carnot curve) with little difference apart from system 2 being higher in all cases. Figure 6-4 is important as it is the basis for several factors such as recovery potential and several efficiency factors.

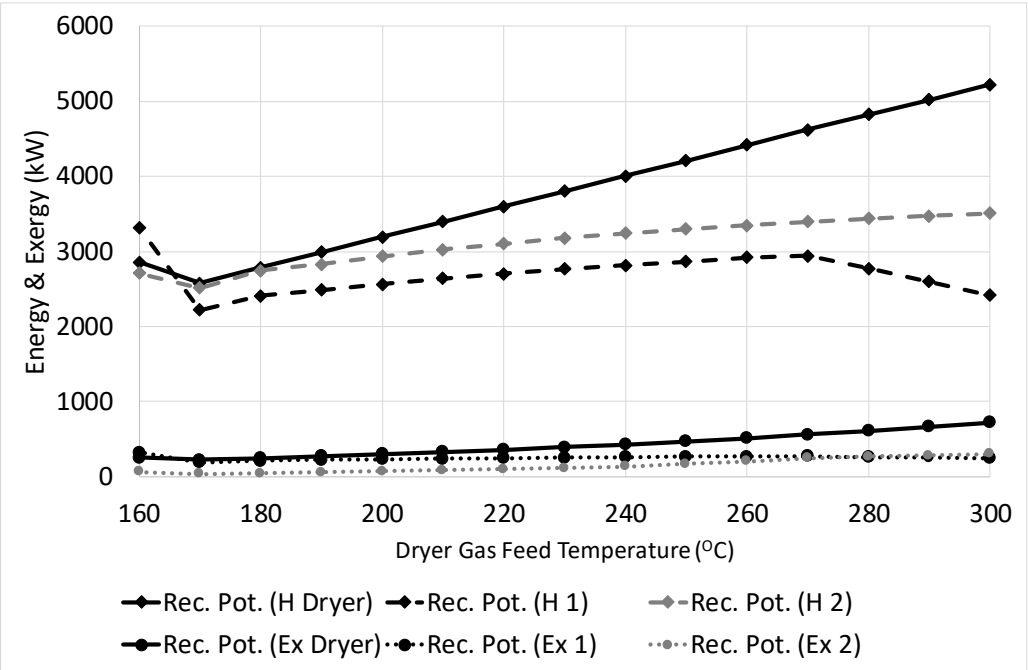

Figure 6-5: The recovery potentials of the dryer and Case 1 and 2.

The recovery potential is one of the factors described above that has a significant meaning in that the recovery is the main way to reduce energy and exergy loss. The results of the raw recovery potential compared with the inlet gas temperature are shown in Figure 6-5. The recovery potentials of the dryer are the maximum recovery, while those of the two systems are similar to each other with Case 2 being slightly higher. It is important to note that both potential recovery curves move away from that of the dryer as the temperature increases. Above 270^{O}C the boiler system has issues with generating enough energy at a sufficient temperature to supply the dryer, and the outlet temperature of the dryer is beyond 100^{O}C (Figure 6-3) meaning this region is not feasible for drying heat sensitive materials such as skim milk powder.

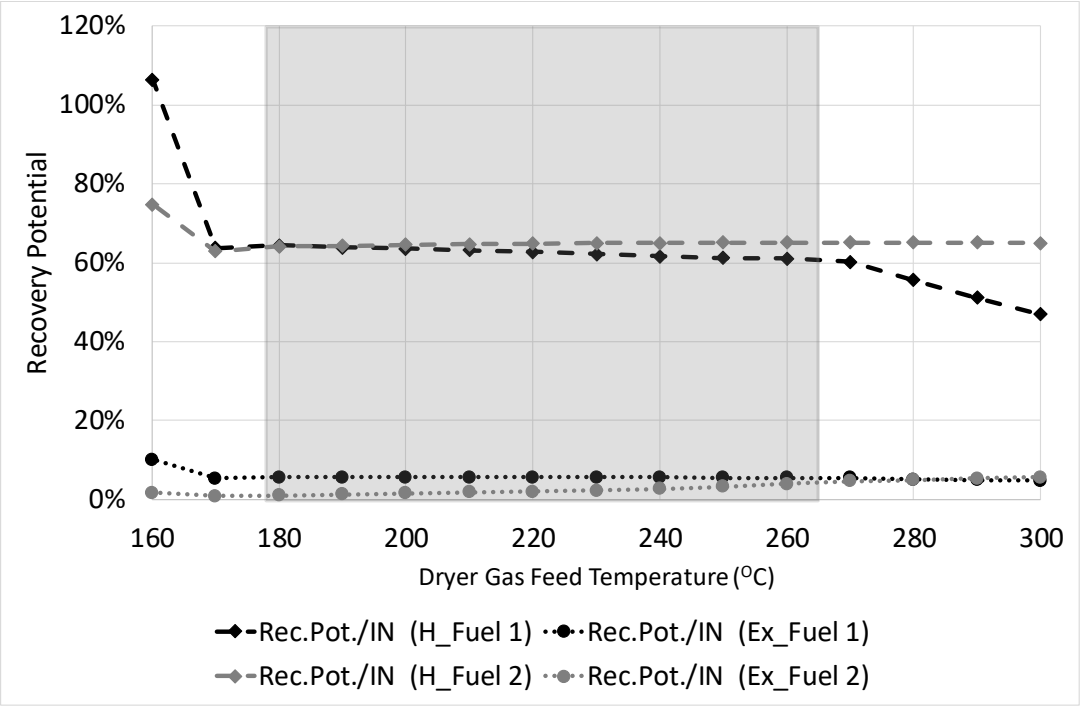

Figure 6-6: Recovery potential as an efficiency.

Figure 6-6 shows the results of comparing Figure 6-5 with Figure 6-4. The recovery potential within the grey area (practical region in the grey box) is an ineffective way of improving recovery for either case. Due to the nature of Case 2, the cost of a compressor will increase significantly as the temperature requirements increase, while on the other side, the

potential to be able to use a turbine to replace the valve increases. Increasing the feed temperature for Case 1 is undesirable with the alternate side effect of the steam pressure requirements becoming increasingly higher to achieve the desired temperature.

The exergy recovery percentage is quite low (compared with the energy recovery) but is an important result, even if it follows the same trend as energy. This result arises because the majority of the energy within the system is thermal in nature, and the comparison is based on overall temperature change.

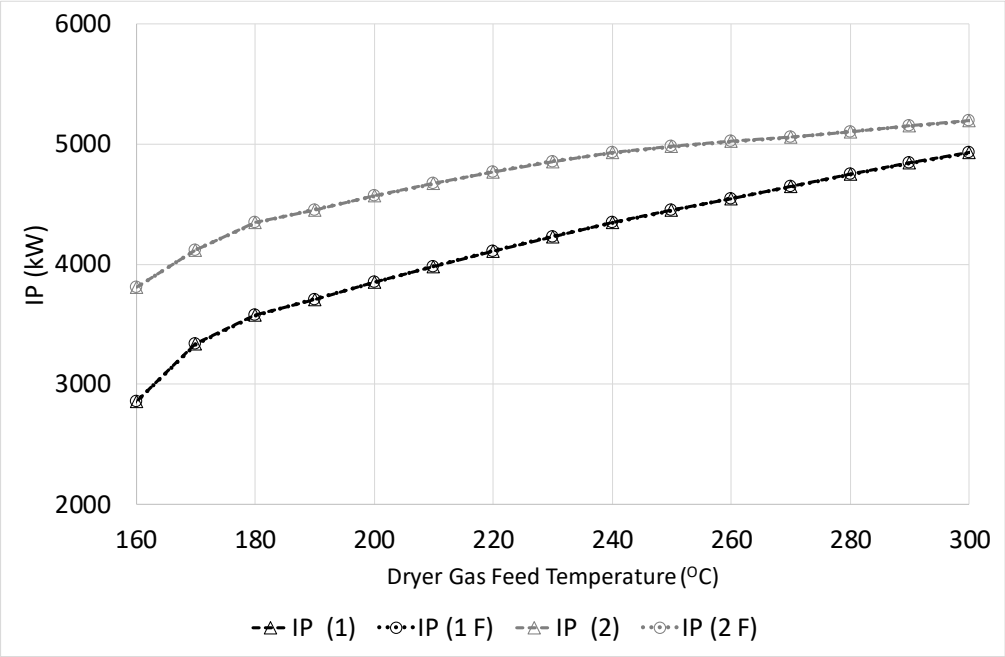

Figure 6-7: The Improvement Potential as a function of the dryer gas feed temperature.

The high value of IP shown in Figure 6-7 for Case 2 is due to the 'inefficient' valve used to return the flow from the compressor to atmospheric pressure, while the value for Case 1 is associated primarily with the utility boiler and its discharge temperature increasing (as the steam temperature increases).

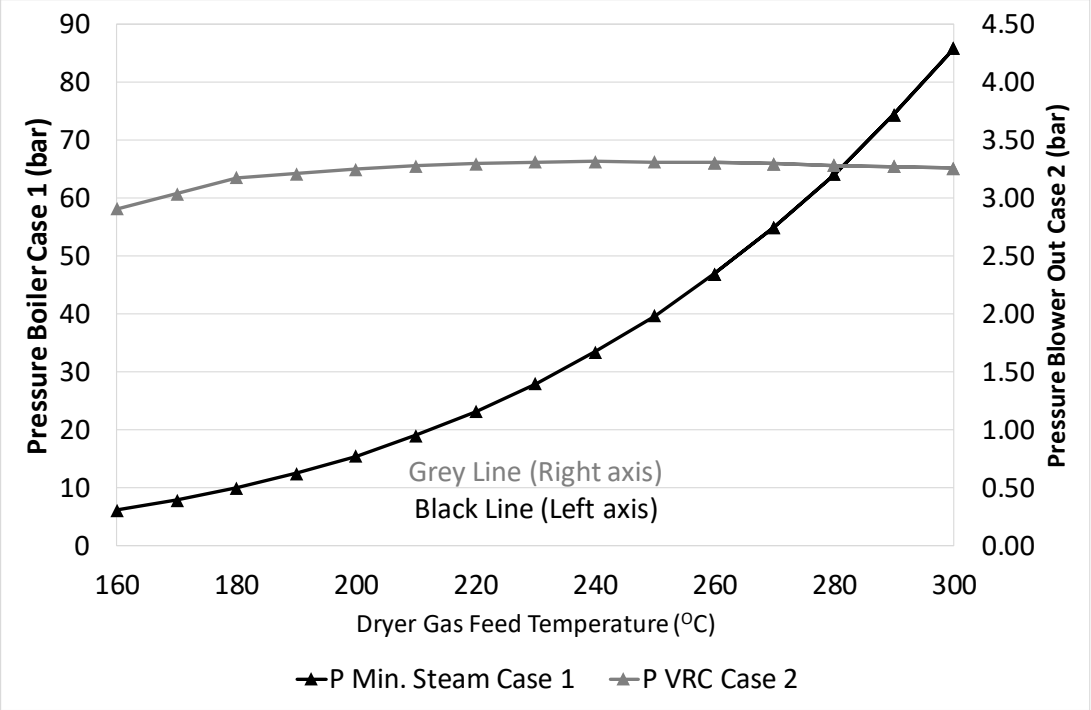

Figure 6-8: The pressure requirements of both systems as a function of dryer gas feed temperature.

Figure 6-8 shows the pressure requirements of both systems, the minimum pressure in the accompanying boiler for case 1 that is required to achieve saturated steam to pre-heat the feed gas, and the outlet pressure for the compressor/blower in case 2. The high pressure in case 1 is significant due to the increased cost of generating the steam, and increased material thickness of the heat exchangers and piping, while the small change in the pressure required for case 2 indicates system flexibility. On the point of the required pressure for Case 2, the pressure has a maximum around 240^{O}C as expected. Above this temperature the outlet pressure appears to decrease, and this decrease is due to the dryer outlet temperature increasing.

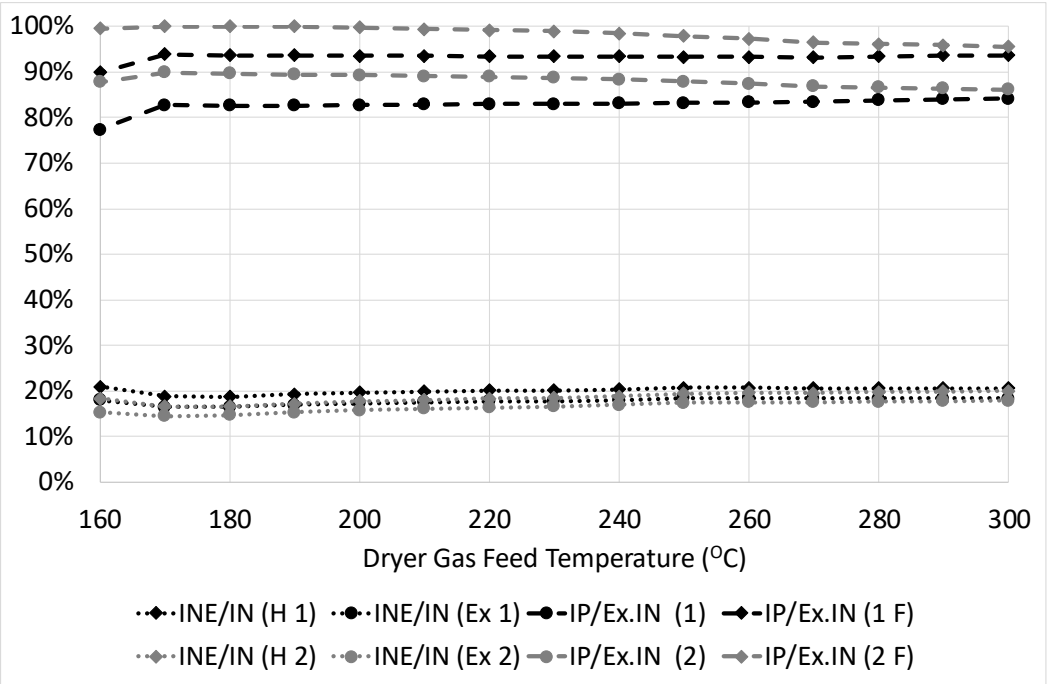

Figure 6-9: The IP and INE/IN as against dryer gas feed temperature.

The Inevitable loss and IP are important results (Figure 6-9) as they both indicate the utilisation of energy and exergy within the system. It is natural that these factors are inverted in their results (shape) since IP determines how much energy or exergy is wasted, while INE looks at the minimum loss associated with the process. The importance is the direction of the slope for each of these factors (again only looking at the practical range), and the optimum point based on these factors gives the minimum point. It is worth noting that while the INE/IN exergy ratio increases for both systems as the dryer gas temperature increases, the IP/IN Case 1 has only a small change (0.26% gas basis and 0.29% on a fuel basis). This result indicates that changing the temperature has a negligible effect on the change in exergy utilisation within the system.

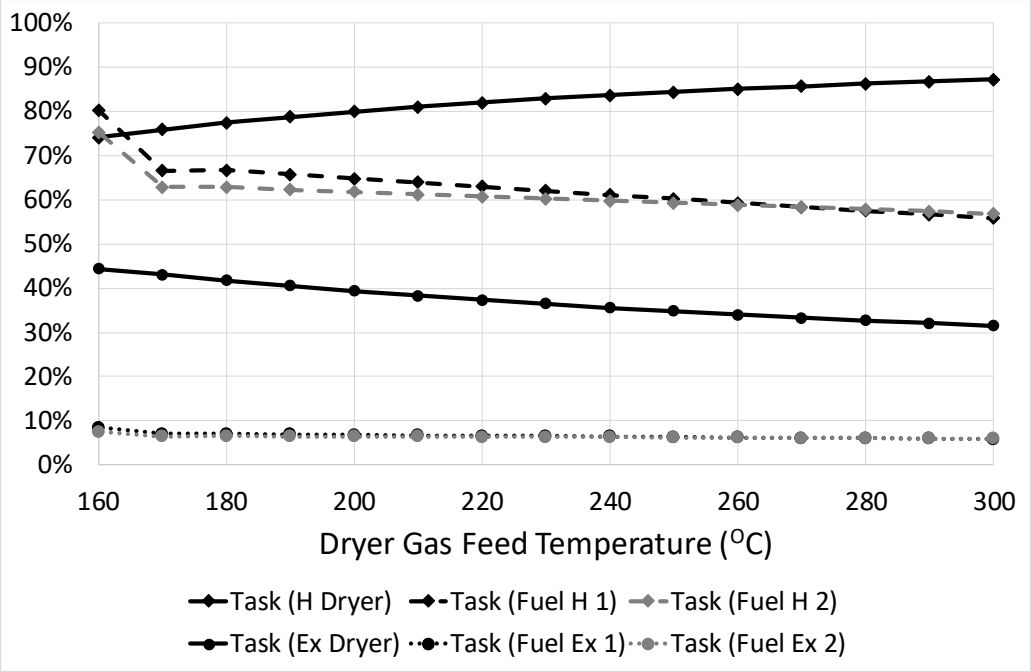

Figure 6-10: Task efficiency of case 1 and case 2 compared with the dryer.

Figure 6-10 shows that while the task efficiency of the dryer increases (on an energy basis) the system inverts it so that the task efficiency decreases significantly as the feed temperature increases. This makes sense when looking at the moisture content curve in Figure 6-3, in that more energy is used to evaporate less moisture at higher temperatures, and this decreases efficiency.

On an exergy basis all three cases are consistent in the way that the task efficiency decreases as the feed gas temperature increases. The best point for the task efficiency is at the lowest practical temperature, and this result may lead to multi-step drying systems being preferred.

With these case studies the results agree that the lowest practical gas feed temperature is the most efficient operating point. On the other hand, other operational factors may be more important, such as a desired solids moisture content or dryer size.

The overall task efficiency is linked with the solids moisture content; only the shape of the relationship between the overall task efficiency and solids outlet moisture content should be considered here - not the scale (as that would be dependent on the system).

The temperature-based profiles indicate that a system-wide optimisation is challenging due to the slightly interactive nature of the system (heat recovery loops). However, most of the results indicate that an increase in temperature (and gas flow) are undesired on both the task and recovery potential basis.

The dryer and parts of the supplementary sections of both cases studied here are limiting. For Case 1, the pre-heating heat exchanger using steam, and the dryer are the worst performers on an exergy basis, while for Case 2, the dryer and the exhaust valve are the worst performers.

Optimisation can be targeted to these areas, in terms of the dryer, the minimum inlet gas temperature to reach the desired output is preferred. This consideration has several effects on the system supporting the dryer, pushing the boiler and compressor to require less energy and less wasted energy within the system as a result.

The energy-based task efficiencies are similar for both systems. The similarity also demonstrates how linked the systems are and that the dryer is the main item in the system. For larger systems, targeting the key units is important for optimisation. Further, the enthalpy-based optimisation is strongly linked to the outlet moisture content as can be seen in Figure 6-10, in contrast to exergy factors, which are linked to system temperatures and flow.

These results demonstrate the usefulness of several factors:

- Simple efficiency is more suited for an overall analysis when comparing different systems or to locate potential areas for further optimisation.
- Task efficiencies are useful for itemised parts of a system and determining if the loss is desired, or wasteful.
- Many of the advanced factors become irrelevant in small systems such as those studied here.

6.8Conclusions

The evaporation potential for Case 1 is 13% better than Case 2 on a fuel and overall basis. However, the recovery potential is higher in Case 2 if the valve is replaced by an improved recovery unit, mainly pressure recovery. The importance of a unit-based approach along

with an overall systems approach is evident in the results. For example, the valve is by far the worst performing unit in Case 2 (more than 50% of total system loss), with the compressor and dryer the next worst performers. The boiler unit(s) are among the worst exergy performers in Case 1, along with the dryer. The valve in Case 2 can be replace by a turbine, that change would involve a higher capital cost than a valve but reduce operating costs.

The solids pre-heater is inefficient in both systems but has a low overall loss and while its efficiency improvement may be high, the gains are an order of magnitude lower than the potential improvement of other units.

Basic factors are useful to simplify larger systems and focus attention to a general area, or to help select process changes. However, in this study using these factors suggest that Case 2 is superior to Case 1, while both cases are improvements on the base case (dryer on its own). More detailed factors such as task, transiting, and recovery all suggest that Case 1 is the preferred system.

From the results, it is clear that Case 1 is a better system than Case 2 while there is potential to improve both systems.

The effect of changing the dryer feed gas temperature are interesting as they suggest that an increased temperature would be inefficient for either system, and the same can be said for flow.

In general, Case 1 is superior in most ways to Case 2, unless the higher energy exhaust from Case 2 can be recovered. As part of a larger system, Case 2 may integrate better than Case 1, and this has not been studied.

These results show the confusing nature of several factors used within the exergy analysis literature, while helping with the interpretation of results in several ways.

Chapter 7 A Comparison of Assessment Methods

The following is an extension of the analyses presented in Chapters 5 and 6. The visualisation of exergy analysis (ExA) is an important requirement to make the analysis more readable, and presentable in reports. This outcome has been one of the major benefits of a Pinch Analysis (PA) in the past. This situation leads into a comparison between PA and ExA, mainly focussing on difficulty level, interpretation and flexibility of each analysis.

Both PA and ExA have limitations and assumptions (outlined in Chapter 2), so these allow some generalisations and simplifications to be made. These simplifications are not suitable for all situations to use in an ExA, so some basic understanding of them is important for them to be used, unlike in PA, which has a set of simple to follow rules.

The following section (7.1) refers to Case 1 in Chapter 6.

7.1Comparing Pinch Analysis and Exergy analysis

To start with, a quick summary of the set-up for Chapter 6 will help set up the rest of this discussion. Performing a PA on the open system (Case 0) results in Case 1 (Figure 7-1). The change is the addition of two heat exchangers, one on the dryer air (E-1), and the other on the boiler air side (E-B2); both are considered economisers, taking flue gas to preheat the feed gas. Since these exchangers are gas-gas heat exchangers, they have a large surface area per unit temperature difference; as such the pseudo temperature difference used in the PA is 20^{O}C, not the typically assumed 10^{O}C [61].

The effect of this change is to reduce the size of the exchanger since it is not necessary to achieve such a small temperature difference (or efficient; both in costs and materials and operating costs) [61] section 3.7. The side-effect is the reduction in recovered energy, a reduced exergy efficiency, and an increase in utilities to further increase the temperature in terms of the dryer gas feed. There is also the issue of energy (exergy) losses to the environment – particularly at higher temperatures where a larger heat exchanger will have a greater exposure to the environment and proportionally higher heat leak [28, 61, 110, 126].

PA gives an effective indication of heat exchanger placement, but it does not indicate how efficient the placement is. The assumptions and rules governing PA assist in process integration.

ExA, on the other hand, analyses effects not normally considered in PA. The extension of the pressure and chemical-based energy that exergy allows may lead to more flexible optimisation beyond just heat exchange systems. The example presented here is a comparison of a compressor and electric heater replacing the energy needed in the traditional system, represented by Case 1.

Both Case 1 and Case 2 systems used in Chapter 6 have been optimised using PA prior to the ExA being applied. As discussed in Chapter 6, exergy analysis shows higher exergy flows to the environment from Case 1 (Boiler) than from Case 2 (VRC), which is information given by ExA, but generally ignored while performing PA. Considering that exergy is a measure of available work potential, the boiler-only system is less work efficient than the vapour recompression system.

An example of the difference between pinch and exergy analysis is the scale of the efficiency value, which is a product of excluding unworkable energy in an energy analysis. The dryer is adiabatic and assumed to almost reach gas-solid equilibrium at the outlet, leaving a small amount of avoidable energy loss on the evaporation basis, and as a result the evaporation efficiency is over 90%.

This situation is contrasted with the exergy efficiency on the basis of evaporation being as low as 38% (Factor 6 in Chapter 6), making the dryer the worst performer of any unit within this system. Exergy changes associated with phase change and the condensed phases are small – especially at low temperatures when compared with the changes in the gas phase. As a result, phase changes and condensed phases are considered insignificant in most applications.

This difference leads to a useful simplification of exergy analysis. The result of this simplification (gas side assumption) is discussed above in the gas side assumption (section 2.9.3).

The exergy efficiency is quite low for the dryer systems in Chapter 6, while the energy efficiency is high. This is due to the energy quality consumption and the energy quality leaving the dryer. Made simpler: the nature of the dryer is inefficient no matter how energy

efficient the dryer is. Using high grade energy to rapidly change a low-grade energy is expensive on an exergy basis, even if the energy efficiency is very high.

For example, if the dryer inlet was a low temperature offset feed ($80^{O}C$ gas feed temperature with recirculation), the dryer's efficiency could potentially be much higher (not plausible for spray dryers, but more suitable for fluidised bed/tray systems). The main inefficiency here is that the mass transfer requires little exergy, while requiring large amounts of energy.

The definition of exergy leads to this difference in the result. Since the exergy within material flows is defined as the work potential to bring the material stream to equilibrium with the environment, some of the exergy in the feed gas is transferred from thermal to chemical exergy. The mechanism for this situation is that the water will tend towards saturation in the vapour phase.

Specifically, the reason why evaporation (at lower temperatures) is low, such as in the drying of sticky, or food type materials, is that the temperature difference is low. Since entropy is heavily reliant on temperature difference from the base (dead) state, the closer to that point at which the evaporation occurs, the closer the entropy comes to equal the energy of evaporation. This situation results in the exergy of evaporation being much lower and is demonstrated in the equation expansion below.

Why Exergy is significantly lower than the Enthalpy for evaporation

$$\frac{\Delta Ex_{\Delta V}}{\Delta H_{\Delta V}} = \frac{m_{\Delta V} \times \left(\Delta h_{\Delta V@T_{\Delta V}} - T_0 \Delta s_{\Delta V@T_{\Delta V}}\right)}{m_{\Delta V} \times \Delta h_{\Delta V@T_{\Delta V}}}$$

Where:

$$\Delta s_{\Delta V@T_{\Delta V}} = \frac{\Delta h_{\Delta V@T_{\Delta V}}}{T_{\Delta V}}$$

$T_{\Delta V}$ and T_0 are in Kelvin

Factor 6

$$\frac{\Delta Ex_{\Delta V}}{\Delta H_{\Delta V}} = \frac{m_{\Delta V} \times \left(\Delta h_{\Delta V@T_{\Delta V}} - T_0 \frac{\Delta h_{\Delta V@T_{\Delta V}}}{T_{\Delta V}}\right)}{m_{\Delta V} \times \Delta h_{\Delta V@T_{\Delta V}}}$$

$$\frac{\Delta Ex_{\Delta V}}{\Delta H_{\Delta V}} = \frac{m_{\Delta V} \times \Delta h_{\Delta V@T_{\Delta V}} \left(1 - \frac{T_0}{T_{\Delta V}}\right)}{m_{\Delta V} \times \Delta h_{\Delta V@T_{\Delta V}}}$$

$$\frac{\Delta Ex_{\Delta V}}{\Delta H_{\Delta V}} = 1 - \frac{T_0}{T_{\Delta V}}$$

As can be seen, the evaporation ratio is more reliant on the temperature at which the evaporation occurs.

7.2Pinch and Exergy Scope and Limitations

A PA on Case 0 indicates that two heat exchangers (one on the dryer air and one on the boiler air side) are possible; both are considered economisers, taking flue gas to preheat the feed gas. Since these exchangers are gas-gas heat exchangers, they have a large surface area per unit temperature difference; as such, the pseudo temperature difference used in the PA is 20^{O}C, not the typically assumed 10^{O}C [61]. The effect of this change is to reduce the size of the exchanger since it is not necessary to achieve such a small temperature difference. The side-effect is the reduction in recovered energy, a reduced exergy efficiency, and an increase in utilities to further increase the temperature in terms of the dryer gas feed. There is also the issue of energy (exergy) losses to the environment – particularly at higher temperatures where a larger heat exchanger will have a greater exposure to the environment and proportionally higher heat losses [28, 61, 110, 126].

PA gives an effective indication of heat exchanger placement but does not indicate how efficient the placement is. The assumptions and rules governing PA assist in process integration.

ExA, on the other hand, analyses effects not normally considered in PA. The extension of the pressure and chemical-based energy amongst other energy forms means that exergy may lead to more flexible optimisations beyond just heat exchange systems. The example presented in Chapter 6 is a comparison of a compressor and electric heater replacing the steam energy needed in the traditional system, represented by Case 1. Both Case 1 and Case 2 systems were optimised using PA prior to the discussion presented in Chapter 6. As discussed previously, exergy analysis shows higher exergy flows to the environment from Case 1 than Case 2, which is extra information given by ExA. Considering that exergy is a measure of work, the boiler-only system is less work efficient than Case 2 for this case.

Another example of the difference between PA and ExA is the efficiency of the dryer used in this chapter. The dryer is adiabatic and assumed to almost reach gas-solid equilibrium at the outlet, leaving a small amount of avoidable energy loss on the evaporation basis, and as a result the energy-based evaporation efficiency is over 90%. This efficiency may be contrasted with the exergy efficiency on the basis of evaporation being as low as 41%, making the dryer the worst performer of any unit within this system. Exergy changes associated with phase change and the condensed phases are small – especially at low temperatures when compared with the changes in the gas phase. As a result, phase changes and condensed phases are considered insignificant in most applications. The inevitable exergy loss within the dryer is high due to the dryer being a simultaneous mass and heat transfer unit operation.

The exergy efficiency is low while the energy efficiency is high due to the energy quality used and the energy quality leaving the dryer. In simple terms, the nature of the dryer is exergy inefficient no matter how energy efficient the dryer is. Using high grade energy to rapidly heat a low-grade energy flow is expensive on an exergy basis, even if the energy efficiency is very high.

For example, if the dryer was replaced with a low temperature offset feed (80^{O}C gas feed temperature with recirculation), the dryer's efficiency would potentially be much higher

(not plausible for spray dryers, but more suitable for fluidised bed/tray systems). The main inefficiency here is that the mass transfer requires little exergy, while requiring large amounts of energy.

The definition of exergy leads to this difference in the result. Since stream exergy is defined as the work potential to bring the stream to equilibrium with the environment, the exergy potential in the feed gas is transferred from thermal exergy to chemical exergy. This change in exergy form occurs by increasing the water fraction to near saturation in the vapour phase.

7.3Visualisation tools for an exergy analysis

It is difficult to discuss these two methods (PA and ExA) without considering the useful visualisation tools presented as part of PA, so finding a similar method for ExA is helpful in making comparisons. There are two commonly used methods, both are useful in their own way. From these two exergy visualisation tools, finding a similar method of comparing visual tools for optimisation potentials and targeting can be achieved. Wall and Gong [24] have assisted in this study by discussing some interesting limitations of PA and describing the concept of exergy, mainly focussing on threshold problems in PA. Continuing from that, the visualisation of the system and results in a similar manner to PA is an important step in making ExA accessible to more engineers.

Visualising the results may assist in the interpretation of the results. Several methods exist, and a few examples will be demonstrated here.

7.3.1Grassman Diagrams

One convenient way to visualise results in energy and exergy analysis is the use of Grassman diagrams, or exergy flow sheeting [30, 31, 91, 110, 127]. Figure 7-2 represents the dryer and separator, which is common to both systems (and effectively represents Case 0, without the required utilities).

Each of the case study systems has a different exergy profile, as shown in Figures 7-2 (Case 1) and 7-3 (Case 2).

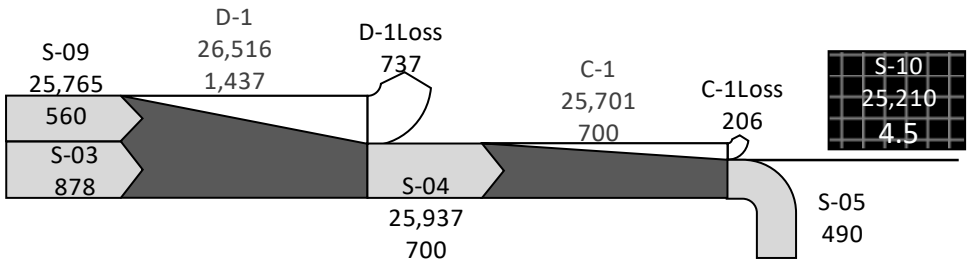

Figure 7-2: Grassman Diagram for the Dryer (D-1) and the cyclone separator (C-1) in all systems.

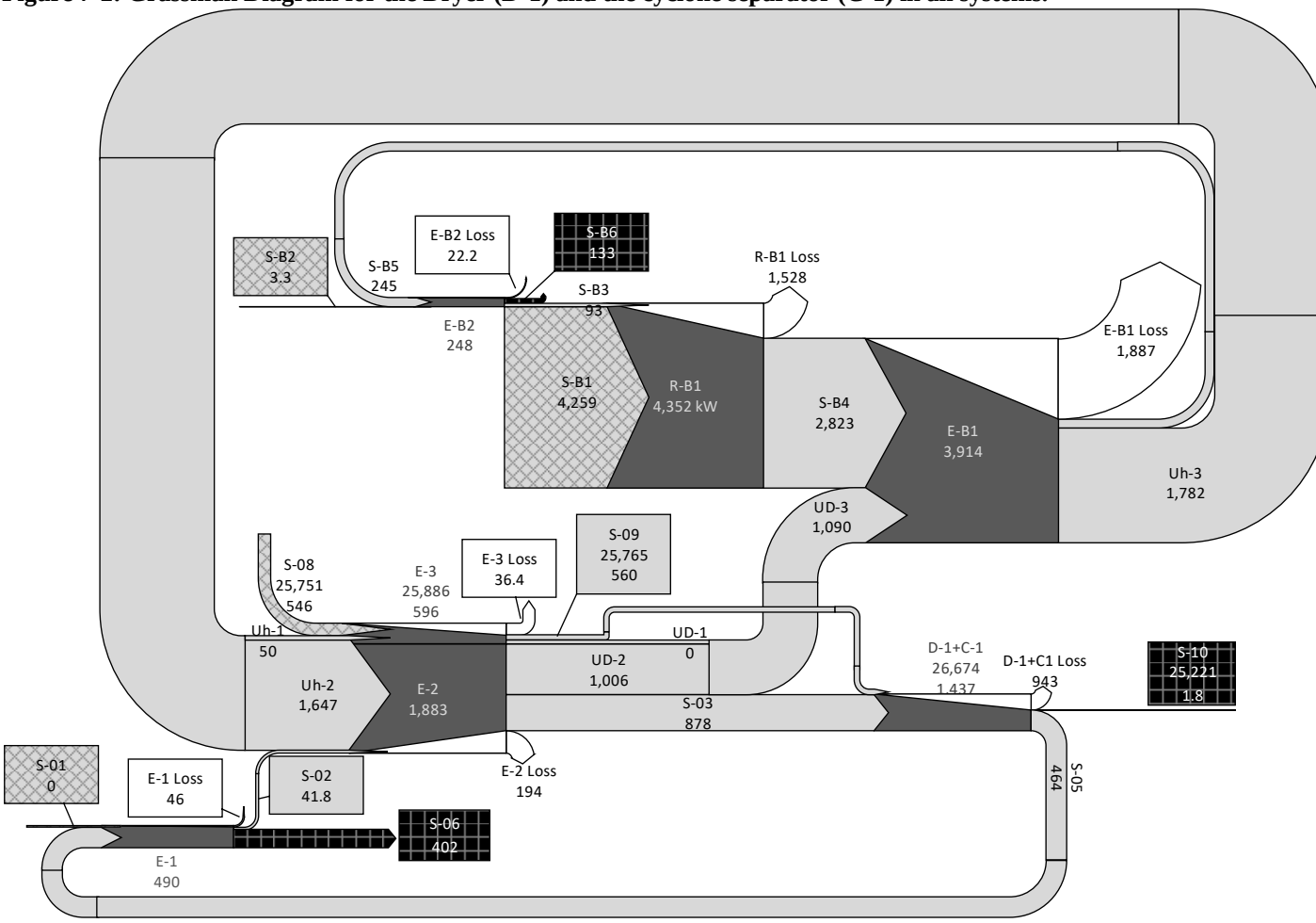

Figure 7-3: The Grassman Diagram for Figure 6-1 (Case 1).

The Grassman diagram of Case 1 (with a combined dryer and solids separator) indicates that the largest exergy losses may be found in E-B1 (steam generating heat exchanger), R-B1 (gas burner) and the dryer unit (D-1+C-1), with small losses found in E-2 (gas pre-heater), E-B2 (boiler economiser) and E-3 (solid-side pre-heater).

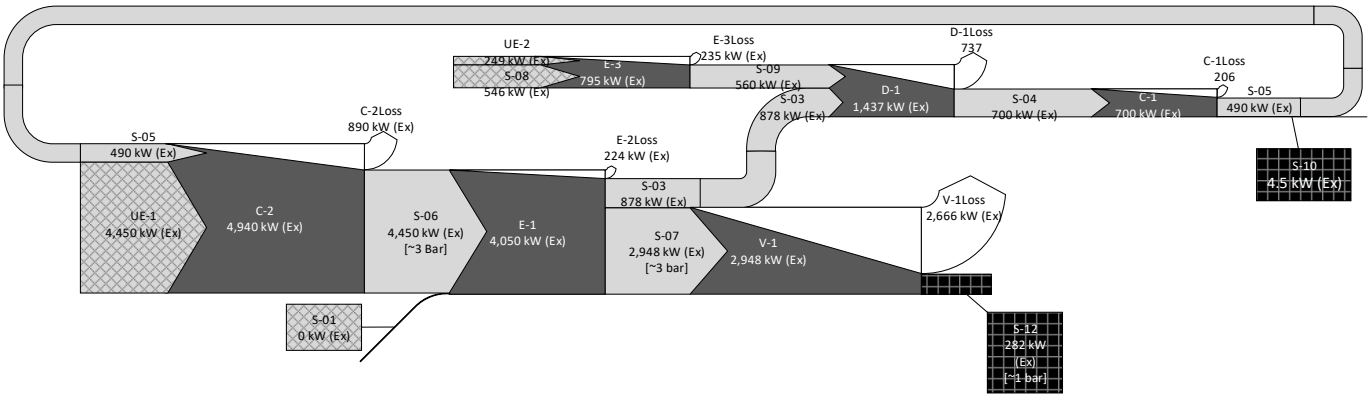

Figure 7-4: The Grassman diagram for Figure 6-2 (Case 2).

The main issue with a visual tool such as Grassman diagrams is scale, especially in the case where the solids chemical potential is taken into account (the number ~25,200 shown in on S-08, S-09, S-10, and is also shown on unit operations E-3 and D-1+C1). The scale of the chemical potential is significantly different to the thermo-mechanical exergy, and this is another reason why using transiting exergy is an important concept.

It is clear that the system in Figure 7-3 is slightly more complex than if E-1 was not used to pre-heat the dryer feed gas, but the saved energy is significant as 88 kW of extra exergy would be vented to the atmosphere, without taking into account the saved fuel (S-B1), as a similar assessment can be drawn from the use of E-B2. Much of the lost exergy is associated with the utility side of the system, meaning that optimisation should be focused in that area of the system. This situation arises because the bulk of the energy loading is in the utility part of the system. Alternatively, the addition of the task efficiency for each unit can help indicate if the loss is required, or not for each unit. The method for calculating the INE has been outlined earlier.

Figure 7-4 shows Case 2, with an electrical heater for the solids pre-heater (E-3) and Compressor to pressurise and heat the off-gas to pre-heat the feed gas (replacing the need for a boiler). The solid feed pre-heater is small compared with the air loop in this system (248 kW vs. 4,450 kW), small enough that the boiler used in Case 1 may be switched over to a resistance (Electric) heater since the amount of power needed in the system would require an onsite transformer for the compressor (C-2). The key area of loss here is now the compressor and valve (V-1), with a much smaller loss associated with E-1. V-1 gives a

significant loss (~53% of total losses) of the exergy in the system, and this is illustrated in Figure 7-4.

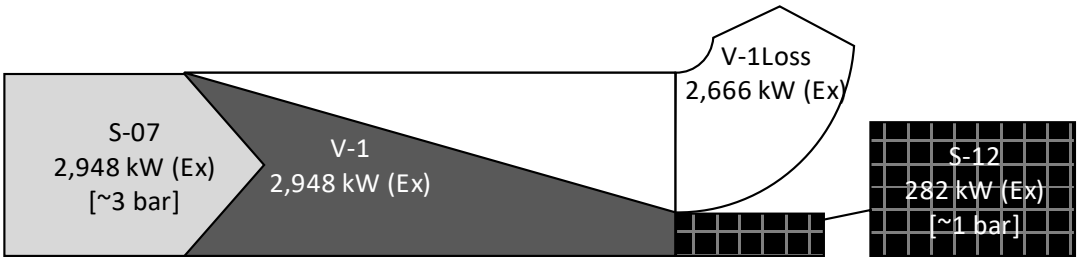

Figure 7-5: The exergy lost from using a valve to reduce the pressure back to 1 atm in Figure 6-2.

The loss associated with just V-1 is shown in Figure 7-5, and the loss in the valve is 90.4% of the fed exergy to the valve, which gives a good indication that a turbine would be a good addition to this system.

7.3.2Energy Level Diagrams

Energy quality may be defined in several ways. In this case study, the values of Ω (exergy to energy ratio) for both natural gas and electricity are the same (unity), natural gas has a value close to unity (or slightly higher, so it can be assumed to be equal to unity). This situation means that exergy and energy have the same values for natural gas and electricity. Since Ω is the ratio of exergy to energy, streams that have low energy contents may have large changes in the Ω value if the exergy changes. These changes in the Ω can be misleading in these cases. This factor has been used in the past to plot exergy as a function of energy for process modification assessment with a degree of success [39, 98].

Table 7-1: Selected boiler flue gas properties for Case 1.

	Case 1	
Gas flow	1.4	$kg.s^{-1}$
Humidity	172	$g_W.kg_{DA}^{-1}$
Exergy content	123	kW
Energy content	499	kW
Ω	0.247	

Table 7-2: Selected dryer flue gas properties for both Case systems.

	Case 1		Case 2	
Gas flow	22.24	$kg.s^{-1}$	22.24	$kg.s^{-1}$
Humidity	59	$g_W.kg_{DA}^{-1}$	59	$g_W.kg_{DA}^{-1}$
Exergy content	409	kW	243	kW
Energy content	3,512	kW	1,813	kW

Ω	0.116	0.134

Since Ω is a ratio (exergy to energy), it needs to be considered along with a scale measure, such as the flow rate. For example, Table 7-2 indicates that for both Case 1 and Case 2, the quality factor (Ω) associated with the discharge gas is similar (0.116 for Case 1, 0.134 for Case 2) but the absolute magnitudes of the exergy flows to the environment are much higher for Case 1 (532 kW-ex; 123 kW from the boiler, 409 kW from the dryer) than Case 2 (243 kW-ex). Considering that the outlet temperature of the flue gas from the economiser on the dryer is higher for Case 2 than Case 1, the dryer in Case 2 has higher exergy and enthalpy flows to the environment.

The visualisation of Omega (or energy quality) can be done in a variety of ways, Figures 7-5 to 7-8 show some interpretations of the same results.

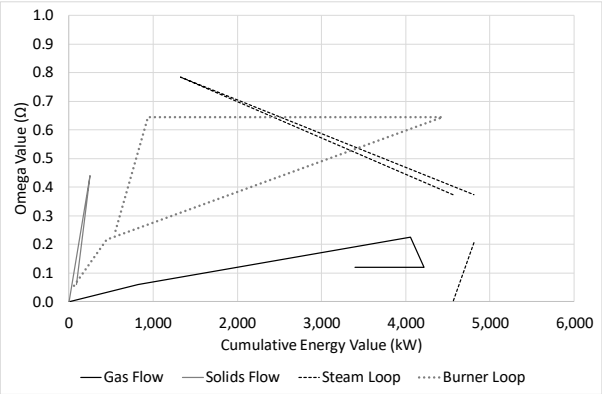

Figure 7-6: Actual values of streams in Case 1.

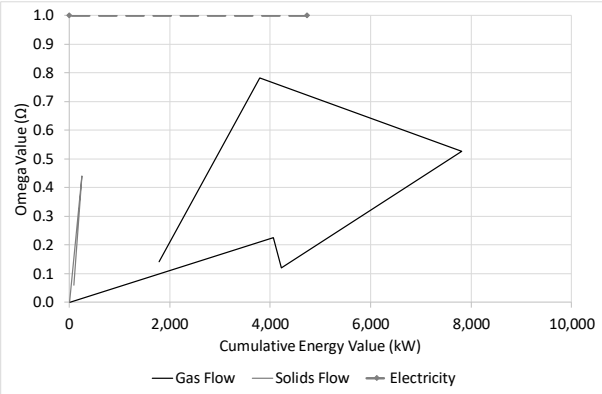

Figure 7-7: Actual values of streams in Case 2.

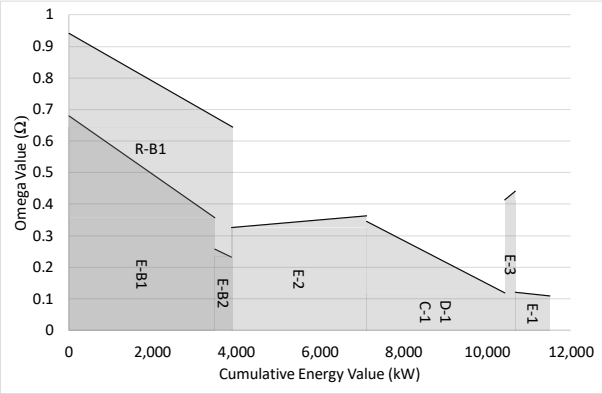

Figure 7-8: Energy Level Diagram (first pass) of Case 1.

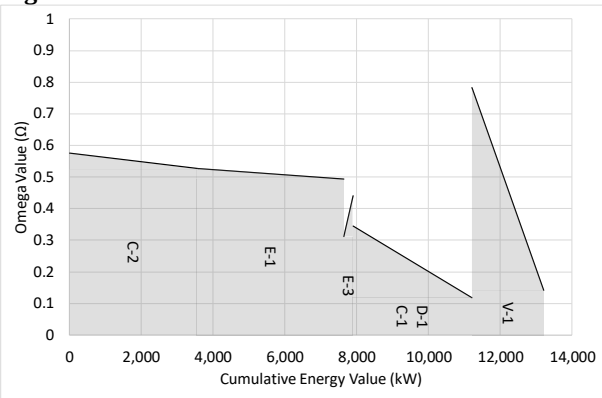

Figure 7-9: Energy Level Diagram (first pass) of Case 2.

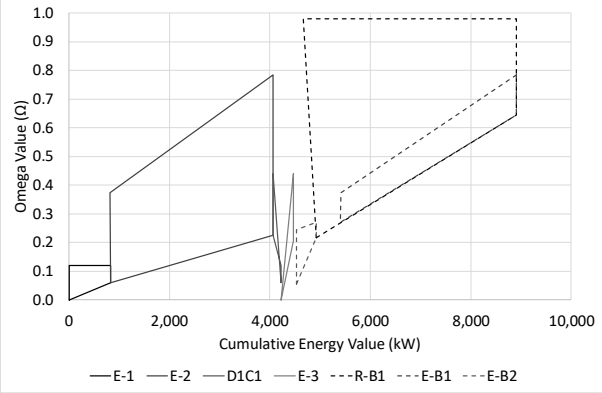

Figure 7-10: A second pass view at energy level diagrams for Case 1.

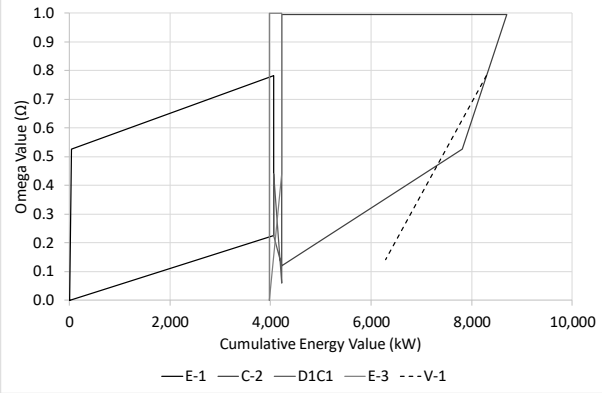

Figure 7-11: A second pass view at energy level diagrams for Case 2.

Figures 7-5 and 7-6 (case 1 and case 2, respectively) show the stream energy quality values at the actual energy flows for each transition used in the next two stages of the visualisation. The boiler system appears to be significantly more compact at this point (an in-out analysis is suitable at this point. It is also apparent that Case 2 (from Figure 7-7) that the potential to recover energy is significantly higher within the gas (the steep slope represents the valve). The disjoined component of the steam cycle in case 1 is due to the steam that is used to pre-heat the solids being assumed to be at a different pressure and temperature to that required to pre-heat the dryer feed gas.

Figures 7-7 and 7-8 (case 1 and case 2, respectively) show the unit operation energy level and energy change (transfer) per unit. This representation is useful as it shows quality loss/gain per unit operation along with quantity. Steep slopes correspond to significant losses within the unit operation. R-B1 has been overlapped with E-B1 and E-B2 to show that, while R-B1 is the general source of energy, the heat transfer is via the two heat exchangers, while one is transferring energy to steam, the other is pre-heating the gas for R-B1. It is also important to note that, while E-3 may have a steep slope, and relatively high quality-level, it is small in comparison to those for other units. The effect of steam condensing is counter intuitive for energy and exergy since the exergy change given by condensing steam is small while the change of energy is large (as discussed in the previous chapter).

A further look at energy quality visualisation allows for pairing streams that display each unit operation as a Rhombus (Figures 7-9 and 7-10) to more clearly show what is causing the slopes in Figures 7-7 and 7-8. This representation is useful as it shows energy and quality

flows being paired up, and how significant each of the heat exchangers are. Large boxes correspond to large losses. It is important to note here, that some of the streams have been flipped in direction to improve visualisation, and to show pairing correctly. This clarification is more evident in the steam loop of Figure 7-11 when compared with Figure 7-7. It is generally preferred that the method used for Figures 7-9 and 7-10 be used for energy level diagrams, with each unit being shifted under the energy source [39, 40, 75, 114].

It is important to point out that Figure 7-10 shows E-B1 and E-B2 within R-B1, and this indicates (similar to what is shown in Figure 7-8) that cyclic systems are interlinked heavily. While in the diagram each unit is shown separately, the loss for a more integrated system may be smaller than each unit taken in isolation (as calculated here). The reason for this result is that the cold streams (if taking a pinch perspective) are above the hot streams in this case, so the quality may appear to be transferred from a cold to a hot stream, even though the energy is being transferred from hot to cold streams. This behaviour is common when a high pressure cold system is being heated by a low pressure hot system and can be confusing at first glance.

Exergy is a measure of energy quality as well as energy quantity. Exergy is not directly connected to costs and, as a result, indicators and correction factors must be used to bring the exergy analysis into the cost domain. Several methods have been introduced to achieve this [31, 108, 128].

7.4Heat loss

Heat loss within the drying system is not accounted for within the model, but it is an important part of the optimisation process. The heat losses associated with a spray dryer can be up to 25% of the energy input [28], and are less significant at lower temperatures.

This effect should be taken into consideration when producing a sensitivity analysis on the energy or exergy saving potential of a real system. A heat loss of 25% can be enough to mitigate significantly more than 25% (minimum) of the heat recovery potential, since heat loss lowers the outlet temperature of the dryer, while needing the feed temperature to increase for the same evaporation rate.

7.5System Complexity

Case 1 has a boiler system which feeds the two pre-heaters for the dryer. The boiler system has three energy change units, while the dryer system has two heat exchangers, a dryer, and a gas-solid separator. Case 1 has an energy recovery heat exchanger on the dryer system (E-1), and the boiler system (E-B2).

Case 2 replaces the gas side pre-heating with the economiser (E-1) and a compressor (C-2). Thus, Case 2 replaces E-1 and E-2 with a larger E-1 which is a gas-gas heat exchanger, and the solids side heat-exchanger in Case 1 with an electrical heating coil. In order for this change to happen, the boiler system is replaced with a compressor and valve. This change mans that Case 2 is four units smaller than the boiler driven Case 1.

On top of the extra units, Case 1's boiler is required to generate high pressure steam (19 Bar) in order to reach the temperature of the feed gas, and the same steam source is used to pre-heat the liquid feed. The compressor in Case 2 is only required to reach 3 Bar by comparison. In Case 2 however, there is a pressure release device to reduce the pressure of the dryer flue gas to 1 atm. This device has a significant exergy loss associated with it, as demonstrated in Figure 7-5.

The large temperature difference associated with the steam for the solids pre-heater (E-3 in Case 1) leads to a large exergy loss for that heat exchanger, while the electrical resistance heater (E-3 in Case 2) can be better insulated but may suffer from other issues such as localised overheating.

A more detailed approach to analysing system complexity may be required in the future, but it is hard to justify a more detailed analysis on the two cases presented here. The only conclusion that can be drawn is that Case 2 has fewer losses internally, while having a larger loss externally (especially if V-1 is not considered).

7.6Conclusions

There are many methods to visualise exergy flows and efficiencies, while they are not as simple in approach to those of PA, they are useful to focus on areas of higher loss within the system. Further work should be done on improving dynamic methods of visualisations for future optimisation methods.

The base case was established in Chapter 5 to help outline the potential recoverable energy for the systems studied in Chapter 6, this was done to create a benchmark for the two cases. It is important to note that the task was defined as evaporating water within the dryer unit. When assessing the system as a whole, the task is still based on the unit of focus (dryer) for the entire system, thereby allowing the factors to be compared as was completed in Chapter 6.

An exergy analysis of the system focuses on other factors outside the heat flow and an energy balance. For example, on an energy basis, a dryer is a reasonable unit operation for the task of evaporating water. However, the amount of lost exergy implies the unit uses significant amounts of high quality energy to perform the task.

Chapter 8 Time and Cost Analysis for the Systems Methods

The interpretation of results from exergy analysis are far from straightforward. This chapter goes through a basic cost comparison to demonstrate that combining methods may yield results that are more straightforward. Performing a costing on a system change, which may be decided based on an exergy analysis may have positive of negative effects on the capital or operating costs of the system. This chapter is a costing of the systems described throughout this thesis (specifically Chapters 4, and 6).

A discussion on the time to complete each method is presented in a conceptual manner is also presented in this chapter, with a focus on what parts of the analysis take the longest in my experience preparing the previous chapters.

8.1Costing Basis and Assumptions

In the interest of dating this analysis correctly, at the time of the analysis there exists no carbon trading or pricing regime for either government or private sector initiation on the east coast of Australia, meaning that a carbon price could not be adjusted.

One factor that removes many of the benefits of electricity over locally burnt gas (for boiler systems) is that for the whole nation of Australia (at the time of the analysis) was made up of 60% coal and 15% natural gas power, with only 17% of power from renewable sources, the remainder from liquid fuel (diesel) generators (83% fossil fuel usage for power) [129-131].

8.2Case 1

8.2.1System Costing

It is important to compare the systems on a cost basis; exergy efficiency improvements must be reasonable and significant on a cost basis to make changes to real systems. This procedure also allows for a comparison of cost methods for energy reduction without going into the complex exergo-economic analysis methods [29, 31, 42, 108, 132]. It should be noted that the methods used to generate an exergo-economic analysis are not straightforward. A full understanding of the basic exergy and exergy methods is essential before using more integrated and advanced tools. The interpretation of the results is the key challenge in exergy analysis, and adding an integrated cost method only adds to the

challenge. For this case, a stand-alone simple cost analysis has been completed to support the exergy analysis results.

The preliminary capital costing (Capex) was sourced from Matche [133], and a commonly used book for design cost estimates [134]. These cost estimates have been corrected to 2019 prices using the (Chemical Engineering Plant Cost Index) CEPCI metric [135, 136]. The results may be seen in Table 8-1, and more detailed tables may be found in Appendix 8B.

Table 8-1: Capex estimates for Case 1.

HX's	$130,000
Boiler	$250,000
Blower	$630,000
Total	**$1,0110,000**

The cost estimate includes two finned-tube heat exchangers with one rated at 1 Bar with a 500 m^2 transfer area (E-1) and the other rated at 20 Bar with a 112 m^2 transfer area (E-2). The boiler heat exchanger was not costed independently, as it was considered to be part of the boiler package. The boiler section was costed as a package including the burner, the boiler (primary heat exchanger), and an economiser rated at 20 Bar with no superheater system. The blower for the Case 1 has been costed based on a power requirement of 1,520 kW (22 $m^3.s^{-1}$ with a maximum pressure increase of 0.6 Bar), the blower is not shown in Figure 6-1.

In terms of the operating expenditure (Opex), there are a few simplifying points to make the comparison less confusing. Limiting the operating cost assessment to just the energy supply cost is enough to compare important aspects of both systems.

Natural gas costs of 85.8 c/day plus 2.76 c/MJ(gas) (9.93 c/kWh) [137] mean that 3,810 kW costs $9,100/day for the boiler in Case 1, and the blower electricity costs are substantial, at $13,000/day (1,770 kW at 33 c/kWh plus 177 c/day). The estimated operating costs are likely to be higher than a real plant of this scale [138, 139], since the cost estimates have been based on the small business standing offer with Australian Gas Light company (AGL) [137, 140]. These offers apply for users using less than 20 MWh/annum of electricity (54.8 kWh/day, the blower requires 36,500 kWh/day), and less than 1.4 TJ/year of natural gas (3.81 MWh/day, the boiler requires 91.44 MWh/day).

Although the operating costs for other considerations have not been added, it is important to note that a moderate pressure boiler (such as the one required for this system) has a significant maintenance cost.

8.2.2Carbon Dioxide Production

Another important part of costing, particularly on an environmental point of view, is carbon accounting.

For Case 1, the amount of CO_2 that is produced is calculated directly from the on-site boiler, and indirectly from the electricity used for the blower and pumps.

The CO_2 emissions have been calculated based on the following data and assumptions:

- The installed power production in the state of NSW, Australia was recorded as 17.4 GW with an average emission rate of 83 MT CO_2-e/year [129-131] for 2018.
- The energy requirement for the blower and pump for Case 1 was estimated to be 1.5 MW (22.03 m^3/s, 0.7 bar ΔP).
- The boiler was assumed to be 80% efficient, so this changes the amount of natural gas burnt to produce the required energy (0.093 kg_{CH4}/s).

This results in 0.256 $kg.s^{-1}$ produced from the boiler and 0.214 $kg.s^{-1}$ produced off site from the electrical requirements of the blower on the dryer. This situation gives a total of 0.47 $kg.s^{-1}$ of CO_2 produced by Case 1.

8.3Case 2

8.3.1System Costing

The preliminary capital costing was sourced from Matche [133], and a common text for design cost estimates [134] and corrected to 2018 prices using the CECPI metric. The results may be seen in Table 8-2.

Table 8-2: Capex estimates for Case 2.

HX's	$250,000
Electric Heater	$24,000
Compressor	$1,400,000
Total	**$1,674,000**

The cost estimate includes one finned tube heat exchanger with a 3,890 m^2 surface area rated at 3 Bar. This area is likely to be oversized since condensation occurs under the studied conditions, while it was assumed to be purely gas-gas in the calculation here. However, a more detailed estimate is unnecessary since the cost of the heat exchanger is over six times smaller than that of the compressor. The electric heater was costed based on a power requirement of 250 kW (The power requirement of this electric heater may seem excessive but is small in context, since the compressor in this system will require a transformer as it requires 3.3 MW, adding 250 kW would not be difficult at that stage). Considering that the cost of the heating element is an order of magnitude lower than that of the boiler package ($24,000 vs $250,000) it is unlikely to be a significant difference.

In terms of the operating expenditure, the energy supply cost is enough to compare both systems. Electricity costs of 11.3 c/kWh(e) plus 177 c/day [140] mean that 3,810 kW costs $26,720 /day for Case 2.

Since none of the equipment is rated at a high pressure (4 Bar maximum), the maintenance costs are likely to be significantly cheaper than in Case 1. Replacing the valve (V-01) with an energy recovery turbine would increase the capital cost and reduce the operating costs, but this replacement option has not been costed for this case.

8.3.2Carbon Dioxide Production

Another important part of costing, particularly on an environmental point of view, is carbon accounting.

For Case 2 all the countable CO_2 production is from the indirect source due to the high amount of electricity used for the compressor and pumps.

The CO_2 emissions have been calculated based on the following data and assumptions:

- The installed power production in the state of NSW, Australia was recorded as 17.4 GW with an average emission rate of 83 MT CO_2-e/year [138, 139, 141] [129-131] for 2018.
- The energy requirement for the blower in Case 2 was estimated to be 3.4 MW (22.03 m^3/s, 2.7 bar ΔP).
- The energy requirement for the thermal heater in Case 2 was estimated at 250 kW.

This situation results in 0.513 $kg.s^{-1}$ produced off site from the electrical requirements of the compressor.

This amount is almost 20% higher than that of Case 1, and this may decrease as the amount of fossil fuel-based power generation in Australia is reduced in the future [138, 139, 141].

8.4Discussion of Costing

While assessing just the energy and exergy effects of each system it is also important to keep thinking about the likelihood of implementing changes, and the fastest way to do this assessment is to consider the costing of systems and any changes that are to be made on a cost basis. Focussing on the operating and capital costs of the systems discussed in this chapter, the boiler only system (Case 1) is superior in terms of both capital and operating cost factors. Moving the costing into the carbon scale is highly dependent on the source of the local electricity generation. In the case of Australia, the power generation consists of a significant percentage of coal power stations, and this means that the carbon cost of electricity is quite high, even when compared to a locally installed gas boiler unit. In areas where power is generated from lower carbon sources, Case 2 would become significantly more attractive for investment.

Table 8-3: Cost summary of the two case studies in Chapter 6.

	Case 1	Case 2
Capital (AU$)	$1,010,000	$1,674,000
Operating (AU$/day)	$22,005	$26,714
Carbon Emissions (T CO_2-e/day)	40.61	44.34

The consideration of non-thermal optimisation does enable alternative methods to be assessed for process changes. This combination of energy, exergy and costing has the potential to be significantly better for process optimisation, the environment and process costings than just thermal optimisation.

A comparison to a case 0 system with no energy recovery is not necessary, as that system would consist of each heating and cooling application having its own utility heat exchanger. This option, while impractical, would allow for smaller heat exchangers with better utility matching options than the pinched system. It would also have one (or two) fewer heat exchangers, bringing the CAPEX down, but the OPEX would be about 20-30% higher (to

account for no energy recovery), but this may be partially offset on the cooling side by discharging the exhaust directly to the atmosphere (at around 60^{O}C). Pinch analysis is generally enough to justify not considering this option.

8.5How Costing Compares with Pinch and Exergy

	Units	Dryer Only	Dryer with no heat recovery	Superheated Steam System*	Boiler-Air System	Air Vapour Recompression System
Unit Operation Count		2	4 dryer +2 boiler loop	3 dryer +3 boiler loop	5 dryer +3 boiler loop	5+ let down valve or paired turbine
Energy Required	kW	4,079	5,298	2,842	4,121	4,714
Exergy Required	kW	765	5,051	860	3,867	4,486
Energy Discharged	kW	4,005	5,027	2,784	3,045	1,734
Exergy Discharged	kW	457	724	608	521	233
PA Energy Saving	kW	-	-	2,473#	1,177	584
ExA Energy Saving	kW	-	-	4,191#	1,184	565
Discharge Reduction**	kW	-	-	1,221	957	2,286
Capital Cost	AU$			$988,000	$1,010,000	$1,674,000
Operating Cost	AU$/d			$21,550	$22,010	$26,720
Carbon Emissions	T CO_2-e/d			38.58	40.61	44.34

NOTE 8-1*: The value for energy and exergy required is based on fuel values determined in Chapter 6. Values for discharged is gas side exhaust only (including boiler system where appropriate). Saving is when compared to dryer with no heat recovery. Full details of the costing are in Appendix B to Chapter 8.
NOTE 8-2: Compared to dryer only, improvements from no recovery options are inflated. VRC system inclusive of valve V-1 (reduction excluding valve is 178 kW)**
NOTE 8-3#: Steam recirculation system and higher outlet temperature give the large saving, heat recovery only exists to preheat the solution phase, natural gas boiler and recirculation blower used.

The steam system was costed with the basis to be the same as that of the boiler-air system but with the boiler replaced with a superheating boiler running at a lower pressure. The cost savings compare closely with the results of chapter 4 in that the superheated steam system has significantly higher heat recovery potential, due to its higher outlet temperature, and recirculation of steam. Other issues exist with the superheated steam system, which are discussed in that chapter. The operating costs are lower than the boiler-air system since not as much steam needs to be raised to heat the gas side of the dryer. The capital cost is lower, again due to the boiler not needing to be as large.

The cost of the VRC system in Chapter 6 is around 67% higher than the boiler driven system for the equivalent task, and also has an operating cost and carbon emission penalty of 21% under the current power generation case in Australia. In the future, this is likely to change,

even to the point of reversal, as power is gradually migrated to lower and zero carbon production sources.

On an exergy basis, the discharge exergy is significant in all systems, and only the VRC system (with valve) has a lower environmental discharge. However, all systems are improvements on the base case. The more expensive systems on a capital basis appear in this case to have a higher energy and exergy requirement, and since this is for the same task, they have a lower effectiveness ratio.

The results of a preliminary costing tend to compare closely with the results of PA and ExA, which is expected, since reducing energy and energy quality requirements will reduce operating costs considerably. Capital costs on the other hand tend to be linked more to the number of unit operations, and the scales of each operation. The gas-gas heat exchangers in the air system are significant in their scale and cost within those systems, and the steam recirculation heat exchanger has the potential to save significant costs (as demonstrated), due to the differences in properties of superheated steam and air under the same temperature and pressure.

8.6Costing Summary

The results of the PA and ExA rankings are also aligned with the results of a preliminary costing analysis. While a boiler driven air dryer system has a lower thermal cost overall, it has a high environmental loss ratio, since the loss to the environment is at lower temperatures (low quality), it has a low recovery use and further recovery would result in higher costs.

The VRC system has a high electricity cost, low thermal cost, and a loss to the environment which is significant in either configuration (valve or not), however, part of this may be negated with the replacement of the valve (V-1) with a pressure recovery turbine to help drive the compression unit. The environmental losses without this unit have a high temperature and pressure (which has a high recovery potential), and this is an important optimisation point for that system.

The costs for the superheated-steam recirculation system are slightly lower than the cost of the boiler driven air system, and adding a VRC to the exhaust steam of this system may yield

improved results again. However, the cost for a system with a higher mechanically driven heat cycle is significant when compared with a chemically driven (combustion boiler) in the case of the other two systems being studied.

A preliminary costing of both systems is also informative for revealing that Case 2 is costlier both initially and to run with the utilities as costed.

Due to the difference in utility types (natural gas vs electricity), a carbon accounting was completed (with natural gas being an onsite emission, while electricity being an offsite one). The results of 0.470 $kg.s^{-1}$ for Case 1 and 0.478 $kg.s^{-1}$ for Case 2 mean that based on current power generation in NSW, Case 1 is less environmentally damaging than Case 2, but this result is dependent on the mix of power generation within the area, and would be different in countries with a lower percentage of coal and gas power generation.

8.7Discussion of the time to complete each method

The methods for each method are outlined in Chapter 2 of this study. The time to complete each method relies on several aspects, the first being data collection.

8.7.1Data Collection

Table 8-4: Required information summary table

Information types	Mass Balance	Inversion Temperature	Energy Balance	Pinch Analysis	Exergy Analysis	Costing
Flows/mass	Yes	Yes	Yes	Yes	Yes	Yes
System model	Partial	No	Yes	Partial	Yes	Yes
Temperatures	No	Yes	Yes	Yes	Yes	No
Heat Capacity	No	Yes	Yes	Yes	Yes	No
Heat of Evaporation	No	Yes	Yes	Yes	Yes	No
Pressures	No	Yes	Yes	No	Yes	Yes
Chemical Potentials	No	No	Yes^	No	Yes	No
Potential energy	No	No	No	No	Yes#	No
Dead State/Standard Conditions	No	No	No	No*	Yes	No

NOTE 8-4^: In the case of reactions, can be ignored otherwise.
NOTE 8-5#: In most cases, this can be ignored, but systems with significant height changes can lead to energy recovery from potential energy. Kinetic energy can be gained from flow profiles and pipe sizing.
NOTE 8-6*: While no, it is useful to separate sub-ambient systems from above ambient systems when performing PA.

Table 8-4 shows the increased level of information as the complexity increases. While most of the information is readily available for each of these information types, flows, temperatures and potential energies are process specific, heat capacities, evaporation energy and chemical potential are material specific and dead state properties are environmental specific (contains chemical equilibrium conditions). None of the information

is challenging to gather, and assumptions (stated in Chapter 2), help to simplify and reduce the time taken at this stage of each of the analysis methods.

The definition of the dead state for exergy analysis can be tricky when dealing with materials that can decompose to the environment, especially if they contain compounds not found in significant proportions. However, aqueous phase chemical potential (condensed phase equilibrium with the environment) has a low impact on exergy values; unless the quantity is extreme or harmful to the environment, this is generally considered insignificant enough to ignore.

In all, most of the methods require an idea of what the system is, so a basic system model is required for most of these to be completed. A mass and energy balance are generally completed around the same time, so no extra information is realistically required.

Costing unit operations is more reliant on having a model built and basic information handy. A costing of chemical plants can be rapid (based on scaling existing plants cost information), to a more detailed unit-by-unit costing, including those for heat exchangers, reactors, dryers and filters.

8.7.2Modelling/Simulation

The modelling and simulation of systems is a time-consuming aspect of any system design. Inversion temperature requires minimal modelling as it is just a comparison of simple kinetics data.

A PA model is relatively easy to put together both graphically and using basic spreadsheets or by hand and only requires thermal data. Minor data manipulation and analysis is required to start with to prepare the cascading energy tables for PA, but that is simple and not time-consuming.

Preparing a model for an ExA is time-consuming due to the complex set of assumptions and simplifications employed for each unit operation, specifically with regards to chemical potential utilisation unit operations and the interactivity of temperature and pressure. This is quite a long process if using spreadsheets. This step is not as straightforward as the previous two methods as the change of results in case studies are seldom linear in nature. With the addition of exergy in some process software (natively or by coded addons), this can

be simplified significantly (care must still be taken at the next stage if relying on this data though).

The results of the ExA should also be tuned to a set of factors (outlined in Chapters 5 and 6) for interpretation. Deciding which factors are suitable for the system being studied is important for the next stage.

For a preliminary costing to be completed, a basic sizing of each unit operation is required, this requires a little bit of work. The main thing to understand is that the cost of a system is unlikely to be a smooth curve as parts of the model change, especially if buying prefabricated units.

8.7.3Interpretation of results

Most of the analysis methods provided here yield little flexibility with respect to the results, a mass balance either balances or not, an IT gives a single temperature, an energy balance either balances or not, PA gives a temperature and minimum thermal utility requirements, and costing gives an estimate of capital and operating costs. On the other hand, ExA depends heavily on which factors were chosen at the previous step. Some factors should be maximised, some minimised, each factor explains different aspects of energy utilisation within the system. The primary initial focus should be to target areas and specific unit operations for closer inspection and optimisation, followed by investigating what implications those changes have on the extended system. It is this last part that means a flexible and detailed model for the system is required, more-so than for PA.

8.7.4Finalising Optimisations

This step of the optimisation hierarchy is more about determining if the change is worth making (to an existing plant, this is harder to justify generally).

For PA, deciding on which heat exchangers to implement, and which ones to exclude from a final system come down to costing, or more specifically, energy saved per transfer area. If a heat exchanger saves a small amount of energy but is quite large (an example is a gas-gas heat exchanger that reduces heating utilities by less than 2% for that line), it is not worth implementing.

For ExA, determining if a change is worth integrating (mechanical equipment such as heat-pumps, vapour recompression, turbine/compressor pairing) is similar in the way that PA's decision tree works, if it takes up a large area and budget for a small gain, then it is not worth adding.

It is just as easy to justify adding (or not) a heat exchanger or mechanical device by looking at a basic costing than to determine suitability based on raw recovery potential using PA and ExA, the main reason for this is that the equipment is required to be sized, at least on a basic level, even for a preliminary costing.

8.7.5Summary of time usage in each method

Table 8-5: Time taken per analysis summary table.

Time per stage	Inversion Temperature	Mass Balance	Costing	Pinch Analysis	Energy Balance	Exergy Analysis
Data Collection	Short	Short	Short	Short	Short-Moderate	Short-Moderate
Modelling/Simulation	Rapid	Short-Moderate	Moderate	Short	Moderate	Intensive
Interpretation	Short	Short	Short	Short	Short	Intensive
Optimisations	N/A	N/A	Short	Rapid	Short	Moderate
Overall	**Rapid**	**Short**	**Short**	**Short**	**Moderate**	**Intensive**

Table 8-5 gives an approximate summary of the above discussed stages for each analysis method, maintaining that due to the available complexity of optimisation pathways available in ExA over the other methods, the modelling aspect of that analysis is quite time consuming. The difficulty in interpreting the results of an exergy analysis is outlined in Chapters 5 and 6.

As Exergy becomes more required, its addition into more sophisticated modelling programs and as methods and the broader understanding in practitioners improves, the less intensive on time use the method is likely to become.

Chapter 9 Concluding remarks

There are multiple levels of analysis for a simple drying system in this work. To understand the complexity and simplicity of each analysis, the scope and methods were defined and briefly explained in Chapters 1 to 3. Each of the tools used here have been demonstrated with the use of case studies to highlight the benefits of each analysis.

The Inversion Temperature for the system(s) in Chapter 4 was estimated at 182^{O}C. Since this is just below the temperature (184^{O}C) where the steam dryer reaches a feasible outlet condition (outlet solids temperature above the dew point), superheated steam dryers are likely to be smaller than air dryers for all feasible drying conditions, while the air system allows for lower inlet temperatures to be used.

For evaporative systems, such as dryers, the use of an Inversion Temperature can assist in drying gas selection when designing a drying system. Pinch Analysis excels at minimising wasted heat from the process, with the caveat that work has already been done to insulate the process from heat losses via equipment to the environment. Exergy Analysis has the potential to be a far more powerful optimisation tool than those currently used in industry.

The recoverable (saved) energy from both the air and steam systems is high using PA at the studied conditions. Pre-heating the feed gas and solids with the dryer outlet gases yields energy savings of 18% for the air system and 8.4% for the steam systems. The steam system has an extra 86.6% of recoverable energy from the condensing of excess steam (a total of 91%), which can be integrated throughout an extended system. This result shows that this rapid analysis can identify a sizable energy saving using the two techniques –IT and PA.

Other key results from Chapter 4 are that the steam dryer sets the pinch temperature, while the air dryer does not set the pinch temperature but rather the fresh inlet gas temperature does this task. This result means that steam drying, when run at 1 atm, works across the Pinch, while the air dryer works above the pinch on its own, i.e. the steam dryer is easier to integrate into other systems. The steam system also has less sensitivity to temperature and flow changes in terms of energy requirements than the air system. This outcome is due to the steam circuit being a recycle stream rather than a once-through system which is commonly used for air drying.

The primary outcome from Chapter 4 is that for rapid assessments, IT and PA are complementary and they provide an engineer with quick assessment tools that compare the potential fixed and variable costs associated with different drying gases. This method indicates the superheated steam dryer has both a faster drying rate (in the unhindered drying period) and a higher energy recovery potential than the air system.

As the need for better energy efficiency and energy effectiveness increases over the coming decades, exergy has the potential to be a leading tool in assisting in these improvements. However, challenges still exist in creating a more streamlined method by which to apply and interpret the results of the analysis. The first principles approach used in this work, which compares the results with other methods such as Preliminary Costing and Pinch Analysis is an important step in demonstrating the power of the tools, and to hopefully make Exergy Analysis more accessible.

Chapter 5 applies an exergy analysis to a dryer unit to highlight some of the challenges with various factor types and the interpretation associated with the variety. The chapter concluded that the dryer is inherently inefficient, in exergy terms, at evaporating the water from the solids. The losses associated with the task are 38%, while the losses associated with the mass transfer and heat transfer are 94% (thermo-mechanical IN/OUT) and 30% (transiting) respectively. This exergy efficiency range is significant considering the overall exergy efficiency is nearly 100% over the entire exergy spectrum.

The IP of 575 kW for the feed of 722 kW shows that the dryer does not appear to be an exergy efficient way of performing this task, but this analysis does not offer an alternative method. The effect of feed temperature for several key variables shows that, depending on the basis of efficiency, various factors give significantly different optimal operating points.

For this system, the optimum operating range in terms of the inevitable exergy loss method is between 215^{O}C and 250^{O}C, which is typical of the conditions used in industry. There appears to be no suitable ‘one-size-fits-all’ efficiency factor for an exergy analysis. A variety of factors, which may be defined as a group, can be used – such as the task efficiency (on the task for the unit operation) and the practical efficiency (based on the task). The INE method is a potential shortcut technique based on the Carnot efficiency and a first law analysis, but there are some limitations for processes that are not exclusively thermal,

where an entropy balance is more correct. The INE method still shows potential as a starting basis of comparison because it shows the scale and the efficiency together, which are both important for targeting areas of the process to improve without doing a full exergy analysis.

Chapter 6 extended the analysis from Chapter 5 to include some systems to feed the dryer, a chemically sourced energy from a thermal boiler was compared with an electrically sourced mechanical compressor to highlight where an exergy analysis may yield results over more traditional methods.

Chapter 6 concluded that the evaporation potential for a natural gas boiler-driven dryer system (Case 1) is 13% better than an electrically-driven Vapour Recompression system (Case 2) on a fuel and overall basis. However, the recovery potential is higher in Case 2 if the valve is replaced by an improved recovery unit, mainly pressure recovery. The importance of a unit-based approach along with an overall systems approach is evident in the results. For example, the valve is by far the worst performing unit in Case 2 (more than 50% of total system loss), with the compressor and dryer the next worst performers. The boiler unit(s) are among the worst exergy performers in Case 1, along with the dryer. The valve in Case 2 can be replace by a turbine. That replacement would involve a higher capital cost than a valve but reduce operating costs.

The solids pre-heater is inefficient in both systems but has a low overall loss. While its efficiency improvement may be high, the gains are an order of magnitude lower than the potential improvement of other units.

In terms of utilising optimisation factors, basic factors are useful to simplify larger systems and focus attention to a general area or to help select process changes. However, in the case study given in Chapter 6, using these factors suggest Case 2 is superior to Case 1, while both cases are improvements on the base case (dryer on its own). More detailed factors such as task, transiting, and recovery all suggest Case 1 is the preferred system.

From the results, it is clear Case 1 is a better system than Case 2, though there is potential to improve both systems.

The effect of changing the dryer feed gas temperature are interesting as they suggest that an increased temperature would be inefficient for either system – and the same can be said for flow.

In general, Case 1 is superior in most ways to Case 2, unless the higher energy exhaust from Case 2 can be recovered. As part of a larger system, Case 2 may integrate better than Case 1, and this has not been studied.

These results show the confusing nature of several factors used within the exergy analysis literature, while helping with the interpretation of results in several ways.

There are many methods to visualise exergy flows and efficiencies, while they are not as simple in approach to those of PA, they are useful to focus on areas of higher loss within the system. Further work should be done on improving dynamic methods of visualisations for future optimisation methods.

Chapter 8 presents the results of the PA and ExA rankings that are aligned with the results of a preliminary costing analysis. While a boiler driven air dryer system has a lower thermal cost overall, it has a high environmental loss ratio since the loss to the environment is at lower temperatures (low quality), it has a low recovery use and further recovery would result in higher costs.

The VRC system has a high electricity cost, low thermal cost, and a loss to the environment which is significant in either configuration (valve or not). However, part of this may be negated with the replacement of the valve (V-1) with a pressure recovery turbine to help drive the compression unit. The environmental losses without this unit have a high temperature and pressure (which has a high recovery potential), and this is an important optimisation point for that system.

The costs for the superheated-steam recirculation system are slightly lower than the cost of the boiler driven air system, and adding a VRC to the exhaust steam of this system may yield improved results again. However, the cost for a system with a higher mechanically driven heat cycle is significant when compared with a chemically driven (combustion boiler) in the case of the other two systems being studied.

A preliminary costing of both systems is also informative, by revealing that Case 2 is costlier both initially and to run with the utilities as costed.

Due to the difference in utility types (natural gas vs electricity), a carbon accounting was completed (with natural gas being an onsite emission and electricity being an offsite emission). The results of 0.470 $kg.s^{-1}$ for Case 1 and 0.478 $kg.s^{-1}$ for Case 2 mean that based on current power generation in NSW, Case 1 is less environmentally damaging than Case 2, but this result is dependent on the mix of power generation within the area, and would be different in countries with a lower percentage of coal and gas power generation.

A discussion of the time taken to complete each analysis is presented in Chapter 8, and this was done in a conceptual manner, suggesting that short-cut methods and sophisticated computer programs may assist in making Exergy Analysis more accessible than it currently is. While Exergy Analysis is not new, it is still considered in its infancy with respect to usage in optimisation and methodology, especially when compared with Pinch Analysis.

References

1. Johnson, P.W.;Langrish, T.A.G. Inversion temperature and pinch analysis, ways to thermally optimize drying processes. Drying Technology, An International Journal, 2011. 29(5): p. 488-507.
2. --- Exergy Analysis of a Spray Dryer: Methods and Interpretations. Drying Technology, An International Journal, 2018. 36(5): p. 578-596.
3. Johnson, P.W.;Langrish, T.A. Interpreting exergy analysis as applied to spray drying systems. International Journal of Exergy, 2020. 31(2): p. 120-149.
4. Baker, C.G.J. Energy efficient dryer operation—An update on developments. Drying Technology, 2005. 23(9): p. 2071-2087.
5. Baker, C.G.J.;Al-Adwani, H.A.H. An evaluation of factors influencing the energy-efficient operation of well-mixed fluidized bed dryers. Drying Technology, 2007. 25(2): p. 311-318.
6. Baker, C.G.J.;McKenzie, K.A. Energy consumption of industrial spray dryers. Drying Technology, 2005. 23(1-2): p. 365-386.
7. Gilmour, J.E.;Oliver, T.N.;Jay, S. Energy use for drying processes: The potential benefits of airless drying. Drying, 1998. 98: p. 573–580.
8. Kudra, T.;Mujumdar, A.S. Advanced drying technologies. 2 ed. 2009: CRC Press. p. xiv, 89-121.
9. Mujumdar, A.S.;Devahastin, S. Fundamental principles of drying, in Guide to Industrial Drying: Principles, Equipment and New Developments, Mujumdar, A.S., Editor. 2001, Colour Publications Pvt, Ltd.: Mumbai, India. p. 1-22.
10. Warren Centre for Advanced Engineering. Industrial energy efficiency in Australia. 2000 [cited 2009 16/11/2009]; Major Energy Project]. Available from: http://thewarrencentre.com.au/projects/past-projects/industrial-energy-efficiency/.
11. Aghbashlo, M.;Mobli, H.;Rafiee, S.;Madadlou, A. A review on exergy analysis of drying processes and systems. Renewable and Sustainable Energy Reviews, 2013. 22: p. 1-22.
12. Langrish, T.A.G. Multi-scale mathematical modelling of spray dryers. Journal of Food Engineering, 2009. 93(2): p. 218-228.
13. Bahu, R.E. Spray drying- maturity or opportunities?, in Eighth International Drying Symposium, Mujumdar, A.S., Editor. 1992, Elsevier: Montreal, Canada. p. 74-91.
14. Ozmen, L.;Langrish, T.A.G. A study of the limitations to spray dryer outlet performance. Drying Technology, 2003. 21(5): p. 895-917.
15. Smith, J.M.;H.C. Van Ness;Abbott, M.M. Introduction to chemical engineering thermodynamics. 6th International ed. 2001, Singapore: McGraw-Hill Book Co. p. 172-184.
16. Sussman, M.V. Elementary general thermodynamics. Addison-Wesley Series in Chemical Engineering, ed. Hoelscher, H.E. 1972, Tufts University-Medford: Addison-Wesley Publishing Company, Inc. p. 246.
17. Kudra, T.;Platon, R.;Navarri, P. Excel-based tool to analyze the energy performance of convective dryers. Drying Technology, 2009. 27(11): p. 1302-1308.
18. Zhelev, T. The conceptual design approach-A process integration approach on the move. Resources Conservation & Recycling, 2007. 50(2): p. 143-157.
19. Zhelev, T.K.;Semkov, K.A. Cleaner flue gas and energy recovery through pinch analysis. Journal of Cleaner Production, 2004. 12(2): p. 165-170.
20. Sciubba, E.;Wall, G. A brief commented history of exergy from the beginnings to 2004. International Journal of Thermodynamics, 2007. 10(1): p. 1-26.
21. Szargut, J. International progress in second law analysis. Energy, 1980. 5(8-9): p. 709-718.
22. IPIECA.org Pinch Analysis. Energy Efficiency 2013 [cited 2013; Efficient use of heat - Pinch Analysis/Utilities optimisation]. Available from: http://www.ipieca.org/resources/energy-efficiency-solutions/efficient-use-of-heat/pinch-analysis/.

23. Aspelund, A.;Berstad, D.O.;Gundersen, T. An extended pinch analysis and design procedure utilizing pressure based exergy for subambient cooling. Applied Thermal Engineering, 2007. 27(16): p. 2633-2649.
24. Wall, G.;Gong, M. Exergy analysis versus pinch technology, in Efficiency, Costs, Optimization, Simulation and Environmental Aspects of Energy Systems, Alvfors, P., Editor. 1996: Royal Institute of Technology, Stockholm, Sweden. p. 451-455.
25. Krajnc, M.;Glavic, P. Energy integration of mechanical heat pumps with process fluid as working fluid. Chemical Engineering Research and Design, 1992. 70(a): p. 407-420.
26. Aghbashlo, M.;Kianmehr, M.H.;Arabhosseini, A. Energy and exergy analyses of thin-layer drying of potato slices in a semi-industrial continuous band dryer. Drying Technology: An International Journal, 2008. 26(12): p. 1501 - 1508.
27. Akpinar, E.K.;Midilli, A.;Bicer, Y. The first and second law analyses of thermodynamic of pumpkin drying process. Journal of Food Engineering, 2006. 72(4): p. 320-331.
28. Dincer, I.;Rosen, M.A. Exergy, energy, environmental and sustainable development. First ed. 2007, Burlington, MA, USA: Elsevier. p. 13, 28-29, 103-107.
29. Gungor, A.;Erbay, Z.;Hepbasli, A. Exergoeconomic analyses of a gas engine driven heat pump drier and food drying process. Applied Energy, 2011. 88(8): p. 2677-2684.
30. --- Exergetic analysis and evaluation of a new application of gas engine heat pumps (GEHPs) for food drying processes. Applied Energy, 2011. 88(3): p. 882-891.
31. Hepbasli, A.;Colak, N.;Hancioglu, E.;Icier, F.;Erbay, Z. Exergoeconomic analysis of plum drying in a heat pump conveyor dryer. Drying Technology: An International Journal, 2010. 28(12): p. 1385 - 1395.
32. Icier, F.;Colak, N.;Erbay, Z.;Kuzgunkaya, E.H.;Hepbasli, A. A comparative study on exergetic performance assessment for drying of broccoli florets in three different drying systems. Drying Technology: An International Journal, 2010. 28(2): p. 193 - 204.
33. Ozgener, L.;Ozgener, O. Exergy analysis of drying process: An experimental study in solar greenhouse. Drying Technology: An International Journal, 2009. 27(4): p. 580 - 586.
34. Topic, R. Mathematical model for exergy analysis for drying plants. Drying Technology, 1995. 13(1): p. 437-445.
35. Ceylan, I.;Aktas, M.;Dogan, H. Energy and exergy analysis of timber dryer assisted heat pump. Applied Thermal Engineering, 2007. 27(1): p. 216-222.
36. Tambunan, A.H.;Manalu, L.P.;Abdullah, K. Exergy analysis on simultaneous charging and discharging of solar thermal storage for drying application. Drying Technology: An International Journal, 2010. 28(9): p. 1107 - 1112.
37. Kuzgunkaya, E.H.;Hepbasli, A. Exergetic performance assessment of a ground source heat pump drying system. International journal of energy research, 2010. 31(8): p. 760-777.
38. Erbay, Z.;Gungor, A.;Hepbasli, A. Exergetic performance assessment of drying of medicinal and aromatic plants by using a pilot scale gas engine driven heat pump dryer, in 17th International Drying Symposium (IDS 2010), Weingärtner, N., Editor. 2010, DECHEMA: Magdeburg, Germany. p. 1195-1202.
39. Feng, X.;Zhu, X.X. Combining pinch and exergy analysis for process modifications. Applied Thermal Engineering, 1997. 17(3): p. 249-261.
40. Wall, G.;Chuang, C.;Ishida, M. Exergy study of the Kalina cycle. Analysis and Design of Energy Systems: Analysis of Industrial Processes, AES, 1989. 10(3): p. 73-77.
41. Gungor, A.;Tsatsaronis, G.;Gunerhan, H.;Hepbasli, A. Advanced exergoeconomic analysis of a gas engine heat pump (GEHP) for food drying processes. Energy Conversion and Management, 2015. 91: p. 132-139.
42. Gungor, A.;Erbay, Z.;Hepbasli, A. Exergoeconomic (thermoeconomic) analysis and performance assessment of a gas engine–driven heat pump drying system based on experimental data. Drying Technology, 2012. 30(1): p. 52-62.

43. Gungor, A.;Erbay, Z.;Hepbasli, A.;Gunerhan, H. Splitting the exergy destruction into avoidable and unavoidable parts of a gas engine heat pump (GEHP) for food drying processes based on experimental values. Energy Conversion and Management, 2013. 73: p. 309-316.
44. Erbay, Z.;Hepbasli, A. Advanced exergy analysis of a heat pump drying system used in food drying. Drying Technology, 2013. 31(7): p. 802-810.
45. Dincer, I.;Midilli, A.;Kucuk, H. Progress in exergy, energy, and the environment. 2014, Switzerland: Springer.
46. Erbay, Z.;Hepbasli, A. Application of conventional and advanced exergy analyses to evaluate the performance of a ground-source heat pump (GSHP) dryer used in food drying. Energy Conversion and Management, 2014. 78: p. 499-507.
47. Han, X.;Liu, M.;Wu, K.;Chen, W.;Xiao, F.;Yan, J. Exergy analysis of the flue gas pre-dried lignite-fired power system based on the boiler with open pulverizing system. Energy, 2016. 106: p. 285-300.
48. Aghbashlo, M.;Mobli, H.;Rafiee, S.;Madadlou, A. Energy and exergy analyses of the spray drying process of fish oil microencapsulation. Biosystems Engineering, 2012. 111(2): p. 229-241.
49. Erbay, Z.;Koca, N. Energetic, exergetic, and exergoeconomic analyses of spray-drying process during white cheese powder production. Drying Technology, 2012. 30(4): p. 435-444.
50. Aghbashlo, M.;Mobli, H.;Madadlou, A.;Rafiee, S. Influence of spray dryer parameters on exergetic performance of microencapsulation process. International Journal of Exergy, 2012. 10(3): p. 267-289.
51. Erbay, Z.;Koca, N. Investigating the effects of operating conditions on the exergetic performance of a pilot–scale spray–drying system. International Journal of Exergy, 2012. 11(3): p. 302-321.
52. Erbay, Z.;Koca, N.;Kaymak-Ertekin, F.;Ucuncu, M. Optimization of spray drying process in cheese powder production. Food and Bioproducts Processing, 2015. 93: p. 156-165.
53. Aghbashlo, M.;Mobli, H.;Rafiee, S.;Madadlou, A. Optimization of emulsification procedure for mutual maximizing the encapsulation and exergy efficiencies of fish oil microencapsulation. Powder technology, 2012. 225: p. 107-117.
54. Sorin, M.;Paris, J. Integrated exergy load distribution method and pinch analysis. Computers and Chemical Engineering, 1999. 23(4): p. 497-507.
55. Sciubba, E.;Ulgiati, S. Emergy and exergy analyses: Complementary methods or irreducible ideological options? Energy, 2005. 30(10): p. 1953-1988.
56. Jørgensen, S.E.;Nielsen, S.N.;Mejer, H. Emergy, environ, exergy and ecological modelling. Ecological Modelling, 1995. 77(2-3): p. 99-109.
57. Nilsson, D. Energy, exergy and emergy analysis of using straw as fuel in district heating plants. Biomass and Bioenergy, 1997. 13(1-2): p. 63-73.
58. Wimmerstedt, R. Steam drying—history and future. Drying Technology, 1995. 13(5): p. 1059-1076.
59. Mujumdar, A.S., ed. Handbook of industrial drying. 3 ed. 2007, CRC Press. Pages.
60. Mujumdar, A.S.;Devahastin, S. Superheated steam drying: An emerging drying technology. 2008: Taastrup, Denmark. p. Presentation 49 slides.
61. Kemp, I.C. Pinch analysis and process integration: a user guide on process integration for the efficient use of energy. Second Edition ed. 2007, Oxford, UK: Butterworth-Heinemann. p. 15-39 and 244-247.
62. Prachayawarakorn, S.;Soponronnarit, S. Superheated-steam drying applied in food engineering, in Innovation in Food Engineering: New Techniques and Products, Maria Laura Passos, C.P.R., Editor. 2009, CRC Press: Boca Raton, FL. p. 331-360.

63. Costa, V.A.F.;Neto da Silva, F. On the rate of evaporation of water into a stream of dry air, humidified air and superheated steam, and the inversion temperature. International Journal of Heat and Mass Transfer, 2003. 46(19): p. 3717-3726.
64. Keey, R.B.;Suzuki, M. On the characteristic drying curve. International Journal of Heat and Mass Transfer, 1974. 17(12): p. 1455-1464.
65. Choicharoen, K.;Devahastin, S.;Soponronnarit, S. Comparative evaluation of performance and energy consumption of hot air and superheated steam impinging stream dryers for high-moisture particulate materials. Applied Thermal Engineering, 2011. 31(16): p. 3444-3452.
66. Suvarnakuta, P.;Devahastin, S.;Soponronnarit, S.;Mujumdar, A.S. Drying kinetics and inversion temperature in a low-pressure superheated steam-drying system. Industrial & Engineering Chemistry Research, 2005. 44(6): p. 1934-1941.
67. Charan, R.;Prasad, S. Energy conservation in milk spray-drying plant. Journal of Food Engineering, 1993. 18(3): p. 247-258.
68. Currie, J.S.;Pritchard, C.L. Energy recovery and plume reduction from an industrial spray drying unit using an absorption heat transformer. Heat Recovery Systems and Combined Heat and Power, 1994. 14(3): p. 239-248.
69. Higa, M.;Freitas, A.J.;Bannwart, A.C.;Zemp, R.J. Thermal integration of multiple effect evaporator in sugar plant. Applied Thermal Engineering, 2009. 29(2-3): p. 515-522.
70. Sieniutycz, S. A development of the relation between drying energy savings and thermodynamic irreversibility. Chemical Engineering Science, 1984. 39(12): p. 1647-1659.
71. Velic, D.;Bilic, M.;Tomas, S.;Planinic, M. Simulation, calculation and possibilities of energy saving in spray drying process. Applied Thermal Engineering, 2003. 23(16): p. 2119-2131.
72. Zbicinski, I. Development and experimental verification of momentum, heat and mass transfer model in spray drying. The Chemical Engineering Journal and the Biochemical Engineering Journal, 1995. 58(2): p. 123-133.
73. Kemp, I.C. Analysis of separation systems by process integration. Journal of Separation Process Technology, 1986. 7(9).
74. --- Reducing dryer energy use by process integration and pinch analysis. Drying Technology, 2005. 23(9): p. 2089 - 2104.
75. Staine, F.;Favrat, D. Energy integration of industrial processes based on the pinch analysis method extended to include exergy factors. Applied Thermal Engineering, 1996. 16(6): p. 497-507.
76. Dincer, I.;Sahin, A.Z. A new model for thermodynamic analysis of a drying process. International Journal of Heat and Mass Transfer, 2004. 47(4): p. 645-652.
77. Syahrul, S.;Hamdullahpur, F.;Dincer, I. Exergy analysis of fluidized bed drying of moist particles. Exergy, An International Journal, 2002. 2(2): p. 87-98.
78. Fushimi, C.;Fukui, K. Simplification and energy saving of drying process based on self-heat recuperation technology. Drying Technology, 2014. 32(6): p. 667-678.
79. Cay, A.;Tarakçıoğlu, I.;Hepbasli, A. Exergetic analysis of textile convective drying with stenters by subsystem models: Part 1-exergetic modeling and evaluation. Drying Technology: An International Journal, 2010. 28(12): p. 1359 - 1367.
80. --- Exergetic analysis of textile convective drying with stenters by subsystem models: Part 2-parametric study on exergy analysis. Drying Technology: An International Journal, 2010. 28(12): p. 1368 - 1376.
81. Zisopoulos, F.K.;Rossier-Miranda, F.J.;van der Goot, A.J.;Boom, R.M. The use of exergetic indicators in the food industry – A review. Critical Reviews in Food Science and Nutrition, 2017. 57(1): p. 197-211.
82. Aghbashlo, M.;Mobli, H.;Rafiee, S.;Madadlou, A. The use of artificial neural network to predict exergetic performance of spray drying process: A preliminary study. Computers and electronics in agriculture, 2012. 88: p. 32-43.

83. Nazghelichi, T.;Aghbashlo, M.;Kianmehr, M.H.;Omid, M. Prediction of energy and exergy of carrot cubes in a fluidized bed dryer by artificial neural networks. Drying Technology, 2011. 29(3): p. 295-307.
84. Nikbakht, A.M.;Motevali, A.;Minaei, S. Energy and exergy investigation of microwave assisted thin-layer drying of pomegranate arils using artificial neural networks and response surface methodology. Journal of the Saudi Society of Agricultural Sciences, 2014. 13(2): p. 81-91.
85. Abdollahi-Demneh, F.;Moosavian, M.A.;Omidkhah, M.R.;Bahmanyar, H. Calculating exergy in flowsheeting simulators: A HYSYS implementation. Energy, 2011. 36(8): p. 5320-5327.
86. Gallo, W.L.R.;Milanez, L.F. Choice of a reference state for exergetic analysis. Energy, 1990. 15(2): p. 113-121.
87. Govin, O.;Diky, V.;Kabo, G.;Blokhin, A. Evaluation of the chemical exergy of fuels and petroleum fractions. Journal of Thermal Analysis and Calorimetry, 2000. 62(1): p. 123-133.
88. Morris, D.R.;Szargut, J. Standard chemical exergy of some elements and compounds on the planet earth. Energy, 1986. 11(8): p. 733-755.
89. Xiang, J.;Calì, M.;Santarelli, M. Calculation for physical and chemical exergy of flows in systems elaborating mixed-phase flows and a case study in an IRSOFC plant. International Journal of Energy Research, 2004. 28(2): p. 101-115.
90. Brodyansky, V.;Sorin, M.;Le Goff, P. The efficiency of industrial processes: exergy analysis and optimization. 1994: Elsevier London.
91. Cornelissen, R.L. Thermodynamics and sustainable development; the use of exergy analysis and the reduction of irreversibility. Laboratory of Thermal Engineering, Department of Mechanical Engineering. Deg. PhD. 1997, Enschede: University of Twente.
92. Farkye, N.;Smith, K.;Schonrock, F.;U.S. Dairy Export Council;LaGrange, V. An overview of changes in the characteristics, functionality and nutritional value of skim milk powder (SMP) during storage, U.S. Dairy Export Council, Editor. 2001: Arlington, VA, USA. p. 7.
93. Alhazmy, M.M. Minimum work requirement for water production in humidification--dehumidification desalination cycle. Desalination, 2007. 214(1-3): p. 102-111.
94. Alpuche, M.G.;Heard, C.;Best, R.;Rojas, J. Exergy analysis of air cooling systems in buildings in hot humid climates. Applied Thermal Engineering, 2005. 25(4): p. 507-517.
95. Rossi, F.;Velázquez, D. A methodology for energy savings verification in industry with application for a CHP (combined heat and power) plant. Energy, 2015. 89: p. 528-544.
96. Shukuya, M.;Hammache, A.;Agency, I.E. Introduction to the concept of exergy-for a better understanding of low-temperature-heating and high-temperature-cooling systems, in VTT Tiedotteita – Research Notes, Kettunen, M. 2002, VTT: Espoo. p. 4-61.
97. Wall, G. Exergetics. 2009: Molndal, Sweden. p. 1-151.
98. Feng, X.;Zhu, X.X.;Zheng, J.P. A practical exergy method for system analysis [of steam power plants]. in 31st Intersociety Energy Conversion Engineering Conference. 1996. Washington, DC; United States of America: IEEE
99. Bilgen, S.;Keleş, S.;Kaygusuz, K. Calculation of higher and lower heating values and chemical exergy values of liquid products obtained from pyrolysis of hazelnut cupulae. Energy, 2012. 41: p. 380-385.
100. Agricultural Research Service Basic Report: 01212, Milk, dry, whole, without added vitamin D Release 28 2015 [cited 2015 2-Nov-15]; also authored by :National Nutrient Database for Standard Reference,]. Available from: http://ndb.nal.usda.gov/ndb/foods/show/181?fgcd=&manu=&lfacet=&format=Abridged&count=&max=25&offset=50&sort=&qlookup=milk.
101. Chemicalbook.com Casein(9000-71-9). 2008 [cited 2012 23 Jan 2013]; Available from: http://www.chemicalbook.com/ProductChemicalPropertiesCB8677929_EN.htm.
102. ScienceLab.com Casein-Hammersten MSDS, in Material Safety Data Sheet:, ScienceLab.com. 2012: Dickinson, TX.

103. McCarthy, O.J.;Singh, H. Physico-chemical properties of milk, in Advanced Dairy Chemistry: Lactose, water, salts and vitamins, Fox, P., Editor. 1997, Springer Us. p. 705-710.
104. Hughes, C.G.;Gray, I.K. Chemical Analysis in the New Zealand Dairy Industry, in Chemical Processes in New Zealand, Chemistry, N.I.o. 2002, New Zealand Dairy Research Institute: Wellington, New Zealand. p. 11.
105. Bilgen, S.;Kaygusuz, K. The calculation of the chemical exergies of coal-based fuels by using the higher heating values. Applied Energy, 2008. 85(8): p. 776-785.
106. Ghannadzadeh, A. Exergetic balances and analysis in a Process Simulator: A way to enhance Process Energy Integration. 2013.
107. Brown, D.;Maréchal, F.;Paris, J. A dual representation for targeting process retrofit, application to a pulp and paper process. Applied Thermal Engineering, 2005. 25(7): p. 1067-1082.
108. Sciubba, E. Beyond thermoeconomics? The concept of extended exergy accounting and its application to the analysis and design of thermal systems. Exergy, An International Journal, 2001. 1(2): p. 68-84.
109. Al-Muslim, H.;Dincer, I.;Zubair, S.M. Effect of reference state on exergy efficiencies of one- and two-stage crude oil distillation plants. International Journal of Thermal Sciences, 2005. 44(1): p. 65-73.
110. Jilek, J.;Young, J.H. Exergy efficiency of a counterflow air/air heat exchanger with vapour condensation. Heat and Mass Transfer, 1993. 28(3): p. 123-130.
111. Rosen, M.A.;Dincer, I. Effect of varying dead-state properties on energy and exergy analyses of thermal systems. International Journal of Thermal Sciences, 2004. 43(2): p. 121-133.
112. Ishida, M.;Kawamura, K. Energy and exergy analysis of a chemical process system with distributed parameters based on the enthalpy-direction factor diagram. Industrial & Engineering Chemistry Process Design and Development, 1982. 21(4): p. 690-695.
113. Marletta, L.;Evola, G.;Sicurella, F. Energy And Exergy Analysis Of Advanced Cycles For Solar Cooling, in Eurosun. 2008, Curran Associates, Inc. NY: Lisbon, Portugal. p. 1-9.
114. Anantharaman, R.;Abbas, O.S.;Gundersen, T. Energy level composite curves--A new graphical methodology for the integration of energy intensive processes. Applied Thermal Engineering, 2006. 26(13): p. 1378-1384.
115. Kuzgunkaya, E.H.;Hepbasli, A. Exergetic performance assessment of a ground source heat pump drying system. International journal of energy research, 2007. 31(8): p. 760-777.
116. Wall, G. Exergetics. 1998: Molndal, Sweden.
117. Smith, J.M.;H.C. Van Ness;Abbott, M.M. Introduction to chemical engineering thermodynamics. 5th International ed. 1996, Singapore: McGraw-Hill Book Co. p. 130, 183-184.
118. Masters, K. Spray drying: An introduction to principles, operational practice and applications. 2 ed. 1976, New York: John Wiley & Sons.
119. Pisecky, J. Handbook of milk powder manufacture. 1997, Søborg: Niro.
120. Reay, D. Energy conservation in industrial drying. Chemical Engineer(London), 1976. July/August(311): p. 507-509.
121. Liu, Y.;Aziz, M.;Kansha, Y.;Bhattacharya, S.;Tsutsumi, A. Application of the self-heat recuperation technology for energy saving in biomass drying system. Fuel processing technology, 2014. 117: p. 66-74.
122. Ranken, M.D. Food industries manual. 2012: Springer Science & Business Media. p. 116.
123. Kim, M.;Bullard, C. A Simple Approach to Performance Analysis of Alternative Refrigerant Rolling-Piston-Type Rotary Compressors. 2001, Air Conditioning and Refrigeration Center, University of Illinois at Urbana-Champaign: Urbana. p. 37.
124. ToolBox., T.E. Optimal Combustion Processes - Fuels and Excess Air The Engineering ToolBox. 2012 Friday, 7 September 2012 5:36:42 PM 2 May 13]; Fuel air mixtures for common fuels].

Available from: http://www.engineeringtoolbox.com/fuels-combustion-efficiency-d_167.html.
125. --- Combustion Efficiency and Excess Air The Engineering ToolBox. 2017 15 June 2017, 16:46:42 16 May 17]; combustion efficiency of common fuels and air ratios]. Available from: http://www.engineeringtoolbox.com/boiler-combustion-efficiency-d_271.html.
126. Hewitt, G.F.;Pugh, S.J. Approximate Design and Costing Methods for Heat Exchangers. Heat Transfer Engineering, 2007. 28(2): p. 76-86.
127. Ozgener, L.;Ozgener, O. Exergy analysis of industrial pasta drying process. International journal of energy research, 2006. 30(15): p. 1323-1335.
128. Creyts, J.;Carey, V. Use of extended exergy analysis to evaluate the environmental performance of machining processes. Journal of Process Mechanical Engineering, 1999. 213(4): p. 247-264.
129. Australian Energy Market Operator Generation Information, in NEM 08-Aug-2019. 2019, Australian Energy Market Operator,.
130. Australian Energy Statistics Table O, Department of the Environment and Energy, Editor. 2019.
131. Department of Environment and Heritage NSW NSW Emissions. 2017. p. Trends in emissions in NSW.
132. Ganjehsarabi, H.;Dincer, I.;Gungor, A. Exergoeconomic analysis of a heat pump tumbler dryer. Drying Technology, 2014. 32(3): p. 352-360.
133. Matches Matches' Process Equipment Cost Estimates. 2007 [cited 2013 01/04/2013]; Cost Estimation Java Calculator]. Available from: http://www.matche.com/EquipCost/.
134. Peters, M.;Timmerhaus, K.;West, R. Plant Design and Economics for Chemical Engineers. 2003: McGraw-Hill Education.
135. Bailey, M.P. Chemical engineering plant cost index (cepci). Chemical Engineering, 2014. 121(2): p. 68.
136. Jenkins, S. Current Economic Trends: CEPCI January (prelim.) and December (final). [news feed] 2017 March 17, 2017 [cited 2017 April 17, 2017]; Business & Economics [Available from: http://www.chemengonline.com/current-economic-trends-cepci-january-prelim-and-december-final/.
137. AGL Regulated offer and standing offer 2013/14 – Jemena Gas Networks in http://www.agl.com.au/~/media/AGL/Residential/Documents/Plans%20and%20Pricing/2013/July/NSW_SRC_Notice_1July2013.pdf, AGL, Editor. 2013. p. 1.
138. ACIL Tasman Projecting changes to prices with changes to electricity contracting levels., in National Electricity Market Modelling, ACIL Tasman. 2011, ACIL Tasman,. p. 85.
139. Bethune, D.G.;Energy Quest esaa Domestic Gas Study Stage 3, in esaa Domestic Gas Study. 2011, Energy Quest: Adelaide. p. 57.
140. AGL AGL NSW Electricity Standing Offer Prices Essential Energy Distribution Zone - Far West1, in http://www.agl.com.au/~/media/AGL/Residential/Documents/Plans%20and%20Pricing/2013/July/NSW_Elec_SRC_Notice_1July2013.pdf, AGL, Editor. 2013. p. 1.
141. Hyslop, P.;ACIL Tasman Projecting changes to prices with changes to electricity contracting levels, in National Electricity Market Modelling. 2011, Energy Supply Association of Australia. p. 85.
142. X-Rates Exchange Rate Average (British Pound, Australian Dollar). 2019 [cited 2019 15/07/19]; Available from: https://www.x-rates.com/average/?from=GBP&to=AUD&amount=1&year=2018.
143. --- Exchange Rate Average (US Dollar, Australian Dollar). 2019 [cited 2019 15/07/19]; Available from: https://www.x-rates.com/average/?from=USD&to=AUD&amount=1&year=2018.

144. Hewitt, G.;Shires, G.;Bott, T.;Mujumdar, A. Process heat transfer. 1994: CRC press Boca Raton, FL.
145. Fox, P. Advanced Dairy Chemistry: Lactose, water, salts and vitamins. 1997: Springer Us.
146. Lactose.com The knowledge database about lactose: Physical properties. 2010 Friday, 25 June 2010 10:41:14 PM [cited 2010 16/12/10]; Available from: http://www.lactose.com/basic/physical_properties.html.

A. Abbreviations

9.1Key Variables

What each variable means:

Task: on a systems basis, this can be defined by the key item or reaction. In this case the drying of solids is the key function, while saving energy/exergy is the key of the analysis. (I.e. Task=evaporation efficiency)

Effective INE: the minimum theoretical loss associated with the task, calculated on a purely ideal basis.

Product Investment: how much of the energy is fed into the final product (in this case, on a solids basis, since this factor uses the solids side of the equation, the change is minimal, and not really useful).

Thermomechanical: temperature and pressure effects only. This definition is satisfactory for most systems without reactions or composition changes (heat exchangers, some phase change is taken into account, and is not important if no outlets are mixed with the environment, in this case diffusion potential changes will cause calculation problems)

Transiting: these factors are representative of the non-inert aspects of the unit operation or system. In this case, the solids chemical potential energy is considered inert and removed from all calculations. This definition is important for systems with high chemical potential that is not used. Using a transiting calculation basis helps focus the analysis on useful areas.

IP (Improvement potential): This is a compound factor which takes the total exergy change and the chosen efficiency factor (transiting-task is best here, in concert with transiting totals) and gives a scale of the inefficiency. Combining this with a factor of IP/IN allows for both scale and importance, i.e. is it better to focus on 10kW @ 4% (i.e. a 4 kW improvement) or 1kW @ 80% (0.8 kW) improvement, so scale is important.

Fuel basis: this refers to the total energy added to the system (inclusive of solution preheating to $60^{O}C$).

Gas side basis: a very high percentage of energy associated with exergy change is associated with the gas side of most systems, which is due to phase change calculations favouring the vapour side of the equation, and the condensed phase only focussing on simple heat (or total mass changes). Also, based on the definition of exergy (energy-entropy), the change of entropy is significantly higher in the gas phase than in the condensed phases. Using the gas side basis for calculations can lead to good estimates, but a more detailed analysis may be required. *(possibly appropriate for targeting with a first pass analysis).*

Task potential: in this case evaporation potential can be determined on several bases:

Fuel use: If all the (above $60^{O}C$) energy fed into the system is given the task of evaporating water @ the solids inlet temperature, how much water can be evaporated.

Gas side: If only the fuel used to preheat the gas side is considered (assume solution is preheated already, this assumption is suitable in this study since the solution preheater takes 250 kW to heat from 25-$60^{O}C$, which is less than 1% of the total energy used within the system). This factor is the energy from burner fuel/compressor used on the gas side pre-heating. This factor is very close for both systems (as expected)

Simple efficiency: OUT_{Tot}/IN_{Tot} (on an exergy basis should be less than unity, on an energy basis this should be unity due to "energy balance". Can be split to be expressed for each phase. Product investment is a good alternative on an energy basis, task is better)

TM efficiency: OUT_{TM}/IN_{TM} (either energy or exergy basis)

Transiting efficiency: OUT_{Trans}/IN_{Trans} (either energy or exergy basis)

Investment: $Invested/IN_{Trans}$ (either energy or exergy basis)

INE: use_{Trans}^{min} (on an energy basis, shortcut exergy calculation, does not make sense when exergy is used in the calculation)

Evap potential: $Fuel/Latent\ Heat@T_{S.IN}$ (either energy or exergy basis)

Improvement Potential: The amount of exergy not used to perform the task. It can be calculated on several bases- ideally it should be done using a transiting basis for the task (commonly used is a total or gas basis using the simple efficiency).

Comparing the inlet vs. the change?

It is important to compare the exergy and energy factor bases in a consistent manner, and this can be achieved on an inlet basis, most factors are 'change/IN'.

Key Terms:

Efficiency: Percentage of energy or exergy used for the process

Effectiveness: Percentage of energy or exergy used to perform the task

Potential: Maximum available on an ideal basis.

Actual: What occurs. This amount is typically lower due to losses through equipment walls, equipment design and constraints, non-ideal behaviour, and non-assumed behaviour (in this case ΔT_{solids}).

What this means is that comparing the potential value with an actual value gives a useful comparison, and a potential to find which one of the above behaviours is the issue.

B. Appendixes

9.2Appendix A to Chapter 5

9.2.1Calculation error analysis

Most of the base figures used in the calculation are accurate to at least two significant figures.

The case study presented in the later part of this chapter shows a smooth curve (except at the point where the outlet temperature reaches the boiling point of water (which occurs at an inlet temperature of around ~270^{O}C) At an inlet temperature of 270^{O}C, the calculation changes to a slightly different form.

On the effect of changing key variables (outside of what was used in the case study), the only parameters that resulted in more than a 1% deviation from the shown results were the inlet gas flowrate and the solids feed moisture content on a thermomechanical (Temperature and Pressure only) basis. Considering that the majority of the key results are percentages, the error propagation is typically subjected to the same variation on both sides of the ratio. The difference between hand calculations (on a very basic level), more detailed calculations, and the results from a sophisticated process modelling software resulted in a variation of +/- 0.5% for Factor 16 in Table 5-3 (η_{Trans}).

The main error, which is largely not used in this chapter, except to explain the need for transiting exergy calculations, is the chemical potential energy of the skim milk powder, with the simulation software estimating a chemical potential energy value of 17,000 KJ/kg compared with the 20,000 KJ/kg calculated using the estimation method provided (up to a 20% error for the chemical potential energy component of exergy).This large relative error is the result of comparing an estimation method (used for fuels) and a sophisticated method integrated within an advanced simulation package.

9.3Appendix B to Chapter 5

9.3.1Several factors which can be used in the analysis of the dryer

Based on the information given in Table 5-1, and the assumptions made in Table 5-2, Table B-1 provides additional supplementary information.

Table B-1: Energy and Exergy values used for calculation of the factors in Table 5-3.

Energy (kW)		Comment	Exergy (kW)		Comment
$\Delta Q_{\Delta V.G}^{TM}$	-2,780	Change of energy from evaporation in the gas phase taking only the TM energy into account.	$\Delta Ex_{\Delta V.G}^{TM}$	-6.4	Change of exergy from evaporation in the gas phase taking only the TM exergy into account.
$\Delta Q_{\Delta TM.G}^{TM}$	2,590	Change of energy from TM change in the gas phase taking only the TM change into account.	$\Delta Ex_{\Delta TM.G}^{TM}$	657	Change of exergy from TM change in the gas phase taking only the TM change into account.
$\Delta Q_{\Delta V.S\&L}^{TM}$	109	Change of energy from evaporation in the condensed phase taking only the TM change into account.	$\Delta Ex_{\Delta V.S\&L}^{TM}$	4.1	Change of exergy from evaporation in the condensed phase taking only the TM change into account.
$\Delta Q_{\Delta TM.S\&L}^{TM}$	80	Change of energy from TM change in the condensed phase taking only the TM change into account.	$\Delta Ex_{\Delta TM.S\&L}^{TM}$	7.2	Change of exergy from TM change in the condensed phase taking only the TM change into account.
			$\Delta Ex_{\Delta V.G}^{diff}$	-359	Change of exergy from evaporation in the gas phase taking only the diffusion change into account.
			$\Delta Ex_{\Delta V.S\&L}^{diff}$	522	Change of exergy from evaporation in the condensed phase taking only the diffusion change into account.
			$\Delta Ex_{\Delta T.G}^{TM} = \Delta Ex_{\Delta TM.G}^{TM}$	657	Temperature based exergy change on the gas side.
			$\Delta Ex_{\Delta T.S\&L}^{TM} = \Delta Ex_{\Delta V.S\&L}^{TM}$	4.1	Temperature based exergy change on the condensed side.
			$\Delta Ex_{\Delta P.G}^{TM}$	0	Pressure based exergy on the gas side.
			$\Delta Ex_{\Delta P.S\&L}^{TM}$	0	Pressure based exergy on the condensed side.
			$\Delta Ex_{\Delta V}^{TM}$	-2.3	$\Delta Ex_{\Delta V.G}^{TM} + \Delta Ex_{\Delta V.S\&L}^{TM}$
			$\Delta Ex_{\Delta T}^{TM}$ $\Delta T_{OUT} = 0$	651	$\Delta Ex_{\Delta T.G}^{TM} + \Delta Ex_{\Delta T.S\&L}^{TM}$
			$\Delta Ex_{\Delta V}^{diff}$	163	$\Delta Ex_{\Delta V.G}^{diff} + \Delta Ex_{\Delta V.S\&L}^{diff}$
			$\Delta Ex_{\Delta V}$	161	$\Delta Ex_{\Delta V}^{diff} + \Delta Ex_{\Delta V}^{TM}$
			ΔEx^{TM}	662	$\Delta Ex_{\Delta T}^{TM} + \Delta Ex_{\Delta V}^{TM}$
			$^{*}\Delta Ex_{Loss}$	825	$\Delta Ex^{TM} + \Delta Ex_{\Delta V}^{diff}$ Or $\Delta Ex_{\Delta T}^{TM} + \Delta Ex_{\Delta V}$
***NOTE B-1:$\Delta Ex_{\Delta T} = \Delta Ex_{\Delta T}^{TM} + \Delta Ex_{\Delta T}^{diff}$ due to the simplifying assumption that the mass transfer occurs isothermally, $\Delta Ex_{\Delta T}^{TM}$ is the same as$\Delta Ex_{\Delta T}$.**					
Q_{IN}	27,400	Total energy fed to the dryer (including chemical potential of solids).	Ex_{IN}	26,500	Total exergy fed to the dryer (including chemical potential of solids).
Q_{IN}^{TM}	4,080	Total TM energy fed to the dryer.	Ex_{IN}^{TM}	733	Total TM exergy fed to the dryer.

$Q_{IN.G}^{TM}$	3,830	TM energy fed to the dryer in the gas phase.	$Ex_{IN.G}^{TM}$	720	Total TM exergy fed to the dryer in the gas phase
Q_{OUT}	27,400	Energy balance.	Ex_{OUT}	25,700	Total exergy leaving the dryer.
Q_{OUT}^{TM}	4,080	Energy balance.	Ex_{OUT}^{TM}	71.3	Total TM exergy leaving the dryer.
$Q_{OUT.G}^{TM}$	4,020	Gas side energy out.*	$Ex_{OUT.G}^{TM}$	69.0	Total exergy leaving the dryer on the gas side.*
***NOTE B-2: Important for energy loss to the environment targeting (waste flue energy)**					
			Ex_{IN}^{diff}	625	Diffusion exergy fed to the dryer.
			$Ex_{IN.G}^{diff}$	31	Diffusion exergy fed to the dryer in the gas phase.
			Ex_{OUT}^{diff}	462	Diffusion exergy exiting the dryer.
			$Ex_{OUT.G}^{diff}$	390	Diffusion exergy exiting the dryer in the gas phase.
Calculated Variables					
$\Delta Q_{\Delta V.min}$	2,590	$\lambda_{\Delta V}\{\Delta Q_{\Delta V}\}@T_{S.OUT} \times \dot{m_{\Delta V}}$	$\Delta Ex_{\Delta V.min}$	284	$\{\Delta Ex_{\Delta V}\}@T_{S.OUT} \times \dot{m_{\Delta V}}$
$\Delta Q_{\Delta V.act}$	2,670	$\Delta Q_{\Delta V.G}^{TM} + \Delta Q_{\Delta V.S\&L}^{TM}$	$\Delta Ex_{\Delta V.act}^{TM}$	-2.3	$\Delta Ex_{\Delta V.G}^{TM} + \Delta Ex_{\Delta V.S\&L}^{TM}$
INE^{TM}	47	INE using $Q_{IN.G}^{TM} - Q_{OUT.G}^{TM}$*	$\Delta Ex_{\Delta V.act}^{diff}$	163	$\Delta Ex_{\Delta V.G}^{diff} + \Delta Ex_{\Delta V.S\&L}^{diff}$
INE_{G}^{TM}	943	INE using $Q_{IN.G}^{TM}$*	$\Delta Ex_{\Delta V.act}$	161	$\Delta Ex_{\Delta V.act}^{diff} + \Delta Ex_{\Delta V.act}^{TM}$
$INE_{\Delta V}$	657	INE using $\Delta Q_{\Delta V.act}$*	Ex_{G}^{Trans}	101	Exergy which is not influenced in the dryer and separator in the gas phase (i.e. can be ignored in analysis).
$INE_{\Delta V.G}^{\Delta T}$	638	In-text Equation 2-27. *	$Ex_{S\&L}^{Trans}$	25,200	Exergy which is not influenced in the dryer and separator in the condensed phase (i.e. can be ignored in analysis).
$INE_{Mix.G}^{\Delta V}$	490	In-text Equation 5-2. *	$T_0 \Delta S_{Gen.ID}$	845	Ideally equivalent to INE_{ID}
$INE_{\Delta V}^{\Delta T}$	657	In-text Equation 5-3. *	$T_0 \Delta S_{Gen.act}$	825	Equivalent to INE.
$INE_{Mix}^{\Delta V}$	471	In-text Equation 5-4. *	$1 - \frac{INE_G}{Q_{G.IN}^{TM}}$	75.4%	Inevitable energy loss ratio.
INE_{Dryer}	1,128	In-text Equation 5-5.	$\frac{\Delta Ex_{\Delta V.ID}}{\Delta Q_{\Delta V.ID}}$	11.0%	Ratio of evaporation exergy use (not particularly useful).
$INE_{Dryer.G}$	1,129	In-text Equation 5-5.	$\Omega_G^{Dryer} = \frac{\Delta Ex_G}{Q_{G.IN}}$	0.08	Unit quality ratio (abstract).

***NOTE B-3:Assuming the INE definition for a boiler suits that of a dryer with $T_{SourceMax}=T_{G.IN}$ and $T_{Sinc}=T_{DP.(YIN)}$.**

9.4Appendix A to Chapter 6

9.4.1Value table

	T	P	n(total)	n_DA	n_S	y()	x()	n_Wub	H_TM	H_tot	H(-trans)	Ex_diff	Ex_TM	Ex_tot	Ex^-CH	Ex(-trans)	Trans Ex	Trans H
Shared Streams																		
S-01	298.2	1.0	0.730	0.723	-	0.010	-	-	0.0	0.0	0.0	0.0	0.0	0.0	0.0	0.0	0.0	0.0
S-03	463.2	1.0	0.730	0.723	-	0.010	-	-	3,525.2	3,525.2	3,525.2	0.0	719.5	719.5	719.5	719.5	0.0	0.0
S-03a	*341.9*	*1.0*	*0.730*	*0.723*	-	*0.010*	-	-	*935.0*	*935.0*	*935.0*	*0.0*	*62.6*	*62.6*	*62.6*	*62.6*	*0.0*	*0.0*
S-03-60c	*333.2*	*1.0*	*0.730*	*0.723*	-	*0.010*	-	-	*747.8*	*747.8*	*747.8*	*0.0*	*40.7*	*40.7*	*40.7*	*40.7*	*0.0*	*0.0*
S-05	341.9	1.0	0.791	0.723	-	0.094	-	-	3,688.5	3,688.5	3,688.5	514.3	394.4	908.7	908.7	908.7	0.0	0.0
S-08	298.2	1.0	0.073	-	0.004	-	19.000	-	0.0	23,300.0	0.0	593.7	0.0	25,751.2	593.7	521.9	25,229.3	23,300.0
S-09	333.2	1.0	0.073	-	0.004	-	19.000	0.033	248.5	23,548.5	248.5	593.7	13.5	25,764.7	607.2	535.4	25,229.3	23,300.0

S-09a	*321.9*	*1.0*	*0.073*	-	*0.004*	-	*2.019*	*0.017*	*2,808.1*	*26,108.1*	*2,808.1*	*759.3*	*198.7*	*26,115.4*	*957.9*	*886.1*	*25,229.3*	*23,300.0*
S-10	321.9	1.0	0.012	-	0.004	-	2.298	-	59.6	23,359.6	59.6	71.8	2.3	25,231.6	74.1	2.3	25,229.3	23,300.0
S-04	335.0	1.0	0.803	0.723	0.004	0.098	1.450	0.071	3,744.8	27,044.8	3,744.8	586.8	350.3	26,094.5	937.0	865.2	25,229.3	23,300.0
S-05-25c	*298.2*	*1.0*	*0.791*	*0.723*	-	*0.032*	-	*0.045*	*696.1*	*696.1*	*696.1*	*217.2*	*0.0*	*217.2*	*217.2*	*217.2*	*0.0*	*0.0*
Boiler Case Streams																		
S-02	321.9	1.0	0.730	0.723	-	0.010	-	-	507.7	507.7	507.7	0.0	19.2	19.2	19.2	19.2	0.0	0.0
S-06	320.4	1.0	0.791	0.723	-	0.094	-	-	3,180.8	3,180.8	3,180.8	514.3	198.9	713.1	713.1	713.1	0.0	0.0
Uh-1	483.2	19.1	0.007	-	-	-	-	0.007	364.6	364.6	263.5	83.7	157.7	241.5	241.5	156.9	84.5	101.1
UD-1	483.1	19.1	0.007	-	-	-	-	0.007	101.1	101.1	0.0	62.1	22.4	84.5	84.5	0.0	84.5	101.1
Uh-2	483.2	19.1	0.088	-	-	-	-	0.088	4,426.7	4,426.7	4,325.6	1,016.7	1,915.3	2,932.0	2,932.0	2,847.5	84.5	101.1
UD-2	483.1	19.1	0.088	-	-	-	-	0.088	1,227.6	1,227.6	1,126.5	754.0	272.6	1,026.5	1,026.5	942.0	84.5	101.1
Uh-3	483.2	19.1	0.095	-	-	-	-	0.095	4,791.2	4,791.2	4,690.1	1,100.5	2,073.0	3,173.5	3,173.5	3,088.9	84.5	101.1
UD-3	483.1	19.1	0.095	-	-	-	-	0.095	1,328.7	1,328.7	1,227.6	816.1	295.0	1,111.1	1,111.1	1,026.5	84.5	101.1
S-B1	298.2	1.0	0.007	-	-	-	-	-	0.0	6,480.6	6,480.6	43.8	0.0	6,608.8	43.8	6,608.8	0.0	0.0
S-B2	298.2	1.0	0.077	-	-	-	-	0.001	0.0	0.0	0.0	1.8	0.0	1.8	1.8	1.8	0.0	0.0
S-B3	483.2	1.0	0.077	-	-	-	-	0.001	417.0	417.0	417.0	1.8	92.6	94.4	94.4	94.4	0.0	0.0
S-B4	2,354.2	1.0	0.082	-	-	-	-	0.012	5,692.4	5,692.4	5,692.4	173.0	3,649.6	3,822.6	3,822.6	3,822.6	0.0	0.0
S-B5	503.2	1.0	0.082	-	-	-	-	0.012	1,001.0	1,001.0	1,001.0	173.0	269.8	442.8	442.8	442.8	0.0	0.0
S-B6	326.2	1.0	0.082	-	-	-	-	0.012	552.5	552.5	552.5	173.0	43.4	216.4	216.4	216.4	0.0	0.0
VRC case Streams																		
S-06	483.2	2.5	0.791	0.723	-	0.094	-	-	7,016.3	7,016.3	7,016.3	514.3	3,569.0	4,083.3	4,083.3	4,083.3	0.0	0.0
S-07	308.2	2.5	0.791	0.723	-	0.094	-	0.052	2,893.3	2,893.3	2,893.3	514.3	1,899.0	2,413.3	2,413.3	2,413.3	0.0	0.0
S-12	406.8	1.0	0.791	0.723	-	0.094	-	-	5,216.4	5,216.4	5,216.4	514.3	1,005.5	1,519.8	1,519.8	1,519.8	0.0	0.0
U-E1	-	-	-	-	-	-	-	-	3,327.8	3,327.8	3,327.8	0.0	3,327.8	3,327.8	3,327.8	3,327.8	0.0	0.0
U-E2	-	-	-	-	-	-	-	-	248.5	248.5	248.5	0.0	248.5	248.5	248.5	248.5	0.0	0.0

NOTE B-4: The rows with a at the end refer to intermediate calculations, the rows with - ##c refer to a temperature change variant, n_Wub refers to unbound water (water which is independent of air or solids)

9.5Appendix A to Chapter 8

9.5.1Pump Power and Discharge Pressure Requirements

Given a particular outlet temperature, the compressor outlet pressure and compressor power estimates may be calculated using Equations B-1 and B-2, respectively.

$$P_{OUT}^{ID} = P_{IN}\left(\frac{T_2}{T_1}\right)^{\frac{k}{k-1}} \quad \text{B-1 [15]}$$

$$And$$

$$P_{OUT}^{Act} = \eta_{Compressor} P_{IN}\left(\frac{T_2}{T_1}\right)^{\frac{k}{k-1}}$$

$$Power_{Est.}^{Adia.} = \left(1000\left(\frac{k}{k-1}\right)P_1 Q_1\left[\left(\frac{P_2}{P_1}\right)\left(\frac{k-1}{k}\right)-1\right]\right) \quad \text{B-2}$$

$$And$$

$$Power_{Est.}^{Act} = \left(\frac{1000}{\eta_{Compressor}}\left(\frac{k}{k-1}\right)P_1 Q_1\left[\left(\frac{P_2}{P_1}\right)\left(\frac{k-1}{k}\right)-1\right]\right)$$

9.6Appendix B to Chapter 8

9.6.1Costing

Since the basis of comparison is the dryer and the separation system, the only part(s) of the plant that have been costed are the capital cost of the heat exchange network, boiler system and compressor, with the operating cost being exclusively a comparison between the electricity for the compressor and the natural gas for the boiler system.

$$A = \frac{\Delta H}{U \Delta T_{LM}} \quad \text{B-3}$$

$$\Delta T_{LM} = \frac{(T_{HH} - T_{HC}) - (T_{CH} - T_{CC})}{LN\left(\frac{T_{HH} - T_{HC}}{T_{CH} - T_{CC}}\right)} \quad \text{B-4}$$

Table B-2: Cost estimations for the two systems major components (excluding the dryer) (summary table, from Table 8-5 to 8-12).

	Case 1	Case 2
HX	$ 130,000	$ 250,000
Boiler	$ 250,000	-
Blower	$ 630,000	-
Compressor	-	$ 1,400,000
Coil Heater	-	$ 24,000
Total	**$ 1,010,000**	**$ 1,674,000**

Table B-3: Various basic conversions used for the estimation.

Curr. conv. =	1.7860	AU$/Pound (2018 average)
	1.3394	AU$/US$ (2018 average)
CEPCI (1982)=	314.0	
CEPCI (1991)=	361.3	
CEPCI (2002)=	395.6	
CEPCI (2007)=	525.4	
CEPCI (2016)=	546.6	
CEPCI (2018)=	603.1	

NOTE B-5: CEPCI from[136] and related sources.
NOTE B-6: Exchange rates calculated from [142, 143].

Table B-4: Pressure correction factor and plate are multiplier used in heat exchanger calculations from Peters, Timmerhaus, West, p 687, figure 14-28 [134].

Operating Pressure	1	20	3	Bar
Pressure correction factor	1	2.4	1	
~ plate area (25% total area)	130.0	30.0	975.0	m^2
	25%			m^2/m^2

Table B-5: Sizing calculations for the 3 heat exchangers.

	Case 1 E-1	Case 1 E-2	Case 2 E-1	
LMTD(counter-flow)				
cLMTD=	21.02	68.19	27.56	K
R=	1.11	8.16	0.54	
θ=	0.50	0.42	0.15	
NTU2=	2.23	4.20	18.42	
P=	0.47	0.00	0.89	
F=	0.88	-	0.65	
LMTD (cross-flow)				
cLMTD (cross)=	18.50		17.91	K
UA Calculations				
U=	100	800	100	$W.m^{-2}.K^{-1}$ *
Q=	465	3,046	3,512	kW
A=Q/U.LMTD				
A=	503	112	3,925	m^2
A=	**510**	**120**	**4,000**	**m^2 ^**
V_{Fl}=	39.8	19.2	26.5	$m^3.s^{-1}$
V_{Fr}=	39.9	27.7	33.7	$m^3.s^{-1}$
Q/dT=	25,200	44,700	196,100	$W.K^{-1}$

***NOTE B-7: First pass estimation values from Hewitt, Shires, Bott, p229 Table 4.5 [144]**
^NOTE B-8: Size rounded up to the nearest two significant figures.

Table B-6: Heat Exchanger Costing from Hewitt, Shires, Bott p229 Table 4.5 [144].

Exchangers	Case 1 E-1	Case 1 E-2	Case 2 E-1				
C_est=	0.650	0.480	0.650	£(1982)/W.K			
p.229 t.4.5	** LP Gas Q/dT~1000*	** Cond. ST Q/dt~30,000*	** HP Gas Q/dT~30,000*				
C_est=	3.982	2.941	3.982	$(2019)/W.K			
Q/dT=	25,843	44,553	193,433	$W.K^{-1}$			
Cost=	$ 100,142	$ 131,390	$ 780,790	$(2019)			
	$ 231,533						
P-Corr. ^	$ 100,142	$ 315,337	**$ 780,790**	$(2019)	**Base**	**$ 420,000**	Cf #
	$ 415,479				**VRC**	**$ 790,000**	
					CR	1.88	

#NOTE B-9: Cost factor method.
^NOTE B-10: Using the pressure correction factors shown in Table B-4.

Table B-7: Heat Exchanger Costing from Peters, Timmerhaus, West p684 Figure 14-20 [134].

Exchangers	Case 1 E-1	Case 1 E-2	Case 2 E-1				
A (trans.) p.684 f.14-20	*503*	*112*	*3,921*	m^2			
	$ 20,000	$ 18,000	$ 120,000	US$(2002)			
	$ 40,839	$ 36,755	$ 245,036	$(2019)			
	$ 77,595						
P-Corr. ^	$ 40,839	$ 88,213	**$ 246,036**		**Base**	**$ 130,000**	graph # finned-tube
	$ 129,052				**VRC**	**$ 250,000**	FH exchanger
					CR	1.92	

#NOTE B-11: Graphical interpolation method.
^NOTE B-12: Using the pressure correction factors shown in Table B-4.

Table B-8: Package Boiler Plant costing with no superheat from Peters, Timmerhaus, West p892 Figure b-3 [134].

Boilers	Case 1 B-01 (0 deg superheat)		Case 2 B-01 (0 deg superheat)*				
Boiler	Basic		Basic		p.892 f.b-3		
Steam Gen		1.73		0.11	kg/s		
		2		**0.8**	kg/s		
Pressure Required		19.07		1.22	Bar		
Used P		**2,860**		**1,825**	**kPa**		
Temperature		230		125	C		
Used T		447		405	C	**Base**	**$ 250,000**
Cost (2002)	$	120,000	$	25,000		**VRC**	$ 52,000
Cost (2019)	**$**	**245,036**	**$**	**51,049**		**CR**	0.21

***NOTE B-13: A check to see if a boiler is worth having.**

Table B-9: Cost of electric immersion heaters from Peters, Timmerhaus, West p624 Figure 15-29 [134]. (extrapolated to be 2x125 kW heaters)

Electric heater		
Rating	250	kW
Cost (2002)	$ 8,500	
Cost (2019)	**$ 23,300**	

Table B-10: Compressor and blower costing for the systems [133].

Blowers and Compressors		
	Case 1 Blower	**Case 2 Compressor #**

V_{FI}=	22.08		22.08	m^2/s		
	46,792		46,792	**ft^3/min**		
Quote ΔP	*0.69*		*8.62*	*Bar*		
Req. ΔP	0.6		2.61	Bar		
Power (E)	2,040		**4,515**	**HP**		
	1,521^		3,367	kW	**Base**	**$ 630,000**
Cost (2007)	$ 409,600	$	1,057,000		**VRC**	**$ 1,400,000**
Cost (2019)	**$ 629,760**	**$**	**1,625,138**		**CR**	2.22

#NOTE B-14: Pressure requirement not low enough for a blower, if Req. ΔP was below 2.1 Bar the cost would be $1,330,000.
^NOTE B-15: Estimate Only.

9.7Appendix C Sample Calculations for a Dryer

Air System

Raw Data

Table B-11: The constants used within the calculations

Reference State Properties			Gas Phase Dead State Properties		
T_0	298.14	K	T_{00}	298.14	K
P_0	101,325	Pa	P_{00}	101,325	Pa
			RH_{00}	27	%
			$\gamma_{DA_{00}}$	0.996	
			$\gamma_{V_{00}}$	0.004	
Constants			**Calculated Constants**		
$\overline{Cp_{DA}}$	28.97	kJ.kmol^{-1}.K^{-1}	$\bar{\rho}_L$	55.35	kmol.m^{-3}
$\overline{Cp_V}$	35.59	kJ.kmol^{-1}.K^{-1}	$\bar{v}_L$	0.0181	m^3.kmol^{-1}
$\overline{Cp_L}$	75.35	kJ.kmol^{-1}.K^{-1}	$\bar{\rho}_S$	4.47	kmol.m^{-3}
$\overline{Cp_S}$	513.43	kJ.kmol^{-1}.K^{-1}	$\bar{v}_S$	0.2237	m^3.kmol^{-1}
mm_{DA}	28.970	kg.kmol^{-1}	R_{DA}	0.000287	kJ.kg.K^{-1} NOTE B-17
mm_V	18.015	kg.kmol^{-1}	R_V	0.000462	kJ.kg.K^{-1} NOTE B-18
mm_L	18.015	kg.kmol^{-1}	β_L	0.000207	K^{-1}
mm_S	342.29	kg.kmol^{-1}	β_S	0.001098	K^{-1} [145] p709-710
$\bar{R}$	0.008314	kJ.kmol^{-1}.K^{-1}			
ρ_L	997	kg.m^{-3} (at 20^{O}C)			
ρ_S	1530	kg.m^{-3} (at 20^{O}C)			

NOTE B-16: The properties of the solid are taken to be those of α-lactose monohydrate for simplicity [146].
NOTE B-17: R_{DA} is $\frac{\bar{R}}{mm_{DA}}$
NOTE B-18: R_V is $\frac{\bar{R}}{mm_V}$

The sample calculation for steam 4 (S-04 in Figure 4-4, Figure 4-7, Figure 6-1, and Figure 6-2) in the process (the dryer outlet) is as follows.

Table B-12: The raw data

Raw Stream Properties, Point 1			Calculated Stream Properties, Point 1		
T_1	330.37	K			
P_1	101,325	Pa			
M_{DA_1}	20.87	kg.s^{-1}	n_{DA_1}	0.7204	kmol.s^{-1}

M_{V_1}	1.21	kg.s^{-1}	n_{V_1}	0.0672	kmol.s^{-1}
M_{L_1}	0.17	kg.s^{-1}	n_{L_1}	0.0094	kmol.s^{-1}
M_{S_1}	1.25	kg.s^{-1}	n_{S_1}	0.0037	kmol.s^{-1}
M_T	23.5	kg.s^{-1}	n_T	0.8007	kmol.s^{-1}
Calculated Stream Properties, Point 1			**Calculated Stream Properties, Point 1**		
x_{DA_1}	0.8998	(eq. B-17)	γ_{DA_1}	0.9147	(eq. B-15)
x_{V_1}	0.0839	(eq. B-17)	γ_{V_1}	0.0853	(eq. B-15)
x_{L_1}	0.0118	(eq. B-17)	γ_{L_1}	0.7210	(eq. B-12)
x_{S_1}	0.0046	(eq. B-17)	γ_{S_1}	0.2790	(eq. B-12)

Now that the stream data is in the four useful forms (mass flow, mole flow, mole fraction, and molar phase fraction) and the calculation constants are determined, it is possible to begin the calculation.

Temperature based Thermo-Mechanical Exergy

First, since there are two interacting phases, it is necessary to determine the interaction using the isotherm calculations. This procedure determines the compositions of point 2 of the system (T_0,P). Once this information is calculated, it is possible to proceed with the exergy calculations for the temperature-based thermo-mechanical exergy.

Using Equation B-5 to determine the partial pressure of water vapour:

$$P_i = \gamma_i P \qquad \text{B-5}$$

$$P_{V_1} = 0.0672 \times 101{,}325$$

$$\boldsymbol{P_{V_1} = 8{,}641.3\ Pa}$$

The temperature at which this vapour pressure causes dew formation, or T_{DP}, can be found using Equation B-6:

$$T_{DP_1} = \frac{3816.44}{18.3036 - \ln\left(\frac{P_{V_1}}{133.3}\right)} + 44.12 \qquad \text{B-6}$$

$$T_{DP_1} = \frac{3816.44}{18.3036 - \ln\left(\frac{8{,}641.3}{133.3}\right)} + 44.12$$

$$\boldsymbol{T_{DP_1} = 314.18\ K}$$

Equation B-7 is used to determine if there is phase change in this pathway. It is also a check to determine if the result from Equation B-6 is reasonable. Phase change occurs if Y_S (humidity above solids)>Y (bulk in gas). Less generally, usually T_G>T_S for drying to occur.

$$\boldsymbol{IF}\ T_{DP_1} \leq T_0, T_{DP_1} = T_0$$
$$\boldsymbol{IF}\ T_{DP_1} \geq T_1, T_{DP_1} = T_1 \qquad \text{B-7}$$

$$298.14\ K < \mathbf{314.18}\ K < 330.27\ K$$
$$T_{DP_1} \text{is reasonable}$$

The above statement means that phase change will occur in the system when the temperature is changed isobarically from T to T_0. For this the amount of water that condenses along this pathway needs to be determined.

Equation B-8 determines the saturation vapour pressure at the end-point. This vapour pressure will act as an upper limit for the amount of water that can be in the air.

$$P_{V_2}^{Sat} = P_{V_0}^{Sat} = 133.3 \times \exp\left(18.3036 - \frac{3816.44}{T_0 - 44.12}\right) \qquad \text{B-8}$$

$$P_{V_0}^{Sat} = 133.3 \times \exp\left(18.3036 - \frac{3816.44}{298.14 - 44.12}\right)$$
$$\boldsymbol{P_{V_0}^{Sat} = 3,540.5\ Pa}$$

Before continuing, finding the limiting flows associated with this point is required, without calculating the isotherm, as will be explained later.

Equation B-9 can be used to calculate the phase fraction associated with the saturation pressure, as follows.

$$\gamma_{V_2}^{Sat} = \frac{P_{V_0}^{Sat}}{P} \qquad \text{B-9}$$

$$\gamma_{V_2}^{Sat} = \frac{3{,}540.5}{101{,}325}$$
$$\boldsymbol{\gamma_{V_2}^{Sat} = 0.0349}$$

And by using Equation B-10 to solve for the molar flow of water vapour, as follows:

$$n_{V_2}^{Sat} = \frac{\gamma_{V_2}^{Sat} n_{DA}}{\left(1 - \gamma_{V_2}^{Sat}\right)} \quad \text{B-10}$$

$$n_{V_2}^{Sat} = \frac{0.0349 \times 0.7204}{(1 - 0.0349)}$$

$$\boldsymbol{n_{V_2}^{Sat} = 0.0261\ kmol.s^{-1}}$$

Then by a water component balance, Equation B-11:

$$n_{L_2}^{Sat} = n_{V_1} + n_{L_1} - n_{V_2}^{Sat} \quad \text{B-11}$$

$$n_{L_2}^{Sat} = 0.0672 + 0.0094 - 0.0261$$

$$\boldsymbol{n_{L_2}^{Sat} = 0.0505\ kmol.s^{-1}}$$

$$\gamma_L = \frac{n_L}{(n_L + n_S)} = \frac{x_L}{(x_L + x_S)} \quad \text{B-12}$$

Next an initial guess for the pressure of the system at point 2 is required. The saturation pressure is known, so it is reasonable to use this as the starting point for the iteration.

$$P_{V_2}^{Initial} = P_{V_0}^{Sat} = 3{,}540.53\ Pa$$

The iterative part of the calculation can then proceed.

Equation B-13 is used to determine the solids and liquid equilibrium condition.

$$\frac{\gamma_{L_2}}{\gamma_{S_2}} = 2.8481 \times \exp\left[-2.306 \times 10^{-3} \times T_0 \times \ln\left(\frac{P_{V_2}^{Sat}}{P_{V_2}}\right)\right] \quad \text{B-13}$$

$$\frac{\gamma_{L_2}}{\gamma_{S_2}} = 2.8481 \times \exp\left[-2.306 \times 10^{-3} \times T_0 \times \ln\left(\frac{3{,}540.5}{3{,}540.5}\right)\right]$$

$$\frac{\gamma_{L_2}}{\gamma_{S_2}} = 2.8481$$

After iteration, a stable solution is reached, as follows:

$$\boldsymbol{\frac{\gamma_{L_2}}{\gamma_{S_2}} = 4.8418}$$

Next it is necessary to solve this for n_{L_2}, which is done with Equation B-14, knowing that the number of moles of solid does not change, $n_{S_2} = n_{S_1}$.

$$n_{L_2} = \frac{\gamma_{L_2}}{\gamma_{S_2}} \times n_{S_2} \quad \text{B-14}$$

$$n_{L_2} = 2.8481 \times 0.0037$$
$$n_{L_2} = 0.0104\ kmol.s^{-1}$$

After iteration, a stable solution is reached, as follows:

$$\boldsymbol{n_{L_2} = 0.0177\ kmol.s^{-1}}$$

Now the solution for n_{V_2} may be found using a water balance, or Equation B-11.

$$n_{V_2} = n_{V_1} + n_{L_1} - n_{L_2} \quad \text{B-11}$$

$$n_{V_2} = 0.0672 + 0.0094 - 0.0104$$
$$n_{V_2} = 0.0662\ kmol.s^{-1}$$

After iteration, a stable solution is reached, as follows:

$$\boldsymbol{n_{V_2} = 0.0589\ kmol.s^{-1}}$$

There is a need to convert this result back into a partial pressure, and this is done by first finding the gas phase fraction that this molar flow represents, Equation B-15. Knowing that $n_{DA_2} = n_{DA_1}$.

$$\gamma_{V_2} = \frac{n_{V_2}}{(n_{V_2} + n_{DA_2})} \quad \text{B-15}$$

$$\gamma_{V_2} = \frac{0.0662}{(0.0662 + 0.7204)}$$
$$\gamma_{V_2} = 0.0842$$

After iteration, a stable solution is reached, as follows:

$$\boldsymbol{\gamma_{V_2} = 0.0756}$$

Now by simply using Equation B-5 again, the partial pressure of vapour at this point can be obtained.

$$P_{V_2} = \gamma_{V_2} P \quad \text{B-5}$$

$$P_{V_2} = 0.0842 \times 101{,}325$$

$$P_{V_2} = 8{,}527.7\ Pa$$

This new P_{V_2} gets substituted into Equation B-13 and repeats until the system reaches a stable solution.

After iteration, a stable solution is reached, as follows:

$$\boldsymbol{P_{V_2} = 7{,}660.7\ Pa}$$

Now it is necessary to check if this is realistic.

$$\boldsymbol{P_{V_2} = 7{,}660.7\ Pa}$$

$$\boldsymbol{P_{V_0}^{Sat} = 3{,}540.5\ Pa}$$

And:

$$\boldsymbol{n_{V_2}(Isotherm) = 0.0589\ kmol.s^{-1}}$$

$$\boldsymbol{n_{V_2}^{Sat} = 0.0261\ kmol.s^{-1}}$$

Since $n_{V_2}^{Sat}$ is the upper limit of the system, the minimum molar value is used, as stated by Equation B-16.

$$n_{V_2}(Actual) = \min\left(n_{V_2}(Isotherm), n_{V_2}^{Sat}\right) \qquad \text{B-16}$$

$$\boldsymbol{n_{V_2} = 0.0261\ kmol.s^{-1}}$$

And by mass balance, or looking up the value that matches it (Calculated above).

$$\boldsymbol{n_{L_2} = 0.0505\ kmol.s^{-1}}$$

To summarise the results:

Table B-13: Data for Point 2

Raw Stream Properties, Point 2			Calculated Stream Properties, Point 2		
T_2	298.14	K			
P_2	101,325	Pa			
M_{DA_2}	20.87	kg.s^{-1}	n_{DA_2}	0.7204	kmol.s^{-1}

M_{V_2}	0.47	kg.s^{-1}	n_{V_2}	0.0261	kmol.s^{-1}
M_{L_2}	0.91	kg.s^{-1}	n_{L_2}	0.0505	kmol.s^{-1}
M_{S_2}	1.25	kg.s^{-1}	n_{S_2}	0.0037	kmol.s^{-1}
M_T	23.5	kg.s^{-1}	n_T	0.8007	kmol.s^{-1}
Calculated Stream Properties, Point 2			**Calculated Stream Properties, Point 2**		
x_{DA_2}	0.8998	(eq. B-17)	γ_{DA_2}	0.9651	(eq. B-15)
x_{V_2}	0.0326	(eq. B-17)	γ_{V_2}	0.0349	(eq. B-15)
x_{L_2}	0.0631	(eq. B-17)	γ_{L_2}	0.9326	(eq. B-12)
x_{S_2}	0.0046	(eq. B-17)	γ_{S_2}	0.0674	(eq. B-12)

At this point it is necessary to identify the component fractions to which Equations B-18, B-22 and B-27 apply, and those to which Equations B-20, B-24 and B-28 apply.

Equations B-18, B-22 and B-27 apply to components with no change in heat capacity, so it is necessary to isolate any phase change part of a component. This procedure is done by taking the minimum of the values at points 1 and 2.

$n_{DA_2} = n_{DA_1}$	Either one.
$n_{V_2} < n_{V_1}$	n_{V_2} is the minimal one.
$n_{L_2} > n_{L_1}$	n_{L_1} is the minimal one.
$n_{S_2} = n_{S_1}$	Either one.

The remaining component is designated $n_{\Delta V}$ and is found by a water component balance:

$$n_{\Delta V}^{T} = n_{V_1} - n_{V_2} \qquad \text{B-11}$$

$$\boldsymbol{n_{\Delta V}^{T} = 0.0261\ kmol.s^{-1}}$$

Hence:

$$\boldsymbol{x_i = \frac{n_i}{n_T}} \qquad \text{B-17}$$

$$\boldsymbol{x_{\Delta V}^{T} = 0.0513}$$

This component requires the use of Equations B-20, B-24 and B-28.

Applying the appropriate formulae to each component

Equation B-18 components:

$$h^T = Cp(T - T_0) \qquad \text{B-18}$$

$$h^T_{DA_1} = x_{DA_1}\overline{Cp_{DA}}(T_1 - T_0)$$
$$h^T_{DA_1} = 0.8998 \times 28.97 \times (330.27 - 298.14)$$
$$\boldsymbol{h^T_{DA_1} = 837\ kJ.kmol^{-1}_T}$$

$$h^T_{V_2} = x_{V_2}\overline{Cp_V}(T_1 - T_0)$$
$$h^T_{V_2} = 0.0326 \times 35.59 \times (330.27 - 298.14)$$
$$\boldsymbol{h^T_{V_2} = 95.9\ kJ.kmol^{-1}_T}$$

$$h^T_{S_1} = x_{S_1}\overline{Cp_S}(T_1 - T_0)$$
$$h^T_{S_1} = 0.0046 \times 513.43 \times (330.27 - 298.14)$$
$$\boldsymbol{h^T_{S_1} = 75.2\ kJ.kmol^{-1}_T}$$

Equation B-20 components: it is necessary to determine the enthalpy associated with the phase change, Equation B-19. The data required for this are readily found in steam tables.

$$\Delta h_{\Delta V} = h_{SatVap}(T_{DP}) - h_{SatLiq}(T_{DP}) \qquad \text{B-19}$$

$$h_{SatVap}(T_{DP}) = 2{,}575.4\ kJ.kg^{-1}$$
$$h_{SatLiq}(T_{DP}) = 171.8\ kJ.kg^{-1}$$
$$\Delta h_{\Delta V} = 2{,}403.5\ kJ.kg^{-1}$$
$$\boldsymbol{\overline{\Delta h_{\Delta V}} = 43{,}299.8\ kJ.kmol^{-1}}$$

Now Equation B-20 can be solved:

$$h^T_{\Delta V} = x^T_{\Delta V}\left[\overline{Cp_V}(T_1 - T_{DP}) + \overline{\Delta h_{\Delta V}} + \overline{Cp_L}(T_{DP} - T_0)\right] \qquad \text{B-20}$$

$$h^T_{\Delta V} = 0.0513 \times [35.59 \times (330.27 - 314.18) + 43{,}299.8 + 75.35 \times (314.18 - 298.14)]$$
$$\boldsymbol{h^T_{\Delta V} = 2{,}312.6\ kJ.kmol^{-1}_T}$$

Now that the enthalpy changes of each component have been calculated, it is possible to add the results together to get the total stream enthalpy change associated with temperature change under isobaric conditions. For this summation, Equation B-21 is used.

$$h_{TM}^{T} = h_{DA_1}^{T} + h_{V_2}^{T} + h_{L_1}^{T} + h_{S_1}^{T} + h_{\Delta V}^{T} \quad \text{B-21}$$

$$h_{TM}^{T} = 837.506 + 95.928 + 28.534 + 75.242 + 2{,}312.59$$

$$\boldsymbol{h_{TM}^{T} = 3{,}349.80\ kJ.kmol^{-1}}$$

Using the same system used for enthalpy (Equations B-18, B-19, B-20 and B-21), the entropy of each component can be calculated, using (Equations B-22, B-23, B-24 and B-25)

Equation B-22 components:

$$T_0 s^T = T_0 Cp \ln\left(\frac{T}{T_0}\right) \quad \text{B-22}$$

$$T_0 s_{DA_1}^{T} = x_{DA_1} T_0 \overline{Cp_{DA}} \ln\left(\frac{T_1}{T_0}\right)$$

$$T_0 s_{DA_1}^{T} = 0.8998 \times 298.14 \times 28.97 \times \ln\left(\frac{330.27}{298.14}\right)$$

$$\boldsymbol{T_0 s_{DA_1}^{T} = 795.4\ kJ.kmol_T^{-1}}$$

$$T_0 s_{V_2}^{T} = x_{V_2} T_0 \overline{Cp_V} \ln\left(\frac{T_1}{T_0}\right)$$

$$T_0 s_{V_2}^{T} = 0.0326 \times 298.14 \times 35.59 \times \ln\left(\frac{330.27}{298.14}\right)$$

$$\boldsymbol{T_0 s_{V_2}^{T} = 35.4\ kJ.kmol_T^{-1}}$$

$$T_0 s_{L_1}^{T} = x_{L_1} T_0 \overline{Cp_L} \ln\left(\frac{T_1}{T_0}\right)$$

$$T_0 s_{L_1}^{T} = 0.0228 \times 298.14 \times 75.35 \times \ln\left(\frac{330.27}{298.14}\right)$$

$$\boldsymbol{T_0 s_{L_1}^{T} = 27.1\ kJ.kmol_T^{-1}}$$

$$T_0 s_{S_1}^{T} = x_{S_1} T_0 \overline{Cp_S} \ln\left(\frac{T_1}{T_0}\right)$$

$$T_0 s_{S_1}^{T} = 0.0046 \times 298.14 \times 513.43 \times \ln\left(\frac{330.27}{298.14}\right)$$

$$\boldsymbol{T_0 s_{S_1}^{T} = 71.5\ kJ.kmol_T^{-1}}$$

Equation B-24 components, for this it is necessary to determine the enthalpy associated with the phase change, or Equation B-23. The data required for this are readily found in steam tables.

$$\Delta s_{\Delta V} = s_{SatVap}(T_{DP}) - s_{SatLiq}(T_{DP}) \quad \text{B-23}$$

$$s_{SatVap}(T_{DP}) = 8.236\ kJ.kg^{-1}.K^{-1}$$
$$s_{SatLiq}(T_{DP}) = 0.586\ kJ.kg^{-1}.K^{-1}$$
$$\Delta s_{\Delta V} = 7.650\ kJ.kg^{-1}.K^{-1}$$
$$\overline{\Delta \boldsymbol{s_{\Delta V}}} = \boldsymbol{137.8\ kJ.kmol^{-1}.K^{-1}}$$

Now Equation B-24 can be solved as follows:

$$T_0 s_{\Delta V}^T = T_0 x_{\Delta V}^T \left[\overline{Cp_V} \ln\left(\frac{T_1}{T_{DP}}\right) + \overline{\Delta s_{\Delta V}} + \overline{Cp_L} \ln\left(\frac{T_{DP}}{T_0}\right)\right] \quad \text{B-24}$$

$$T_0 s_{\Delta V}^T = 298.14 \times 0.0513 \times \left[35.59 \times \ln\left(\frac{330.27}{314.18}\right) + 137.8 + 75.35 \times \ln\left(\frac{314.18}{298.14}\right)\right]$$
$$\boldsymbol{T_0 s_{\Delta V}^T = 2,195.4\ kJ.kmol_T^{-1}}$$

Now that the entropy changes of each component have been obtained, the addition of each component gives the total stream enthalpy change associated with temperature change under isobaric conditions. For this step Equation B-25 is used.

$$T_0 s_{TM}^T = T_0 s_{DA_1}^T + T_0 s_{V_2}^T + T_0 s_{L_1}^T + T_0 s_{S_1}^T + T_0 s_{\Delta V}^T \quad \text{B-25}$$

$$T_0 s_{TM}^T = 795.378 + 35.379 + 27.099 + 71.458 + 2{,}195.41$$
$$\boldsymbol{T_0 s_{TM}^T = 3,124.7\ kJ.kmol^{-1}}$$

Similarly the exergy can be calculated with the above results, using Equation B-26, or directly using Equations B-27, B-19, B-24 and B-28.

$$e_{TM}^T = h_{TM}^T - T_0 s_{TM}^T \quad \text{B-26}$$

$$e_{TM}^T = 3{,}349.80 - 3{,}124.73$$
$$\boldsymbol{e_{TM}^T = 225.1\ kJ.kmol^{-1}}$$

$$e_{TM}^T = \overline{Cp}\,(T - T_0) - T_0 \overline{Cp} \ln\left(\frac{T}{T_0}\right) \quad \text{B-27}$$

$$e_{TM}^{T} = x_{\Delta V}\left[\overline{Cp_V}\left[T - T_{DP} - T_0 \ln\left(\frac{T}{T_{DP}}\right)\right] + \overline{Cp_L}\left[T_{DP} - T_0 - T_0 \ln\left(\frac{T_{DP}}{T_0}\right)\right] + \Delta h_{\Delta V} - T_0 \Delta s_{\Delta V}\right] \quad \text{B-28}$$

Now that the temperature based thermo-mechanical exergy has been obtained, the pressure based thermo-mechanical exergy can now be calculated.

Pressure based Thermo-Mechanical Exergy

Again, starting with the isotherm and mass balance of the system. Point 2 data can be found in Table B-13, and the constants can be found in Table B-11.

The dew point temperature is of no consequence here as this is an isothermal calculation; instead, the saturation pressure at the reference temperature is used.

$$P_{V_0}^{Sat} = P_{V_2}^{Sat} = 133.3 \times \exp\left(18.3036 - \frac{3816.44}{T_0 - 44.12}\right) \quad \text{B-8}$$

Therefore

$$P_{V_0}^{Sat} = 3{,}450.5\ Pa$$

If there is a change in pressure in the system, which in this case there is not, the molar fraction of the vapour in the gas phase will change. At lower pressures it will increase, while according to the above calculation, which is only dependant on temperature, the total pressure of the vapour will not.

i.e.

$$\gamma_{V_0}^{Sat} \neq \gamma_{V_2}^{Sat}\ and\ \frac{P_{V_0}^{Sat}}{P_0} \neq \frac{P_{V_2}^{Sat}}{P_2}$$

Therefore

$$P_{V_0}^{Sat} = 3{,}450.5\ Pa$$

And calculate the new $\gamma_{V_0}^{Sat}$

$$\gamma_{V_0}^{Sat} = \frac{P_{V_0}^{Sat}}{P_0} \quad \text{B-9}$$

$$\gamma_{V_0}^{Sat} = \frac{3{,}450.5}{101{,}325}$$

$$\boldsymbol{\gamma_{V_0}^{Sat} = 0.0349}$$

And by using Equation B-10 to solve for the molar flow of water vapour:

$$n_{V_0}^{Sat} = \frac{\gamma_{V_0}^{Sat} n_{DA}}{\left(1 - \gamma_{V_0}^{Sat}\right)} \qquad \text{B-10}$$

$$n_{V_0}^{Sat} = \frac{0.0349 \times 0.7204}{(1 - 0.0349)}$$

$$\boldsymbol{n_{V_0}^{Sat} = 0.0261\ kmol.s^{-1}}$$

Then by a water component balance, Equation B-11:

$$n_{L_0}^{Sat} = n_{V_2} + n_{L_2} - n_{V_0}^{Sat} \qquad \text{B-11}$$

$$n_{L_0}^{Sat} = 0.0672 + 0.0094 - 0.0261$$

$$\boldsymbol{n_{L_0}^{Sat} = 0.0505\ kmol.s^{-1}}$$

Next the initial guess for the pressure of the system at point 0 is made. The saturation pressure is known from the previous calculation, so using it as the starting point for the iteration is suitable.

$$P_{V_0}^{Initial} = P_{V_0}^{Sat} = 3{,}540.53\ Pa$$

Now the iterative part of the calculation begins.

Equation B-13 is used to determine the solids and liquid equilibrium condition.

$$\frac{\gamma_{L_0}}{\gamma_{S_0}} = 2.8481 \times \exp\left[-2.306 \times 10^{-3} \times T_0 \times \ln\left(\frac{P_{V_0}^{Sat}}{P_{V_0}}\right)\right] \qquad \text{B-13}$$

$$\frac{\gamma_{L_0}}{\gamma_{S_0}} = 2.8481 \times \exp\left[-2.306 \times 10^{-3} \times T_0 \times \ln\left(\frac{3{,}540.5}{3{,}540.5}\right)\right]$$

$$\frac{\gamma_{L_0}}{\gamma_{S_0}} = 2.8481$$

After the iteration reaches a stable solution this becomes:

$$\frac{\boldsymbol{\gamma_{L_0}}}{\boldsymbol{\gamma_{S_0}}} = \mathbf{4.8418}$$

Solving for n_{L_2}, this is done with Equation B-14, knowing that the number of moles of solid does not change, $n_{S_0} = n_{S_2}$.

$$n_{L_0} = \frac{\gamma_{L_0}}{\gamma_{S_0}} \times n_{S_0} \qquad \text{B-14}$$

$$n_{L_0} = 2.8481 \times 0.0037$$
$$n_{L_0} = 0.0104\ kmol.s^{-1}$$

After the iteration reaches a stable solution this becomes:

$$\boldsymbol{n_{L_0} = 0.0177\ kmol.s^{-1}}$$

Now solving for n_{V_0} by using a water balance, or Equation B-11.

$$n_{V_0} = n_{V_2} + n_{L_2} - n_{L_0} \qquad \text{B-11}$$

$$n_{V_0} = 0.0672 + 0.0094 - 0.0104$$
$$n_{V_0} = 0.0662\ kmol.s^{-1}$$

After the iteration reaches a stable solution this becomes:

$$\boldsymbol{n_{V_0} = 0.0589\ kmol.s^{-1}}$$

Converting this back into pressure, is done by first finding the gas phase fraction that this molar flow represents, Equation B-15. Knowing that $n_{DA_0} = n_{DA_2}$.

$$\gamma_{V_0} = \frac{n_{V_0}}{\left(n_{V_0} + n_{DA_0}\right)} \qquad \text{B-15}$$

$$\gamma_{V_0} = \frac{0.0662}{(0.0662 + 0.7204)}$$
$$\gamma_{V_0} = 0.0842$$

After the iteration reaches a stable solution this becomes:

$$\boldsymbol{\gamma_{V_0} = 0.0756}$$

Now by simply using Equation B-5 again, the partial pressure of vapour can be determined at this point.

$$P_{V_0} = \gamma_{V_0} P \qquad \text{B-5}$$

$$P_{V_0} = 0.0842 \times 101{,}325$$
$$P_{V_0} = 8{,}527.7\ Pa$$

This new P_{V_0} gets substituted into Equation B-13 and repeats until the system solves.

After the iteration reaches a stable solution this becomes:

$$\boldsymbol{P_{V_0} = 7{,}660.7\ Pa}$$

Now it is necessary to check if this is realistic.

$$\boldsymbol{P_{V_0} = 7{,}660.7\ Pa}$$

$$\boldsymbol{P_{V_0}^{Sat} = 3{,}540.5\ Pa}$$

And:

$$\boldsymbol{n_{V_0}(Isotherm) = 0.0589\ kmol.s^{-1}}$$

$$\boldsymbol{n_{V_0}^{Sat} = 0.0261\ kmol.s^{-1}}$$

Since $n_{V_0}^{Sat}$ is the upper limit of the system, the minimum molar value is taken, as stated by Equation B-16.

$$n_{V_0}(Actual) = \min\left(n_{V_0}(Isotherm), n_{V_0}^{Sat}\right) \qquad \text{B-16}$$

$$\boldsymbol{n_{V_0} = 0.0261\ kmol.s^{-1}}$$

By mass balance, or looking up the value that matches it (Calculated above).

$$\boldsymbol{n_{L_0} = 0.0505\ kmol.s^{-1}}$$

To summarise the results:

Table B-14: Data for Point 0

Raw Stream Properties, Point 0			Calculated Stream Properties, Point 0		
T_0	298.14	K			
P_0	101,325	Pa			
M_{DA_0}	20.87	kg.s^{-1}	n_{DA_0}	0.7204	kmol.s^{-1}
M_{V_0}	0.47	kg.s^{-1}	n_{V_0}	0.0261	kmol.s^{-1}
M_{L_0}	0.91	kg.s^{-1}	n_{L_0}	0.0505	kmol.s^{-1}
M_{S_0}	1.25	kg.s^{-1}	n_{S_0}	0.0037	kmol.s^{-1}
M_T	23.5	kg.s^{-1}	n_T	0.8007	kmol.s^{-1}
Calculated Stream Properties, Point 0			**Calculated Stream Properties, Point 0**		
x_{DA_0}	0.8998	(eq. B-17)	γ_{DA_0}	0.9651	(eq. B-15)
x_{V_0}	0.0326	(eq. B-17)	γ_{V_0}	0.0349	(eq. B-15)
x_{L_0}	0.0631	(eq. B-17)	γ_{L_0}	0.9326	(eq. B-12)
x_{S_0}	0.0046	(eq. B-17)	γ_{S_0}	0.0674	(eq. B-12)

It is clear that there is no change in this pathway for the sample calculation, so this next section is redundant, but is important for systems where there is a change in pressure, so the calculation method for the pressure based exergy will be described.

At this point the component fractions are identified to which Equations B-29, B-34 and B-40 apply, and to which components use Equations B-30, B-35 and B-41 apply, and those to which Equations B-31, B-36, B-32, B-37 and B-42 apply.

Equations B-29, B-34 and B-40 apply to the gas phase components with no change in heat capacity. This step is done by taking the minimum of the values at points 0 and 2.

$n_{DA_0} = n_{DA_2}$	Either one.
$n_{V_0} = n_{V_2}$	Either one.

Equations B-30, B-35 and B-41 apply to the solids and liquid phase components with no change in heat capacity. This calculation is done by taking the minimum of the values of point 0 and point 2.

$n_{L_0} = n_{L_2}$	Either one.
$n_{S_0} = n_{S_2}$	Either one.

The remaining component is designated $n_{\Delta V}$ and is found by a water component balance:

$$n_{\Delta V}^{P} = n_{V_2} - n_{V_0}$$

$$\boldsymbol{n_{\Delta V}^{P} = 0\ kmol.s^{-1}}$$

$$\boldsymbol{x_{\Delta V}^{P} = 0}$$

This component requires the use of Equations B-31, B-36, B-32, B-37 and B-42.

Applying the appropriate formulas to each component

Equation B-29 components:

$$H_{Gas}^{P} = 0 \qquad \text{B-29}$$

$$\boldsymbol{h_{DA_2}^{P} = 0\ kJ.kmol_T^{-1}}$$

$$\boldsymbol{h_{V_2}^{P} = 0\ kJ.kmol_T^{-1}}$$

Equation B-30 components:

$$H_{S\&L}^{P} = V(1 - T_0\beta)(P - P_0) \qquad \text{B-30}$$

$$h_{L_2}^{P} = x_{L_2}\overline{v_L}(1 - T_0\beta_L)(P - P_0)$$
$$h_{L_2}^{P} = 0.063 \times 0.0181 \times (1 - 298.14 \times 0.00021) \times (101{,}325 - 101{,}325)$$
$$\boldsymbol{h_{L_2}^{P} = 0\ kJ.kmol_T^{-1}}$$

$$h_{S_2}^{P} = x_{S_2}\overline{v_S}(1 - T_0\beta_S)(P - P_0)$$
$$h_{L_2}^{P} = 0.0046 \times 0.2237 \times (1 - 298.14 \times 0.0011) \times (101{,}325 - 101{,}325)$$
$$\boldsymbol{h_{L_2}^{P} = 0\ kJ.kmol_T^{-1}}$$

Equation B-32 components: for this it is necessary to do some further calculation, in order to determine the enthalpy associated with the phase change, or Equation B-31. The data required for this calculation are readily found the in steam tables.

$$\Delta h_{\Delta V} = h_{SatVap}(P_V) - h_{SatLiq}(P_V) \qquad \text{B-31}$$

$$h_{SatVap}(P_V) = 2{,}574.78\ kJ.kg^{-1}$$
$$h_{SatLiq}(P_V) = 170.43\ kJ.kg^{-1}$$
$$\Delta h_{\Delta V} = 2{,}404.35\ kJ.kg^{-1}$$
$$\overline{\Delta \boldsymbol{h}_{\Delta \boldsymbol{V}}} = \boldsymbol{43{,}302.3\ kJ.kmol^{-1}}$$

Now Equation B-32 can be solved as follows:

$$h^P_{\Delta V} = x_{\Delta V}\left[\overline{\Delta h_{\Delta V}} + \overline{v_L}(1 - T_0\beta_L)(P - P_0)\right] \quad \text{B-32}$$

$$h^P_{\Delta V} = 0 \times [43{,}302 + 0.0181 \times (1 - 298.14 \times 0.000207) \times (101{,}325 - 101{,}325)]$$
$$\boldsymbol{h^P_{\Delta V} = 0\ kJ.kmol^{-1}_T}$$

Now that the enthalpy changes of each component have been obtained, each of them is added together to get the total stream enthalpy change associated with temperature change under isobaric conditions. For this step Equation B-33 is used.

$$h^P_{TM} = h^P_{DA_2} + h^P_{V_2} + h^P_{L_2} + h^P_{S_2} + h^P_{\Delta V} \quad \text{B-33}$$

$$h^P_{TM} = 0 + 0 + 0 + 0 + 0$$
$$\boldsymbol{h^P_{TM} = 0\ kJ.kmol^{-1}}$$

Using the same system for enthalpy (Equations B-29, B-30, B-32 and B-33), the entropy of each component can be calculated, using (Equations B-34, B-35, B-37 and B-38)

Equation B-34 components:

$$S^P_{Gas} = -n\bar{R}\ln\left(\frac{P}{P_0}\right) \quad \text{B-34}$$

$$T_0 s^P_{DA_2} = -x_{DA_2} T_0 \bar{R}\ln\left(\frac{P_2}{P_0}\right)$$
$$T_0 s^P_{DA_2} = -0.8998 \times 298.14 \times 0.008314 \times \ln\left(\frac{101{,}325}{101{,}325}\right)$$
$$\boldsymbol{T_0 s^P_{DA_2} = 0\ kJ.kmol^{-1}_T}$$

$$T_0 s^P_{V_2} = -x_{V_2} T_0 \bar{R}\ln\left(\frac{P_2}{P_0}\right)$$

$$T_0 s_{V_2}^P = -0.0326 \times 298.14 \times 0.008314 \times \ln\left(\frac{101{,}325}{101{,}325}\right)$$

$$\boldsymbol{T_0 s_{V_2}^P = 0\ kJ.kmol_T^{-1}}$$

Equation B-35 components are:

$$S_{S\&L}^P = -\beta V(P - P_0) \qquad \text{B-35}$$

$$T_0 s_{L_2}^P = -x_{L_2} T_0 \beta_L \overline{v_L}(P_2 - P_0)$$

$$T_0 s_{L_2}^P = -0.0631 \times 298.14 \times 0.000207 \times 0.0181 \times (101{,}325 - 101{,}325)$$

$$\boldsymbol{T_0 s_{L_2}^P = 0\ kJ.kmol_T^{-1}}$$

$$T_0 s_{S_2}^P = -x_{S_1} T_0 \beta_S \overline{v_S}(P_2 - P_0)$$

$$T_0 s_{S_2}^P = -0.0046 \times 298.14 \times 0.001098 \times 0.2237 \times (101{,}325 - 101{,}325)$$

$$\boldsymbol{T_0 s_{S_2}^P = 0\ kJ.kmol_T^{-1}}$$

Equation B-37 components. For this it is necessary to do some more calculation, in order to determine the enthalpy associated with the phase change, or Equation B-36. The data required for this are readily found in steam tables.

$$\Delta s_{evap} = s_{SatVap}(P_V) - s_{SatLiq}(P_V) \qquad \text{B-36}$$

$$s_{SatVap}(P_V) = 8.243\ kJ.kg^{-1}.K^{-1}$$

$$s_{SatLiq}(P_V) = 0.582\ kJ.kg^{-1}.K^{-1}$$

$$\Delta s_{\Delta V} = 7.661\ kJ.kg^{-1}.K^{-1}$$

$$\boldsymbol{\overline{\Delta s_{\Delta V}} = 137.975\ kJ.kmol^{-1}.K^{-1}}$$

Equation B-37 can then be solved.

$$T_0 s_{\Delta V}^P = T_0 x_{\Delta V}\left[-\bar{R}\ln\left(\frac{P}{P_0}\right) + \overline{\Delta s_{\Delta V}} - \overline{v_L}\beta_L(P - P_0)\right] \qquad \text{B-37}$$

$$T_0 s_{\Delta V}^P = 298.14 \times 0 \times \left[-0.008314 \times \ln\left(\frac{101{,}325}{101{,}325}\right) + 137.98 - 0.0181 \times 0.000207 \times (101{,}325 - 101{,}325)\right]$$

$$\boldsymbol{T_0 s_{\Delta V}^P = 0\ kJ.kmol_T^{-1}}$$

Now that the entropy changes of each component have been obtained, simply adding them together to get the total stream enthalpy change associated with temperature change under isobaric conditions is possible. For this step Equation B-38 is used.

$$T_0 s_{TM}^P = T_0 s_{DA_2}^P + T_0 s_{V_2}^P + T_0 s_{L_2}^P + T_0 s_{S_2}^P + T_0 s_{\Delta V}^P \quad \text{B-38}$$

$$T_0 s_{TM}^P = 0 + 0 + 0 + 0 + 0$$

$$\boldsymbol{T_0 s_{TM}^P = 0\ kJ.kmol^{-1}}$$

Similarly, the exergy can be calculated with the above results, using Equation B-39 or directly using Equations B-40, B-41, B-31, B-36 and B-42.

$$e_{TM}^P = h_{TM}^P - T_0 s_{TM}^P \quad \text{B-39}$$

$$e_{TM}^P = 0 - 0$$

$$\boldsymbol{e_{TM}^{TP} = 0\ kJ.kmol^{-1}}$$

$$e_{TM_{Gas}}^P = \bar{R} T_0 \ln\left(\frac{P}{P_0}\right) \quad \text{B-40}$$

$$e_{TM_{S\&L}}^P = \overline{v_{Ave}}(P - P_0) \quad \text{B-41}$$

$$e_{TM}^P = x_{\Delta V}\left[T_0 \bar{R} \ln\left(\frac{P}{P_0}\right) + \overline{\Delta h_{\Delta V}} - \overline{\Delta s_{\Delta V}} + \overline{v_L}(P - P_0)\right] \quad \text{B-42}$$

Chemical Exergy

Start with the isotherm and mass balance of the system. Point 0 data can be found in Table B-14 and the constants can be found in Table B-11.

The considerations that need to be reviewed first are:

- What restrictions does the system have to work with?

- Exergy is considered the maximum work potential, therefore, there is no resistance to changes. Therefore, the assumption that the water vapour disperses faster than the water evaporates under isothermal and isobaric conditions is suitable.

- What basis is to be used for the diffusion coefficient?
    - The basis will be to treat the mass transfer component as part of the final phase and adding the exergy of the change separately.

If there is a change of pressure in the system, which in this case there is not, the molar fraction of the vapour in the gas phase will change. At lower pressures, it will increase, while according to the above calculation, which is only dependant on temperature, the total pressure of the vapour will not increase.

i.e.

$$\gamma_{V_A}^{Sat} = \gamma_{V_0}^{Sat} \; and \; \frac{P_{V_A}^{Sat}}{P_{00}} = \frac{P_{V_0}^{Sat}}{P_0}$$

This value is the same as the result from the pressure-based exergy section.

$$\boldsymbol{\gamma_{V_A}^{Sat} = 0.0349}$$
$$\boldsymbol{n_{V_A}^{Sat} = 0.0261 \; kmol.s^{-1}}$$
$$\boldsymbol{n_{L_A}^{Sat} = 0.0505 \; kmol.s^{-1}}$$

Next the final vapour pressure of the system needs to be calculated, P_{00}. This calculation uses a constant value of the dead-state phase fraction of the water vapour defined earlier.

$$P_{V_{00}} = \gamma_{V_{00}} P_{00} \qquad \text{B-5}$$

$$P_{V_{00}} = 0.0913 \times 101{,}325$$
$$\boldsymbol{P_{V_{00}} = 968.3 \; Pa}$$

Using Equation B-13, the solid and liquid equilibrium compositions at the dead state can be determined.

$$\frac{\gamma_{L_{00}}}{\gamma_{S_{00}}} = 2.8481 \times \exp\left[-2.306 \times 10^{-3} \times T_0 \times \ln\left(\frac{P_{V_{00}}^{Sat}}{P_{V_{00}}}\right)\right] \quad \text{B-13}$$

$$\frac{\gamma_{L_{00}}}{\gamma_{S_{00}}} = 2.8481 \times \exp\left[-2.306 \times 10^{-3} \times T_0 \times \ln\left(\frac{3{,}540.5}{968.3}\right)\right]$$

$$\boldsymbol{\frac{\gamma_{L_{00}}}{\gamma_{S_{00}}} = 1.1680}$$

Next solving for n_{L_2} using Equation B-14. Noting that the number of moles of solid does not change, the calculation gives $n_{S_{00}} = n_{S_0}$.

$$n_{L_{00}} = \frac{\gamma_{L_{00}}}{\gamma_{S_{00}}} \times n_{S_{00}} \quad \text{B-14}$$

$$\boldsymbol{n_{L_{00}} = 0.0043\ kmol.s^{-1}}$$

n_{V_A} can then be found by using a water balance, Equation B-11.

$$n_{V_A} = n_{V_0} + n_{L_0} - n_{L_{00}} \quad \text{B-11}$$

$$n_{V_A} = 0.0261 + 0.0505 - 0.0043$$

$$\boldsymbol{n_{V_A} = 0.0723\ kmol.s^{-1}}$$

To summarise the results:

Table B-15: Data for Point A

Raw Stream Properties, Point A			**Calculated Stream Properties, Point A**		
T_0	298.14	K			
P_0	101,325	Pa			
M_{DA_A}	20.87	kg.s^{-1}	n_{DA_A}	0.7204	kmol.s^{-1}
M_{V_A}	1.30	kg.s^{-1}	n_{V_A}	0.0723	kmol.s^{-1}
M_{L_A}	0.08	kg.s^{-1}	$n_{L_{00}}$	0.0043	kmol.s^{-1}
M_{S_A}	1.25	kg.s^{-1}	$n_{S_{00}}$	0.0037	kmol.s^{-1}
M_T	23.5	kg.s^{-1}	n_T	0.8007	kmol.s^{-1}
Calculated Stream Properties, Point A			**Calculated Stream Properties, Point A**		
x_{DA_A}	0.8998	(eq. B-17)	γ_{DA_A}	0.9087	(eq. B-15)
x_{V_A}	0.0903	(eq. B-17)	γ_{V_A}	0.0913	(eq. B-15)
x_{L_A}	0.0053	(eq. B-17)	γ_{L_A}	0.5387	(eq. B-12)
x_{S_A}	0.0046	(eq. B-17)	γ_{S_A}	0.4613	(eq. B-12)

It is clear that the only change that has occurred here is that some of the water has vaporised isothermally, and isobarically. The energies involved in such a process need to be determined in order to completely account for the work or lost work of the system. In order

to determine the enthalpy associated with the phase change, Equation B-31, the data required for these calculations are readily found in steam tables.

$$\Delta h_{\Delta V} = h_{SatVap}(P_V) - h_{SatLiq}(P_V) \quad \text{B-31}$$

$$h_{SatVap}(P_V) = 2{,}512.82\ kJ.kg^{-1}$$
$$h_{SatLiq}(P_V) = 27.33\ kJ.kg^{-1}$$
$$\Delta h_{\Delta V} = 2{,}485.49\ kJ.kg^{-1}$$
$$\overline{\Delta \boldsymbol{h_{\Delta V}}} = \boldsymbol{44{,}763.68\ kJ.kmol^{-1}}$$

Solving Equation B-43:

$$h_{\Delta V_A}^{CH} = x_{\Delta V_A}\left[\overline{\Delta h_{\Delta V}} + \overline{v_L}(1 - T_0\beta_L)(P - P_0)\right] \quad \text{B-43}$$

Since there is no change in overall pressure, this calculation simply becomes:

$$h_{\Delta V_A}^{CH} = x_{\Delta V_A}\overline{\Delta h_{\Delta V}}$$
$$h_{\Delta V_A}^{CH} = (0.0326 - 0.0903) \times 44{,}763.7$$
$$\boldsymbol{h_{\Delta V_A}^{CH} = -2{,}583\ kJ.kmol_T^{-1}}$$

Similarly, to determine the enthalpy associated with the phase change, Equation B-36, the data required for this calculation are readily found in steam tables.

$$\Delta s_{\Delta V} = s_{SatVap}(P_V) - s_{SatLiq}(P_V) \quad \text{B-36}$$

$$s_{SatVap}(P_V) = 8.987\ kJ.kg^{-1}.K^{-1}$$
$$s_{SatLiq}(P_V) = 0.099\ kJ.kg^{-1}.K^{-1}$$
$$\Delta s_{\Delta V} = 8.888\ kJ.kg^{-1}.K^{-1}$$
$$\overline{\Delta \boldsymbol{s_{\Delta V}}} = \boldsymbol{160.1\ kJ.kmol^{-1}.K^{-1}}$$

Solving Equation B-44 gives:

$$T_0 s_{\Delta V_A}^{CH} = T_0 x_{\Delta V}\left[-\bar{R}\ln\left(\frac{P}{P_0}\right) + \overline{\Delta s_{\Delta V}} - \overline{v_L}\beta_L(P - P_0)\right] \quad \text{B-44}$$
$$T_0 s_{\Delta V_A}^{CH} = T_0 x_{\Delta V_A}\overline{\Delta s_{\Delta V}}$$

$$T_0 s_{\Delta V_A}^{CH} = 298.14 \times (0.0326 - 0.0903) \times 160.1$$
$$\boldsymbol{T_0 s_{\Delta V_A}^{CH} = -2{,}754.15\ kJ.kmol_T^{-1}}$$

Similarly the exergy can be calculated with the above results, using Equation B-45.

$$e_{\Delta V_A}^{CH} = h_{\Delta V_A}^{CH} - T_0 s_{\Delta V_A}^{CH} \quad \text{B-45}$$

$$e_{\Delta V_A}^{CH} = -2{,}583 \; - -2{,}754$$

$$\boldsymbol{e_{\Delta V_A}^{CH} = 171.3\ kJ.kmol^{-1}}$$

The final part of the calculation is the most detailed, which is because the components at Point A can diffuse and come into complete equilibrium with the environment. This diffusion has a driving force and can potentially generate work, thus it contains exergy.

The procedure is carried out by taking each individual component and changing its partial pressure, or concentration, between the two states (Points A and 00) while maintaining the composition of the other components. This calculation can be written as Equation B-46.

$$e^{CH} = \sum_{i=0}^{\infty} \left(\mu_{i_0} - \mu_{i_{00}}\right)_{T_0,P_0} x_{i_A} \quad \text{B-46}$$

Since the liquid and solids components have been taken to a point of equilibrium with the environment, and each other. The need to determine what the diffusion, or mixing, exergy is for the gas phase is required. This procedure can be done using Equation B-47.

$$e_{i_{Gas}}^{CH} = T_0 \bar{R} x_{i_A} \ln\left(\frac{\gamma_{i_A}}{\gamma_{i_{00}}}\right) \quad \text{B-47}$$

Recalling the data required to solve Equation B-47, shown in Table B-16.

Table B-16: The Data required to solve the remaining Chemical exergy

Raw Stream Properties, Point A			Raw Stream Properties, Point 00		
T_0	298.14	K	T_{00}	298.14	K
x_{DA_A}	0.8998				
x_{V_A}	0.0903				
γ_{DA_A}	0.9087		$\gamma_{DA_{00}}$	0.9904	
γ_{V_A}	0.0913		$\gamma_{V_{00}}$	0.0096	
$\bar{R}$	0.008314	kJ.kmol^{-1}.K^{-1}			

Solving for the dry air component gives:

$$e_{DA}^{CH} = T_0 \bar{R} x_{DA_A} \ln\left(\frac{\gamma_{DA_A}}{\gamma_{DA_{00}}}\right)$$

$$e_{DA}^{CH} = 298.14 \times 0.008314 \times 0.8998 \times \ln\left(\frac{0.9087}{0.9904}\right)$$

$$\boldsymbol{e_{DA}^{CH} = -0.1920\ kJ.kmol^{-1}}$$

And for the vapour, the solution is:

$$e_V^{CH} = T_0 \bar{R} x_{V_A} \ln\left(\frac{\gamma_{V_A}}{\gamma_{V_{00}}}\right)$$

$$e_V^{CH} = 298.14 \times 0.008314 \times 0.0903 \times \ln\left(\frac{0.0913}{0.0096}\right)$$

$$\boldsymbol{e_V^{CH} = 0.5053\ kJ.kmol^{-1}}$$

Now, utilising Equation B-48.

$$e^{CH} = e_{DA}^{CH} + e_V^{CH} + e_L^{CH} + e_S^{CH} + e_{\Delta V_A}^{CH} \qquad \text{B-48}$$

$$e^{CH} = e_{DA}^{CH} + e_V^{CH} + 0 + 0 + e_{\Delta V_A}^{CH}$$

$$e^{CH} = -0.1920 + 0.5053 \pm 7.672$$

$$\boldsymbol{e^{CH} = -7.3589\ kJ.kmol^{-1}}$$

Quality Factor

Now that all of the exergy components have been determined, it is possible to determine the quality factor for the calculated point in the system. Equations B-49, B-50 and B-51 may be used to complete this calculation.

$$h = h_{TM}^{T} + h_{TM}^{P} + h_{\Delta V_A}^{CH} \qquad \text{B-49}$$

$$h = 3{,}350 + 0 + (-2{,}583)$$

$$\boldsymbol{h = 767\ kJ.kmol^{-1}}$$

$$e = e_{TM}^{T} + e_{TM}^{P} + e^{CH} \qquad \text{B-50}$$

$$e = 225.1 + 0 + (-7.3589)$$

$$\boldsymbol{e = 217.7\ kJ.kmol^{-1}}$$

$$\Omega = \frac{e}{h} \qquad \text{B-51}$$

$$\Omega = \frac{217.7}{767}$$

$$\boldsymbol{\Omega = 0.284}$$

Values of Omega (Ω) are representative of exergy quality. This must be a number between 0 and 1 for systems that have a driving force to the ambient conditions. If the number is negative, or greater than 1, work must be done on the system, and no useful work can be extracted from the system [39, 98].

9.8Appendix D Sample Calculations of Carious Factors

9.8.1Calculation data

Data used:

Base Values			Molar Masses		
Label	**Value**	**Units**	**Label**	**Value**	**Units**
T_{00}	298.15	K	mm_{DA}	28.858	kg.kmol^{-1}
T_{00}	25	C	mm_V	18.015	kg.kmol^{-1}
P_{00}	101325	Pa	mm_L	18.015	kg.kmol^{-1}
P_{00}	1.01325	Bar	mm_S	342.290	kg.kmol^{-1}
$P_{v_0}^{sat}$	0.03170	Bar	mm_{fuel}	16.042	kg.kmol^{-1}
RH_{00}	27	%	mm_{O_2}	31.999	kg.kmol^{-1}
$\gamma_{DA_{00}}$	0.9785		mm_{N_2}	28.013	kg.kmol^{-1}
$\gamma_{V_{00}}$	0.022		mm_{CO_2}	44.010	kg.kmol^{-1}
$\overline{v_L}$	0.0181	m^3.kmol^{-1}			
$\overline{v_S}$	0.2237	m^3.kmol^{-1}	$\overline{\Delta h_{\Delta V@T_0}}$	43,987	kJ.kmol^{-1}
β_L	0.00021	K^{-1}	$\overline{T_0 \Delta s_{\Delta V@T_0}}$	43,987	kJ.kmol^{-1}
β_S	0.0011	K^{-1} [103]	$\overline{\Delta h_{\Delta V@T_S^{IN}}}$	42,474	kJ.kmol^{-1}
R	8.31446	kJ.kgmol^{-1}.K^{-1}	$\overline{T_0 \Delta s_{\Delta V@T_S^{IN}}}$	38,013	kJ.kmol^{-1}
$\Delta T_{Dryer_{out}}$	20	C			
Cp Values (mass)			**Cp Values (mol)**		
Cp_{DA}	1.011	kJ.kg^{-1}.K^{-1}	$\overline{Cp_{DA}}$	29.189	kJ.kmol^{-1}.K^{-1}
Cp_V	2.000	kJ.kg^{-1}.K^{-1}	$\overline{Cp_V}$	36.030	kJ.kmol^{-1}.K^{-1}
Cp_L	4.180	kJ.kg^{-1}.K^{-1}	$\overline{Cp_L}$	75.303	kJ.kmol^{-1}.K^{-1}
Cp_S	1.500	kJ.kg^{-1}.K^{-1}	$\overline{Cp_S}$	513.435	kJ.kmol^{-1}.K^{-1}
Cp_{fuel}	2.226	kJ.kg^{-1}.K^{-1}	$\overline{Cp_{fuel}}$	35.711	kJ.kmol^{-1}.K^{-1}
Cp_{O_2}	0.918	kJ.kg^{-1}.K^{-1}	$\overline{Cp_{O_2}}$	29.375	kJ.kmol^{-1}.K^{-1}
Cp_{N_2}	1.040	kJ.kg^{-1}.K^{-1}	$\overline{Cp_{N_2}}$	29.134	kJ.kmol^{-1}.K^{-1}
Cp_{CO_2}	0.846	kJ.kg^{-1}.K^{-1}	$\overline{Cp_{CO_2}}$	37.232	kJ.kmol^{-1}.K^{-1}

Dryer Initial Conditions		
$\dot{m_{G_{IN}}}$	21	$kg.s^{-1}$
Y_{IN}	0.006	$kg_W.kg_{DA}^{-1}$
$Y_{IN.n}$	0.010	$mol_W.mol_{DA}^{-1}$
$\dot{m_{S_{IN}}}$	2.5	$kg.s^{-1}$
X_{IN}	1	$kg_W.kg_S^{-1}$
$X_{IN.n}$	19.00	$mol_W.mol_S^{-1}$
$\dot{n_{DA_{IN}}}$	0.72	$kmol.s^{-1}$
$\dot{n_{S_{IN}}}$	0.0037	$kmol.s^{-1}$
$T_{G_{IN}}$	190	C
$T_{G_{IN}}$	463.15	K
$T_{S_{IN}}$	60	C
$T_{S_{IN}}$	333.15	K

9.8.2Calculations

Gas side energy and exergy

The following calculations belongs to the results shown on page Energy flows

Case 0 on page 167.

$$H_{G_{IN}} = n_{DA_{IN}}\overline{Cp_{DA}}(T - T_0) + n_{V_{IN}}\left[\overline{Cp_V}(T - T_0) + \overline{\Delta h_{\Delta V@T_0}}\right] \quad \text{2-31}$$

$$= n_{DA_{IN}}\left(\overline{Cp_{DA}}(T - T_0) + Y_{IN.n}\left(\overline{Cp_V}(T - T_0) + \overline{\Delta h_{\Delta V@T_0}}\right)\right) \quad \text{2-32}$$

$$= 0.72\big(29.189(463.15 - 298.15) + 0.010(36.030(463.15 - 298.15) + 43{,}987)\big)$$

$$= kmol.s^{-1}\big(kJ.kmol^{-1}.K^{-1}K + kmol_W.kmol_{DA}^{-1}(kJ.kmol^{-1}.K^{-1}K + kJ.kmol^{-1})\big)$$

$$= 3{,}525\ kW$$

$$Ex_{G_{IN}} = \dot{n_{G_{IN}}}\left((h-h_0) - T_0(s-s_0) + \sum_{i=0}^{inf}(\mu_i - \mu_0)x_i\right) \quad \text{2-30, 2-39, 2-40}$$

$$= \dot{n_{DA_{IN}}}\overline{Cp_{DA}}(T-T_0) + \dot{n_{V_{IN}}}\left[\overline{Cp_V}(T-T_0) + \overline{\Delta h_{\Delta V@T_0}}\right]$$
$$- T_0\dot{n_{DA_{IN}}}\overline{Cp_{DA}}\ln\left(\frac{T}{T_0}\right) - T_0\dot{n_{V_{IN}}}\left[\overline{Cp_V}\ln\left(\frac{T}{T_0}\right) + \overline{\Delta s_{\Delta V@T_0}}\right]$$

$$= n_{DA_{IN}}\left(\overline{Cp_{DA}}\left(T - T_0\left(1+\ln\left(\frac{T}{T_0}\right)\right)\right)\right.$$
$$\left. + Y_{IN.n}\left(\overline{Cp_V}\left(T - T_0\left(1+\ln\left(\frac{T}{T_0}\right)\right)\right) + \overline{\Delta h_{\Delta V@T_0}} - T_0\overline{\Delta s_{\Delta V@T_0}}\right)\right)$$

$$= 0.72\left(29.189\left(463.15 - 298.15\left(1+\ln\left(\frac{463.15}{298.15}\right)\right)\right)\right.$$
$$+ 0.010\left(36.030\left(463.15 - 298.15\left(1+\ln\left(\frac{463.15}{298.15}\right)\right)\right)\right.$$
$$\left.\left. + 43{,}987 - 43{,}987\right)\right)$$

$$= kmol.s^{-1}\big(kJ.kmol^{-1}.K^{-1}K$$
$$+ kmol_W.kmol_{DA}^{-1}(kJ.kmol^{-1}.K^{-1}K + kJ.kmol^{-1}$$
$$- kJ.kmol^{-1})\big)$$

$$= 0.72\big(29.189(33.6786)$$
$$+ 0.010(36.030(33.6786) + 43{,}987 - 43{,}987)\big)$$

$$= 719.5\ kW$$

NOTE B-19: The chemical potential has been ignored, and the effect or Pressure on exergy has also been ignored as the pressure is at the dead state pressure.

Evaporation Calculations

$$\dot{n_{\Delta V.act}} = 1.099\ kg.s^{-1}; 0.061\ kmol.s^{-1}$$

Calculated using a mass and energy balance with iteration,

$$\dot{n_{\Delta V.pot_Q}} = \frac{\dot{n_{G_{IN}}}\overline{Cp_G}(T_G^{IN} - T_S^{IN})}{\Delta H_{\Delta V@T_S^{IN}}}$$

$$= \frac{n_{DA}(Cp_{DA} + Y_{IN.n}Cp_V)(T_G^{IN} - T_S^{IN})}{\Delta H_{\Delta V@T_S^{IN}}}$$

$$= \frac{0.72(29.189 + 0.010 \times 36.030)(463.15 - 333.15)}{42{,}474}$$

$$= \frac{kmol.s^{-1}(kJ.kmol^{-1}.K^{-1} + kmol_W.kmol_{DA}^{-1}.kJ.kmol^{-1}.K^{-1})(}{kJ.kmol^{-1}}$$

$$= 0.06535\ kmol.s^{-1}$$

$$m_{\Delta V.\dot{pot}_{Ex}} = \frac{m_{G_{IN}}^{\cdot}\overline{Cp_G}\left(T_G^{IN} - T_S^{IN} - T_0 \ln\left(\frac{T_G^{IN}}{T_S^{IN}}\right)\right)}{\Delta H_{\Delta V@T_S^{IN}} - T_0\Delta S_{\Delta V@T_S^{IN}}}$$

$$= \frac{n_{DA}(Cp_{DA} + Y_{IN.n}Cp_V)\left(T_G^{IN} - T_S^{IN} - T_0 \ln\left(\frac{T_G^{IN}}{T_S^{IN}}\right)\right)}{\Delta H_{\Delta V@T_S^{IN}} - T_0\Delta S_{\Delta V@T_S^{IN}}}$$

$$= \frac{0.72(29.189 + 0.010 \times 36.030)\ \left(463.15 - 333.15 - 273.15 \ln\left(\right.\right.}{42{,}474 - 38{,}013}$$

$$= \frac{0.72(29.189 + 0.010 \times 36.030)\ (40.009)}{4{,}461}$$

$$= \frac{kmol.s^{-1}(kJ.kmol^{-1}.K^{-1} + kmol_W.kmol_{DA}^{-1}.kJ.kmol^{-1}.K^{-1})(}{kJ.kmol^{-1}}$$

$$= 0.1521\ kmol.s^{-1}$$

$$\eta_{\Delta V.H_{G.IN}} = \frac{n_{\Delta V.act}^{\cdot}}{n_{\Delta V.\dot{pot}_Q}}$$

$$= \frac{0.0610}{0.06535} = \mathbf{79}\%$$

$$\eta_{\Delta V.Ex_{G.IN}^{TM}} = \frac{n_{\Delta V.act}^{\cdot}}{n_{\Delta V.\dot{pot}_{Ex}}}$$

$$= \frac{0.0610}{0.1521} = \mathbf{41}\%$$

9.9Appendix E Visual Basic Code for MSExcel Modelling of a dryer

PLEASE NOTE: any reference to 'water97_v13' refers to an excel steam table addon found freely on the web (https://www.cheresources.com/invision/files/file/34-thermodynamic-and-transport-properties-of-water-and-steam/).

```
Public Const T_conv As Double = 273.14     'add to C, subtract from K
Public Const P_conv As Double = 100000     'multiply bar, divide Pa
Public Const T_00 As Double = 298.15       'K=25oC
Public Const P_00 As Double = 1.01325      'Bar=1atm
Public Const mf0_O2 As Double = 0.209818117126608     'Bar partial pressure
Public Const mf0_N2 As Double = 0.789682255754957     'Bar partial pressure
Public Const mf0_CO2 As Double = 4.99627118435682E-04  'Bar partial pressure
Public Const mf0_H2O As Double = 0.0095205709     'Bar partial pressure

Public Const mm_DA As Double = 28.858      'kg.kmol-1
Public Const mm_W As Double = 18.015       'kg.kmol-1
Public Const mm_S As Double = 342.29       'kg.kmol-1
Public Const mm_o2 As Double = 31.9988     'kg.kmol-1
Public Const mm_n2 As Double = 28.01348    'kg.kmol-1
Public Const mm_co2 As Double = 44.0098    'kg.kmol-1
Public Const mm_F As Double = 16.04246     'kg.kmol-1

Public Const Cpa As Double = 1.011         'kJ.kg-1.K-1
Public Const Cpl As Double = 4.18276       'kJ.kg-1.K-1
Public Const Cps As Double = 1.5           'kJ.kg-1.K-1
Public Const Cpv As Double = 2             'kJ.kg-1.K-1
Public Const cpo2 As Double = 0.918        'kJ/kg.K@300K
      http://www.engineeringtoolbox.com/oxygen-d_978.html
Public Const cpn2 As Double = 1.04         'kJ/kg.K@300K
      http://www.engineeringtoolbox.com/nitrogen-d_977.html
Public Const cpco2 As Double = 0.846       'kJ/kg.K@300K
      http://www.engineeringtoolbox.com/carbon-dioxide-d_974.html
```

```
Public Const cpf As Double = 2.226        'kJ/kg.K@300K
      http://www.engineeringtoolbox.com/methane-d_980.html
Public Const Ta As Double = 190           'oC
Public Const Ts As Double = 60            'oC
Public Const R As Double = 8.31446        'kJ.kgmol-1.K-1

Public Const Cp_DA As Double = mm_DA * Cpa      'kJ.kmol-1.K-1
Public Const Cp_V As Double = mm_W * Cpv        'kJ.kmol-1.K-1
Public Const Cp_L As Double = mm_W * Cpl        'kJ.kmol-1.K-1
Public Const Cp_S As Double = mm_S * Cps        'kJ.kmol-1.K-1
Public Const Cp_o2 As Double = mm_o2 * cpo2     'kJ.kmol-1.K-1@300K
Public Const Cp_n2 As Double = mm_n2 * cpn2     'kJ.kmol-1.K-1@300K
Public Const Cp_co2 As Double = mm_co2 * cpco2  'kJ.kmol-1.K-1@300K
Public Const Cp_f As Double = mm_F * cpf        'kJ.kmol-1.K-1@300K
Public Const k_air As Double = 1.4              'from compressor power sheet

Public Const spec_v_L As Double = 0.0181   'm3.kmol-1
Public Const spec_v_S As Double = 0.2237   'm3.kmol-1
Public Const Th_exp_L As Double = 0.00021  'K-1
Public Const Th_exp_S As Double = 0.0011   'K-1 [29] p709-710

Public Const HHV_S_raw As Double = 18640    'kJ.kg-1 *Using Formulae
Public Const HHV_f_raw As Double = 58780    'kJ.kg-1 *Using Formulae
' *HHV=341C+1,323H+68S-15.3A-120(O+N)
' ^^b=1.047+0.0154H/C+0.0562O/C+0.5904N/C(1-0.175H/C)
Public Const ExCh_S_raw As Double = 15933 '20126   'kJ.kg-1 ^^Using Formulae (b*LHV)
Public Const ExCh_f_raw As Double = 58332 '59545   'kJ.kg-1 ^^Using Formulae (b*LHV)

Public Const HHV_S As Double = HHV_S_raw * mm_S     'kJ.kmol-1
Public Const HHV_f As Double = HHV_f_raw * mm_F     'kJ.kmol-1

Public Const ExCh_S As Double = ExCh_S_raw * mm_S   'kJ.kmol-1
```

```
Public Const ExCh_f As Double = ExCh_f_raw * mm_F   'kJ.kmol-1
Function Tdp(p, n_da, n_wt)                 'dew point temperature calculation
   If n_da + n_wt = 0 Then
      Tdp = T_00 + 100
   ElseIf n_wt = 0 Then
      Tdp = T_00
   Else
      Tdp = water97_v13.tSatW(p * n_wt / (n_da + n_wt))
   End If
End Function
Function pp_w_max(t)                        'saturation partial pressure at temperature
   If t < T_00 Then
      pp_w_max = water97_v13.pSatW(T_00)
   Else
      pp_w_max = water97_v13.pSatW(t)
   End If
End Function
Function isoSkimMilk(t, p, n_da, n_wt, n_s)     'the isotherm limit for skim milk if solids
      present
Dim pp, pp_sat, n_vcalc As Double
   n_vcalc = n_v(t, p, n_da, n_wt, n_s)

   pp_sat = pp_w_max(t)
   If n_da = 0 Then
      pp = p
   ElseIf pp = pp_sat Then
      pp = pp_sat
   Else
      pp = n_v(t, p, n_da, n_wt, n_s) / (n_da + n_v(t, p, n_da, n_wt, n_s)) * p
   End If
   isoSkimMilk = 2.8481 * Exp(-0.002306 * t * WorksheetFunction.ImLn(pp_sat / pp))
End Function
```

```
Function n_v_iso(t, p, n_da, n_wt, n_s)        'isothermal vapour maximum
   If n_s = 0 Then
      n_v_iso = n_wt
   Else
      n_v_iso = n_wt - n_s * isoSkimMilk(t, p, n_da, n_wt, n_s)
   End If
   If n_v_iso < 0 Then
      n_v_iso = 0
   End If
End Function
Function n_v(t, p, n_da, n_wt, n_s)            'maximum n_V at point T,P
Dim n_vset, n_viso, pp_w, pp_wsat, t_dp, n_Vsat As Double
   If p = 0 Then
      p = P_00
   End If
   pp_wsat = pp_w_max(t)
   n_v = n_wt
   If n_da + n_v = 0 Then
      pp_w = p
      t_dp = 373.15
   Else
      pp_w = n_v / (n_da + n_v) * p
      t_dp = Tdp(p, n_da, n_wt)
   End If
   Select Case n_da = 0
      Case True
      Select Case n_s = 0
         Case True
            Select Case t > t_dp
               Case True
                  n_v = n_wt
               Case False
```

```
            n_v = 0
        End Select
    Case False
        Select Case t < t_dp
            Case True
                n_v = 0
            Case False
                n_v = n_wt
        End Select
    End Select
Case False
If pp_wsat > p Then
    n_Vsat = n_wt
Else
    n_Vsat = n_da * pp_wsat / (p - pp_wsat)
End If
n_viso = n_wt + 1
Select Case n_s = 0
    Case True
        Select Case t > t_dp
            Case True
                n_v = n_wt
            Case False
                n_v = n_Vsat
        End Select
    Case False
        Select Case t > t_dp
            Case True
            If n_wt = 0 Then
                n_v = 0
            Else
                Count = 0
```

```
                While n_viso <> n_v And Count < 20
                  'n_viso = n_v_iso(t, p, n_da, n_wt, n_s)
                  n_viso = (n_wt - n_s * 2.8481 * Exp(-2.306 * 10 ^ -3 * t *
    WorksheetFunction.Ln(pp_wsat / (p * n_v / (n_v + n_da)))))
                  n_v = (n_wt - n_s * 2.8481 * Exp(-2.306 * 10 ^ -3 * t *
    WorksheetFunction.Ln(pp_wsat / (p * n_viso / (n_viso + n_da)))))
                  Count = Count + 1
                Wend
                n_v = WorksheetFunction.Min(n_wt, n_viso, n_Vsat)
              End If
              Case False
                n_v = WorksheetFunction.Min(n_wt, n_Vsat)
            End Select
          End Select
        End Select
      If n_v > n_wt Then
        n_v = n_wt
      ElseIf n_v <= 0 Then
        n_v = 0
      End If
End Function
Function n_l(t, p, n_da, n_wt, n_s)          'n_L at point T,P by water balance
    n_l = n_wt - n_v(t, p, n_da, n_wt, n_s)
End Function
'POINT SPECIFIC VARIABLES, Hsatvap(T), Hsatliq(T), T0Ssatvap(T), T0Ssatliq(T), H(T), T0S(T)
Function Hsv_T(t, p, n_da, n_wt)          'POINT SPECIFIC VARIABLES, Hsatvapw(T)
    Hsv_T = water97_v13.enthalpySatVapTW(t) * mm_W
End Function
Function Hsl_T(t, p, n_da, n_wt)          'POINT SPECIFIC VARIABLES, Hsatliqw(T)
    Hsl_T = water97_v13.enthalpySatLiqTW(t) * mm_W
End Function
Function TSsv_T(t, p, n_da, n_wt)          'POINT SPECIFIC VARIABLES, T0Ssatvapw(T)
```

```
   TSsv_T = water97_v13.entropySatVapTW(t) * mm_W * T_00
End Function
Function TSsl_T(t, p, n_da, n_wt)          'POINT SPECIFIC VARIABLES, T0Ssatliqw(T)
   TSsl_T = water97_v13.entropySatLiqTW(t) * mm_W * T_00
End Function
Function Hw(t, p, n_da, n_wt)              'POINT SPECIFIC VARIABLES, Hw(T)
Dim pp, pp_sat As Double
   pp_sat = pp_w_max(t)
   pp = pp_sat
   If n_da = 0 Then
      pp = p
   Else
      If pp > (p * n_wt / (n_da + n_wt)) Then
         pp = p * n_wt / (n_da + n_wt)
      End If
   End If
   Hw = water97_v13.enthalpyW(t, pp) * mm_W
End Function
Function TSw(t, p, n_da, n_wt)             'POINT SPECIFIC VARIABLES, T0Sw(T)
Dim pp, pp_sat As Double
   pp_sat = pp_w_max(t)
   pp = pp_sat
   If n_da = 0 Then
      pp = p
   End If
   If pp > (p * n_wt / (n_da + n_wt)) Then
         pp = p * n_wt / (n_da + n_wt)
   End If
   TSw = water97_v13.entropyW(t, pp) * mm_W * T_00
End Function
'ENTHALPY OF THE SYSTEM CALCULATION
Function H_W(t, p, n_da, n_wt, n_s)        'saturated water enthalpy
```

```
    If t > Tdp(p, n_da, n_wt) Then
        H_W = Hw(t, p, n_da, n_wt) * n_wt
    Else
        H_W = Hsv_T(t, p, n_da, n_wt) * n_v(t, p, n_da, n_wt, n_s) + Hsl_T(t, p, n_da, n_wt) *
        n_l(t, p, n_da, n_wt, n_s)
    End If
    If T_00 > Tdp(P_00, n_da, n_wt) Then
        H_W = H_W - Hw(T_00, P_00, n_da, n_wt) * n_wt + n_v(T_00, P_00, n_da, n_wt, n_s) *
        (Hsv_T(T_00, P_00, n_da, n_wt) - Hsl_T(T_00, P_00, n_da, n_wt))
    Else
        H_W = H_W - (Hsv_T(T_00, P_00, n_da, n_wt) * n_v(T_00, P_00, n_da, n_wt, n_s) +
        Hsl_T(T_00, P_00, n_da, n_wt) * n_l(T_00, P_00, n_da, n_wt, n_s)) + n_v(T_00, P_00,
        n_da, n_wt, n_s) * (Hsv_T(T_00, P_00, n_da, n_wt) - Hsl_T(T_00, P_00, n_da, n_wt))
    End If
End Function
'ENTROPY OF THE SYSTEM CALCULATION
Function TS_W(t, p, n_da, n_wt, n_s)      'saturated water entropy
    If t > Tdp(p, n_da, n_wt) Then
        TS_W = TSw(t, p, n_da, n_wt) * n_wt
    Else
        TS_W = TSsv_T(t, p, n_da, n_wt) * n_v(t, p, n_da, n_wt, n_s) + TSsl_T(t, p, n_da, n_wt) *
        n_l(t, p, n_da, n_wt, n_s)
    End If
    If T_00 > Tdp(P_00, n_da, n_wt) Then
        TS_W = TS_W - TSw(T_00, P_00, n_da, n_wt) * n_wt + n_v(T_00, P_00, n_da, n_wt, n_s)
        * (TSsv_T(T_00, P_00, n_da, n_wt) - TSsl_T(T_00, P_00, n_da, n_wt))
    Else
        TS_W = TS_W - (TSsv_T(T_00, P_00, n_da, n_wt) * n_v(T_00, P_00, n_da, n_wt, n_s) +
        TSsl_T(T_00, P_00, n_da, n_wt) * n_l(T_00, P_00, n_da, n_wt, n_s)) + n_v(T_00, P_00,
        n_da, n_wt, n_s) * (TSsv_T(T_00, P_00, n_da, n_wt) - TSsl_T(T_00, P_00, n_da, n_wt))
    End If
End Function
```

```
'EXERGY CALCULATION
Function Ex_W(t, p, n_da, n_wt, n_s)        'saturated water exergy
   Ex_W = H_W(t, p, n_da, n_wt, n_s) - TS_W(t, p, n_da, n_wt, n_s)
End Function
'DRY AIR COMPONENTS
Function H_DA(t, p, n_da)                   'DRY AIR enthalpy
   H_DA = n_da * Cp_DA * (t - T_00)
End Function
Function TS_DA(t, p, n_da)                  'DRY AIR entropy
   TS_DA = n_da * T_00 * (Cp_DA * WorksheetFunction.Ln(t / T_00) - R *
      WorksheetFunction.Ln(p / P_00) * 100)
End Function
Function Ex_DA(t, p, n_da)                  'EXERGY of dry air component
   Ex_DA = n_da * (Cp_DA * (t - T_00 * (1 + WorksheetFunction.Ln(t / T_00))) + T_00 * R *
      WorksheetFunction.Ln(p / P_00) * 100)
End Function
'DRY SOLID COMPONENTS
Function H_s(t, p, n_s)                     'DRY solid enthalpy
   H_s = n_s * Cp_S * (t - T_00) + n_s * spec_v_S * (1 - T_00 * Th_exp_S) * (p - P_00) * 100
End Function
Function TS_s(t, p, n_s)                    'DRY solid entropy
   TS_s = n_s * T_00 * (Cp_S * WorksheetFunction.Ln(t / T_00)) - n_s * spec_v_S * Th_exp_S
      * T_00 * (p - P_00) * 100
End Function
Function Ex_s(t, p, n_s)                    'EXERGY of dry solid component
   Ex_s = n_s * (Cp_S * (t - T_00 * (1 + WorksheetFunction.Ln(t / T_00))) - spec_v_S * (p -
      P_00) * 100)
End Function
'system calculations
Function Ex_TM(t, p, n_da, n_wt, n_s)       'exergy base complex
   Ex_TM = Ex_DA(t, p, n_da) + Ex_W(t, p, n_da, n_wt, n_s) + Ex_s(t, p, n_s)
End Function
```

```
Function H_TM(t, p, n_da, n_wt, n_s)        'enthalpy base complex
   H_TM = H_DA(t, p, n_da) + H_W(t, p, n_da, n_wt, n_s) + H_s(t, p, n_s)
End Function
Function H_w_simple(t, p, n_da, n_wt, n_s)  'simple water enthalpy
Dim nv, nl As Double
   nv = n_v(t, p, n_da, n_wt, n_s)
   nl = n_wt - nv
   H_w_simple = (nv * Cp_V + nl * Cp_L) * (t - T_00) + nv * lambdaH_T(T_00, P_00, n_da,
      n_wt) + nl * spec_v_L * (1 - T_00 * Th_exp_L) * (p - P_00) * 100
End Function
Function TS_w_simple(t, p, n_da, n_wt, n_s) 'simple water entropy
Dim nv, nl As Double
   nv = n_v(t, p, n_da, n_wt, n_s)
   nl = n_l(t, p, n_da, n_wt, n_s)
   TS_w_simple = T_00 * ((nv * Cp_V + nl * Cp_L) * WorksheetFunction.Ln(t / T_00) + nv *
      lambdaTS_T(t, p, n_da, n_wt) / T_00 - nl * spec_v_L * Th_exp_L * (p - P_00) * 100)
End Function
Function Ex_w_simple(t, p, n_da, n_wt, n_s) 'simple water exergy
   Ex_w_simple = H_w_simple(t, p, n_da, n_wt, n_s) - TS_w_simple(t, p, n_da, n_wt, n_s)
End Function
Function H_simple(t, p, n_da, n_wt, n_s)    'simple enthalpy
   H_simple = H_DA(t, p, n_da) + H_s(t, p, n_s) + H_w_simple(t, p, n_da, n_wt, n_s)
End Function
Function TS_simple(t, p, n_da, n_wt, n_s)   'simple entropy
   TS_simple = TS_DA(t, p, n_da) + TS_s(t, p, n_s) + TS_w_simple(t, p, n_da, n_wt, n_s)
End Function
Function Ex_simple(t, p, n_da, n_wt, n_s)   'simple exergy
   Ex_simple = H_simple(t, p, n_da, n_wt, n_s) - TS_simple(t, p, n_da, n_wt, n_s)
End Function
Function lambdaH_T(t, p, n_da, n_wt)        'evaporation enthalpy
   lambdaH_T = Hsv_T(t, p, n_da, n_wt) - Hsl_T(t, p, n_da, n_wt)
End Function
```

```
Function lambdaTS_T(t, p, n_da, n_wt)      'evaporation entropy
   lambdaTS_T = TSsv_T(t, p, n_da, n_wt) - TSsl_T(t, p, n_da, n_wt)
End Function
'Fuel and Flue COMPONENTS
Function H_flue(t, p, n_o2, n_n2, n_co2, n_f) 'flue and fuel enthalpy
   H_flue = (n_o2 * Cp_o2 + n_n2 * Cp_n2 + n_co2 * Cp_co2 + n_f * Cp_f) * (t - T_00)
End Function
Function TS_flue(t, p, n_o2, n_n2, n_co2, n_f) 'flue and fuel entropy
   TS_flue = (n_o2 * Cp_o2 + n_n2 * Cp_n2 + n_co2 * Cp_co2 + n_f * Cp_f)
   TS_flue = TS_flue * (T_00 * WorksheetFunction.Ln(t / T_00))
   Dim X As Double
   X = WorksheetFunction.Ln(p / P_00)
   TS_flue = TS_flue - (n_o2 + n_n2 + n_co2 + n_f) * R * T_00 * X
End Function
Function Ex_flue(t, p, n_o2, n_n2, n_co2, n_f) 'flue and fuel exergy
   Ex_flue = H_flue(t, p, n_o2, n_n2, n_co2, n_f) - TS_flue(t, p, n_o2, n_n2, n_co2, n_f)
End Function
Function H_Ch(n_s, n_f) 'chemical energy of fuel and SMP
   H_Ch = n_s * HHV_S + n_f * HHV_f
End Function
Function Ex_Ch(n_s, n_f) 'chemical exergy of fuel and SMP
   Ex_Ch = n_s * ExCh_S + n_f * ExCh_f
End Function
Function T_v_out(n_da, n_wt, n_s, t_in, p_in, p_out, q_in) 'valve outlet temperature
   Dim resid, dt, dpv, A As Double
   n = 0
   A = Cp_DA * n_da + Cp_V * n_wt
   dpv = (A * T_00 * (p_in - p_out))
   dt = dpv / A
   t_out = t_in + dt
   resid = q_in - H_TM(t_out, p_out, n_da, n_wt, n_s)
   While Round(resid, 7) <> 0 And n < 50
```

```
        t_out = t_out + resid / A
        resid = q_in - H_TM(t_out, p_out, n_da, n_wt, n_s)
        If n_l(t_out, p_out, n_da, n_wt, n_s) > 0 Then
            resid = resid - n_l(t_out, p_out, n_da, n_wt, n_s) * lambdaH_T(t_out, p_out, n_da,
        n_wt)
        End If
        n = n + 1
    Wend
T_v_out = t_out
End Function
Function p_comp_req(t_in, t_out) 'compressor outlet pressure estimate (75% adiabatic
        efficiency)
    p_comp_req = (P_00 * (t_out / t_in) ^ (k_air / (k_air - 1))) * 0.75
End Function
Function fuel_req(q_in1, q_out1) 'fuel requirement estimate (not used)
    fuel_req = (q_in1 - q_out1) / HHV_f_raw
End Function
Function T_hx_out(n_da, n_wt, n_s, q_1_in, q_1_out, q_2_in, t_2_in, p_in) 'heat
        exchanger outlet temperature estimate, fails if change of state occurs
    Dim deltaq, resid, t_est, A, n_cond As Double
    deltaq = q_1_in - q_1_out
    n = 0
    A = (n_da * Cp_DA + n_wt * Cp_V + n_s * Cp_S)
    resid = deltaq
    t_est = t_2_in + deltaq / A
    While Round(resid, 7) <> 0 And n < 500
        resid = H_TM(t_est, p_in, n_da, n_wt, n_s)
        resid = deltaq + q_2_in - resid
        t_est = t_est + resid / A
        n = n + 1
    Wend
    T_hx_out = t_est
```

```
End Function
Function T_hx_out_p(n_o2, n_n2, n_co2, n_wt, q_1_in, q_1_out, q_2_in, t_2_in, p_in)
    'heat exchanger outlet temperature estimate (flue), fails if change of state occurs
  Dim deltaq, resid, t_est, t_est1, A, n_da, n_cond As Double
  deltaq = q_1_in - q_1_out
  n = 0
  n_da = n_o2 + n_n2 + n_co2
  A = (n_o2 * Cp_o2 + n_n2 * Cp_n2 + n_co2 * Cp_co2 + n_wt * Cp_V)
  resid = deltaq
  t_est = t_2_in + deltaq / A
  While Round(resid, 7) <> 0 And n < 500
    resid = H_TM(t_est, p_in, n_da, n_wt, 0)
    resid = deltaq + q_2_in - resid
    t_est = t_est + resid / A
    n = n + 1
  Wend
  T_hx_out_p = t_est
End Function
Function ex_diffusion(n_da, n_wt, n_s, n_f, n_o2, n_n2, n_co2, nn_l, nn_v) 'diffusion
    calculations
Dim inter, mfo, mfn, mfc, mfvw, mflw, ntot As Double
If n_da > 0 Then
  n_o2 = n_da * mf0_O2
  n_n2 = n_da * mf0_N2
  n_co2 = n_da * mf0_CO2
  n_da = 0
End If
'determine change to gas composition from fuel
'solids assumed un-reactive (thus omitted)
If n_f > 0 Then
  n_o2 = 2 * n_f + n_o2 - 2 / 3 * n_f
  n_co2 = n_co2 + 1 / 3 * n_f
```

```
    n_wt = n_wt + 2 / 3 * n_f
    n_n2 = n_n2 + 2 * 0.8 / 0.2 * n_f
End If
'set-up variables
n_da = n_o2 + n_n2 + n_co2 + n_da
n_wt = n_wt + nn_l + nn_v
ntot = n_da + n_wt
mfo = n_o2 / ntot
mfn = n_n2 / ntot
mfc = n_co2 / ntot
If nn_l > 0 Or nn_v > 0 Then
    mfvw = nn_v / ntot
    mflw = nn_l / ntot
Else
    mfvw = n_v(T_00, P_00, n_da, n_wt, n_s) / ntot
    mflw = n_l(T_00, P_00, n_da, n_wt, n_s) / ntot
End If
'start diffusion calculations
If n_da = 0 Then
    If nn_v = 0 Then
        inter = Abs(n_wt * R * T_00 * WorksheetFunction.Ln(1 / water97_v13.pSatW(T_00)))
    Else
        If mfvw = 0 Then
            inter = 0
        Else
            inter = Abs(mfvw * R * T_00 * ntot * WorksheetFunction.Ln(mfvw / mf0_H2O))
            inter = inter + Abs(mflw * R * T_00 * ntot * WorksheetFunction.Ln(mfvw /
        water97_v13.pSatW(T_00)))
        End If

    End If
ElseIf n_wt = 0 Then
```

```
   inter = Abs(n_o2 * R * T_00 * WorksheetFunction.Ln(mfo / mf0_O2))
   inter = inter + Abs(n_n2 * R * T_00 * WorksheetFunction.Ln(mfn / mf0_N2))
   inter = inter + Abs(n_co2 * R * T_00 * WorksheetFunction.Ln(mfc / mf0_CO2))
Else
   inter = Abs(n_o2 * R * T_00 * WorksheetFunction.Ln(mfo / mf0_O2))
   inter = inter + Abs(n_n2 * R * T_00 * WorksheetFunction.Ln(mfn / mf0_N2))
   inter = inter + Abs(n_co2 * R * T_00 * WorksheetFunction.Ln(mfc / mf0_CO2))
   inter = inter + Abs(mfvw * R * T_00 * ntot * WorksheetFunction.Ln(mfvw / mf0_H2O))
   inter = inter + Abs(mflw * R * T_00 * ntot * WorksheetFunction.Ln(mfvw /
      water97_v13.pSatW(T_00)))
End If
ex_diffusion = inter
End Function
Function enthalpy(t, p, n_da, n_wt, n_s, n_f, n_o2, n_n2, n_co2) 'overall enthalpy
      calculation
If n_da > 0 Then
   n_o2 = n_da * mf0_O2
   n_n2 = n_da * mf0_N2
   n_co2 = n_da * mf0_CO2
Else
   n_da = n_o2 + n_n2 + n_co2
End If
enthalpy = H_flue(t, p, n_o2, n_n2, n_co2, n_f)
enthalpy = enthalpy + H_W(t, p, n_da, n_wt, n_s) 'H_w_simple(t, p, n_da, n_wt, n_s)
enthalpy = enthalpy + H_s(t, p, n_s) + H_Ch(n_s, n_f)
'n_v0 = mf0_H2O * n_da / (1 - mf0_H2O)
'If n_v(T_00, P_00, n_da, n_wt, n_s) > n_v0 Then
'    enthalpy = enthalpy - n_v0 * lambdaH_T(T_00, P_00, n_da, n_wt)
'ElseIf n_v(T_00, P_00, n_da, n_wt, n_s) <= n_v0 Then
' enthalpy = enthalpy - (n_v(T_00, P_00, n_da, n_wt, n_s) - n_v0) * lambdaH_T(T_00, P_00,
      n_da, n_wt)
'End If
```

```
End Function
Function exergy(t, p, n_da, n_wt, n_s, n_f, n_o2, n_n2, n_co2) 'overall exergy calculation
If n_da > 0 Then
   n_o2 = n_da * mf0_O2
   n_n2 = n_da * mf0_N2
   n_co2 = n_da * mf0_CO2
Else
   n_da = n_o2 + n_n2 + n_co2
End If
exergy = Ex_flue(t, p, n_o2, n_n2, n_co2, n_f) + Ex_s(t, p, n_s) + Ex_Ch(n_s, n_f)
exergy = exergy + ex_diffusion(0, n_wt, n_s, n_f, n_o2, n_n2, n_co2, 0, 0)
exergy = exergy + Ex_W(t, p, n_da, n_wt, n_s) ' Ex_w_simple(t, p, n_da, n_wt, n_s)
End Function
Function dryer_tg_o(t_g_in, n_da, yn_in, t_s_in, n_s, xn_in, offset)
Dim lam, n_v2, n_v1, T_int, t_s, T_g, H_in, H_resid, n_wt As Double
'determine standard variables
n_wt = yn_in * n_da + xn_in * n_s
'Determine goal enthalpy as a check
H_in = enthalpy(t_g_in, P_00, n_da, n_da * yn_in, 0, 0, 0, 0, 0) + enthalpy(t_s_in, P_00, 0,
      n_s * xn_in, n_s, 0, 0, 0, 0)
'starting guesses
T_g = t_g_in
t_s = Tdp(P_00, n_da, n_wt)
n_v1 = yn_in * n_da
n_v2 = n_v(t_s, P_00, n_da, n_wt, n_s)
lam = lambdaH_T(t_s, P_00, n_da, n_wt)
n = 0
H_resid = H_in
'begin loop
While n < 100 And H_resid <> 0
   'set-up required variables
   T_int = T_g
```

```
    n_v2 = n_v(t_s, P_00, n_da, n_wt, n_s)
    'determine how much enthalpy is not accounted for
    H_resid = H_in - enthalpy(T_int, P_00, n_da, n_v2, 0, 0, 0, 0, 0)
    H_resid = H_resid - enthalpy(t_s, P_00, 0, n_wt - n_v2, n_s, 0, 0, 0, 0)
    'convert H to temperature on gas phase only
    resid_T = (H_resid / (n_da * Cp_DA + n_v2 * Cp_V + (n_wt - n_v2) * Cp_L + n_s * Cp_S)) *
       0.6
    T_g = T_int + resid_T
    n_v1 = n_v(T_g - offset, P_00, n_da, n_wt, n_s)
    t_s = T_g - offset
    'progress values
    n = n + 1
Wend
`flip the result so it is easier to access via cell functions
Dim vector(1 To 4) As Double
vector(1) = T_g
vector(2) = t_s
vector(3) = resid_T
vector(4) = n 'check timout
If Application.Caller.Rows.Count > 1 Then
    dryer_tg_o = Application.Transpose(vector)
Else
    dryer_tg_o = vector
End If
End Function
Function T_SP(x_n)
Dim x_m, t_Glass_w, t_glass_s As Double
'glass transistion temperature of water -137C, of lactose is 101C
'x_n is in mol/mol, x_m must be in kg/kg
x_m = x_n * mm_W / mm_S
t_Glass_w = -137
t_glass_s = 101
```

```
T_SP = ((1 - x_m) * t_glass_s + x_m * t_Glass_w) / (1 + 7.48 * x_m) + 23.3
End Function
```